Journal of Hydrology 529 (2015) 1313–1323

Contents lists available at ScienceDirect

Journal of Hydrology

journal homepage: www.elsevier.com/locate/jhydrol

Environmental tracers for elucidating the weathering process in a phosphogypsum disposal site: Implications for restoration

Rafael Pérez-López [a,*], José M. Nieto [a], Jesús D. de la Rosa [a,b], Juan P. Bolívar [c]

[a] Department of Geology, University of Huelva, Campus 'El Carmen', 21071 Huelva, Spain
[b] Associate Unit CSIC – University of Huelva "Atmospheric Pollution", Center for Research in Sustainable Chemistry (CIQSO), University of Huelva, 21071 Huelva, Spain
[c] Department of Applied Physics, University of Huelva, Campus 'El Carmen', 21071 Huelva, Spain

ARTICLE INFO

Article history:
Received 2 March 2015
Received in revised form 20 July 2015
Accepted 26 August 2015
Available online 1 September 2015
This manuscript was handled by Laurent Charlet, Editor-in-Chief, with the assistance of Pedro J. Depetris, Associate Editor

Keywords:
Phosphogypsum
Geochemical tracers
Rare earth elements
Cl/Br mass ratio
Estuary of Huelva

SUMMARY

This study provides geochemical data with the aim of identifying and tracing the weathering of phosphogypsum wastes stack-piled directly on salt-marshes of the Tinto River (Estuary of Huelva, SW Spain). With that purpose, different types of highly-polluted acid solutions were collected in the stack. Connection between these solutions and the estuarine environment was studied by geochemical tracers, such as rare earth elements (REE) and their North American Shale Composite (NASC)-normalized patterns and Cl/Br ratios. Phosphogypsum-related wastewaters include process water stored on the surface, pore-water contained in the phosphogypsum profile and edge outflow water emerging from inside the stack. Edge outflow waters are produced by waterlogging at the contact between phosphogypsum and the nearly impermeable marsh surface and discharge directly into the estuary. Process water shows geochemical characteristics typical of phosphate fertilizers, i.e. REE patterns with an evident enrichment of heavy-REE (HREE) with respect to middle-REE (MREE) and light-REE (LREE). By contrast, REE patterns of deeper pore-water and edge outflows are identical to those of Tinto River estuary waters, with a clear enrichment of MREE relative to LREE and HREE denoting influence of acid mine drainage. Cl/Br ratios of these solutions are very close to that of seawater, which also supports its estuarine origin. These findings clearly show that process water is not chemically connected with edge outflows through pore-waters, as was previously believed. Phosphogypsum weathering likely occurs by an upward flow of seawater from the marsh because of overpressure and permeability differences. Several recommendations are put forward in this study to route restoration actions, such as developing treatment systems to improve the quality of the edge outflow waters before discharging to the receiving environment.

1. Introduction

Some estuarine areas in Europe have undergone extensive industrialization over the past half-century due to their relatively flat surface, the nearby water availability and the proximity of the sea as a means of communication. Among these areas, a huge complex of chemical and petrochemical industries was installed in the surroundings of the Estuary of Huelva, a system formed by the confluence of the Tinto and Odiel Rivers (SW Spain). In this industrial area, several factories focus on the production of phosphoric acid for fertilizers. This manufacturing process is based on wet chemical attack of phosphate rock ore (fluorapatite, $Ca_5(PO_4)_3F$) with sulfuric acid (H_2SO_4) to produce phosphoric acid (H_3PO_4) as a commercial product and a low-value waste composed mainly by gypsum ($CaSO_4{\cdot}2H_2O$) known as phosphogypsum. The process can be summarized in the following reaction (Eq. (1)):

$$Ca_5(PO_4)_3F + 5H_2SO_4 + 10H_2O \rightarrow 3H_3PO_4 + 5CaSO_4 \cdot 2H_2O + HF \quad (1)$$

Phosphogypsum broadly contains metal(loid)s and radionuclides (Rutherford et al., 1994), also that produced by the industries located at the Estuary of Huelva (Bolívar et al., 1996; Pérez-López et al., 2007). Consequently, the market is poor for such waste and, hence, its production leads to stacking in large disposal areas close to the industrial plant, where phosphogypsum is often exposed to weathering conditions (Tayibi et al., 2009). In the Estuary of Huelva, the stack contains phosphogypsum produced for 40 years, i.e. approx. 1000 ha and 100 Mt. This dump covers the salt-marshes associated with the Tinto River estuary, less than 1 km from the city of Huelva. Phosphogypsum piles have even greater area than that of the city (approx. 1100 ha). These wastes

* Corresponding author. Tel.: +34 95 921 9819; fax: +34 95 921 9810.
E-mail address: rafael.perez@dgeo.uhu.es (R. Pérez-López).

http://dx.doi.org/10.1016/j.jhydrol.2015.08.056
0022-1694/

are currently considered a NORM (naturally occurring radioactive material) substance and, therefore, its proximity to the urban area has awakened considerable social concern in recent years.

The mountain of waste has caused evident loss of a landscape with great ecological value and has a strong visual and landscape impact. Similar unimpacted salt-marshes on the Odiel River estuary were declared a UNESCO Biosphere Reserve in 1983 and RAMSAR-NATURA wetlands site in 1989. Fertilizer plants ceased dumping in December 2010 by decision of the Spanish National Court. However, the old stacks still remain on the salt-marshes of the Tinto River. Most of the potentially toxic impurities contained in phosphogypsum are associated with the easily mobile fraction, which is transferred to the environment in extremely acidic solutions (Pérez-López et al., 2010a). The stack base is directly in contact with the marsh soil surface. Marshes have a high content of organic matter whose oxidative decomposition leads to oxygen consumption and strongly anaerobic conditions. In the weathering profile of the phosphogypsum pile, some of the mobile metals are removed from solution by precipitation of insoluble metal sulfides in this anaerobic zone by activity of sulfate-reducing bacteria (Pérez-López et al., 2011; Castillo et al., 2012).

Pérez-López et al. (2011) clarified the redox geochemical processes occurring along the weathering profile and concretely the role of the underlying salt-marsh in the natural attenuation of contamination and, hence, in mitigating part of the phosphogypsum impact on the estuarine environment. However, several sources of highly-polluted acidic water can be recognized in the waste pile. On the one hand, surface ponds storing waters from the industrial processes, known as process waters, are directly on the pile. On the other hand, groundwater is retained above the relatively impermeable marsh surface, forcing a lateral flow through deeper saturated zones of the waste that emerges on the edge of the stack. These springs, known as edge outflow waters, drain the phosphogypsum pile and discharge directly into the Estuary of Huelva. Hence, the phosphogypsum stack is not totally watertight at present. Some of these leachates have been previously characterized from a radiological point of view (Gázquez et al., 2014), but no information has yet been published on the content of metallic impurities.

Phosphogypsum stacks are presently submitted to continuous weathering. There are some guidelines taken by the regional government for the implementation of future actions aimed at remediating the phosphogypsum disposal area (Junta de Andalucía, 2009). These already existing guidelines include, roughly, the following priority actions: (1) to remove process water from surface ponds, (2) to pump out and remove the pore-water of the piles to prevent leakages around the edges of the stack, (3) to treat ex situ the extracted wastewater in a treatment system, and (4) to cover the phosphogypsum surface by artificial-soil amendments with a drainage system to facilitate the evacuation of rainwater. This preliminary report states that the process water is the primary route of dispersion of pollutants to the aqueous environment, both by its volume and by its chemical characteristics, and thus its removal must be carried out urgently. Moreover, these guidelines also indicate that infiltration of ponded process water downward to groundwater is the direct cause of diffuse and point edge outflows toward the estuary, i.e. process water and edge outflows are linked through porous media. However, these preliminary guidelines were issued without proving the possible connection between these solutions and with an obvious lack of information on the weathering process involved in leaching and transport of contaminants from the stack to the estuarine environment. Thus, the present study aims to bridge this gap using geochemical indicators, e.g. ionic compositions and fractionation of rare earth elements (REE), as environmental tracers of the phosphogypsum weathering process. This information will be invaluable for the design and optimization of remediation actions.

2. Environmental setting

The Estuary of Huelva is on a mesotidal mixed-energy coast with a tidal range of 1–3 m and a tidal prism between 37 and 82 hm^3 during a tidal half-cycle (6 h) (Grande et al., 2000). Surprisingly, the phosphogypsum stack is located within the tidal prism of this estuary. The fertilizer plant has produced and deposited phosphogypsum with a rate of 2.5 Mt/year from 1968 to 2010. Currently, four zones are clearly recognized within the dumping area. In future plans for restoration, zones 1 and 4 (approx. 750 ha) are considered to be already restored by only covering the phosphogypsum with a layer of natural soil. Neither of these *a priori* restored zones have process water in surface ponds. In zones 2 and 3 (approx. 450 ha), the uncovered phosphogypsum is directly exposed to weathering (see in Fig. 1). The phosphogypsum management policy changed in 1997, following the OSPAR convention (OSPAR, 2002, 2007). Until then, 80% of produced phosphogypsum was transported and deposited in the four zones of the stack with seawater using an open-circuit pipe system, reaching an average height of 5 m. The water, after waste decantation, with around 20% of phosphogypsum was directly poured into the Odiel River estuary, and this was dispersed by the tidal action reaching finally the Atlantic Ocean (Martínez-Aguirre et al., 1996; Bolívar et al., 2000, 2002).

From 1997 to the end of 2010, all the phosphogypsum produced was stored in zone 2 using a closed-circuit system with freshwater as process water, forming a pyramidal pile of up to 30 m in height. Thereafter, there has been no 'direct' release to the estuary up to date (Villa et al., 2009). The closed circulation system of process waters includes the creation of the surface pond and a series of perimeter channels for collecting and incorporating acidic leachates from the phosphogypsum weathering into the closed circuit. According to the restoration guidelines of the regional government (Junta de Andalucía, 2009), these channels collect most of the infiltrating water in zone 2 and, therefore, the potential risk for the ecological receptors by 'indirect' leakage of edge outflows in this area would be presumably minimal.

In contrast, zone 3 is an abandoned area without restoration activities where no disposal of phosphogypsum has occurred since 1997. Since then, its function has been to store process water in a central pond that is part of the closed-circuit freshwater system installed after the change of management policy (Fig. 1). This process water is conducted through pipes from zone 2 of the stack. Since the cessation of phosphogypsum production in 2010, water circulation remains active and carries process water to zone 3 to be subjected to evaporation with the purpose of reducing its volume. However, zone 3 does not have any measures to prevent leached water from phosphogypsum weathering from reaching the surrounding environment. In fact, there are numerous points and diffuse sources of edge outflow that comprise a total annual flow of approx. 90,000 m^3 (Tragsatec, 2010). For this reason, this study focuses on the assessment of the potential contamination from this zone of the phosphogypsum stack, which may be representative of the overall disposal area.

3. Materials and methods

3.1. Sampling points

Geochemical tracers of the weathering processes in the phosphogypsum stack were studied by sampling in May 2013 (Fig. 1): (1) pore-solutions of phosphogypsum samples collected at approx. 0.5 m intervals from the stack surface to the underlying marsh surface using a soil sampling auger (bore-hole C; samples C1–C14), (2) edge outflow leachates reaching the Estuary of Huelva (samples

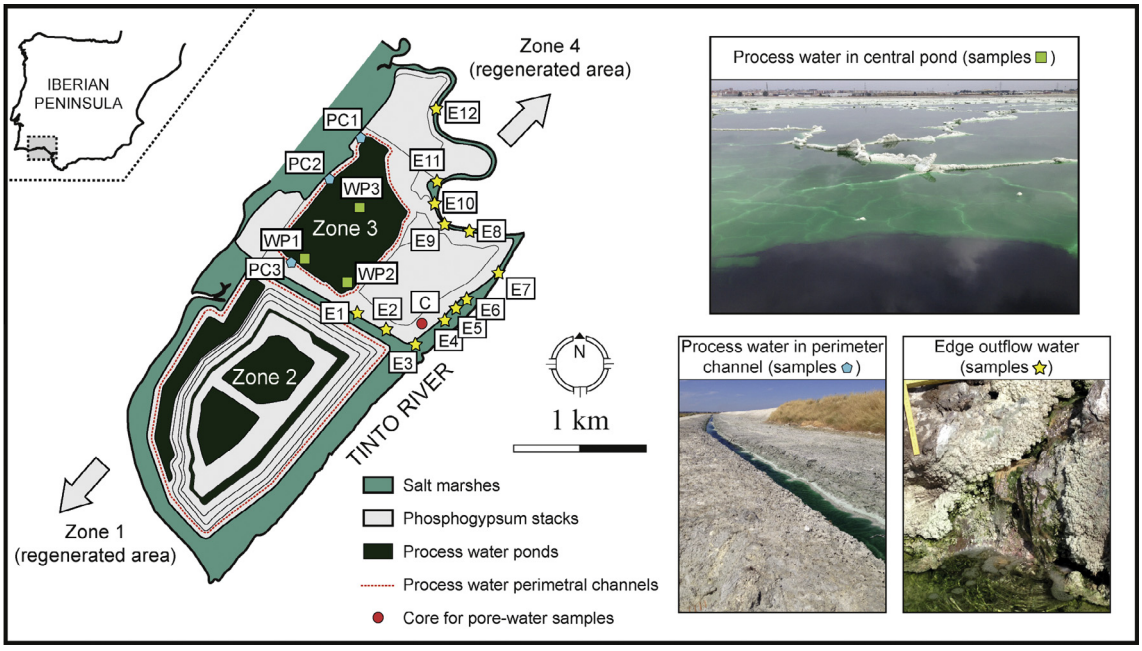

Fig. 1. Location map of the phosphogypsum disposal piles on the salt-marshes of the Tinto River. Some field pictures of the process water (both in the central pond and perimeter channel) and the edge outflow water are also shown.

E1–E12), and (3) process water in the central pond (samples WP1–WP3) and in the perimeter channel (samples PC1–PC3). Given that the idea would be to check whether the possible infiltration of the ponded process water reaches the edge through the waste porosity and contaminates the estuarine environment, the core site was specifically chosen close to the contour of the phosphogypsum stack (Fig. 1).

For upper pore-water samples, solution extraction and filtration were simultaneously conducted using suction cup lysimeters and hollow-fiber tube sampler devices (Rhizon samplers; Eijkelkamp Agrisearch Equipment, Netherlands), which were inserted into the wet samples collected with the soil auger. For deeper pore-water samples, due to high waterlogging, solutions were easily extracted by centrifugation and then filtered with 0.45 μm membrane filters. The edge outflow and process water samples were also filtered with 0.45 μm membrane filters.

3.2. Analytical procedures

The pH, redox potential (Eh) and electrical conductivity (EC) were measured in the field, except for the pore-waters that were measured immediately in the laboratory after extraction, using a portable Multiparametric Crison Mm 40+ meter. Redox potential was corrected in order to obtain the Eh with respect to the standard hydrogen electrode (Nordstrom and Wilde, 1998). Filtered solutions were divided into three aliquots, one not acidified for anion analysis, one acidified with nitric acid to pH = 1 for major and trace element analysis, and one buffered to pH 4.5 with an ammonium acetate/acetic acid buffer and Fe(II) complexed with a phenantroline solution for Fe(II)/(III) determination according to the method outlined by Rodier (1996).

Concentrations of anions in phosphogypsum-related wastewater solutions were analyzed by high performance liquid chromatography (HPLC) using a Metrohm 883 basic ion chromatograph (IC) plus equipped with a Metrosep A Supp 5 250/4.0 column. These wastewater solutions were also analyzed using Inductively Coupled Plasma-Atomic Emission Spectroscopy (ICP-AES; Jobin Yvon Ultima 2) for determination of major elements (Al, Ca, Fe, K, Mg, Mn, Na, P and S) and Inductively Coupled Plasma-Mass Spectroscopy (ICP-MS; Agilent 7700) for trace elements (As, Cd, Co, Cr, Cu, Ni, Pb, Sb, U, Zn and REE). Detection limits were: 0.2 mg/L for S; 0.1 mg/L for Na; 0.05 mg/L for Fe, K and Mg; 0.02 mg/L for Al, Ca, Mn and P; and 1 μg/L for the trace elements. In the analyses of ICP-AES and ICP-MS, calibration with sets of standards was performed and the regression coefficient exceeded 0.999. Three laboratory standards, prepared with metal concentrations within the range of the samples, were analyzed with every 10 samples to check for accuracy. Furthermore, dilutions from 1:10 to 1:200 were performed to ensure that the concentration of the samples was within the concentration range of the standards. Blank solutions with the same acid matrix as the samples were also analyzed. The average measurement error was less than 5%. The charge balance error between cations and anions was within 10%, calculated with the PHREEQC code (Parkhurst and Appelo, 2005) to check the quality of the analyses.

Determinations of Fe(II) and total Fe (following reduction with hydroxylamine hydrochloride) in the wastewater solutions were immediately undertaken in the laboratory by colorimetry at 510 nm using a Hach DR/890 colorimeter on the same day of the sampling. The detection limit was 0.3 mg/L and precision was better than 5%; Fe(III) was calculated as the difference between total Fe and Fe(II).

3.3. NASC-normalized REE patterns

REE fractionation has been shown to be a feasible tool to identify pollution sources and trace possible impacts on ecological receptors (Noack et al., 2014 and references therein). In order to better determine fractionation processes, it is useful to normalize absolute REE concentrations to a reference material such as North American Shale Composite (NASC), which has been widely used in numerous geochemical studies (Gromet et al., 1984). Cerium anomalies $(Ce/Ce^{*})_{NASC}$ were calculated from the expression $Ce_{NASC}/\sqrt{[La_{NASC}\cdot Pr_{NASC}]}$. Moreover, the shape of the NASC-normalized REE patterns was described using the $(La/Gd)_{NASC}$ and $(La/Yb)_{NASC}$ ratios, being La representative of the light-REE (LREE),

Gd of the middle-REE (MREE) and Yb of the heavy-REE (HREE). However, using a single REE ratio as representative of the whole suite could hamper the interpretation of REE patterns in the case of exclusive fractionation affecting only one of the elements in the ratio. In fact, some processes cause a curvature effect, upward concave (V-type for depletion) or convex (Λ-type for enrichment), in the MREE whole segment whose identification could not be well-evaluated by the normalized ratios. Thus, Pérez-López et al. (2010b) proposed the E_{MREE} parameter to quantify these curved MREE signatures with higher sensitivity than the traditional parameters. The index E_{MREE} allows quantifying the curvature as the normalized maximum vertical difference between the polynomial curve fitting of the MREE region and its theoretical *Y*-axis position in the absence of enrichment or depletion (see details in Pérez-López et al., 2010b). The quality of the fit, and hence the significance of the curve formed by data points, can be quantified by the squared correlation coefficient, R^2. The value of E_{MREE} is positive for convex-up MREE-signatures, negative for concave-up MREE-signatures and around zero for flat patterns.

4. Results

Phosphogypsum consists almost entirely of gypsum (90–95 wt %), along with minor amounts of quartz. However, this waste by-product is not inert, but contains relatively high concentrations of contaminants (Pérez-López et al., 2007). Except some elements with chemical affinity to Ca (e.g., Ra, Sr, Y), most of the contaminant impurities are partitioned into the commercial phosphoric acid during the manufacturing process (Bolívar et al., 1996, 2009; Pérez-López et al., 2010a). However, phosphogypsum deposited in the stack contains a small residual fraction of free acids: mainly phosphoric acid and, to a lesser extent, sulfuric and hydrofluoric acids. These acids make phosphogypsum a source of extreme acidity and dangerousness. Sulfuric acid is the excess of reagent used for chemical digestion of phosphate rock ore; whereas phosphoric and hydrofluoric acids are the products of the reaction (see Eq. (1)). The resulting phosphoric acid is separated in the industrial process and further processed for sale. However, residual amounts of phosphoric acid can remain within the waste porosity. This residual phosphoric acid also explains the high content of pollutants of the waste by-product. The geochemical characteristics of the solutions derived from phosphogypsum are described below.

4.1. Elemental contaminant concentrations

4.1.1. Pore-water

The water table in the bore-hole of the phosphogypsum stack during the sampling campaign was at a depth of 2.5 m; while the surface of the salt-marsh was found at 8 m. Along the vertical profile, pore-water pH values decrease with depth from 3.55 to 2.05 (Fig. 2a); whereas EC values increase from 3.38 mS/cm to 59.7 mS/cm (Fig. 2b). Eh is maintained with values of around 480 mV between 2.5 and 6 m depth, but then decreases progressively toward the marsh to 385 mV (Fig. 2c).

Concomitant with the increase of EC, there is also an increase of the sum of the major anions in solution. Based on the major element concentrations, the phosphogypsum pile could be divided into two well-defined zones: (1) an upper zone to a depth of 5.5 m where solutions mainly show high S and P concentrations, with values that progressively increase to 2867 and 1881 mg/L, respectively; and (2) a deeper zone from 5.5 to 8 m where S and P concentrations are maintained around those levels and Cl strongly dominates the pore-water composition with values that increase sharply up to 19334 mg/L (Fig. 3a). Total S and P concentrations obtained by ICP-AES are equal to the S and P concentrations obtained by HPLC as sulfate and phosphate species, respectively, if one considers molar concentrations; except for S in the deepest samples in contact with the marsh where there is up to around 40% of other reduced sulfur species. Similarly, Br concentrations increase progressively to a maximum value of 86.2 mg/L in the deepest zones (Fig. 3b). Chloride/Br ratios can provide information on the origin of the water. Upper pore-waters have Cl/Br ratios between 3.30 and 59.9 (average of 31.9 ± 20.1), whereas Cl/Br ratios vary between 120 and 235 (average of 191 ± 44.1) for deeper pore-waters (Fig. 3b). As for F, concentrations increase up to values of 4290 mg/L at 4 m depth and then decrease down to constant values of about 500 mg/L (Fig. 3a).

For metals, Fe exhibits the highest concentrations. Iron concentrations increase progressively with depth from 1.1 mg/L to 1117 mg/L, with the sharpest increase occurring in the last meter (Fig. 3c). Most of the total Fe corresponds to Fe(II), with percentages totaling 100% in the deepest zones. For the remaining trace metals, most are strongly and positively correlated with phosphate concentrations in solution, which confirms the industrial origin of this association. The concentrations of these metals progressively increase to a maximum around 5.0–6.0 m depth, as occurred with S and P concentrations (Fig. 4). Below this zone, concentrations of most metals decrease toward the contact with the marsh. This decrease occurs gradually for Co, Ni, Cu, As, Cd, Sb and U and parallels the decrease in the Eh values (see red arrows in Figs. 2c and 4). Concentrations in the deepest zone are not as low as near the surface. For Pb, although its concentration decreases with depth from 5.5 m, the values increase in the last meter.

4.1.2. Edge outflow water

As stated before, wastewater leaching from the phosphogypsum stack does not infiltrate into the marsh. The extensive accumulation of water observed during sampling above the last meter before the relatively impermeable marsh surface could be, at least partly, drained away through 12 edge outflows sampled on the perimeter of zone 3 of the phosphogypsum stack (samples E). These samples correspond to point sources reaching the Estuary of Huelva, either directly or indirectly through secondary tidal channels. The samples E1, E2, E11 and E12 (Fig. 1) are edge outflows that are dammed in inactive perimeter channels, which are susceptible to overflow and easily reach the estuary. The main geochemical characteristics of these edge outputs are extreme acidity (pH of 2.03 ± 0.10), high EC values (40.3 ± 9.88 mS/cm) and high concentration of anions and cations (Table 1). The concentrations are very similar to those found in the pore-water of the deepest part of the weathering profile. Thus, Cl/Br ratios of most edge outflow waters are in the same order of magnitude as deeper pore-solutions, with an average value of 228 ± 70.4. Two samples have been excluded from these calculations for presenting significantly higher values (samples E6 and E11; Table 1).

4.1.3. Process water

Process water collected in the active perimeter channels (samples PC) shows geochemical characteristics similar to those found in deeper pore-water and edge outflow water, although with relatively higher concentrations as this water comes directly from the industrial process and is concentrated in the closed-circuit system. It is worthwhile to highlight its low pH (1.42 ± 0.24) and high EC (59.4 ± 4.32 mS/cm), as well as high elemental concentrations (Table 2). The geochemical features of ponded process water (samples WP) are indicative of the intense evaporation that occurs in this central pond and that acts to concentrate acidity and contaminants, reaching pH values of 0.31 ± 0.06 and EC of 87.1 ± 27.4 mS/cm. The concentrations of P and metals are about three times higher than that found in the active perimeter channels (Table 2). Of all the phosphogypsum-related leachates, these are certainly

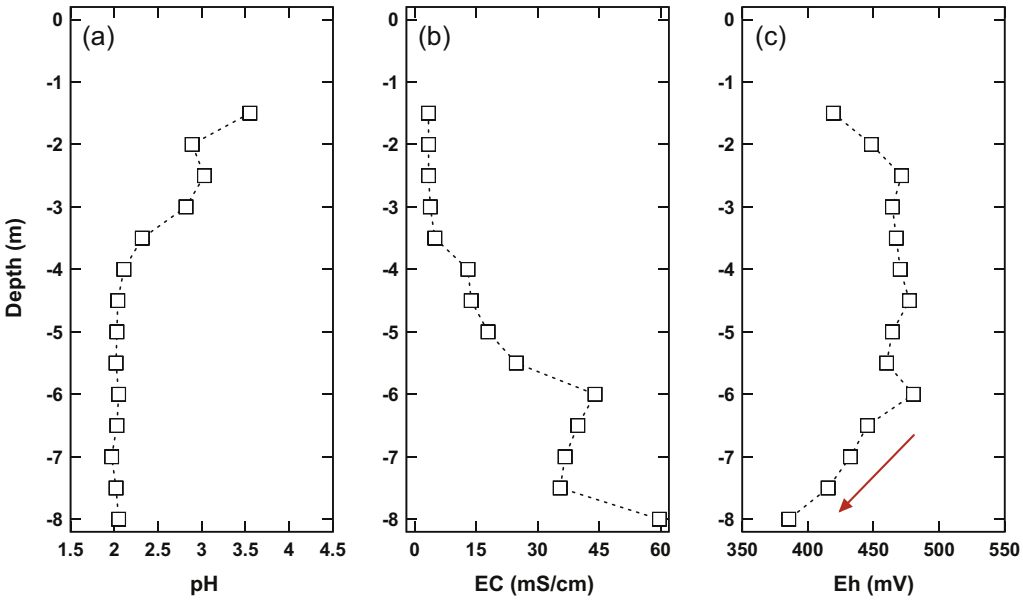

Fig. 2. Evolution with depth of (a) pH, (b) EC and (c) Eh in pore-water solutions from phosphogypsum samples.

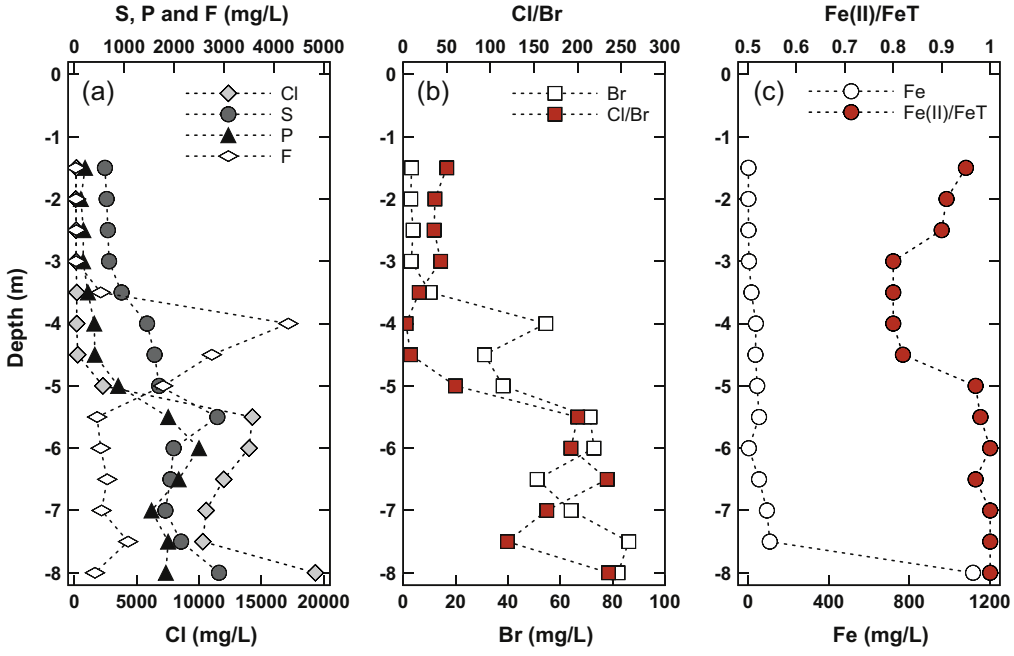

Fig. 3. Evolution with depth of major element concentrations [(a) Cl, S, P, F (b) Br and (c) Fe] in pore-water solutions from phosphogypsum samples. The Cl/Br and Fe(II)/Fe_{total} ratios are also shown in (b) and (c), respectively.

the most acidic and enriched in contaminants. All process waters have lower Cl/Br ratios than edge outflows and deeper pore-waters, but in the same order of magnitude as upper pore-waters, with average values of 53.4 ± 14.4 and 44.6 ± 10.2 for samples of the active perimeter channels and of the central pond, respectively (Table 2).

4.2. Rare earth element concentrations

Concentrations of all REE in the samples of phosphogypsum-related wastewaters are shown in the Table S1 (see electronic supplement). Table S1 also shows the sum of total REE (ΣREE), the values of the Ce anomaly, the normalized $(La/Gd)_{NASC}$ and $(La/Yb)_{NASC}$ ratios, and the E_{MREE} parameter for all samples. Higher ΣREE concentrations are found by far in the process water samples, i.e. both in the perimeter channels (average of 5.21 mg/L) and mainly in the central pond (average of 12.4 mg/L), which is as expected due to concentration in the closed-circuit and more recently to evaporation. ΣREE contents of edge output waters (average of 139 μg/L) and pore-waters (average of 60.4 μg/L) are within the same order of magnitude, but with significantly lower values than those in the process water. All samples of phosphogypsum-related waters

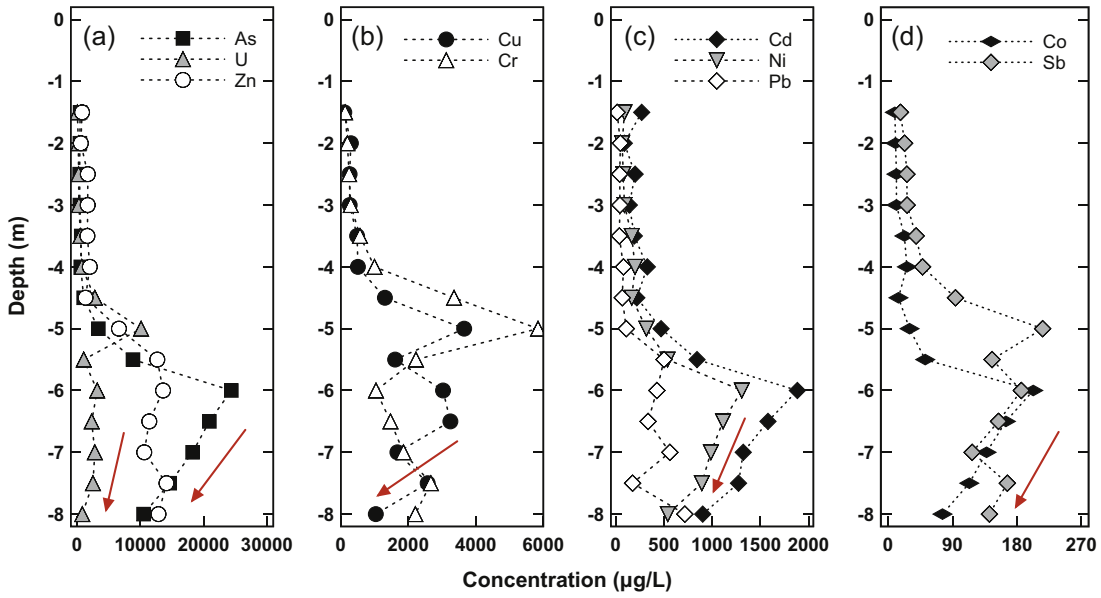

Fig. 4. Evolution with depth of trace element concentrations [(a) As, U, Zn, (b) Cu, Cr, (c) Cd, Ni, Pb and (d) Co, Sb] in pore-water solutions from phosphogypsum samples.

show NASC-normalized REE patterns with a strong negative Ce anomaly, with average values of $(Ce/Ce^*)_{NASC}$ ranging between 0.20 and 0.38 (Supplementary Table S1 and Fig. 5).

With respect to NASC-normalized ratios, edge outflow waters and pore-waters show average $(La/Gd)_{NASC}$ values closer to unity (1.24 and 0.86, respectively) than those of $(La/Yb)_{NASC}$, which are higher than unity (2.84 and 1.76, respectively). These values indicate that there is not a clear fractionation of LREE with respect to MREE, and only a slight enrichment of LREE with respect to HREE can be observed. E_{MREE} values do not indicate any type of curvature in upper pore-water samples (up to 5.5 m deep) because most curves fitting the MREE segments show a value of $R^2 < 0.50$ (Fig. 5a). However, both deeper pore-water (from 5.5 m to 8.0 m deep) and edge outflow samples are characterized by a positive value of E_{MREE} of $+0.63 \pm 0.20$ (average R^2 of 0.79) and $+0.39 \pm 0.07$ (average R^2 of 0.94), respectively. These values are consistent with the presence of an enrichment or convex-up curvature in MREE (Λ-type) observed visually in the NASC-normalized patterns (Fig. 5b and c), which is not indicated by the conventional $(La/Gd)_{NASC}$ ratio.

Average $(La/Gd)_{NASC}$ and $(La/Yb)_{NASC}$ values for process water, both in the perimeter channels (average of 0.59 and 0.28, respectively) and in the central pond (average of 0.56 and 0.23, respectively), show an evident enrichment in HREE with respect to LREE, and in MREE with respect to LREE. In this case, normalized $(La/Gd)_{NASC}$ and $(La/Yb)_{NASC}$ ratios certainly describe the shape of the REE patterns, as observed in Fig. 5d. Regarding the convexity index, although patterns are fitted with curves having average R^2 of 0.99, the value obtained for E_{MREE} is $+0.13 \pm 0.01$, which shows that distributions are relatively flatter in the MREE segment than those observed for deeper pore-water and edge outflow solutions. In principle, this difference in the NASC-normalized REE distribution could allow investigation of the possible connections between the various types of phosphogypsum-related wastewaters.

5. Discussion

5.1. Environmental tracers for the weathering process

All phosphogypsum wastewater samples exhibit similar chemical characteristics, i.e. extreme acidity and high loads of contaminants. These solutions represent the true environmental risk of the phosphogypsum stack, rather than the solid waste. Cessation of damming process water on the stack and the high degree of evaporation that it has undergone in recent years make that these solutions have even more extreme characteristics that distinguish them from the other phosphogypsum-related solutions. However, there was probably a greater chemical similarity between all wastewater solutions during industrial activity and before evaporation. Therefore, ruling out a possible connection between the process water and the edge outflows is not so obvious.

Based on our results, one could use geochemical tracers to reveal the connection between phosphogypsum wastewaters and its possible influence on the Estuary of Huelva. Using geochemical tools should be straightforward because there are two clearly contrasting geochemical endmembers; i.e. fertilizer production and salt-marshes of the Tinto River. The NASC-normalized REE distribution patterns (Fig. 5) together with the Cl/Br ratio (Fig. 6) are distinct and, therefore, both tools could be used as geochemical tracers of both environments. At one extreme, fertilizers are usually characterized by a Cl/Br mass ratio ranging from 30 to 120 (Otero et al., 2005). Plotting Br vs. Cl concentrations (Fig. 6) in phosphogypsum wastewaters, it is clearly observed that the process water is in the range of typical values for fertilizers, as expected. Likewise, both the marked negative Ce anomaly and HREE enrichment with respect to MREE and LREE in the NASC-normalized REE patterns are also typical of phosphate rock-derived fertilizers and phosphogypsum (McArthur and Walsh, 1985; Otero et al., 2005).

At the other extreme, in systems with possible marine influence it is widely known that the Cl/Br ratio can be also used as a natural tracer, especially to identify the existence of saline intrusion in groundwater flow (e.g. Sánchez-Martos et al., 2002). Thus, the Cl/Br mass ratio is close to 290 for seawater. Notably, edge outflow waters in the phosphogypsum stack have Cl/Br ratios close to seawater (Fig. 6), except the two samples with higher values. These higher values of Cl/Br ratio could be related to the dissolution of halite in estuarine marsh zones with precipitation of evaporitic salts (Stober and Bucher, 1999; Göb et al., 2013). Moreover, NASC-normalized REE patterns in the edge outflows show a convex-up curvature in the MREE whole segment. This convex signature enriched in MREE is perfectly consistent with a Tinto

Table 1
Compilation of pH, electrical conductivity, redox potential, Cl/Br ratio and elemental contaminant analysis in the edge outflow water samples.

	pH	EC (mS/cm)	Eh (mV)	Cl/Br	Major elements (mg/L)						Trace elements (μg/L)									
					Cl	Br	F	Fe	P	S	As	Cd	Co	Cr	Cu	Ni	Pb	Sb	U	Zn
Edge outflow water																				
E1	1.83	61.8	579	226	21609	95.6	307	58.1	3049	2350	33518	2594	357	1622	4276	2075	422	241	3505	21402
E2	1.98	27.0	527	111	5890	53.0	727	23.4	1650	1914	17987	1162	184	4977	5754	983	409	363	6120	12278
E3	2.10	31.4	452	185	9275	50.1	695	77.6	1329	1656	14291	982	95.3	1840	1642	698	60.2	107	2537	6668
E4	2.17	31.4	460	192	8563	44.7	571	84.1	1500	1643	11895	1135	101	1611	1286	836	95.2	188	2459	7293
E5	2.06	38.6	451	336	10152	30.2	472	55.0	2077	1751	16427	1479	204	3189	2569	1176	134	228	3404	13517
E6	2.03	46.9	432	2075	15831	7.63	399	52.9	1986	1862	21980	1648	193	1850	2590	1151	254	221	2512	15460
E7	2.04	34.4	450	203	9281	45.8	437	62.6	1572	1800	17598	1354	200	1616	2742	999	188	311	2349	15303
E8	2.13	38.8	447	220	11741	53.3	448	69.4	1224	2048	11717	1187	212	2005	2416	1443	24.2	256	1752	15185
E9	1.93	47.7	453	352	15579	44.3	518	84.9	2845	1900	19148	2632	273	4497	4992	1987	235	190	5917	19033
E10	2.17	34.3	451	217	10905	50.3	444	46.6	1629	1882	17744	1359	232	3691	3942	2320	40.3	244	3647	15714
E11	1.93	50.4	561	1559	16291	10.4	365	18.0	2715	2090	22951	3095	544	3116	4960	2638	80.7	207	6741	20415
E12	2.02	40.4	532	234	11755	50.3	532	20.2	1778	1889	19074	1531	338	2103	2988	1778	146	232	4235	12712
Mean	2.03	40.3	483	492	12239	44.6	493	54.4	1946	1899	18694	1680	244	2676	3346	1507	174	232	3765	14582
Standard deviation	0.10	9.88	51.4	632	4330	22.5	125	23.7	610	196	5808	695	123	1192	1414	636	134	63.5	1660	4563

Table 2
Compilation of pH, electrical conductivity, redox potential, Cl/Br ratio and elemental contaminant analysis in the process water samples.

	pH	EC (mS/cm)	Eh (mV)	Cl/Br	Major elements (mg/L)						Trace elements (μg/L)									
					Cl	Br	F	Fe	P	S	As	Cd	Co	Cr	Cu	Ni	Pb	Sb	U	Zn
Process water in perimeter channel																				
PC1	1.32	54.4	511	50.0	9910	198	1047	239	16504	2038	43484	16022	1061	52904	17984	9851	1174	686	47225	92036
PC2	1.24	62.3	629	40.9	13856	338	1013	263	19628	2430	58671	20939	1395	72213	23614	12814	1289	928	63683	120010
PC3	1.69	61.4	606	69.1	19069	276	851	86.0	21347	1607	68372	20705	1800	40267	19715	14903	597	518	41295	120676
Mean	1.42	59.4	582	53.4	14278	271	970	196	19160	2025	56843	19222	1419	55128	20438	12523	1020	711	50734	110907
Standard deviation	0.24	4.32	62.6	14.4	4594	70.4	105	96.1	2456	411	12544	2774	370	16089	2884	2539	371	206	11599	16346
Process water in central pond																				
WP1	0.38	103	647	39.3	28748	732	724	856	55129	3807	143588	55538	3486	179561	61249	33304	2371	2368	155027	298017
WP2	0.28	102	701	38.1	30992	813	691	975	63362	4053	161474	61859	3861	203440	67621	36928	2586	2626	174721	338497
WP3	0.28	55.4	719	56.4	29565	524	715	897	60093	4211	155595	60864	3918	202749	64330	37509	2419	2609	171689	325982
Mean	0.31	87.1	689	44.6	29769	690	710	909	59528	4024	153553	59421	3755	195250	64400	35914	2459	2534	167146	320832
Standard deviation	0.06	27.4	37.5	10.2	1136	149	17.1	60.2	4145	203	9116	3399	235	13591	3186	2279	113	144	10604	20725

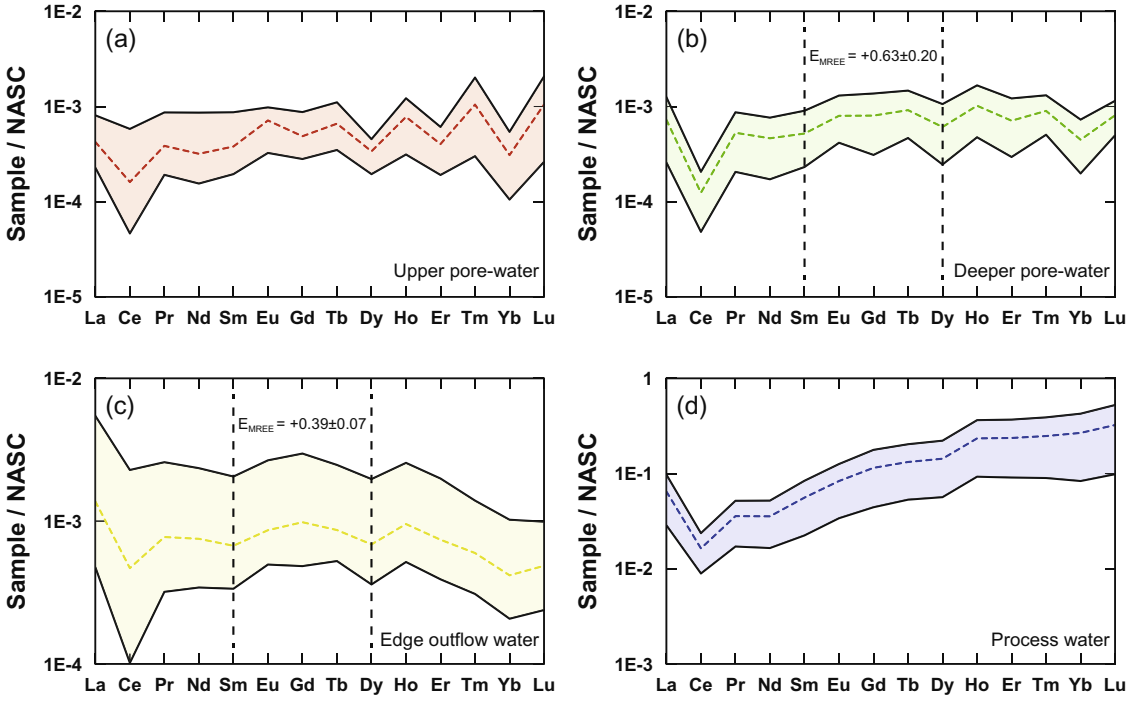

Fig. 5. NASC-normalized REE patterns for (a) upper pore-water, (b) deeper pore-water, (c) edge outflow water and (d) process water. The shadowed area refers to the variability range and dash line to the mean value.

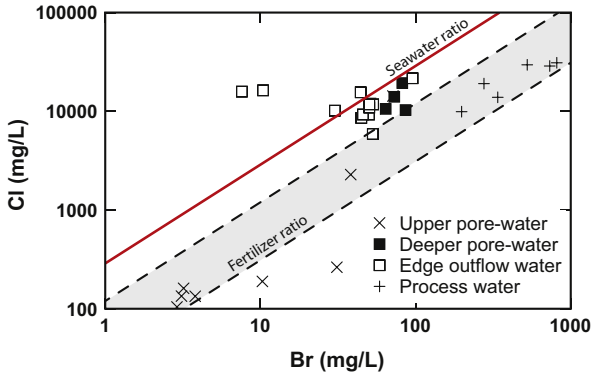

Fig. 6. Chlorine vs. bromine concentrations of the phosphogypsum wastewater solutions. Ratios for seawater and fertilizers derived from Sánchez-Martos et al. (2002) and Otero et al. (2005), respectively.

estuarine water source (Elbaz-Poulichet and Dupuy, 1999; Borrego et al., 2005).

On the other hand, pore-water solutions show the influence of both geochemical environments depending on the depth. Pore-water in shallower zone with high concentrations of S and P in relation to Cl (up to 5.5 m deep) shows NASC-normalized REE patterns with an absence of MREE enrichment and marked negative Ce anomaly, as well as low values of Cl/Br ratio close to those found in the process water (Fig. 6). In contrast, in pore-water in deeper zones with very high Cl concentrations (from 5.5 to 8 m deep), the Cl/Br ratio is similar to that found in the edge outflows, being also close to that of seawater (Fig. 6). These deeper solutions, although with a negative Ce anomaly indicative of phosphogypsum-related pollution, also have a convex-up curvature in MREE similar to that observed in the edge outflows.

REE patterns observed in deeper pore-water and edge outflows with a region of MREE upward convex (Λ-type) are characteristic of environments affected by acid mine drainage (AMD) and, in that sense, the Tinto River is an outstanding example of contamination by this type of acidic water resulting from sulfide oxidation in abandoned mining environments (e.g., Olías et al., 2006; Cánovas et al., 2007; Nieto et al., 2007). Indeed, the Tinto River along with the Odiel and Guadiana Rivers drain one of the largest massive sulfide provinces in the world, i.e. the Iberian Pyrite Belt (IPB), and most of their fluvial basins are affected by AMD. The E_{MREE} values quantified in the current study for deep pore-water solutions and edge outflows of the phosphogypsum stack are congruent with those obtained in Pérez-López et al. (2010b) and Delgado et al. (2012) in these AMD environments.

A comparison of average patterns shows a good agreement of the REE distribution in deeper pore-water and edge outflows with the distribution for the waters of the Tinto River in the estuary (Fig. 7). In the Tinto River estuary, most of AMD-related contaminants precipitate in the mixing zone between river and seawater; however, estuarine water preserves the NASC-normalized pattern enriched in the MREE segment (Elbaz-Poulichet and Dupuy, 1999). The only difference between both REE patterns is the

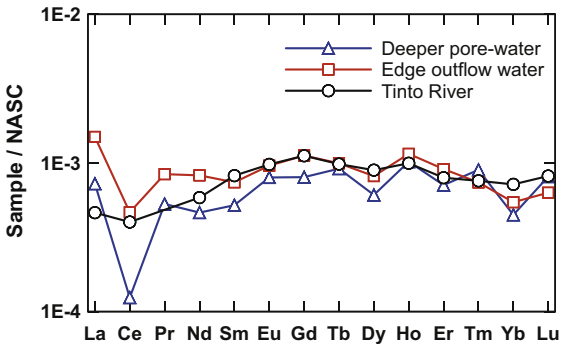

Fig. 7. Comparative diagram showing average NASC-normalized REE patterns for deeper pore-waters and edge outflow waters (see also Fig. 5), and Tinto River estuary (Elbaz-Poulichet and Dupuy, 1999).

marked Ce anomaly existing in deeper pore-water and edge outflows. Therefore, it is possible to suggest that there is a clear connection between deeper pore-water and edge outflows and that water leaching the phosphogypsum-related pollution is of estuarine origin. Such seawater fills the pores in the deepest zones of the phosphogypsum stack, leaches the contaminants, inheriting the Ce anomaly, and transports them through the edge outflows to the Estuary of Huelva.

The existence of seawater in the interstices of the gypsum by-product could be expected in this disposal area. As discussed above, phosphogypsum was transported and disposed of as an aqueous slurry with seawater taken from the Estuary of Huelva; a practice that was discontinued in 1997 when the dumping ceased in zone 3. Likely, this stock of seawater in the pores may be responsible for transporting contaminants from the stack to the estuarine environment. Furthermore, some previous technical reports pointed to the existence of a possible recharge of seawater in deeper pores of the stack. This recharge seems to be a constant source that is produced by overpressure of the phosphogypsum stack on the marsh surface. In fact, it was observed that free water at the contact between stack and marsh was under excessive pressure, causing the water to abruptly rise to the surface during drilling operations (Tragsatec, 2010). It is likely that this over-pressure also causes a continuous upward flow of the relict seawater entrapped in the pores of the salt-marsh sediments that feeds the deeper pore-water of the stack. Upward flow may be encouraged by the distinct difference in permeability between marsh and stack materials. In addition, because of its localization within the estuarine tidal prism, we cannot ignore a possible contribution from seawater intrusion in deeper zones of the phosphogypsum stack during high tidal cycles. Hence, this marsh-seawater source could be the main weathering agent of the phosphogypsum stack, which is congruent with the Cl/Br ratios and REE patterns observed both in deeper pore-water and in edge outflows.

The process of continuous recharge of the pore-water in the deeper zone of the phosphogypsum stack by rising seawater contained in the marsh would be also consistent with the results of the chemical evolution of pore-water in the weathering profile. The concentration of contaminants in the shallowest part is relatively lower likely due to rainwater washout. However, these values increase with depth to 5.0–6.0 m where the maximum concentrations occur. Below this depth, the decrease in concentration observed in most of the contaminants, mainly Co, Ni, Cu, As, Cd, Sb and U, in the last two meters may reflect the effect of dilution by the upward flow of seawater (see red arrows in Fig. 4). It is also possible that some of these elements are removed by sulfide precipitation at the contact with the marsh surface by activity of sulfate-reducing bacteria, which would be consistent with the drop of Eh (see red arrow in Fig. 2c) and the presence of high concentrations of reduced S species in this deeper zone (Pérez-López et al., 2011).

5.2. Implications for restoration of the phosphogypsum stacks

As stated in the introduction, some general guidelines have been already established for the future restoration of zones 2 and 3 of the waste disposal area (Junta de Andalucía, 2009). Our findings suggest some key ideas for the successful restoration of the phosphogypsum stack. Firstly, it would be crucial to remove and treat ex situ the process water. In this regard, we agree with previous guidelines recommended in this priority action due to the extreme acidity and high pollutant load of these solutions dammed on the stack. However, our results of Cl/Br ratios and REE patterns show that there is not an obvious chemical connection, or at least extremely weak, between process water and edge outflows reaching the estuary, unlike what was indicated in the previous restoration report. Indeed, removal of process water and covering the stack surface with natural soil likely would not lead to the cessation of edge outflows. The main origin of these edge outflows appears to be continuous recharge of relict seawater contained in the pores of the underlying salt-marsh flowing upward due to overpressure of the marsh by the phosphogypsum stack.

Secondly, the next action would be to cover the stack with an impermeable barrier. Although edge outflows are of marine origin and there is no chemical connection of these solutions with other weathering agents, we do not have data to rule out a possible hydraulic connection between meteoric water infiltration, deeper pore-water and tidal water level. In fact, deep pore-water circulation could be promoted by hydraulic pressure of the infiltrating rainwater. Therefore, the covering of the stack must be of natural soil but with some type of waterproof barrier. Finally, we propose collecting edge outflows and treating them, as was also pointed out by the previous guidelines. Since edge flow could only be avoided with an insulating bottom cover to prevent access of seawater from the marsh, which would be technically not viable, we strongly recommend continuous monitoring of edge outflows and subsequent channeling to a passive treatment system for acidic waters (see for instance Macías et al., 2012) before discharge to the Estuary of Huelva.

The leaching of phosphogypsum by deep seawater intrusion and the use of waterproof barriers in the upper covering were not taken into consideration in previously restored zones 1 and 4; therefore, it is strongly advisable to check for the existence of edge outflows discharging directly into the estuary in both zones. Supposedly, the currently active perimeter channels collect the leachates of zone 2; however, outer channels of this zone are not on the edge but 2 m height above the marsh level. Thus, it is also strongly recommend to check for possible edge outflows in this zone of the stack. The recommendations suggested by this study should be considered for both the restoration of zones 2 and 3 and the improvement of the previous restoration actions in zones 1 and 4 of the phosphogypsum stack. Using Cl/Br ratios and REE patterns could be extremely promising and provide useful information for managers to use in identifying, characterizing, and assessing other environmental systems globally threatened by wastewater runoff from phosphogypsum stacks.

6. Conclusions

Effectively retiring a phosphogypsum stack requires knowledge of the main processes controlling the weathering and release of contaminants to the surrounding environment. In the Estuary of Huelva, a retired phosphogypsum stack derived from phosphate fertilizer manufacturing rests on salt-marshes of the Tinto River (SW Spain). This waste by-product consists mainly of gypsum; however, high concentrations of acidity and mobile contaminants are present in the solutions contained in the stack, i.e. process water in a reservoir on the surface and interstitial pore-water. Moreover, waterlogging at the contact between the phosphogypsum stack and the surface of the marsh causes a lateral groundwater flow that emerges at the edge of the stack, known as edge outflow, and that transports contaminants to the estuary. Based on rare earth elements and Cl/Br ratios as geochemical tracers, two clearly distinct environments can be distinguished in the present study. On the one hand, process water has typical characteristics of phosphate fertilizer and phosphogypsum, with NASC-normalized REE patterns strongly enriched in HREE. Whereas, on the other hand, deep pore-waters and edge outflows have a characteristic fingerprint that points to the acid mine drainage-impacted Tinto River, with NASC-normalized REE patterns showing an enrichment or convex-up curvature in the MREE segment as

well as Cl/Br ratios indicative of seawater. This distinction rules out process water as the source for edge outflows reaching the estuary by infiltration through porous media. The main vector of contaminants to the estuary is relic seawater that was used to deposit phosphogypsum as a slurry in the stack and that seems to be recharged by an upward flow from the salt-marsh by overpressuring. This new insight of the weathering process should substantially change the future plans for restoration of the phosphogypsum stack and suggests improvements in the preliminary mitigation actions already taken in some of the zones of the disposal area.

Acknowledgements

This work was supported by the Government of Andalusia through the research project 'Phosphogypsum: from the environmental assessment as a waste to its revaluation as a resource (P12-RNM-2260)'. R. Pérez-López also thanks the Spanish Ministry of Science and Innovation and the 'Ramón y Cajal Subprogramme' (MICINN-RYC 2011). The analytical assistance of María Jesús Vílchez, María Beltrán and Laura González from the CIDERTA Research Institute of the University of Huelva is gratefully acknowledged. We would also like to thank Dr. Laurent Charlet (Editor-in-Chief) and two anonymous reviewers for the support and comments that significantly improved the quality of the original paper. This is a publication from CEIMAR Publication series.

Appendix A. Supplementary material

Supplementary data associated with this article can be found, in the online version, at http://dx.doi.org/10.1016/j.jhydrol.2015.08.056.

References

Bolívar, J.P., García-Tenorio, R., García-León, M., 1996. On the fractionation of natural radioactivity in the production of phosphoric acid by the wet acid method. J. Radional. Nucl. Chem. 214, 77–78.

Bolívar, J.P., García-Tenorio, R., Vaca, F., 2000. Radioecological study of an estuarine system located in the South of Spain. Water Res. 34, 2941–2950.

Bolívar, J.P., García-Tenorio, R., Más, J.L., Vaca, F., 2002. Radioactive impact in sediments from an estuarine system affected by industrial waste releases. Environ. Int. 27, 639–645.

Bolívar, J.P., Martín, J.E., García-Tenorio, R., Pérez-Moreno, J.P., Mas, J.L., 2009. Behaviour and fluxes of natural radionuclides in the production process of a phosphoric acid plant. Appl. Radiat. Isotopes 67, 345–356.

Borrego, J., López-González, N., Carro, B., Lozano-Soria, O., 2005. Geochemistry of rare earth elements in Holocene sediments of an acidic estuary: environmental markers (Tinto river estuary, Southwestern Spain). J. Geochem. Explor. 86, 119–129.

Cánovas, C.R., Olías, M., Nieto, J.M., Sarmiento, A.M., Cerón, J.C., 2007. Hydrogeochemical characteristics of the Tinto and Odiel Rivers (SW Spain). Factors controlling metal contents. Sci. Total Environ. 373, 363–382.

Castillo, J., Pérez-López, R., Sarmiento, A.M., Nieto, J.M., 2012. Evaluation of organic substrates to enhance the sulfate-reducing activity in phosphogypsum. Sci. Total Environ. 439, 106–113.

Delgado, J., Pérez-López, R., Galván, L., Nieto, J.M., Borski, T., 2012. Enrichment of rare earth elements as environmental tracers of contamination by acid mine drainage in salt marshes: a new perspective. Mar. Pollut. Bull. 64, 1799–1808.

Elbaz-Poulichet, F., Dupuy, C., 1999. Behaviors of rare earth elements at the freshwater-seawater interface of two acid mine rivers: the Tinto and Odiel (Andalucia, Spain). Appl. Geochem. 14, 1063–1072.

Gázquez, M.J., Mantero, J., Mosqueda, F., Bolívar, J.P., García-Tenorio, R., 2014. Radioactive characterization of leachates and efflorescences in the neighbouring areas of a phosphogypsum disposal site as a preliminary step before its restoration. J. Environ. Radioact. 137, 79–87.

Göb, S., Loges, A., Nolde, N., Bau, M., Jacob, D.E., Markl, G., 2013. Major and trace element compositions (including REE) of mineral, thermal, mine and surface waters in SW Germany and implications for water-rock interaction. Appl. Geochem. 33, 127–152.

Grande, J.A., Borrego, J., Morales, J.A., 2000. A study of heavy metal pollution in the Tinto-Odiel estuary in southwestern Spain using factor analysis. Environ. Geol. 39, 1095–1101.

Gromet, L.P., Dymek, R.F., Haskin, L.A., Korotev, R.L., 1984. The "North American shale composite": its compilation, major and trace element characteristics. Geochim. Cosmochim. Acta 48, 2469–2482.

Junta de Andalucía, 2009. Prescripciones prioritarias para la redacción del proyecto de recuperación de las balsas de fosfoyesos en las marismas de Huelva. Technical report, Huelva, Spain, p. 18. Available from <http://www.juntadeandalucia.es/medioambiente/portal_web/web/temas_ambientales/vigilancia_y_prevencion_ambiental/planificacion/plan_calidad_huelva_2010_15/criterios_directrices_recuperacion_2.pdf>.

Macías, F., Caraballo, M.A., Rötting, T.S., Pérez-López, R., Nieto, J.M., Ayora, C., 2012. From highly polluted Zn-rich acid mine drainage to non-metallic waters: implementation of a multi-step alkaline passive treatment system to remediate metal pollution. Sci. Total Environ. 433, 323–330.

Martínez-Aguirre, A., García-León, M., Gascó, C., Travesí, A., 1996. Anthropogenic emissions of 210Po, 210Pb and 226Ra in an estuarine environment. J. Radioanal. Nucl. Ch. 207, 357–367.

McArthur, J.M., Walsh, J.N., 1985. Rare earth geochemistry of phosphorites. Chem. Geol. 47, 191–220.

Nieto, J.M., Sarmiento, A.M., Olías, M., Cánovas, C.R., Riba, I., Kalman, J., Delvalls, T.A., 2007. Acid mine drainage pollution in the Tinto and Odiel rivers (Iberian Pyrite Belt, SW Spain) and bioavailability of the transported metals to the Huelva Estuary. Environ. Int. 33, 445–455.

Noack, C.W., Dzombak, D.A., Karamalidis, A.K., 2014. Rare earth element distributions and trends in natural waters with a focus on groundwater. Environ. Sci. Technol. 48, 4317–4326.

Nordstrom, D.K., Wilde, F.D., 1998. Reduction-oxidation potential (electrode method), in: National field manual for the collection of water quality data. U. S. Geological Survey Techniques of Water-Resources Investigations, Book 9, chapter 6.5.

Olías, M., Cánovas, C.R., Nieto, J.M., Sarmiento, A.M., 2006. Evaluation of the dissolved contaminant load transported by the Tinto and Odiel rivers (South West Spain). Appl. Geochem. 21, 1733–1749.

OSPAR, 2002. Discharges of radioactive substances into the maritime area by non-nuclear industry. Radioactive Substances Series. Publication No. 161. OSPAR Commission, London, 60 p.

OSPAR, 2007. PARCOM Recommendation 91/4 on Radioactive Discharges: Spanish Implementation Report. Radioactive Substances Series. Publication No. 342. OSPAR Commission, London, 49 p.

Otero, N., Vitòria, L., Soler, A., Canals, A., 2005. Fertiliser characterisation: major, trace and rare earth elements. Appl. Geochem. 20, 1473–1488.

Parkhurst, D.L., Appelo, C.A.J., 2005. PHREEQC-2 version 2.12: a hydrochemical transport model. <http://wwwbrr.cr.usgs.gov>.

Pérez-López, R., Álvarez-Valero, A., Nieto, J.M., 2007. Changes in mobility of toxic elements during the production of phosphoric acid in the fertilizer industry of Huelva (SW Spain) and environmental impact of phosphogypsum wastes. J. Hazard. Mater. 148, 745–750.

Pérez-López, R., Nieto, J.M., López-Coto, I., Aguado, J.L., Bolívar, J.P., 2010a. Dynamics of contaminants in phosphogypsum of the fertilizer industry of Huelva (SW Spain): From phosphate rock ore to the environment. Appl. Geochem. 25, 705–715.

Pérez-López, R., Delgado, J., Nieto, J.M., Márquez-García, B., 2010b. Rare earth element geochemistry of sulphide weathering in the São Domingos mine area (Iberian Pyrite Belt): a proxy for fluid-rock interaction and ancient mining pollution. Chem. Geol. 276, 29–40.

Pérez-López, R., Castillo, J., Sarmiento, A.M., Nieto, J.M., 2011. Assessment of phosphogypsum impact on the salt-marshes of the Tinto river (SW Spain): role of natural attenuation processes. Mar. Pollut. Bull. 62, 2787–2796.

Rodier, J., 1996. L'analyse de l'eau: eaux naturelles, eaux résiduaires, eaux de mer, 8th ed. Dunod, Paris, 1383p.

Rutherford, P.M., Dudas, M.J., Samek, R.A., 1994. Environmental impacts of phosphogypsum. Sci. Total Environ. 149, 1–38.

Sánchez-Martos, F., Pulido-Bosch, A., Molina-Sánchez, L., Vallejos-Izquierdo, A., 2002. Identification of the origin of salinization in groundwater using minor ions (Lower Andarax, Southeast Spain). Sci. Total Environ. 297, 43–58.

Stober, I., Bucher, K., 1999. Origin of salinity of deep groundwater in crystalline rocks. Terra Nova 11, 181–185.

Tayibi, H., Choura, M., López, F.A., Alguacil, F.J., López-Delgado, A., 2009. Environmental impact and management of phosphogypsum. J. Environ. Manage. 90, 2377–2386.

Tragsatec, 2010. Servicio para la recuperación de las balsas de fosfoyesos en las Marismas de Huelva. Fase de diagnóstico y propuesta de regeneración. Technical report ref. TEC0002159, España.

Villa, M., Mosqueda, F., Hurtado, S., Mantero, J., Manjón, G., Periañez, R., Vaca, F., García-Tenorio, R., 2009. Contamination and restoration of an estuary affected by phosphogypsum releases. Sci. Total Environ. 408, 69–77.

Science of the Total Environment 553 (2016) 42–51

Contents lists available at ScienceDirect

Science of the Total Environment

journal homepage: www.elsevier.com/locate/scitotenv

Pollutant flows from a phosphogypsum disposal area to an estuarine environment: An insight from geochemical signatures

Rafael Pérez-López [a,*], Francisco Macías [a], Carlos Ruiz Cánovas [a], Aguasanta Miguel Sarmiento [b], Silvia María Pérez-Moreno [c]

[a] Department of Geology, University of Huelva, Campus 'El Carmen', 21071 Huelva, Spain
[b] Department of Geodynamics and Palaeontology, University of Huelva, Campus 'El Carmen', 21071 Huelva, Spain
[c] Department of Applied Physics, University of Huelva, Campus 'El Carmen', 21071 Huelva, Spain

HIGHLIGHTS

- Acidity and contaminants from phosphogypsum leaching are released to an estuary.
- Already-restored zones act as a pollution source just as unrestored zones.
- Cl/Br ratios and REE patterns were suitable to assess the restoration inefficiency.
- Changes in the remediation strategies of the phosphogypsum stack are hence necessary.

GRAPHICAL ABSTRACT

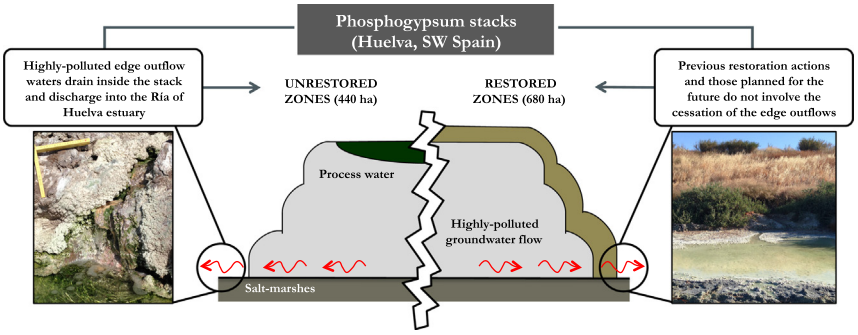

ARTICLE INFO

Article history:
Received 2 December 2015
Received in revised form 10 February 2016
Accepted 10 February 2016
Available online xxxx

Editor: D. Barcelo

Keywords:
Phosphogypsum stack
Acid leachates
Contaminant
Restoration
Estuary of Huelva

ABSTRACT

Phosphogypsum wastes from phosphate fertilizer industries are stockpiled in stacks with high contamination potential. An assessment of the environmental impact, including the use of geochemical tracers such as rare earth elements (REE) and Cl/Br ratios, was carried out in the phosphogypsum stack located at the Estuary of Huelva (SW Spain). Inside the pile, highly polluted acid pore-waters flows up to the edge of the stack, emerging as small fluvial courses, known as edge outflows, which discharge directly into the estuary. The disposal area is divided into four zones; two unrestored zones with surface ponds of industrial process water and two a priori already-restored zones. However, an extensive sampling of edge outflows conducted in the perimeter of the four zones demonstrates the high potential of contamination of the whole stack, including those zones that were supposedly restored. These solutions are characterized by a pH of 1.9 and concentrations of 6100 mg/L for P, 1970 mg/L for S, 600 mg/L for F, 200 mg/L for NH_4^+, 100 mg/L for Fe, 10–30 mg/L for Zn, As and U, and 1–10 mg/L for Cr, Cu and Cd. Preliminary restoration actions and those planned for the future prioritize removal of ponded process water and cover of the phosphogypsum with artificial topsoil. These actions presuppose that the ponded process water percolates through the porous medium towards the edge up to reach the estuary. However, geochemical tracers rule out this connection and point to an estuarine origin for these leachates, suggesting a possible tidal-induced leaching of the waste pile in depth. These findings would explain the ineffectiveness of preliminary restoration measures and should be considered for the development of new action plans.

* Corresponding author.
E-mail address: rafael.perez@dgeo.uhu.es (R. Pérez-López).

http://dx.doi.org/10.1016/j.scitotenv.2016.02.070
0048-9697/

1. Introduction

The production of phosphoric acid (H_3PO_4) by fertilizer industry following the wet chemical digestion of phosphate rock (fluorapatite, $Ca_5(PO_4)_3F$) with sulfuric acid (H_2SO_4) generates huge amounts of a waste known as phosphogypsum (gypsum, $CaSO_4 \cdot 2H_2O$). The overall reaction is (Eq. (1)):

$$Ca_5(PO_4)_3F + 5H_2SO_4 + 10H_2O \rightarrow 3H_3PO_4 + 5CaSO_4 \cdot 2H_2O + HF + \text{Heat.} \quad (1)$$

The phosphate rock is commonly concentrated by flotation prior to phosphoric acid manufacturing. The flotation process is enhanced by the addition of chemical reagents such as ammonium hydroxide or amine. The final phosphogypsum is soaked with the chemical reactants used and the products obtained in the industrial process, which leads to the existence of interstitial acidic solutions containing high concentrations of mainly phosphate, but also of sulfate, fluoride and often ammonium (Lottermoser, 2010). Phosphate corresponds to the fraction of residual phosphoric acid obtained as product that cannot be effectively separated in the industrial process for sale. On the other hand, phosphate rocks also contain metal and radionuclides as impurities that are released during the industrial process and finally concentrated in the reaction products (Rutherford et al., 1994). Most of toxic elements, including U and Th, are transferred from the phosphate rock to the phosphoric acid (Bolívar et al., 2009; Pérez-López et al., 2010). Thus, the residual phosphoric acid trapped in the interstices of phosphogypsum particles explains the acidic nature and the high contaminant release potential under leaching conditions of this waste. Moreover, these impurities limit the commercial use of the phosphogypsum.

Phosphogypsum is transported and dumped as an aqueous slurry in huge, aboveground stockpiles, without any prior treatment, known as stacks. These stacks are often vulnerable to weathering, and contaminant leaching can occur and cause serious environmental damage (see review in Tayibi et al., 2009). Moreover, contaminants in phosphogypsum-affected environments can be transferred finally to living beings (Boryło et al., 2013). Most of dumping areas are located in coastal regions close to phosphoric acid production plants. Some examples of potential leaching from phosphogypsum stacks to coastal environments are described in detail in the Santos-Cubatão estuarine system (Brazil; Sanders et al., 2013), in the Lebanese coast (El Samad et al., 2014) and in the Gulf of Gabes (Tunisia; El Zrelli et al., 2016), among many others.

Of particular interest is the case of the phosphogypsum stack located at the estuary formed by the confluence of the Tinto and Odiel Rivers, the so-called Ría of Huelva estuary (SW Spain). Since the beginning of the fertilizer production, phosphogypsum was transported and deposited over the Tinto River salt-marshes in several decantation zones. In this environment, phosphogypsum deposition may be influenced by physical and geochemical processes associated with estuarine systems (Sanders et al., 2013). The presence of the residual phosphoric acid trapped in the interstices of the gypsum particles makes the piles behave as an unconfined aquifer, clearly distinguishing an unsaturated zone and a saturated zone with contaminated groundwater flow (Pérez-López et al., 2011). The piles are directly settled on bare marshland soils without any type of isolation, which act as an impermeable barrier that withholds groundwater in depth and forces the water to flow laterally. When the groundwater reaches the edge of the stack, polluted water emerges forming superficial drainages, known as edge outflows, which release high load of contaminants into the estuary. Therefore, the leakages from the phosphogypsum stacks pose a potential risk to the ecological receptors (Bolívar et al., 2002; Borrego et al., 2013). Nevertheless, the Ría of Huelva also receives huge amounts of contaminants through the Tinto and Odiel Rivers. Both rivers are intensively affected by acid mine drainage from sulfide oxidation in the more than one hundred abandoned mines in the Iberian Pyrite Belt (Olías et al., 2006).

Preliminary restoration actions were carried out for some disposal modules of the phosphogypsum stack by following guidelines included in a report from the regional government (Junta de Andalucía, 2009). The same restoration guidelines are planned to be performed in unrestored zones. As far as we know, most studies characterizing the contamination from edge outflows focus mainly on one of the unrestored zone of the phosphogypsum stack (e.g. Gázquez et al., 2014; Martínez-Sánchez et al., 2014; Pérez-López et al., 2015). The research reported here expands the preliminary studies to the rest of the unrestored stack and to those zones that have already been supposedly restored. Thus, the main objective of this study is to assess the efficiency of the previous restoration measures since it is of paramount importance to optimize future restoration criteria for the whole phosphogypsum stack. The obtained results will provide useful information for managers to use in assessing other environmental systems globally threatened by leakages from phosphogypsum stacks, particularly in coastal regions.

2. Material and methods

2.1. Study area

Phosphogypsum was produced by several phosphate fertilizer plants and deposited over Tinto River salt-marshes from 1968 to 2010, when the dumping ceased under a decision of the Spanish National Court. These fertilizer facilities commonly imported phosphate ore from Morocco to manufacture the phosphoric acid. The total amount of stockpiled phosphogypsum is around 100 Mt (approx. 1200 ha of surface) at <300 m of the Huelva city (Fig. 1). The stack lies within the tidal prism of the Ría of Huelva, which ranges from 37 to 82 hm^3 during a tidal half-cycle (6 h) (Grande et al., 2000). The climate of the area is Mediterranean with annual average precipitation of 490 mm, mainly during autumn and winter, and temperature of 19.2 °C (1990–2010; from National Meteorology Institute). From 1968 to 1997, phosphogypsum was transported using seawater to several decantation zones that reached up to 10 m in height on average. After decantation, seawater used for transport along with the remaining 20% of phosphogypsum was directly released to the estuary without any treatment despite showing high acidity and pollutant concentrations. The enforcement of more strict environmental regulations in 1997 compelled the factory to avoid any direct discharge to the estuary according to the OSPAR convention (OSPAR, 2002; 2007). The new waste management plan proposed two main measures to fulfill this goal; on the one hand, the deposit of phosphogypsum in a large pyramidal pile over a single, previously-used zone; and on the other hand, the implementation of a closed-circuit system for transport and settling of phosphogypsum using freshwater instead of seawater. The closed-circuit system, also known as process water circuit, included the existence of ponds to store water in the central part of the stacks and different perimeter channels collecting all lixiviates from the piles and returning them to the closed-loop. Presently, the successive changes in environmental regulations have led to the existence of four different zones or modules within the stack (Fig. 1):

- Zone 1 (35 Mt; 400 ha and 2–3 m in height) was closed and restored in 1992 by adding a 25 cm layer of natural soil and vegetation over the bare phosphogypsum. Phosphogypsum is not visually observed and there are not perimeter channels or process water ponded on the top part.
- Zone 2 (25 Mt; 240 ha and up to 30 m in height) is the large pyramidal pile of phosphogypsum deposited after 1997 with the new waste management plan. This zone has been active until discharge stopped in 2010. Restoration measures have not been adopted and, hence, this module is currently exposed to weathering. Ponds with process

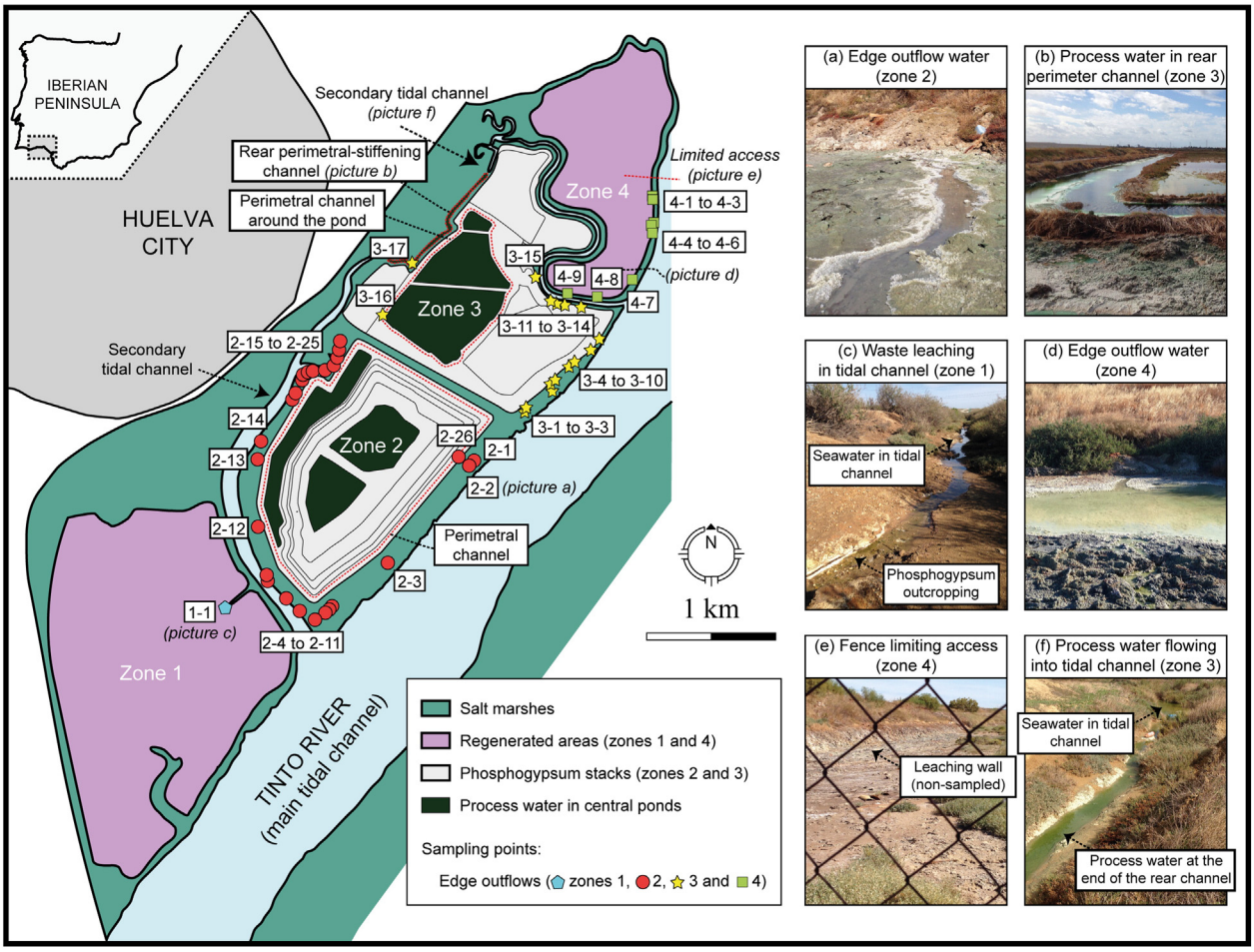

Fig. 1. Location map of the phosphogypsum disposal piles on the salt-marshes of the Tinto River and sampling points of edge outflows. Some field pictures are also shown (see explanation in the text). Additional geographic details are available as Supplemental data.

water are located on the surface, which are surrounded by a network of perimeter channels in order to collect the acidic lixiviates. According to the restoration guidelines of the regional government (Junta de Andalucía, 2009), these channels collect most of infiltrating waters and, although the existence of some diffuse drainage cannot be dismissed, the impact of this zone on the estuarine environment is supposedly minimal.

- Zone 3 (15 Mt; 200 ha and 8–12 m in height) is a sector where phosphogypsum was disposed until 1997. Since then, this zone has been subject to weathering and no preventive measures have been adopted to minimize the environmental impact (e.g. covers to avoid leaching). In fact, numerous edge outflows draining the pile and reaching the estuary have been previously reported (e.g. Pérez-López et al., 2015). For this reason, this zone has been precisely the focus of previous studies. This zone has been used since 1997 to store process water in surface ponds.
- Zone 4 (30 Mt; 280 ha and 8–10 m in height) is a sector where phosphogypsum was also disposed of before 1997. This zone has been also restored by the addition of a cover over the bare phosphogypsum to prevent weathering. This cover is more complex than that of zone 1 and comprises the following layers (in ascending order): a 1 m layer of building wastes, a 2 m layer of theoretically inert industrial wastes and 30–50 cm layer of topsoil. As in zone 1, zone 4 has not ponded process water and the phosphogypsum is not visible.

The Spanish National Court obliged the fertilizer factory to develop an environmental restoration plan of the affected marshland. This plan was presented in 2014 and is based on the removal of process water ponds and the cover of zones 2 and 3 to limit water infiltration. These measures are in agreement with the previous guidelines prioritized by the regional government, which state that the infiltration of process water stored in the ponds through the porous media and its subsequent emergence as edge outflows is the main pathway of pollutant dispersion to the estuary (Junta de Andalucía, 2009). This action plan omits any measure in zones 1 and 4 based on the assumption that the previous restoration (elimination of process water and the installation of covers) successfully eliminated all discharges into the estuary. However, Pérez-López et al. (2015) recently studied by geochemical tracers the weathering process in the zone 3 of the phosphogypsum stack. The main results of this work strongly disagree with the pollutant dispersion pathway assumed by both the regional government and the fertilizer factory, which is the base of the restoration plan. These authors reveal the absence of chemical connection between process water ponded on the surface of the stack and edge outflows reaching the estuary, at least for zone 3. On this basis it is essential to verify the current state of zone 2 as potential source of pollutants into the estuary, as well as to compare the unrestored zones 2 and 3 with already-restored zones 1 and 4.

2.2. Sampling and analysis of edge outflow water

The perimeter of the four zones of the phosphogypsum stack was inspected in May–June 2014 in order to locate possible edge outflows and collect the corresponding samples (Fig. 1). In addition, some samples of process water contained in perimeter channels of zones 2 and

3 were taken. For a better understanding of the study area, localization of all sampling points can be seen by Google Earth™ using the Keyhole Markup Language (KML) file available as electronic supplement. The pH, redox potential and electrical conductivity (EC) were measured in the field using a portable Multiparametric Crison MM 40 + equipment. Measured redox potential was referenced to the standard hydrogen electrode (Eh), as proposed by Nordstrom and Wilde (1998). Water samples were filtered with 0.45 μm membrane filters and divided into three aliquots; one unacidified for anion and ammonium determination, one acidified with HNO_3 to pH < 1 for major and trace element analysis, and the other one was buffered to pH 4.5 with an ammonium acetate/acetic acid buffer and Fe(II) complexed with a phenantroline solution for Fe(II)/(III) determination according to the method outlined by Rodier (1996). As long as possible, the float method was used to estimate the flow rate at the sampling points.

Concentrations of anions (Br, Cl and F) and ammonium in all the unacidified samples were analyzed by high performance liquid chromatography (HPLC) using a Metrohm 883 basic ion chromatograph (IC) plus equipped with Metrosep columns. The acidified samples were analyzed using Inductively Coupled Plasma-Atomic Emission Spectroscopy (ICP-AES; Jobin Yvon Ultima 2) for determination of major elements (Al, Ca, Fe, K, Mg, Mn, Na, P and S) and Inductively Coupled Plasma-Mass Spectroscopy (ICP-MS; Agilent 7700) for trace elements (As, Cd, Co, Cr, Cu, Ni, Pb, Sb, U, Zn and REE). Detection limits were: 0.2 mg/L for S; 0.1 mg/L for Na; 0.05 mg/L for Fe, K and Mg; 0.02 mg/L for Al, Ca, Mn and P; and 0.1 μg/L for trace elements. All analyzes were performed in the laboratories of the University of Huelva. Three laboratory standards, prepared with concentrations within the range of the samples, were analyzed with every 10 samples to check for accuracy. Furthermore, dilutions were performed to ensure that the concentration of the samples was within the concentration range of the standards. Blank solutions with the same acid matrix as the samples were also analyzed. The average measurement error was <5%. Determination of Fe (II) and total Fe (following reduction with hydroxylamine hydrochloride) in the solutions was immediately undertaken in the laboratory on the same day of the sampling by colorimetry at 510 nm using a SHIMADZU UVmini-1240 spectrophotometer. The detection limit was 0.3 mg/L and measurement error was better than 5%; Fe(III) was calculated as the difference between total Fe and Fe(II).

Rare earth elements (REE) have been widely used as tracers of geochemical processes (see review in Noack et al., 2014; and references therein). For the study of earth surface processes, such as weathering, REE concentrations are often normalized using the North-American Shale Composite (NASC) values (Gromet et al., 1984). Moreover, in this study the shape of the NASC-normalized REE patterns was described using the NASC-normalized ratios, $(MREE/LREE)_{NASC}$ and $(HREE/MREE)_{NASC}$, which were calculated as the average of all permutations of those inter-element ratios. The LREE (light-REE) included in the ratio calculation were La, Pr, Nd, and Sm; the MREE (middle-REE) were Gd, Tb, and Dy; and the HREE (heavy-REE) were Ho, Er, Tm, Yb, and Lu. Both Ce and Eu were excluded from calculation due to their anomalous redox activity. Stolpe et al. (2013) proposed these normalized ratios to avoid using a single representative of a whole group, which would be not advisable for the interpretation of REE patterns in the case of exclusive fractionation affecting only one of the elements in the ratio.

3. Results

3.1. Elemental contaminant concentrations

Leachate samples were collected at fifty-three sites around the perimeter of the four zones of the phosphogypsum stack, including those already-restored zones where supposedly leakages should not occur (Fig. 1). Detailed hydrogeochemical information for these samples is compiled in Table S1 (see electronic supplement). All samples have similar characteristics; i.e. extreme acidity and high EC values, which correlate with high dissolved concentrations of anions and cations, some of them potentially toxic. Of the total sampling points, fifty samples strictly correspond to edge outflows whose average values of pH, EC and major anions and cations for each zone of the stack can be seen in Figs. 2 and 3. The remaining three samples (2–26, 3–16 and 3–17) are from solutions contained in perimeter channels of zones 2 and 3 and their chemical composition is detailed in Table S1. All edge outflow solutions and some samples of the perimeter channels discharge to the estuarine waters directly or indirectly through secondary tidal channels. The measured flow rates range from 0.1 to 1.5 L/s with an average value of 0.2 L/s. In the following, the geochemical characteristics of the edge outflows of the areas that are being considered for immediate restoration (zones 2 and 3) will be compared with those observed in previously-restored areas (zones 1 and 4).

3.1.1. Unrestored zones

Twenty-six acid leachates were collected at zone 2 of the phosphogypsum stack (Fig. 1; see example in picture (a)). Of these leachates, twenty-five samples strictly correspond to edge outflows reaching the estuarine environment (samples 2–1 to 2–25; Table S1). These edge leachates are by far more acidic and polluting than those found in other zones of the stack; with the lowest pH values and the significantly highest concentrations of P, F, NH_4^+ and metallic impurities such as Fe (mainly as Fe(II)), Zn, As, U, Cr, and minor contents of other elements such as Cd, Co, Cu, Ni and Pb (Figs. 2 and 3). On the contrary, edge outflows of this zone show lower concentrations of Cl and S than the rest (Fig. 2). On the other hand, the sample 2–26 corresponds to acid water of the outermost perimeter channel of zone 2 (Fig. 1), which presents acidity and element concentrations that are slightly higher but within the same order of magnitude as the remaining edge outflow samples of this zone (Table S1). Chloride/Br ratios can provide information on the origin of the water (Davis et al., 1998). In this sense, both edge outflows and channeled water of zone 2 have Cl/Br mass ratio values of 143 ± 42.4, on mean (±standard deviation), and 59, respectively (Table S1).

Seventeen acid leachates were collected at zone 3 of the phosphogypsum stack (Fig. 1), of which fifteen samples are point edge outflows discharging into the estuarine environment (samples 3–1 to 3–15; Table S1). In the edge outflows of zone 3, average values of pH are slightly higher and concentrations of P, F, NH_4^+ and metallic impurities are significantly lower than in those of zone 2 (Figs. 2 and 3). Instead, these solutions have higher concentrations of Cl and, to a lesser extent, S (Fig. 2). As shown in Fig. 1, this zone has a perimeter channel exclusively around the ponded process water and another perimeter-stiffening channel at the back of the stack, where samples 3–16 and 3–17 were taken, respectively (see picture (b) in Fig. 1). Acidity and contaminant level in this channeled water is much higher than in the edge outflows (even than in those of zone 2) (Table S1). Chloride/Br ratios of most edge outflow solutions of zone 3 are higher (mean of 300 ± 118) than that of the rear perimeter channel (180) and, especially, than that of the perimeter channel surrounding the process water ponded on the surface (40.3) (Table S1).

3.1.2. Already-restored zones

Zones 1 and 4 of the phosphogypsum stack are characterized by having no water in ponds or perimeter channels. One unique acid leachate was found and sampled in zone 1 (Fig. 1; see picture (c)). This sample does not strictly correspond to an edge outflow, but it is likely produced by interaction of seawater with phosphogypsum outcropping in a small tidal channel during the rising tide (sample 1–1; Table S1). After interaction, the resulting solutions during the lowering tide are already acidic. So, because of the cyclic nature of tides, this channel provides a continuous supply of acidity and contaminants to the estuary. Nevertheless, acidity and concentrations of P, NH_4^+, F and other metallic impurities in this tidal channel are significantly lower than in edge outflows

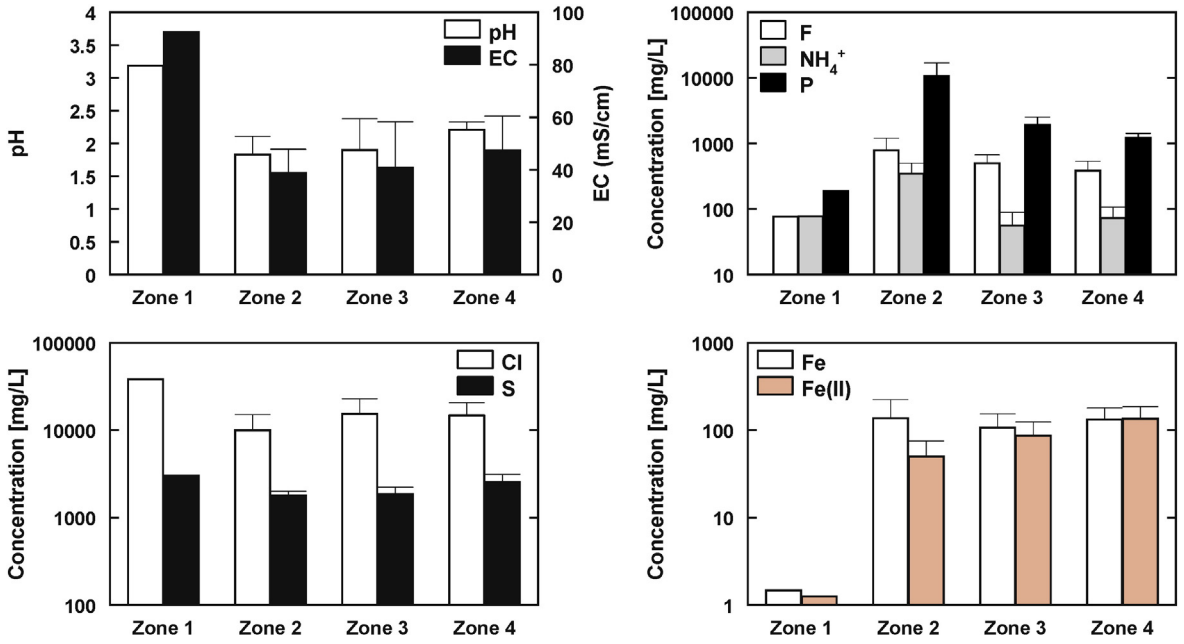

Fig. 2. Values of pH, EC and concentration of major elements (Cl, F, Fe, NH_4^+, P and S) in edge outflows of the four zones of the phosphogypsum stack. Both mean and standard deviation are shown graphically for each zone.

of the other zones of the stack due to the dilution effect exerted by estuarine waters (Figs. 2 and 3).

Finally, zone 4 has acidic and polluting leakages in up to 9 discharging points (Fig. 1; see example in picture (d)). However, sampling could be carried out only in the half of this zone of the stack because a fence restricts the access to the rest. Nevertheless, many edge outflows can be observed at a glance through the fence (see picture (e) in Fig. 1). All collected samples correspond to edge outflows (samples 4–1 to 4–9; Table S1), which also show acidic pH values but slightly higher than in zones 2 and 3. Concentrations of P, F, NH_4^+ and most of metals are close to those observed in zone 3 and often even lower (Figs. 2 and 3). Regarding other elements, concentrations of S in zones 1 and 4 and those of Cl in zone 1 are the highest of all edge outflows sampled in the whole stack (Fig. 2). In addition, Cl/Br mass ratio values of 373 for the leachate of zone 1 and of 195 ± 22.5, on mean, for edge outflows of zone 4 were observed (Table S1).

3.2. Rare earth element concentrations

Concentrations of REE in the leachates of the four zones of the phosphogypsum stack are shown in Table S2 (see electronic supplement). Values of ΣREE as well as the normalized $(HREE/MREE)_{NASC}$ and

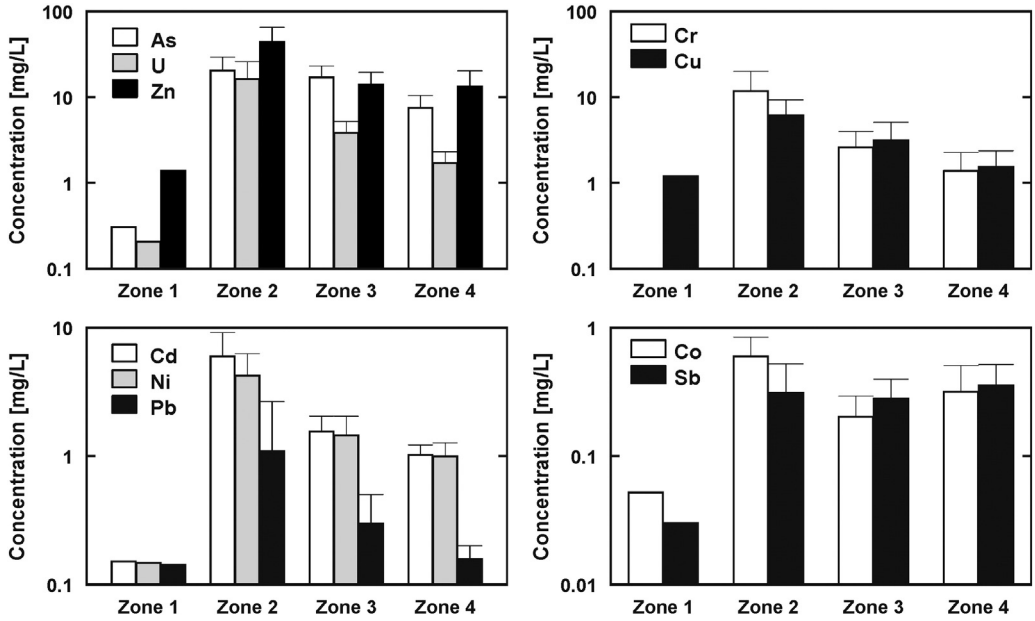

Fig. 3. Concentration of trace elements (As, Cd, Co, Cr, Cu, Ni, Pb, Sb, U and Zn) in edge outflows of the four zones of the phosphogypsum stack. Both mean and standard deviation are shown graphically for each zone.

$(MREE/LREE)_{NASC}$ ratios are also shown in Table S2. Around 30% of samples showed REE (mainly HREE) concentrations close to the detection limit of ICP-MS and, for this reason, they were not considered in the interpretations based on the REE pattern shape.

In the edge outflow samples, the highest ΣREE concentrations are found by far in zone 2 (334 ± 161 μg/L) followed by zone 3 (120 ± 75.2 μg/L) and then by zone 4 (40.0 ± 21.1 μg/L), which is in accordance with the overall trend observed for pollutants. The only sample of zone 1 shows concentrations of most REE below the detection limit. Concerning the water of the perimeter channels, sample 2–26 of zone 2 presents ΣREE values in the same order of magnitude as the edge outflows of this zone (387 μg/L); however, samples 3–16 and 3–17 of zone 3 exhibit concentrations of up to two and one order of magnitude higher (23,700 and 2666 μg/L, respectively) than the remaining samples of the four zones of the stack.

NASC-normalized REE patterns of edge outflows seem to be similar from one zone to another of the phosphogypsum stack (Fig. 4). However, normalized ratios reveal some differences in the REE distribution. In general, edge outflow waters show clearly higher $(MREE/LREE)_{NASC}$ values than unity than those of $(HREE/MREE)_{NASC}$, which are closer to unity (Table S2). These ratios indicate that there is an enrichment of MREE with respect to LREE and a flattening of the pattern in the HREE range. This distribution can be observed specially in zone 2 with mean values of $(MREE/LREE)_{NASC}$ and $(HREE/MREE)_{NASC}$ of 1.73 ± 0.19 and 1.01 ± 0.12, respectively (Fig. 4a). However, mean values of $(MREE/LREE)_{NASC}$ and $(HREE/MREE)_{NASC}$ decrease notably in edge outflows of zone 3 (1.43 ± 0.16 and 0.98 ± 0.11, respectively; Fig. 4b) and, mainly, of zone 4 (1.33 ± 0.04 and 0.83 ± 0.04, respectively; Fig. 4c). In fact, edge outflows of zone 4 have patterns where enrichment of MREE with respect to LREE is observed but there is a slight depletion of HREE with respect to MREE (Fig. 4c).

The acid water from the outer perimeter channel of zone 2, sample 2–26, shows a NASC-normalized REE pattern with identical distribution to that found in the edge outflows of this zone (Fig. 4a), with ratios in the same order of magnitude ($(MREE/LREE)_{NASC}$ = 2.03 and $(HREE/MREE)_{NASC}$ = 0.95) (Table S2). Instead, waters contained in the perimeter channels of zone 3, samples 3–16 and 3–17, exhibit normalized patterns with a slight increase of the enrichment of MREE with respect to LREE ($(MREE/LREE)_{NASC}$ = 2.23 and 2.52, respectively) and, mainly, with a significant enrichment of HREE with respect to MREE ($(HREE/MREE)_{NASC}$ = 1.71 and 1.84, respectively) (Table S2). The strong enrichment in the HREE segment of both samples makes that these solutions have completely different REE patterns in comparison with the rest of samples of the phosphogypsum stack (Fig. 4b). In principle, this difference in the NASC-normalized REE distribution could allow investigation of the possible sources of edge outflow waters discharging into the estuary.

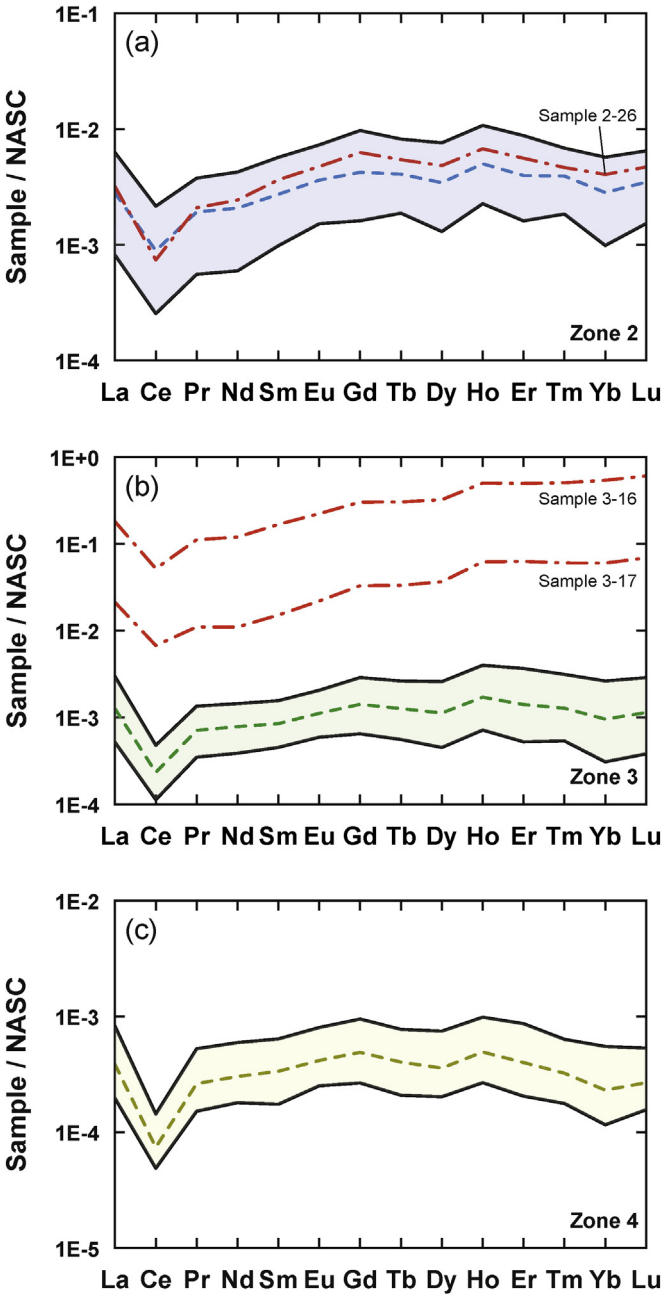

Fig. 4. NASC-normalized REE patterns for edge outflows of (a) zone 2, (b) zone 3 and (c) zone 4 of the phosphogypsum stack; shadowed area = variability range and dash line = mean value. Red dashed-dot lines refer to the normalized patterns for the three samples of perimeter channels.

4. Discussion

4.1. Source of edge outflow waters

The origin of all polluting solutions related to the phosphogypsum stack located at the Ría of Huelva can be traced using geochemical indicators such as NASC-normalized REE patterns and Cl/Br ratios Pérez-López et al. (2015). In this scenario, it is possible to identify two clearly contrasting geochemical environments. On the one hand, Tinto River estuary waters are characterized by REE patterns with an up-convex curvature in the MREE segment, which results in an enrichment of MREE with respect to both LREE ($(MREE/LREE)_{NASC}$ = 1.60) and HREE ($(HREE/MREE)_{NASC}$ = 0.83), according to the pattern reported by Elbaz-Poulichet and Dupuy (1999). In addition, estuarine water has Cl/Br mass ratios close to 290 (obtained from the Cl and Br concentrations found in Barba-Brioso et al., 2010), which is the typical value of seawater (Davis et al., 1998). On the other hand, freshwater used in the industrial process since 1997 acquires REE patterns with an upward positive trend of clear enrichment of MREE with respect to LREE ($(MREE/LREE)_{NASC}$ = 3.02) and of HREE with respect to MREE ($(HREE/MREE)_{NASC}$ = 2.08), according to the pattern of the ponded process water in zone 3 reported by Pérez-López et al. (2015). According to this latter work, these solutions also have a Cl/Br mass ratio of around 45. Both REE pattern and Cl/Br ratio are typical geochemical characteristics of fertilizers derived from phosphate rock (Otero et al., 2005).

Values typical of Tinto estuarine water and process water ponded on the stacks can be used as end-members in plots of $(HREE/MREE)_{NASC}$ vs. $(MREE/LREE)_{NASC}$ and Cl vs. Br in order to guess the origin of the solutions (Fig. 5). Considering the ideal mixing line between end-members, most of the edge outflows of the phosphogypsum stack are closer to the estuarine water end-member; although there are

significant differences from one zone to another of the stack, as discussed above. Thus, in zone 2 there are more edge outflows with a relatively greater influence for the process water end-member in comparison to the edge outflows of the remaining zones. These samples have patterns with relatively higher enrichment in HREE with respect to MREE and in MREE with respect to LREE, moving slightly away from the estuarine water end-member in the graph of REE (Fig. 5a). The influence of both sources is best observed by representing Cl/Br ratios, since all edge outflows are perfectly aligned in a wide range of mixing between the two end-members (Fig. 5b).

Some contribution of the process water source is also observed, although to a lesser extent, in some of the edge outflows of zone 3. These samples broadly have higher estuarine influence since the enrichment in HREE with respect to MREE is negligible and only an enrichment in MREE with respect to LREE is observed (Fig. 5c); in addition, Cl/Br values are closer to those of seawater (Fig. 5d). Finally, all edge outflows of zone 4 are characterized by presenting characteristics that are attributable exclusively to the Tinto estuarine water, with enrichment in MREE with respect to both LREE and HREE and Cl/Br ratios closer to the typical values of seawater as well (Fig. 5e,f). Such marine

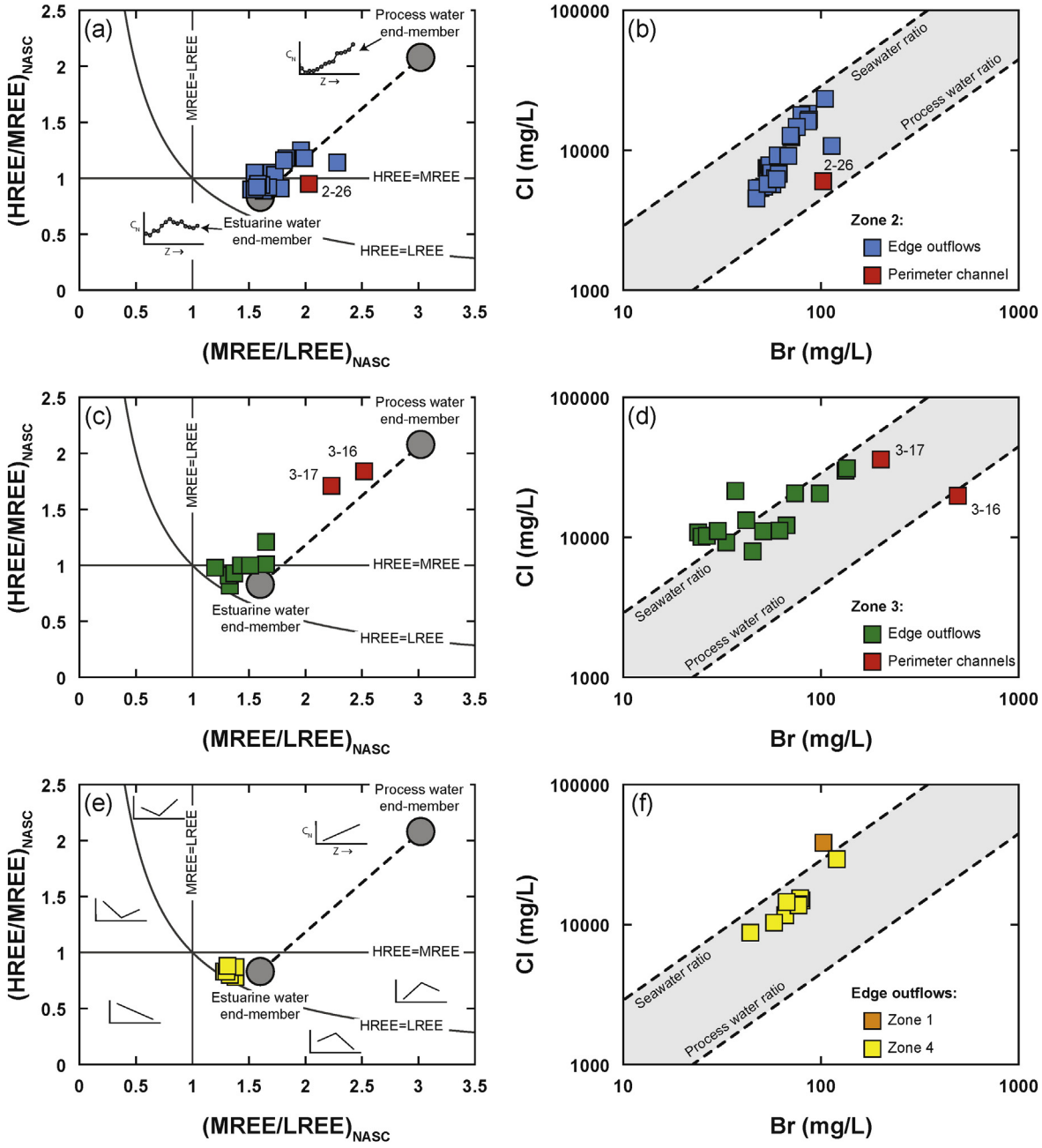

Fig. 5. Plots of $(HREE/MREE)_{NASC}$ vs. $(MREE/LREE)_{NASC}$ ratios (left side) and Cl vs. Br concentrations (right side) for the samples collected in (a, b) zone 2, (c, d) zone 3 and (e, f) zones 1 and 4 of the phosphogypsum stack. Note that legends of (a), (c) and (e) are the same as in (b), (d) and (f), respectively. In the NASC-normalized ratio plot, insets have been included in (a) to show the raw data for process and estuarine waters; in addition, schematic insets have been inserted in (e) for illustrating the general shape of the REE profile in the different fields of the graph (see more explanation in Stolpe et al., 2013). In these insets, C_N refers to the NASC-normalized concentration and Z→ refers to the REE in order by their increasing atomic number. REE pattern and Cl/Br ratio for the estuarine/sea-water end-member were taken from Elbaz-Poulichet and Dupuy (1999) and Davis et al. (1998), respectively; whereas both data for the process water end-member were taken from Pérez-López et al. (2015).

influence is also seen in the only sample collected in zone 1 according to the Cl/Br ratio, as expected from its location in a tidal channel (Fig. 5f).

These results are consistent with the history of dumping of the four zones of the phosphogypsum stack. The marine influence in the edge outflows is due to the use of estuarine waters for transport and settling of phosphogypsum slurries in the disposal area from 1968 to 1997. This estuarine water dissolves contaminants associated with residual phosphoric acid but a fraction remains in the interstitial space of the waste after decantation, being subsequently released from the edges of the stack to the estuary. During this time period, the circuit system was open and, hence, seawater is used only once and hardly loses its typical imprint of Cl/Br ratio and REE pattern. This stock of contaminated estuarine water fills the pores of the phosphogypsum in the whole depth profile of zones 1, 3 and 4. However, dumping sequence in zone 2 comprises a first filling stage with seawater before 1997 and a second stage with freshwater after 1997 following the change in phosphogypsum management policy. In this second stage, the continuous reuse of freshwater in a closed-loop system yielded a highly acidic and pollutant process water with the characteristic imprint of phosphate fertilizers according to its Cl/Br ratio and REE distribution. Thus, edge outflows of zone 2 mainly show an estuarine origin from the first filling stage, but with a notable contribution of the process water from the second filling stage. This fact explains why edge outflows of zone 2 have higher concentrations of P, NH_4^+ and contaminants than edge outflows from zones 1, 3 and 4. On the other hand, the higher marine influence in edge outflows of zones 1, 3 and 4 also explain the highest concentrations of Cl and S observed in comparison with those of zone 2.

As for samples from perimeter channels, water of the outermost perimeter channel of zone 2 has a REE distribution comparable to the estuarine water end-member but with a slight influence of process water, i.e. values similar to those found in the edge outflows of this zone (Fig. 5a). The geochemical similarity between these solutions suggests that the outer perimeter channel may intercept part of the emerging groundwater lateral flow before discharging to the outside. However, this channel is not at the same elevation as the stack basement but approx. 2 m height above the marsh. This would be also congruent with the lower value of Cl/Br ratio and the higher element concentrations in relation to edge outflows due likely to a larger contribution of the process water from the second filling stage (Fig. 5b). Therefore, it is also possible to suggest that much of the groundwater lateral flow is not intercepted and emerges to the surface up to reach the estuarine environment. In fact, there are numerous edge outflows around the whole perimeter of this zone of the stack; i.e. both towards the main tidal channel in the front part and towards the secondary channel embracing the back part (Fig. 1).

On the other hand, samples from the two perimeter channels of zone 3 are completely different to the rest of samples as they reveal a clear connection with the process water end-member according to the shape of REE patterns (Fig. 5c). Process water in this zone is not in the gypsum pores but in surface ponds. The possible infiltration of ponded process water seems to be successfully intercepted by both perimeter channels. This is certainly reasonable since the channels are very close to the surface ponds (Fig. 1). Presently, the ponded process water is subjected to evaporation in order to reduce its volume, which explains the extreme levels of contamination of these samples. It is important to highlight that the rear perimeter channel is on the same level as the marsh surface so it could be effective in collecting edge outflows in this part. However, the front and side parts have not any perimeter channel in the base of the marsh to prevent groundwater flow, which explains the numerous edge outflows observed towards the main tidal channel and the secondary channel surrounding this zone of the stack. Nevertheless, although it may seem surprising, the rear perimeter channel is connected to the secondary tidal channel and the acidic waters go directly to the estuary (see picture (f) in Fig. 1). Entry of seawater to this channel could explain the relatively closer REE pattern to the estuarine water end-member (Fig. 5c) and the relatively higher values of Cl/Br ratio with respect to the perimeter channel surrounding the ponded process water (Fig. 5d).

4.2. Evaluation of previous and future restoration actions

This study reports the existence of leakages from the unrestored zones of the phosphogypsum stack, which are currently a source of pollution to the Ría of Huelva. These findings are in disagreement with the previous restoration guidelines established by the regional government at least for zone 2 (Junta de Andalucía, 2009). In fact, this zone 2 exhibits the highest number of edge outflows along its perimeter; despite having numerous perimeter channels in order to collect the acidic leakages. In addition, leachates of zone 2 are the most polluting observed in comparison with those of the remaining zones of the stack.

In zone 3 many sources of pollution had already been previously recognized in the edge (Pérez-López et al., 2015). Nearly no influence of process water on the chemistry of most of these leachates suggests almost nonexistent, or strongly diluted, connection between process water ponded on the surface and edge outflows, which confirms what was pointed out in that latter study. It seems to be that the process water stored on surface only infiltrates up to the perimeter channels due to their proximity but does not reach the front or side edge of the stack. The discharge of contaminants occurs mainly through the seawater contained in the pores of the waste. In addition, Pérez-López et al. (2015) proposed for zone 3 the existence of a possible continuous recharge of seawater in the deeper zone of the phosphogypsum stack according to some evidences observed in previous technical reports (Tragsatec, 2010). The phosphogypsum weathering likely occurs by seawater intrusion in deeper zones of the stack because of its localization within the estuarine tidal prism.

Edge outflows of zone 2 are influenced by process water in a wide range of mixing. However, these solutions still preserve a marine character, which allow us to extend to this zone the interpretations made for zone 3. On the one hand, process water surely comes from a second filling stage, as stated before. Disconnection between process water ponds and edge outflows seems evident since the thickness of phosphogypsum in zone 2 is greater than in zone 3 and therefore infiltration from the surface pond to the basement and edges of the stack is highly unlikely. Definitely, the process water of the central ponds in zones 2 and 3 would not act as a source of edge outflows that reach the estuary by infiltration through porous media, which again contradicts previous restoration guidelines provided by the regional government (Junta de Andalucía, 2009). On the other hand, zone 2 shows the highest number of edge outflows because the amount of stack-piled phosphogypsum and, therefore, the thickness of the saturated zone as well as the volume of water stored in pores is substantially greater than in the remaining zones. In addition, we cannot ignore a possible contribution from seawater intrusion in deeper zones of the phosphogypsum stack. According to these results, future restoration actions in unrestored zones involving removal of process water ponds and cover of the stack surface with natural soil would not necessarily lead to the cessation of edge outflows. This statement can be confirmed by comparison of these zones with already-restored zones.

Regarding already-restored zones, the absence of edge outflows in zone 1 is probably due to the low thickness of phosphogypsum (2–3 m), which determines that whole profile of weathering corresponds to unsaturated zone; i.e. there is not a large stock of water in the deep pores that can flow laterally to emerge superficially at the edges. Thus, capacity of acidity and metal release is unquestionable owing to the nature of these wastes; however, pollution production is limited by the availability of weathering agents acting as hydrological drivers. On the contrary, zone 4 present a similar number of edge outflows to zone 3. This seems reasonable since both zones have similar thickness of phosphogypsum and, hence, seawater stored in the pores should be also of the same order of magnitude. It is therefore possible to confirm that the absence of process water ponds and presence of a complex

artificial-soil cover does not prevent leakages from the stack to the estuary. The only effect observed is the lack of influence of process water in the chemical composition of edge outflows, which are slightly less polluting for some toxic elements.

The results obtained in zone 4 allow once more the extension of the weathering model of zones 2 and 3 to even already-restored zones of the stack. The implementation of complex surface covers would have not any effect as restoration measure on pollution reaching the estuary through the edge outflows. The release of contaminants into the estuary would be only avoided by channeling and treatment of edge outflows before discharge. Therefore, it can be concluded that future restoration measures planned for zones 2 and 3 shall not involve the interruption of indirect leachates to the estuary. These data are in line with the need for an imminent change in the restoration strategies that the fertilizer company has proposed for the environmental regeneration of zones 2 and 3 of the phosphogypsum stack. It is also a priority to include zone 4 in the new restoration plans since preliminary actions seem to have been futile. Concerning zone 1, also previously-restored, its potential to generate acid leachates during the contact with weathering agents is lower. Nevertheless, it contributes to the pollution of the estuarine environment and should be also included in the new plans of regeneration.

Considering all sampling points, the measured flow values would result approximately in a bulk discharge of 335,000 m^3/y, which is in the same order of magnitude as some data found elsewhere (Tragsatec, 2010). Nevertheless, these values must be underestimated because of the existence of diffuse groundwater flow in the edge difficult to quantify. The result of multiplying the average concentration of all sampling points by bulk flow shows that the phosphogypsum stack releases enormous quantities of dissolved contaminants into the estuary: 42 ton/y of Fe, 12 ton/y of Zn, 6.9 ton/y of As, 4.2 ton/y of U, 3.5 ton/y of Cr, 1.8 ton/y of Cu, 1.6 ton/y of Cd and 1.2 ton/y of Ni, among others. On the other hand, Olías et al. (2006) calculated the fluvial metal contribution to the Ría of Huelva from mining districts between 1995 and 2003, showing that mean contaminants discharge is around 7922 ton/y of Fe, 3475 ton/y of Zn, 1721 ton/y of Cu, 36 ton/y of As, 36 ton/y of Ni and 11 ton/y of Cd. If comparing with these figures, phosphogypsum stack release represents, for the comparable metals, <3% of the total content, except for As and Cd which are highly remarkable, with values of up to 16% and 13%, respectively. Most importantly, and particularly for Cd, is the fact that this toxic metal behaves conservatively in the estuary (Hierro et al., 2014). The polluting power of the phosphogypsum stack is especially significant if one considers that the stack has an extension of 12 km^2 while fluvial basins have an area of 3979 km^2. Furthermore, the effluents from the phosphogypsum might lead to the contribution of new contaminants (non-mining related) such as phosphate, fluoride, ammonium and uranium.

5. Conclusions

This paper focuses on a phosphogypsum stack as potential contamination source to the Ría of Huelva estuary (SW Spain). The phosphate fertilizer factory ceased dumping in 2010, thus an imminent restoration of the area is planned. In particular, the study evaluates the future restoration works planned for some disposal zones by comparing with other zones that have been already restored following the same action guidelines. It is the general belief that the edge leakages or outflows draining inside the stack and discharging into the estuary have its origin in the infiltration of industrial process water ponded on the surface of the unrestored zones through the porous medium. Thus, planned restoration measures involve removal of ponded process water and cover with topsoil. However, some geochemical tracers such as REE patterns and Cl/Br ratios have allowed us to rule out the ponded process water as main vector of contaminants and suggest that these restoration actions would not involve the cessation of the leaching. The acid leachates have geochemical signatures typically found in seawater due to a possible connection between the stack and the estuary by saline intrusion. In this sense, already-restored zones act as a pollution source on the estuary through edge outflows just as unrestored zones, which strengthens this argument and reveals the inefficiency of adopted measures. According to this study, it is of critical importance to define again the basic guidelines for the development of restoration actions for the whole phosphogypsum stack in order to limit the exposure of estuarine ecosystems to acidity and toxic contaminants. Indeed, the contaminant contribution discharged into the estuary from the phosphogypsum stack is around 15% for both As and Cd of the total content when considering the pollution related to mining activities, which are highly toxic elements that can considerably affect the biota. This study also reveals that geochemical tracers such as Cl/Br ratios and REE patterns may be very valuable for the scientific community devoted to researching pollutant pathways, assessing long-term impacts mainly on coastal environments and optimizing restoration actions in other potentially polluting phosphogypsum stacks worldwide.

Acknowledgements

This work was supported by the Government of Andalusia through the research project 'Phosphogypsum: from the environmental assessment as a waste to its revaluation as a resource (P12-RNM-2260)'. R. Pérez-López also thanks the Spanish Ministry of Science and Innovation and the 'Ramón y Cajal Subprogramme' (MICINN-RYC 2011). C.R. Cánovas was funded by the European Union's Seventh Framework Program, Marie Skłodowska-Curie actions and the Ministry of Economy, Innovation, Science and Employment of the Junta de Andalucia by the program TalentHub (COFUND - Grant Agreement 291780). The analytical assistance of María Jesús Vílchez from the CIDERTA of the University of Huelva is gratefully acknowledged. We would also like to thank Dr. Damià Barceló (Editor-in-Chief) and five anonymous reviewers for the support and comments that significantly improved the quality of the original paper.

Appendix A. Supplementary data

Supplementary data associated with this article can be found in the online version, at http://dx.doi.org/10.1016/j.scitotenv.2016.02.070. These data include Google maps of the most important areas described in this article.

References

Barba-Brioso, C., Fernández-Caliani, J.C., Miras, A., Cornejo, J., Galán, E., 2010. Multi-source water pollution in a highly anthropized wetland system associated with the estuary of Huelva (SW Spain). Mar. Pollut. Bull. 60, 1259–1269.

Bolívar, J.P., García-Tenorio, R., Más, J.L., Vaca, F., 2002. Radioactive impact in sediments from an estuarine system affected by industrial waste releases. Environ. Int. 27, 639–645.

Bolívar, J.P., Martín, J.E., García-Tenorio, R., Pérez-Moreno, J.P., Mas, J.L., 2009. Behaviour and fluxes of natural radionuclides in the production process of a phosphoric acid plant. Appl. Radiat. Isot. 67, 345–356.

Borrego, J., Carro, B., Grande, J.A., de la Torre, M.L., Valente, T., Santisteban, M., 2013. Control factors on the composition of superficial sediments in estuaries of the coast of Huelva (SW Spain): a statistical approach. J. Iber. Geol. 39, 223–232.

Boryło, A., Nowicki, W., Skwarzec, B., 2013. The concentration of trace metals in selected cultivated and meadow plants collected from the vicinity of a phosphogypsum stack in Northern Poland. Pol. J. Environ. Stud. 22, 347–356.

Davis, S.N., Whittemore, D.O., Fabryka-Martin, J., 1998. Uses of chloride/bromide ratios in studies of potable water. Groundwater 36, 338–350.

El Samad, O., Aoun, M., Nsouli, B., Khalaf, G., Hamze, M., 2014. Investigation of the radiological impact on the coastal environment surrounding a fertilizer plant. J. Environ. Radioact. 133, 69–74.

El Zrelli, R., Courjault-Radé, P., Rabaoui, L., Castet, S., Michel, S., Bejaoui, N., 2016. Heavy metal contamination and ecological risk assessment in the surface sediments of the coastal area surrounding the industrial complex of Gabes city, Gulf of Gabes. SE Tunisia. Mar Pollut Bull http://dx.doi.org/10.1016/j.marpolbul.2015.10.047.

Elbaz-Poulichet, F., Dupuy, C., 1999. Behaviors of rare earth elements at the freshwater-seawater interface of two acid mine rivers: the Tinto and Odiel (Andalucia, Spain). Appl. Geochem. 14, 1063–1072.

Gázquez, M.J., Mantero, J., Mosqueda, F., Bolívar, J.P., García-Tenorio, R., 2014. Radioactive characterization of leachates and efflorescences in the neighbouring areas of a phosphogypsum disposal site as a preliminary step before its restoration. J. Environ. Radioact. 137, 79–87.

Grande, J.A., Borrego, J., Morales, J.A., 2000. A study of heavy metal pollution in the Tinto-Odiel estuary in southwestern Spain using factor analysis. Environ. Geol. 39, 1095–1101.

Gromet, L.P., Dymek, R.F., Haskin, L.A., Korotev, R.L., 1984. The "North American shale composite": its compilation, major and trace element characteristics. Geochim. Cosmochim. Acta 48, 2469–2482.

Hierro, A., Olías, M., Cánovas, C.R., Martín, J.E., Bolívar, J.P., 2014. Trace metal partitioning over a tidal cycle in an estuary affected by acid mine drainage (Tinto estuary, SW Spain). Sci. Total Environ. 497/498, 18–28.

Junta de Andalucía, 2009. Prescripciones Prioritarias Para la Redacción Del Proyecto de Recuperación de Las Balsas de Fosfoyesos en Las Marismas de Huelva. España, Technical report Available from http://www.juntadeandalucia.es/medioambiente/portal_web/web/temas_ambientales/vigilancia_y_prevencion_ambiental/planificacion/plan_calidad_huelva_2010_15/criterios_directrices_recuperacion_2.pdf.

Lottermoser, B.G., 2010. Mine Wastes: Characterization, Treatment and Environmental Impacts. third ed. Springer-Verlag, Berlin, Heidelberg.

Martínez-Sánchez, M.J., Pérez-Sirvent, C., García-Lorenzo, M.L., Martínez-López, S., Bech, J., García-Tenorio, R., Bolívar, J.P., 2014. Use of bioassays for the assessment of areas affected by phosphate industry wastes. J. Geochem. Explor. 147, 130–138.

Noack, C.W., Dzombak, D.A., Karamalidis, A.K., 2014. Rare earth element distributions and trends in natural waters with a focus on groundwater. Environ. Sci. Technol. 48, 4317–4326.

Nordstrom, D.K., Wilde, F.D., 1998. Reduction-oxidation potential (electrode method). National Field Manual for the Collection of Water Quality Data. U.S. Geological Survey Techniques of Water-Resources Investigations (Book 9, chapter 6.5).

Olías, M., Cánovas, C.R., Nieto, J.M., Sarmiento, A.M., 2006. Evaluation of the dissolved contaminant load transported by the Tinto and Odiel rivers (South West Spain). Appl. Geochem. 21, 1733–1749.

OSPAR, 2002. Discharges of Radioactive Substances Into the Maritime Area by Non-nuclear Industry. Radioactive Substances Series. Publication No. 161. OSPAR Commission, London.

OSPAR, 2007. PARCOM Recommendation 91/4 on Radioactive Discharges: Spanish Implementation Report. Radioactive Substances Series. Publication No. 342. OSPAR Commission, London.

Otero, N., Vitòria, L., Soler, A., Canals, A., 2005. Fertiliser characterisation: major, trace and rare earth elements. Appl. Geochem. 20, 1473–1488.

Pérez-López, R., Nieto, J.M., López-Coto, I., Aguado, J.L., Bolívar, J.P., 2010. Dynamics of contaminants in phosphogypsum of the fertilizer industry of Huelva (SW Spain): from phosphate rock ore to the environment. Appl. Geochem. 25, 705–715.

Pérez-López, R., Castillo, J., Sarmiento, A.M., Nieto, J.M., 2011. Assessment of phosphogypsum impact on the salt-marshes of the Tinto river (SW Spain): role of natural attenuation processes. Mar. Pollut. Bull. 62, 2787–2796.

Pérez-López, R., Nieto, J.M., de la Rosa, J.D., Bolívar, J.P., 2015. Environmental tracers for elucidating the weathering process in a phosphogypsum disposal site: implications for restoration. J. Hydrol. 529, 1313–1323.

Rodier, J., 1996. L'analyse de l'eau: eaux naturelles, eaux résiduaires, eaux de mer. eighth ed. Dunod, Paris.

Rutherford, P.M., Dudas, M.J., Samek, R.A., 1994. Environmental impacts of phosphogypsum. Sci. Total Environ. 149, 1–38.

Sanders, L.M., Luiz-Silva, W., Machado, W., Sanders, C.J., Marotta, H., Enrich-Prast, A., Bosco-Santos, A., Boden, A., Silva, E.V., Santos, I.R., Patchineelam, S.R., 2013. Rare earth element and radionuclide distribution in surface sediments along an estuarine system affected by fertilizer industry contamination. Water Air Soil Pollut. 224, 1742–1749.

Stolpe, B., Guo, L., Shiller, A.M., 2013. Binding and transport of rare earth elements by organic and iron-rich nanocolloids in Alaskan rivers, as revealed by field-flow fractionation and ICP-MS. Geochim. Cosmochim. Acta 106, 446–462.

Tayibi, H., Choura, M., López, F.A., Alguacil, F.J., López-Delgado, A., 2009. Environmental impact and management of phosphogypsum. J. Environ. Manag. 90, 2377–2386.

Tragsatec, 2010. Servicio para la recuperación de las balsas de fosfoyesos en las Marismas de Huelva. Fase de diagnóstico y propuesta de regeneración España: Technical report ref. TEC0002159 .

Journal of Hazardous Materials 331 (2017) 99–108

Contents lists available at ScienceDirect

Journal of Hazardous Materials

journal homepage: www.elsevier.com/locate/jhazmat

An anomalous metal-rich phosphogypsum: Characterization and classification according to international regulations

Francisco Macías[a,*], Carlos R. Cánovas[a], Pablo Cruz-Hernández[a], Sergio Carrero[a], Maria P. Asta[b], José Miguel Nieto[a], Rafael Pérez-López[a]

[a] Earth Sciences Department, University of Huelva, Campus "El Carmen", E-21071 Huelva, Spain
[b] Ecole Polytechnique Fédérale de Lausanne, Environmental Microbiology Laboratory (EML), Station 6, CH-1015 Lausanne, Switzerland

HIGHLIGHTS

- Leaching tests used by EU and US environmental rules were applied to phosphogypsum.
- Phosphogypsum from Huelva shows anomalously high metal levels.
- High mobility of contaminants was found under different weathering scenarios.
- Discrepancies between EU and US regulations were observed regarding hazardousness.
- We propose a complementary protocol based on the risk for the aquatic life.

ARTICLE INFO

Article history:
Received 5 September 2016
Received in revised form 27 January 2017
Accepted 12 February 2017
Available online 21 February 2017

Keywords:
Leaching tests
Hazardousness classification
Aquatic life risk
Arsenic anomaly

ABSTRACT

Phosphogypsum is the main waste generated by the phosphate fertilizer industry. Despite the high level of pollutants found in phosphogypsum and the proximity of stacks to cities, there are no specific regulations for the management of this waste. This study addresses this issue by applying to phosphogypsum, from a fertilizer plant in Huelva (SW Spain), the leaching tests proposed by the current European and US environmental regulations for wastes management and classification. Two main conclusions were obtained: 1) the anomalous metal and metalloid concentrations (e.g. As, Fe, Pb, Sb, Mn, V and Cu) and higher mobility observed in the Huelva phosphogypsum compared to other stacks worldwide, and 2) the discrepancies observed between EU and US regulations dealing with hazardousness classification of these materials. This latter finding suggests the need to use complementary assessment protocols to obtain a better characterization and classification of these wastes. An evaluation of the potential risk to the aquatic life according to the US EPA regulation is proposed in this study. The results warn about the acute and chronic effects on the aquatic life of this waste and suggest the adoption of more strict measures for a safe disposal of phosphogypsum stacks.

1. Introduction

Phosphate fertilizer industry plays a key role to maintain the levels of farming production worldwide. This industry needs phosphoric acid for the fertilizer production, which is mainly obtained from the manufacturing process of phosphate rock by the "wet acid method" [1]. In this method, the previously washed phosphate rock is concentrated by flotation and digested with sulfuric acid to obtain phosphoric acid and an unwanted by-product known as phosphogypsum. For every ton of phosphoric acid manufactured, 5 tons of phosphogypsum are generated. Considering that the world phosphate rock production is increasing as well as the P_2O_5 consumption from fertilizers, then, the world phosphogypsum production is expected to reach values around 100–280 Mt per year [2].

The geochemical characteristics of phosphogypsum are strongly influenced by the ore phosphate rock composition and by the chemical behavior of impurities released during manufacturing process [3]. Thus, although phosphogypsum is mainly composed by gypsum ($CaSO_4{\cdot}2H_2O$), this waste also contains some impurities such as phosphate, sulfate and fluoride, mainly in form of residual acids, toxic trace elements (e.g. As, Cd, Cr, Cu or Zn) and radionuclides from uranium decay series. Then, the management,

* Corresponding author.
E-mail addresses: francisco.macias@dgeo.uhu.es, francisco.macias.suarez@gmail.com (F. Macías).

http://dx.doi.org/10.1016/j.jhazmat.2017.02.015
0304-3894/

environmental policy and potential recycling of these wastes depend on the type and amount of impurities. From all the phosphogypsum generated in the world, only the 15% is recycled, mainly as building materials [1]. The remaining 85% is disposed of in large stacks, commonly in coastal areas, without any treatment and exposed to weathering processes. During operation, phosphogypsum is commonly stockpiled near the fertilizer plant over a composite liner to avoid infiltration. Upon closure, the stack is often capped with an impermeable layer to avoid leaching of contaminants.

Despite the high content of contaminants found in phosphogypsum and the proximity of stacks to cities, it is especially surprising that there are no specific regulations for the management of this waste. Furthermore, the phosphogypsum leaching capacity and the compliance of leachates to current regulations have not been properly addressed. There are several works dealing with the environmental impact of radionuclides contained in phosphogypsum, which suggest managing this by-product in radioactive waste landfills [e.g. 1,4]. However, only few researches have been focused on the trace metals leachability during weathering processes or on the behavior of phosphogypsum stacks, based on leaching protocols, for management strategies according to international rules [5,6]. In this sense, the high variability in phosphogypsum chemical composition associated to the different nature of phosphate rock, type of wet acid process performed and the release of contaminants during acid phosphoric manufacturing may cause significant differences on the leaching behavior among piles. Owing to this variability, the research on metal release from stacks worldwide under different weathering scenarios is of crucial importance.

Therefore, the present study addresses this issue by applying to phosphogypsum, from a fertilizer plant in Huelva (SW Spain), the leaching tests proposed by the current European and US environmental regulations for wastes management and classification (EN 12457-2 [7] and TCLP [8], respectively). In addition, owing to the intense interaction of Huelva phosphogypsum with seawater, leaching tests with this weathering agent have been also performed. The results of these tests have been compared with, to our knowledge, the only case reported worldwide applying these leaching protocols: the Mulberry stacks (Florida, US) [5]. Additionally, the potential risk to the aquatic life under different weathering scenarios has been studied by comparing the leachates composition to the so-called Criterion Continuous Concentration and Criterion Maximum Concentration from the National Recommended Water Quality Criteria of the US EPA [9]. The results obtained in this study will fill a gap in the knowledge of the potential pollutant release of these wastes under different weathering agents and help decision makers to determine the best cost-effective and environmentally safe disposal practices for these wastes.

2. Huelva phosphogypsum stack

The phosphoric acid production in the city of Huelva since 1967–2010 has caused the dumping of around 100Mt of phosphogypsum directly on 12 km^2 of salt-marshes of the Tinto River estuary, less than 100 m from the urban core (Fig. 1). The Huelva phosphogypsum is divided into four different zones within the stack (Fig. 1); zones 1 and 4 account for 65 Mt of phosphogypsum deposited over 680 ha, with heights ranging from 2 to 10 m. Both zones have been restored by conventional dry-covers to prevent weathering. Despite to this fact, highly-polluted acid leachates are directly discharged into the estuary [10]. Zones 2 and 3 are unrestored areas, accounting up to 40 Mt of phosphogypsum deposited over 440 ha, with average heights of 30 and 8 m, respectively. In both zones, the number and pollution grade of the acid discharges are far greater than those from the already-restored zones 1 and 4 [10].

The singularity of the Huelva phosphogypsum stack relies on two outstanding circumstances: a) the waste was deposited over the marshland without any type of isolation, and b) the piles are located within the tidal prism of the estuary. As a consequence, the Huelva phosphogypsum is subject to three different weathering scenarios. Firstly, the wastes are subject to weathering by rainwater (at least zones 2 and 3), where in semiarid climates rainfall events are scarce but intense. Secondly, due to its location within the estuarine system, the stack is also affected by the weathering of seawater during tidal cycles. Finally, owing to the absence of composite liners in the bottom of the stack, the residue is in direct contact with the organic matter-rich marshland; for this reason,

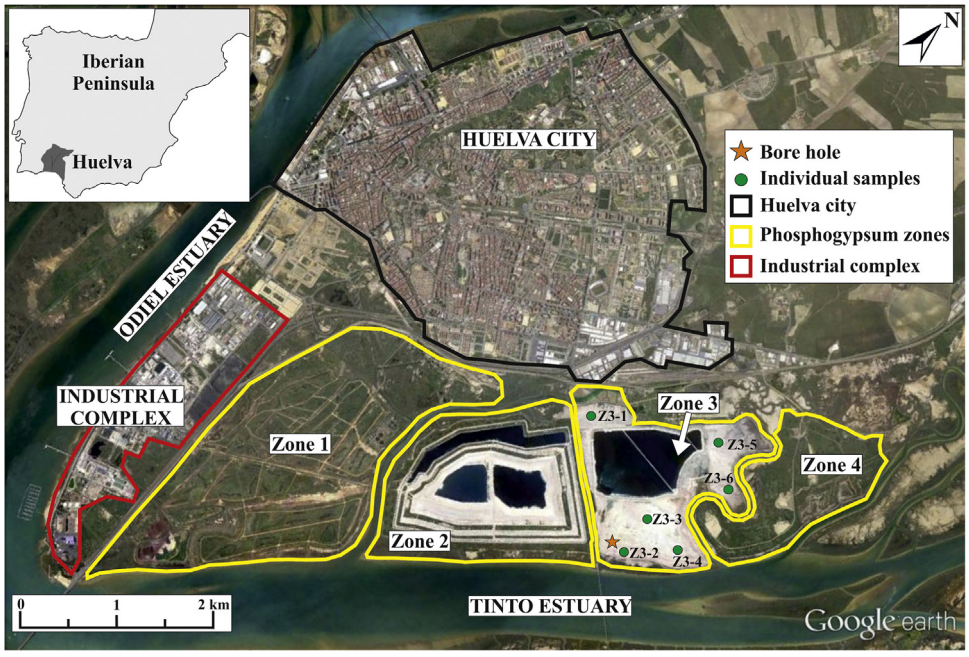

Fig. 1. Location map of the Huelva phosphogypsum stack with bore-hole and individual sampling points indicated. Image from Google Earth© software.

the upward flow of seawater and the downward flow of rainwater may interact with the stack, causing the weathering of the phosphogypsum under reducing conditions [6]. Detailed information about environmental setting of the Huelva stack and its pollution capacity can be found elsewhere [6,10].

3. Materials and methods

3.1. Sampling and analysis of total composition of Huelva phosphogypsum

Phosphogypsum solid samples were collected in the zone 3 of the stack (Fig. 1) in November 2015, from a bore-hole at different depths (0.5, 1.6, 2.9, 3.5, 4.1, 5.6, 7 and 8.1 m). The two shallowest samples correspond to unsaturated zone (0.5 and 1.6 m samples), whereas the remaining samples correspond to saturated zone (from 2 to 8.1 m). The deepest sample represents the stack basement directly in contact with the estuarine marsh soils. Additionally, 6 surface phosphogypsum samples (Z3-1–Z3-6) were collected in different locations of the zone 3 for seawater leaching experiments (Fig. 1). After collection, samples were immediately frozen and lyophilized to preserve their characteristics.

The chemical composition of the samples was obtained by analyses after aqua-regia pseudo-total digestion. These data were compared to those obtained from different leaching protocols with the purpose of quantifying the proportion of pollutants released by each weathering process simulated. This chemical extraction has been traditionally used to determine the pseudo-total metal content in environmental samples with good recovery percentages regarding the total content. Thus, 10 mL of aqua-regia (12 mol L^{-1} HCl and 15.8 mol L^{-1} HNO_3 in the ratio 3:1) were added to 1 g of phosphogypsum in Teflon reactors and reacted for 20 h in a fume cupboard, and then, simmered on a hot plate for 1 h at 100 °C. The digestates were diluted with deionized water and stored refrigerated at 4 °C until analysis.

3.2. Leaching protocols for management and hazardousness assessment

Three different leaching tests were performed to assess the waste management and disposal according to its hazardousness. On the one hand, the phosphogypsum was subject to leaching protocols established by current regulations on waste disposal using both EU standard EN 12457-2 [7] and US standard TCLP [8] leaching tests. On the other hand, the release of pollutants under seawater interaction was studied by leaching with seawater. All these leaching tests simulate the potential weathering agents that may currently release pollutants from the stacks, which will be briefly described below.

The EN 12457-2 leaching test is applied to assess the acceptance for disposal of a waste in European landfill sites, and has been widely used in mineral-processing wastes [e.g. 11,12]. The experimental concentrations obtained in the test must be normalized to the sample weight in order to be compared with the limit threshold values issued by the European Council Decision [13] as criterion for the acceptance of wastes in three types of landfill sites: landfills for inert wastes, non-hazardous wastes and hazardous wastes. The test was conducted by mixing phosphogypsum samples with deionized water at a liquid to solid ratio of 10:1, followed by stirring for 24 h, centrifugation and filtration of the supernatant and determination of dissolved elements. In addition, the use of deionized water in this test allows us to estimate the potential leaching of pollutants by phosphogypsum through contact with rainwater.

The TCLP leaching test [8] was originally designed to simulate co-disposal with municipal wastes, although its applicability has been extended for the hazardousness classification of mineral-processing wastes [14] regarding to the regulated limits of certain inorganic pollutants [e.g. 11,15,16]. Additionally, metal concentrations in TCLP leachates can be also employed as limits to determine if a specific waste needs to be submitted to an universal treatment standard (UTS) to accomplish with Land Disposal Restrictions (LDR, EPA 530-R-01-007) [17]. The test was performed according to the method 1311 of the US EPA [8]. The samples were extracted for 18 h by stirring on a shaker with a liquid to solid ratio of 20:1. The extractant must be chosen as function of waste pH. For samples with pH <5, such as the Huelva phosphogypsum, an acetic acid solution buffered to pH 4.9 was used as extractant. Following the extraction, samples were centrifuged, the supernatant filtered, acidified with HNO_3 and stored refrigerated at 4 °C until analysis. In this case, leaching of phosphogypsum with organic acids would simulate the leaching processes when the upward flow from the basement and/or the downward flow by meteoric water from the surface interact with rich organic matter environments from the salt-marshes.

Finally, the simulation of weathering by seawater was performed in 6 samples by mixing with seawater at a liquid to solid ratio of 10:1, followed by stirring for 24 h. Afterwards, filtration of the supernatant and determination of dissolved elements or pollutants were performed. Seawater used during this leaching test was obtained in the coast of Atlantic Ocean near to the city of Huelva.

3.3. Analytical methodology

Major element (Al, Fe, Mn and S) concentrations were obtained using Inductively Coupled Plasma-Atomic Emission Spectroscopy (ICP-AES; Jobin Yvon Ultima 2) and trace element (As, Ba, Be, Cd, Co, Cr, Cu, Mo, Ni, Pb, Sb, Se, Sn, Tl, V and Zn) contents by Inductively Coupled Plasma-Mass Spectroscopy (ICP-MS; Agilent 7700). Detection limits were: 0.2 mg/L for S; 0.05 mg/L for Al and Fe; 0.02 mg/L for Mn; and 0.2 μg/L for trace elements. All analyses were performed in the laboratories of the University of Huelva. Three laboratory standards, prepared with concentrations within the range of the samples, were analyzed every 10 samples to check for accuracy. Furthermore, dilutions were performed to ensure that the concentration of the samples was within the concentration range of the standards. Blank solutions with the same matrix as the samples were also analyzed. The average measurement error was <5%.

3.4. Comparison with other phosphogypsum stacks worldwide

With the aim of checking remarkable differences of the waste by-products in various phosphoric industries, the total chemical composition of Huelva phosphogypsum has been compared with that reported for other phosphogypsum stacks around the world. Data were obtained from stacks located at Florida, Idaho and Louisiana reported by Mostary [5], Luther et al. [18] and Carbonell-Barrachina et al. [19], respectively; from Brazilian phosphogypsums published by Oliveira et al. [20], da Conceicao et al. [21] and Silva et al. [22]; from Canadian phosphogypsum reported by Rutherford et al. [23]; and from Tunisian and Jordanian stacks described by Choura et al. [24] and Abed et al. [25], respectively.

Also for comparison purposes, data after applying the TCLP and EN standardized leaching tests in phosphogypsum from a giant stack located at Mulberry (Florida, US) [5] were used. Phosphate mining in Florida is one of the state's largest industries, and produces approximately 40 Mt of phosphogypsum per year [5], accounting between 14 and 40% of worldwide phosphogypsum production. In this US state, more than one billion tons of phosphogypsum are permanently stored in over 25 giant stacks, some of them with up to 60 m in height and 2 km^2 in extension [26]. For this reason, it seems reasonable to consider Mulberry

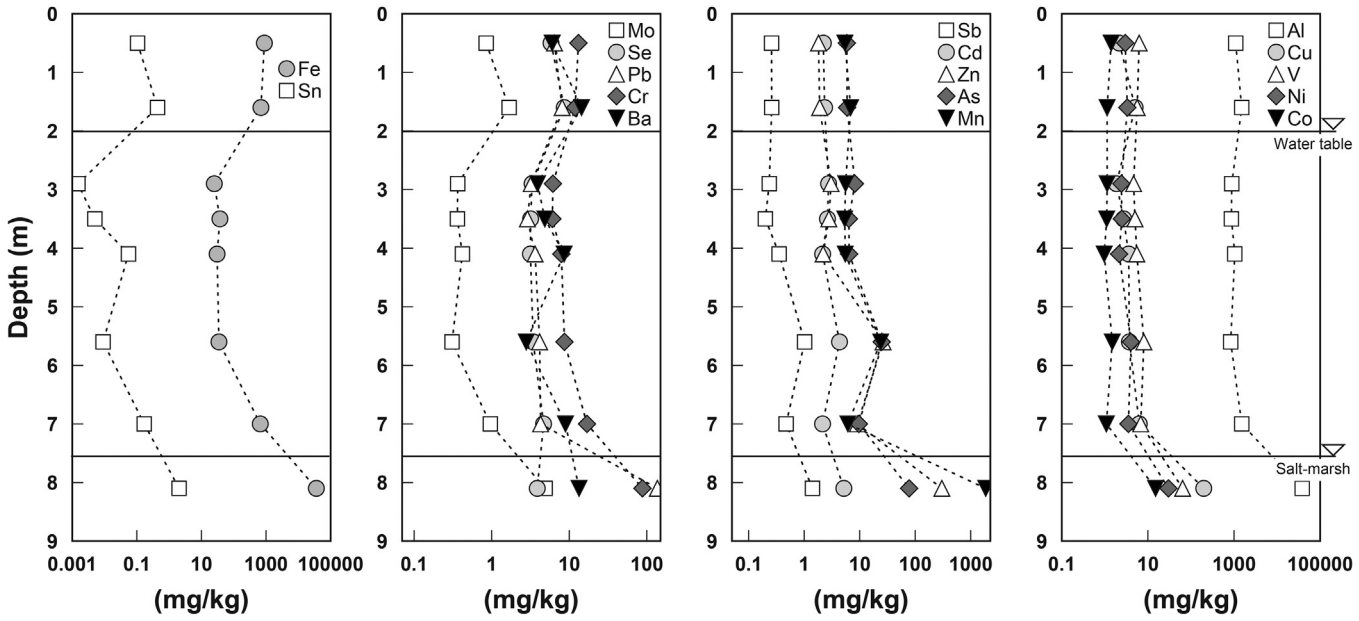

Fig. 2. Metal content of the Huelva phosphogypsum at different depths (see text for explanation).

phosphogypsum as a representative stack worldwide. Mostary [5] collected samples from four locations on the stack walls at different depths along the first 0.6 m. Then, samples collected from different depths for each location were thoroughly mixed to get a homogenous sample, obtaining finally a total of 8 samples. To our knowledge, this is the only case worldwide applying the EU standard EN 12457-2 and US standard TCLP leaching tests to phosphogypsum.

4. Results and discussion

4.1. Chemical composition of Huelva phosphogypsum and comparison with other phosphogypsum stacks

The Huelva stack acts as an anthropogenic aquifer system, with clearly differentiated unsaturated (0–2 m) and saturated zones (from 2 m depth to the bare marsh). This latter zone is subject to a strongly reducing environment, especially the phosphogypsum located at the bottom of the stack. This feature promotes chemical gradients along the profile, and therefore, different responses to weathering may be expected.

As can be observed in Fig. 2, most elements analyzed reached the highest concentrations in the bottom of the profile (with the exception of Se). This fact is due to sulfate-reducing processes occurring in the contact of phosphogypsum with bare marshland soils [27,28] that promote precipitation and trapping of metals of the pore-waters into metallic sulfides. However, a slight enrichment is observed for Fe and other trace metals (i.e. Sn, Ba, Cr, Pb, Se and Mo) in the unsaturated zone (0–2 m) compared to the saturated zone (except to the bottom, in contact with the marshland; Fig. 2).

The chemical composition of the three zones identified in the Huelva stack, i.e. unsaturated, saturated and marshland contact zones, has been compared with that reported in others stacks around the world (Fig. 3). As can be observed, Huelva phosphogypsum exhibits the same range of concentrations for most elements as those reported worldwide, with the exception of the bottom material where enrichments in Fe, Pb, Sb, Mn, V, Cu, Co, Ni and Cr are observed in relation to the rest of stacks (Fig. 3). However, the most striking feature is the anomalously high concentration of As observed along the whole profile, i.e. between 1 and 2 orders of magnitude higher than that found in the rest of reported stacks worldwide. The most probable origin of this anomalously high concentration of As in the Huelva phosphogypsum could be related with the quality of the sulfuric acid used during the industrial process. The sulfuric acid used during phosphoric acid manufacturing in Huelva was mainly obtained by pyrite roasting and SO_2 recovery [29]. The pyrite used came from the Tharsis Mines which contained up to 0.4% of As [30], thus, the high level of As in the sulfuric acid may have been transferred to the phosphogypsum.

These results highlight the singularity of Huelva stack as an anomalous As and metal-rich phosphogypsum among the cases reported worldwide, especially in the bottom of the stack where Fe, Pb, Sb, Mn, V, Cu, Co, Ni and Cr are trapped as a consequence of the interaction between the phosphogypsum and the organic matter-rich marshland soils. As a difference of most phosphogypsum deposits worldwide, Huelva was not stockpiled over an impermeable liner but on bare marshland soils [10]. If these metal and metalloids, anomalously enriched in Huelva, were easily mobilized by weathering agents, the current state of the Huelva stack may pose a serious threat to the environment.

4.2. Management assessment and hazardousness classification based on international regulations

Owing to the anomalously high As concentration along the profile and high metal concentrations observed in the deepest zone of the Huelva stack, its hazardousness and the suitability for landfill disposal must be addressed. Table 1 shows the regulatory limits for waste acceptance at landfills in EU [13], and the results of the EN 12457-2 leaching test applied to the Huelva depth profile. For comparative purposes, the results reported in Mulberry [5] with the same test are also included.

According to these results, the unsaturated zone of the Huelva stack could be considered as a non-hazardous waste because sulfate and Cd exceed the limit of 6000 mg/kg and 0.04 mg/kg respectively, established for inert wastes landfills. On the other hand, the saturated zone may be considered as a hazardous material due to the high concentrations of As leached and, therefore, it must be deposited in landfills for this type of wastes. As well as the saturated

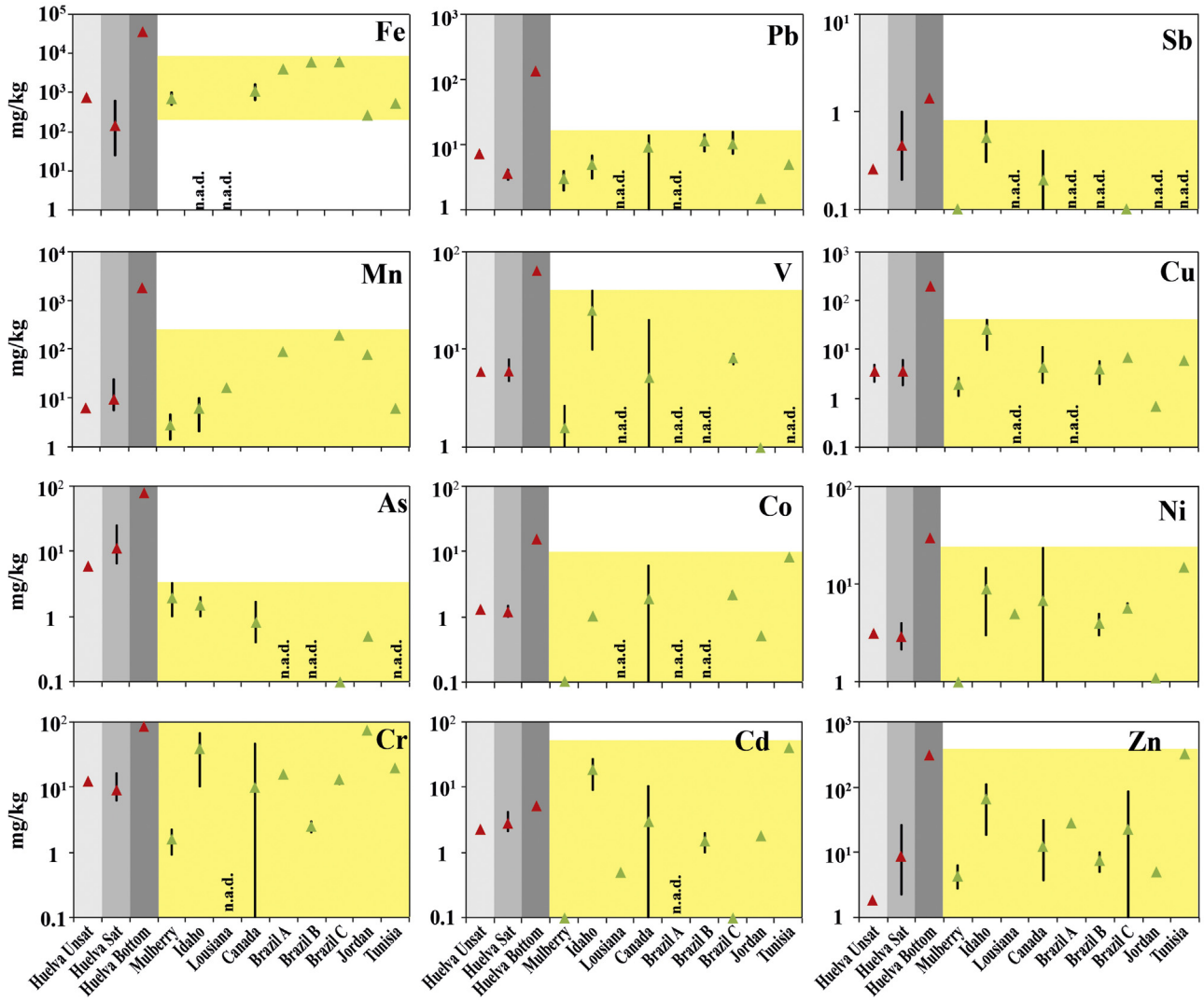

Fig. 3. Content in metal and metalloids of Huelva phosphogypsum profile and comparison with other phosphogypsum stacks worldwide. Max, min and mean values are plotted. n.a.d. (no available data).

Table 1
Results of the EN 12457-2 leaching test applied to the Huelva depth profile and Mulberry phosphogypsum stack, and comparison with the regulatory limits for waste acceptance at landfills in EU. Data in mg/kg.

Landfills for:	As	Ba	Cd	Cr	Cu	Mo	Ni	Pb	Sb	Se	Zn	$SO4^{2-}$
Inert wastes	0.5	20	0.04	0.5	2	0.5	0.4	0.5	0.06	0.1	4	6000
Non-hazardous wastes	2	100	1	10	50	10	10	10	0.7	0.5	50	20000
Hazardous wastes	25	300	5	70	100	30	40	50	5	7	200	50000
Huelva depth profile (m):												
0.5	0.03	0.19	0.12	b.d.l	0.03	0.04	0.09	b.d.l	b.d.l	0.06	0.31	13758
1.6	0.09	0.20	0.11	b.d.l	0.04	0.05	0.10	0.02	b.d.l	0.07	0.32	14067
2.9	4.24	0.29	0.35	0.22	0.78	0.02	0.43	0.13	0.03	0.02	2.63	15045
3.5	3.72	0.29	0.34	0.33	0.74	0.02	0.41	0.14	0.04	0.02	2.57	14799
4.1	3.47	0.35	0.38	0.39	1.52	0.02	0.48	0.17	0.05	0.02	2.57	16168
5.6	3.22	0.28	0.35	0.34	1.26	0.03	0.38	0.11	0.06	0.03	6.73	18082
7	6.71	0.30	0.42	0.26	0.70	0.02	0.46	0.10	0.04	0.03	9.16	16739
8.1	6.76	0.23	1.78	0.03	1.78	0.18	1.06	0.01	0.05	0.10	24.7	18028
Mulberry (n = 8)												
Max	b.d.l	1.20	b.d.l	b.d.l	3.40	2.00	0.80	b.d.l	b.d.l	b.d.l	5.80	n.a.d
Min	b.d.l	0.40	b.d.l	b.d.l	1.80	0.40	0.20	b.d.l	b.d.l	b.d.l	2.00	n.a.d
Mean	b.d.l	0.80	b.d.l	b.d.l	2.40	1.00	0.40	b.d.l	b.d.l	b.d.l	3.60	n.a.d

b.d.l (below detection limit), n.a.d (no available data).

Table 2
Results of the TCLP leaching test (method 1311 of US EPA) applied to the Huelva depth profile and Mulberry phosphogypsum stack, and comparison with the regulatory limits established by the Land Disposal Restrictions (LDR, EPA 530-R-01-007). Data in mg/L.

Limits:	As	Ba	Cd	Cr	Ni	Pb	V	Zn	Se	Sb	Be	Tl
TCLP	5	100	1	5	n.r.l	5	n.r.l	n.r.l	1	n.r.l	n.r.l	n.r.l
UTS	5	21	0.11	0.6	11	0.75	1.6	4.3	5.7	1.15	1.22	0.2
Huelva depth profile (m):												
0.5	0.002	0.027	0.010	b.d.l	0.011	0.002	b.d.l	0.026	b.d.l	b.d.l	b.d.l	b.d.l
1.6	0.006	0.026	0.008	b.d.l	0.012	0.005	b.d.l	0.021	0.004	b.d.l	b.d.l	b.d.l
2.9	0.213	0.036	0.019	0.005	0.026	0.008	0.015	0.124	b.d.l	0.002	b.d.l	b.d.l
3.5	0.185	0.034	0.020	0.008	0.027	0.009	0.033	0.126	b.d.l	0.003	b.d.l	b.d.l
4.1	0.177	0.041	0.022	0.005	0.029	0.004	0.028	0.121	b.d.l	0.003	b.d.l	b.d.l
5.6	0.345	0.032	0.024	0.005	0.027	0.001	0.019	0.419	b.d.l	0.002	b.d.l	b.d.l
7	0.156	0.028	0.020	0.007	0.024	0.001	0.018	0.304	b.d.l	0.002	b.d.l	b.d.l
8.1	0.400	0.030	0.127	0.008	0.068	0.008	0.075	1.591	0.004	0.004	b.d.l	0.001
Mulberry (n = 8)												
Max	b.d.l	0.16	b.d.l	0.04	0.07	b.d.l	b.d.l	0.29	b.d.l	b.d.l	n.a.d	n.a.d
Min	b.d.l	0.07	b.d.l	0.02	0.01	b.d.l	b.d.l	0.05	b.d.l	b.d.l	n.a.d	n.a.d
Mean	b.d.l	0.11	b.d.l	0.03	0.03	b.d.l	b.d.l	0.14	b.d.l	b.d.l	n.a.d	n.a.d

n.r.l (no referenced limit), b.d.l (below detection limit), n.a.d (no available data).

zone, the phosphogypsum deposited in the bottom of the stack in contact with the marshland soils also exceeds the values of non-hazardous wastes for As and Cd. Thus, this zone of the stack must be also deposited in a hazardous waste landfill. The trend on metal and metalloids release in depth by EN 12457-2 leaching test is in agreement with the trend observed for total chemical composition (Fig. 2). In summary, the mobility of As and Cd confers the Huelva stacked material the classification of hazardous waste according to EU regulations. On the other hand, the Mulberry phosphogypsum should be considered as a non-hazardous waste according to the EU regulation by the release of Cu, Mo, Ni and Zn; only these metals exceed the threshold limits for inert waste landfills (Table 1). Unlike Huelva, As and Cd were below the detection limit for Mulberry (Table 1), elements which confer the hazardousness to the Huelva pile.

According to US EPA regulation [8,14], the Huelva and Mulberry phosphogypsums can be considered as non-hazardous wastes due to the fact that the TCLP limits are not exceeded in any case (Table 2). The Mulberry phosphogypsum neither exceeds the UTS limits nor must therefore be treated before disposal to accomplish with Land Disposal Restrictions [17]. However, the waste stored in the bottom of the Huelva stack releases Cd at concentrations that exceed the UTS limit, so this zone of the stack must be treated before disposal. Most elements considered in the TCLP (mainly highly toxic, e.g. As, Cd, Pb, V) were below the detection limit in the extractants from Mulberry, unlike in the Huelva phosphogypsum where remarkable concentrations were reached. This pattern is in line with that of chemical composition and of deionized water leaching results obtained in Huelva and Mulberry, highlighting the anomalous metal and metalloid concentrations and higher mobility observed in the Huelva phosphogypsum.

The discrepancies between EU and US regulations dealing with hazardousness classifications of mineral processing wastes have been previously reported [11], which suggests the need to use complementary assessment protocols to obtain a better characterization and classification of these wastes. In case of discrepancies, a detailed investigation of the potential effects on the aquatic life should be performed in order to assure a safe waste disposal and a risk minimization to the environment.

4.3. Environmental impact on aquatic life under different weathering scenarios

The impact of this anomalously metal-rich phosphogypsum on the aquatic life has been studied under different weathering scenarios: (1) weathering by rainwater (simulated by EN 12457-2 leaching test), which may occur in the unrestored zones of Huelva stack during rainfall events; (2) weathering under reducing conditions (simulated by TCLP leaching test), which may occur in the lowest part of saturated zones and in the bottom of Huelva pile; and (3) weathering by seawater, which may occur during tidal cycles. The impact of these weathering scenarios on the aquatic life has been assessed by comparison with the criteria established by the US EPA. In this sense, the Criterion Continuous Concentration is the threshold value above which a certain element poses a significant risk to the majority of species in waters if chronic exposure is maintained. On the other hand, the Criterion Maximum Concentration represents the acute exposure to a metal, that is, the highest one-hour average concentration that should not result in unacceptable effects on aquatic organisms.

Tables 3 and 4 show the Criterion Continuous Concentration and Criterion Maximum Concentration limits, and the metal and metalloid release after EN 12457-2 and TCLP tests in the Huelva and Mulberry phosphogypsum stacks, respectively. As can be observed, only Al and, at a lesser extent, Zn exceed the limits in Mulberry, which pose a risk for aquatic life by both elements upon acute and chronic exposure. The metal exposure for aquatic life under rainfall weathering and reducing conditions of Huelva phosphogypsum is even more severe; Cd exceeds both limits along the whole profile while other pollutants (Al, As, Pb, Ni, Se and Zn) show exceedance of one of the two limits at different depths. Only Fe, Cu and Cr values remained below the threshold limits of the aquatic life criteria established by the US EPA along the whole profile. In addition to As and Cd, the release of other toxic metals (e.g. Pb, Se or Zn) under rainfall weathering and reducing conditions poses a risk to the aquatic life. The comparison with Mulberry highlights, once again, the hazardous nature of the Huelva stack and warns about the acute and chronic effects on the aquatic life during rainfall events and reducing conditions.

The interaction of seawater with Huelva stack also causes a significant release of toxic metals. Both limits for Cd were exceeded in all samples and for As in two cases (Table 5). The rest of the elements exceeded Criterion Continuous Concentration and/or Criterion Maximum Concentration limits in one or several samples (with the exception of Cu). Once more, both Cd and As appear to be the most mobile and harmful elements in Huelva phosphogypsum, which agree well with the anomalous total chemical composition and the release observed for these elements under previous weathering scenarios. Unfortunately, to our knowledge there is no data available to compare with these findings. There is only one work

Table 3
Results of the leaching experiments with deionized water and comparison with the Mulberry results and the Criterion Continuous Concentration and Criterion Maximum Concentration limits established in the aquatic life criteria by the US EPA (see text for explanation). Data in mg/L.

US EPA Water Quality Criteria limits:	Al	As	Cd	Cr	Cu	Fe	Pb	Ni	Se	Zn
Criterion Continous Concentration	0.087	0.15	0.00025	0.085	1.3	1	0.0025	0.052	0.005	0.12
Criterion Maximun Concentration	0.75	0.34	0.002	0.586	n.r.l	n.r.l	0.065	0.47	n.r.l	0.12
Huelva depth profile (m):										
0.5	5.279*	0.003	0.012*	b.d.l	0.003	0.005	b.d.l	0.009	0.006**	0.032
1.6	5.450*	0.009	0.011*	b.d.l	0.004	b.d.l	0.002	0.010	0.007**	0.032
2.9	1.692*	0.428*	0.035*	0.022	0.078	0.083	0.013**	0.043	0.002	0.265*
3.5	1.590*	0.384*	0.035*	0.034	0.076	0.180	0.014**	0.042	0.002	0.265*
4.1	1.434*	0.350*	0.038*	0.039	0.153	0.470	0.017**	0.048	0.002	0.260*
5.6	1.152*	0.335**	0.036*	0.036	0.131	0.400	0.011**	0.040	0.003	0.699*
7	1.111*	0.697*	0.044*	0.027	0.073	0.801	0.011**	0.048	0.003	0.951*
8.1	6.371*	0.729*	0.192*	0.003	0.193	0.051	0.002	0.114**	0.011**	2.668*
Mulberry (n = 8):										
Max	2.210*	b.d.l	b.d.l	b.d.l	0.170	b.d.l	b.d.l	0.040	b.d.l	0.290*
Min	1.200*	b.d.l	b.d.l	b.d.l	0.090	b.d.l	b.d.l	0.010	b.d.l	0.100
Mean	1.630*	b.d.l	b.d.l	b.d.l	0.120	b.d.l	b.d.l	0.020	b.d.l	0.180*

*Both US EPA Water Quality Criteria limits have been exceeded and **only Criterion Continuous Concentration has been exceeded. n.r.l (no referenced limit), b.d.l (below detection limit).

Table 4
Results of the leaching experiments with organic acid and comparison with the Mulberry results and the Criterion Continuous Concentration and Criterion Maximum Concentration limits established in the aquatic life criteria by the US EPA (see text for explanation). Data in mg/L.

US EPA Water Quality Criteria limits:	Al	As	Cd	Cr	Cu	Fe	Pb	Ni	Se	Zn
Criterion Continous Concentration	0.087	0.15	0.00025	0.085	1.3	1	0.0025	0.052	0.005	0.12
Criterion Maximun Concentration	0.75	0.34	0.002	0.586	n.r.l	n.r.l	0.065	0.47	n.r.l	0.12
Huelva depth profile (m):										
0.5	2.032*	0.002	0.010*	b.d.l	0.001	b.d.l	0.002	0.011	b.d.l	0.026
1.6	1.682*	0.006	0.008*	b.d.l	b.d.l	b.d.l	0.005**	0.012	0.004	0.021
2.9	0.575**	0.213**	0.019*	0.005	0.033	b.d.l	0.008**	0.026	b.d.l	0.124*
3.5	0.625**	0.185**	0.020*	0.008	0.031	b.d.l	0.009**	0.027	b.d.l	0.126*
4.1	0.493**	0.177**	0.022*	0.005	0.064	b.d.l	0.004**	0.029	b.d.l	0.121*
5.6	0.481**	0.345*	0.024*	0.005	0.028	b.d.l	0.001	0.027	b.d.l	0.419*
7	0.530**	0.156**	0.020*	0.007	0.041	b.d.l	0.001	0.024	b.d.l	0.304*
8.1	4.817*	0.400*	0.127*	0.008	0.377	b.d.l	0.008**	0.068**	0.004	1.591*
Mulberry (n = 8):										
Max	2.180*	b.d.l	b.d.l	0.04	0.060	0.580	b.d.l	0.070**	b.d.l	0.290*
Min	1.660*	b.d.l	b.d.l	0.02	0.010	0.320	b.d.l	0.010	b.d.l	0.050
Mean	1.860*	b.d.l	b.d.l	0.03	0.030	0.470	b.d.l	0.030	b.d.l	0.140*

*Both US EPA Water Quality Criteria limits have been exceeded and **only Criterion Continuous Concentration has been exceeded. n.r.l (no referenced limit), b.d.l (below detection limit).

Table 5
Results of the leaching experiments with seawater and comparison with the Criterion Continuous Concentration and Criterion Maximum Concentration limits established in the aquatic life criteria by the US EPA (see text for explanation). Data in mg/L.

US EPA Water Quality Criteria limits:	Al	As	Cd	Cr	Cu	Fe	Pb	Ni	Se	Zn
Criterion Continous Concentration	0.087	0.15	0.00025	0.085	1.3	1	0.0025	0.052	0.005	0.12
Criterion Maximun Concentration	0.75	0.34	0.002	0.586	n.r.l	n.r.l	0.065	0.47	n.r.l	0.12
Huelva individual samples:										
Z3-1	0.300**	b.d.l	0.018*	b.d.l	b.d.l	b.d.l	b.d.l	0.008	b.d.l	b.d.l
Z3-2	0.600**	0.550*	0.141*	0.360**	0.434	1.490*	b.d.l	0.178**	0.020**	1.190*
Z3-3	0.300**	b.d.l	0.012*	b.d.l	b.d.l	b.d.l	b.d.l	0.010	b.d.l	b.d.l
Z3-4	0.200**	b.d.l	0.012*	b.d.l	0.004	b.d.l	b.d.l	0.015	b.d.l	0.010
Z3-5	0.400**	0.830*	0.089*	0.030	0.409	0.220	0.030**	0.087**	b.d.l	0.629*
Z3-6	0.100**	0.050	0.025*	b.d.l	0.008	b.d.l	b.d.l	0.025	b.d.l	0.031

*Both US EPA Water Quality Criteria limits have been exceeded and **only Criterion Continuous Concentration has been exceeded. n.r.l (no referenced limit), b.d.l (below detection limit).

focused on the interaction between phosphogypsum and seawater [31], which only deals with the U release under this weathering agent. This is probably due to the lower values of metals contained in phosphogypsum worldwide compared to the anomalously high metal concentrations observed in Huelva. Thus, little attention has been paid to this issue up to now.

4.4. Potential release of metal and metalloids from different weathering agents; implication for remediation strategies

As indicated in the previous section, the Criterion Continuous Concentration and Criterion Maximum Concentration limits are exceeded with different elements, then, a relative hazardousness order for weathering agents in Huelva stack could be established as: seawater > rainwater > reducing conditions. However, the

Table 6
Percentages of elements released respect to pseudo-total composition for the weathering agents simulated.

		pH	Al	As	Cd	Cr	Cu	Fe	Pb	Ni	Se	Zn
Total depth profile (mg/kg)	Unsaturated	n.a	1301	5.90	2.30	12.5	3.60	791	7.30	3.20	7.20	1.80
	Saturated	2.12	1029	11.1	2.80	9.20	3.60	158	3.60	2.90	3.60	8.70
	Bottom	2.15	38303	77.7	5.20	87.9	197	36121	137	30.0	3.90	301
Rainwater (%)	Unsaturated		4.1	1.0	4.9	0.0	1.1	0.0	0.1	2.9	0.9	16.9
	Saturated		1.4	49.2	14.2	3.9	31.2	7.1	3.7	15.8	0.7	84.5
	Bottom		0.2	8.7	34.3	0.0	0.9	0.0	0.0	3.5	2.6	8.2
Reducing conditions (%)	Unsaturated		3	1.3	8.2	0.0	2.0	0.0	0.9	7.1	0.4	25.8
	Saturated		1.1	45.0	15.9	1.5	27.9	0.0	2.8	19.3	0.0	76.4
	Bottom		0.3	10.3	48.9	0.2	4.9	0.0	0.1	4.5	2.2	10.5
Total individual samples (mg/kg)	Z3-1	6.66	1923	b.d.l	2.1	3.6	b.d.l	300	4.4	1.4	b.d.l	4.2
	Z3-2	2.49	1627	6.4	2.8	16.7	3.3	208	10.8	2.7	b.d.l	13.1
	Z3-3	6.35	1314	b.d.l	1.6	9.9	b.d.l	299	3.6	0.9	b.d.l	1.9
	Z3-4	6.41	1275	b.d.l	1.4	20.3	b.d.l	287	2.8	0.9	1.2	2.3
	Z3-5	3.04	1244	11.6	2.3	11.2	2.2	216	3.2	1.9	b.d.l	9.9
	Z3-6	6.35	1001	b.d.l	1.4	3.6	b.d.l	120	2.0	1.1	b.d.l	2.4
Seawater (%)	Z3-1		0.6	0.0	8.8	0.0	0.0	0.0	0.0	5.9	0.0	0.0
	Z3-2		1.5	86.1	49.8	21.4	100.0	7.2	0.0	66.7	0.0	90.6
	Z3-3		0.9	0.0	7.5	0.0	0.0	0.0	0.0	11.4	0.0	0.0
	Z3-4		0.6	0.0	8.6	0.0	0.0	0.0	0.0	17.2	0.0	4.4
	Z3-5		1.3	71.7	38.5	2.7	100.0	1.0	9.4	45.5	0.0	63.5
	Z3-6		0.4	0.0	17.9	0.0	0.0	0.0	0.0	24.0	0.0	13.2

potential release of metal and metalloids from each weathering agent interacting with the stack must be quantified as well as the factors controlling these processes. Table 6 shows the percentage of each pollutant released with respect to the total chemical composition for the phosphogypsum samples and for the weathering agents used. As it is shown, the rainwater weathering and the leaching under reducing conditions cause the release of high percentages of As, Cd, Cu, Ni and Zn in the saturated and bottom zones of the profile. Except for Cd, the remaining pollutants are leached in higher percentages in saturated zone than in the contact zone of phosphogypsum with marshland soils. These findings are supported by other studies [27,28] which evidence the key role played by sulfate-reducing processes on the contaminant attenuation in phosphogypsum stacks.

On the other hand, the percentages released by seawater are exceptionally high for two of the six samples (Z3-2 and Z3-5). In these samples, the percentages of As, Cd, Cr, Cu, Ni, and Zn released under seawater leaching were twice or three times higher than those obtained with rainwater and reducing conditions, which is consistent with the hazardousness order established for the weathering agents from the US EPA water quality criteria limits. However, the metal and metalloid release potential in the remaining four samples with seawater was low, only Cd and Ni were released at significant rates in these samples (Table 6). The different release rates observed in samples subject to tidal influence within the stack may be related to chemical changes produced during the exposure to weathering agents. Phosphogypsum samples exposed to leaching by meteoric or estuarine waters may have lost most of residual acids and soluble trace elements originally present in comparison to other samples with a lesser contact with these agents. As can be seen in Table 6, the samples with lower potential to release metals and metalloids correspond to those with pH values close to neutrality. The alkalinity contained in seawater is high enough to neutralize the residual acid still contained in these samples, causing metal and metalloid depletion in the leaching solution; only the most mobile metals, such as, Cd and Zn remain in solution. This pH dependence of metal and metalloid release from the phosphogypsum samples has been previously pointed out by Pérez-López et al. [32], who reported a good correlation ($R^2 = 0.79$) between pH and P, which is indicative of H_3PO_4 residual content.

These results have serious implications for restoration strategies and the environmental impact on the surrounding environment. Despite the high potential to release metals and metalloids shown by rainwater, the settlement of impermeable barriers, i.e. clay covers, to avoid water infiltration would mitigate the impact of this weathering agent on the metals and metalloids release to the environment. However, the absence of any isolation barrier in the base of the stack may cause the interaction of estuarine waters with phosphogypsum. Marshland soils act as a nearly impermeable barrier that withholds groundwater in depth and forces the water to flow laterally. When the groundwater reaches the edge of the stack, polluted water emerges forming superficial drainages, known as edge outflows, which release a high load of contaminants into the estuary [10]. According to this latter work, both As and Cd are the main contaminants reaching the estuary through edge outflow waters in highly remarkable percentages in relation to other pollution sources. These findings are in agreement with the results of the leaching tests performed in this study (Table 6) and may pose a great environmental concern. Both toxic pollutants, especially Cd, behave conservatively in estuarine waters [33], which not only poses a significant risk to the majority of species by chronic exposure but may also result in unacceptable effects on these organisms under acute exposure.

Therefore, despite the absence of specific regulations on the management and disposal of these by-products, the hazardousness evidenced by the present study justifies the exploration of alternative restoration measures to avoid the transference of pollutants from these wastes to the environment. Some discrepancies were observed according to the leaching protocols performed based on international regulations (i.e. EU and US). In this sense, these wastes must be deposited in properly conditioned landfills for hazardous wastes according to the EU regulations and in non-hazardous waste landfills after treatment (for Cd removal) according to the US regulation. However, other more cost-effective and environmentally-friendly such as reutilization of this waste or recycling of compounds contained should be also addressed. This later issue has been recently evaluated for Huelva phosphogypsum, suggesting that this waste is a potential source of critical raw materials [34] or Ca for mineral carbon sequestration [35].

5. Conclusions

Despite the high content of contaminants found in phosphogypsum and the proximity of stacks to cities, it is surprising the absence of specific regulations for the management of this waste and the lack of information of metal and metalloid release under different weathering scenarios. This study tries to fill this gap by applying different leaching protocols to the phosphogypsum generated in the Huelva fertilizer plant (SW Spain), assessing the compliance of leachates to current international regulations.

Compared to other stacks around the world, enrichment in Fe, Pb, Sb, Mn, V, Cu, Co, Ni and Cr is observed in the Huelva phosphogypsum. However, the most remarkable finding is the anomalously high concentration of As observed along the whole profile, i.e. between 1 and 2 orders of magnitude higher than those observed in the rest of reported stacks worldwide. This is attributed to the quality of the sulfuric acid used in the manufacturing process (i.e. from As-rich pyrite roasting). The mobility of metals and metalloids under different weathering agents (i.e. rainfall, reducing conditions and seawater) acting simultaneously in Huelva stack was assessed and compared to that reported by, to our knowledge, the only case worldwide applying some of these protocols to phosphogypsum; the giant stack of Mulberry (Florida, US).

The mobility of As and Cd confers the Huelva stacked material the classification of hazardous waste according to EU regulations, while the Mulberry should be considered as a non-hazardous waste by the release of Cu, Mo, Ni and Zn. However, according to US EPA regulation both the Huelva and Mulberry can be considered as non-hazardous wastes due to TCLP limits were not exceeded in any case, although in the case of Huelva, the phosphogypsum must be treated before disposal because exceed the Cd UTS limit for the bottom zone. Two main conclusions can be raised from this comparison: 1) the anomalous metal and metalloid concentrations and higher mobility observed in Huelva compared to Mulberry and 2) the discrepancies observed between EU and US regulations dealing with hazardousness classification of these materials. This latter finding suggests the need to use complementary assessment protocols to obtain a better characterization and classification of these wastes. For this reason, the assessment of the potential effects on the aquatic life under different scenarios has been performed.

The exceedance of limits for Al and, at a lesser extent, Zn in Mulberry phosphogypsum may pose a risk for aquatic life upon acute and chronic exposure. The metal exposure for aquatic life under rainfall weathering and reducing conditions of Huelva is even more severe; Cd exceeds the US EPA water quality criteria limits along the whole profile while other pollutants (Al, As, Pb, Ni, Se and Zn) shows exceedance of these limits at different depths. Only Fe, Cu and Cr values remained below the threshold limits of the aquatic life criteria established by the US EPA along the whole profile. This highlights the higher environmental risk caused by the stockpiling of these wastes in comparison to that of Mulberry and justifies the disposal of these wastes in landfills for hazardous wastes.

The results of this study must be taken into account in the already-started restoration plan of the Huelva phosphogypsum, which only contemplates the use of conventional dry-covers; this situation will mitigate the weathering by rainwater, however, the stack would be subject to seawater weathering. The impact of this weathering agent strongly depends on the acidity balance between the estuarine waters and the acidic phosphogypsum pore-waters. The existence of acid and metal rich outflows from restored zones by dry-covers implies the need of alternative restoration measures to explore new routes for recycling and reuse of these by-products or, at least, to mitigate the metal and metalloid pollution by disposal in landfills for hazardous wastes.

Acknowledgements

This work was supported by the Government of Andalusia through the research project 'Phosphogypsum: from the environmental assessment as a waste to its revaluation as a resource (P12-RNM-2260)'. Authors also want to especially thank the funding support for the Experts Committee on "The environmental diagnosis and the proposal of restoration measures for the phosphogypsum stacks of Huelva", appointed by the City Hall of Huelva. C.R Cánovas was funded by the European Union's Seventh Framework Program, Marie Skłodowska-Curie actions (COFUND–Grant Agreement 291780) and the Ministry of Economy, Innovation, Science and Employment of the Junta de Andalucía. S. Carrero was supported by a research pre-doctoral fellowship AP2010-2117 (Spanish Ministry of Education, Spain). M.P. Asta has received economical support from the Spanish Ministry of Science and Innovation through a Research Contract from the "Juan de la Cierva Subprogram". We would also like to thank Dr. Diana S. Aga (Editor) and two anonymous reviewers for the support and comments that improved the quality of the original paper.

References

[1] H. Tayibi, M. Choura, F.A. López, F.J. Alguacil, A. López-Delgado, Environmental impact and management of phosphogypsum, J. Environ. Manage. 90 (2009) 2377–2386.
[2] J. Yang, W. Liu, L. Zhang, B. Xiao, Preparation of load-bearing building materials from autoclaved phosphogypsum, Constr. Build. Mater. 23 (2009) 687–693.
[3] B.G. Lottermoser, Mine Wastes: Characterization, Treatment and Environmental Impacts, third ed., Springer-Verlag, Berlin, Heidelberg, 2010.
[4] P.M. Rutherford, M.J. Dudas, R.A. Samek, Environmental impacts of phosphogypsum, Sci. Total Environ. 149 (1994) 1–38.
[5] S. Mostary, Trace Metals Leachability Characterization of Phosphogypsum, University of Florida, 2011 (last Accessed 2 September 2016) http://ufdcimages.uflib.ufl.edu/UF/E0/04/30/79/00001/mostary_s.pdf.
[6] R. Pérez-López, J.M. Nieto, J.D. de la Rosa, J.P. Bolivar, Environmental tracers for elucidating the weathering process in a phosphogypsum disposal site: implications for restoration, J. Hydrol. 529 (2015) 1313–1323.
[7] EN 12457-2, Characterization of Waste, Compliance Test for Leaching of Granular Wastes Materials and Sludges, Part 2: One Stage Batch Test at a Liquid to Solid Ratio of 10 l kg-1 for Materials with Particle Size Below 4 mm (without or with Size Reduction), European Committee of Standardization, CEN/TC 292,12/02/2002, p. 28.
[8] US EPA. (US Environmental Protection Agency), TCLP, Method 1311, Rev 0. In SW-846: Test Methods for Evaluating Solid Waste, Physical/Chemical Methods, Office of Solid Waste, Washington, DC, 1992.
[9] US EPA. (US Environmental Protection Agency), National Recommended Water Quality Criteria. http://www2.epa.gov/wqc/national-recommended-water-quality-criteria. (last Accessed 2 September 2016).
[10] R. Pérez-López, F. Macías, C.R. Cánovas, A.M. Sarmiento, S.M. Pérez-Moreno, Pollutant flows from a phosphogypsum disposal area to an estuarine environment: an insight from geochemical signatures, Sci. Total Environ. 553 (2016) 42–51.
[11] F. Macías, M.A. Caraballo, J.M. Nieto, Environmental assessment and management of metal-rich wastes generated in acid mine drainage passive remediation systems, J. Hazard. Mater. 229–230 (2012) 107–114.
[12] M. Vemic, F. Bordas, G. Guibaud, E. Joussein, J. Labanowski, P.N.L. Lens, E.D. van Hullebusch, Mineralogy and metals speciation in Mo rich mineral sludges generated at a metal recycling plant, Waste Manage. 38 (2015) 303–311.
[13] EC Decision 2003/33/CE, Council Decision of 19 December 2002 establishing criteria and procedures for the acceptance of waste at landfills pursuant to Article16 of an Annex II to Directive 1999/31/EC, Off. J. L 011, 16/01/2003 pp. 0027–0049.
[14] US EPA. (US Environmental Protection Agency), Applicability of the Toxicity Characteristic Leaching Procedure to Mineral Processing Wastes, United States Environmental Protection Agency, Washington, DC, April 1998, p. 28.
[15] L.R.P. de Andrade Lima, L.A. Bernardez, L.A.D. Barbosa, Characterization and treatment of artisanal gold mine tailings, J. Hazard. Mater. 150 (2008) 747–753.
[16] S.R. Al-Abed, G. Jegadeesan, J. Purandare, D. Allen, Leaching behavior of mineral processing waste: comparison of batch and column investigations, J. Hazard. Mater. 153 (2008) 1088–1092.
[17] US EPA. (US Environmental Protection Agency), Land Disposal Restrictions, Rules and Regulations, http://www.epa.gov/osw/hazard/tsd/ldr/regs.htm. (last Accessed 2 September 2016).
[18] S.M. Luther, M.J. Dudas, P.M. Rutherford, Radioactivity and chemical characteristics of Alberta phosphogypsum, Water Air Soil Pollut. 69 (3) (1993) 277–290.

[19] A. Carbonell-Barrachina, R.D. DeLaune, A. Jugsujinda, Phosphogypsum chemistry under highly anoxic conditions, Waste Manage. 22 (2002) 657–665.
[20] M.L.S. Oliveira, C.R. Ward, M. Izquierdo, C.H. Sampaio, I.A.S. de Brum, R.M. Kautzmann, S.C. Sabedot, X. Querol, L.F.O. Silva, Chemical composition and minerals in pyrite ash of an abandoned sulphuric acid production plant, Sci. Total Environ. 430 (2012) 34–47.
[21] F.T. da Conceicao, D.M. Bonotto, Radionuclides, heavy metals and fluorine incidence at Tapira phosphate rocks Brazil, and their industrial (by) products, Environ. Pollut. 139 (2006) 232–243.
[22] N.C. da Silva, M. Cipriani, M.H. Taddei, E.A. Fernandes, Leaching Assessment of Radioactive and Non-Radioactive Elements from Brazilian Phosphogypsum. 2 International Symposium on Technologically Enhanced Natural Radiation, Book of Abstracts, Brazil, 1999, p. 124.
[23] P.M. Rutherford, M.J. Dudas, J.M. Arocena, Radioactivity and elemental composition of phosphogypsum produced from three phosphate rock sources, Waste Manage. Res. 13 (1995) 407–423.
[24] M. Choura, M. Keskes, F. Cherif, J. Rouis, Study of the mechanical strength and leaching behavior of phosphogypsum in a sulfur in matrix, Jacobs J. Civil Eng. 1 (1) (2015) 001.
[25] A.M. Abed, R. Sadaqah, M.A. Kuisi, Uranium and potentially toxic metals during the mining, beneficiation, and processing of phosphorite and their effects on ground water in Jordan, Mine Water Environ. 27 (2008) 171–182.
[26] M. Fischetti, Phosphorus lake. Strip-mining Florida to fertilize the nation, Sci. Am. 303 (5) (2010) 62–63.
[27] F. Papanicolaou, S. Antoniou, I. Pashalidis, Redox chemistry of sulphate and uranium in a phosphogypsum tailings dump, J. Environ. Radioactiv. 101 (2010) 601–605.
[28] J. Castillo, R. Pérez-López, A.M. Sarmiento, J.M. Nieto, Evaluation of organic substrates to enhance the sulfate-reducing activity in phosphogypsum, Sci. Total Environ. 439 (2012) 106–113.
[29] A. Sáinz, El SO_2 en Huelva: la historia de una contaminación. Consejería de Medio Ambiente, Dirección general de Prevención y Calidad Ambiental (2005), 182 pp. http://www.juntadeandalucia.es/medioambiente/consolidado/publicacionesdigitales/30-212_EL_SO2_EN_HUELVA_LA_HISTORIA_DE_UNA_CONTAMINACION/30-212.htm. (last Accessed 2 September 2016).
[30] I. Pinedo Vara, Piritas de Huelva Su historia, minería y aprovechamiento, Summa, Madrid, Spain, 1963.
[31] M. Lysandrou, I. Pashalidis, Uranium chemistry in stack solutions and leachates of phosphogypsum disposed at a coastal area in Cyprus, J. Environ. Radioactiv. 99 (2008) 359–366.
[32] R. Pérez-López, J.M. Nieto, I. López-Coto, J.L. Aguado, J.P. Bolívar, Dynamics of contaminants in phosphogypsum of the fertilizer industry of Huelva (SW Spain): From phosphate rock ore to the environment, Appl. Geochem. 25 (2010) 705–715.
[33] A. Hierro, M. Olías, M.E. Ketterer, F. Vaca, J. Borrego, C.R. Cánovas, J.P. Bolívar, Geochemical behavior of metals and metalloids in an estuary affected by acid mine drainage (AMD), Environ. Sci. Pollut. Res. 21 (2014) 2611–2627.
[34] C.R. Cánovas, R. Pérez-López, F. Macías, S. Chapron, J.M. Nieto, S. Pellet-Rostaing, Exploration of fertilizer industry wastes as potential source of critical raw materials, J. Clean. Prod. 143 (2017) 497–505.
[35] I. Romero-Hermida, A. Santos, R. Pérez-López, R. García-Tenorio, L. Esquivias, V. Morales-Flórez, New method for carbon dioxide mineralization based on phosphogypsum and aluminium-rich industrial wastes resulting in valuable carbonated by-products, J. CO2 Util. 18 (2017) 15–22.

Journal of Hazardous Materials 350 (2018) 154–161

Contents lists available at ScienceDirect

Journal of Hazardous Materials

journal homepage: www.elsevier.com/locate/jhazmat

Sulfate reduction processes in salt marshes affected by phosphogypsum: Geochemical influences on contaminant mobility

Rafael Pérez-López[a,*], Sergio Carrero[a,b], Pablo Cruz-Hernández[a,c], Maria P. Asta[d], Francisco Macías[a], Carlos R. Cánovas[a], Clara Guglieri[e], José Miguel Nieto[a]

[a] Department of Earth Sciences & Research Center on Natural Resources, Health and the Environment (Natur HE), University of Huelva, Campus 'El Carmen', 21071, Huelva, Spain
[b] Department of Earth and Planetary Science, University of California Berkeley, McCone Hall, CA, 94720-4767, Berkeley, USA
[c] Department of Mining Engineering, University of Chile, Av. Tupper 2069, 8370451, Santiago, Chile
[d] École Polytechnique Fédérale de Lausanne, Environmental Microbiology Laboratory (EML), Station 6, CH-1015, Lausanne, Switzerland
[e] Elettra-Sincrotrone Trieste, s.s. 14 km 165.3, 34149, Basovizza, Trieste, Italy

GRAPHICAL ABSTRACT

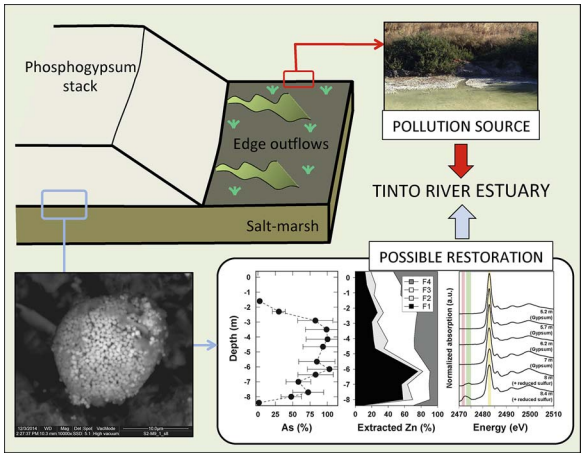

ARTICLE INFO

Keywords:
Phosphogypsum
Salt-marsh
Sulfate reduction
Metal removal
XANES

ABSTRACT

Sulfate reduction and its associated contaminant immobilization in marsh soils supporting a phosphogypsum stack was examined by pore-water and solid analysis, selective extractions, microscopy and sulfur K-edge X-ray absorption near-edge structure (XANES) spectroscopy. The negative impact of this stack on estuarine environments is a concerning problem. In the weathering profile, total concentrations of most pollutants increase with depth; instead, dissolved contents in pore-waters increase to middle of the saturated zone but then decrease drastically down to reach the marsh due to sulfide precipitation. Excess of acid-volatile sulfide plus pyritic sulfur over metals bound to the oxidizable fraction indicates that sulfide precipitation is the main mechanism responsible for metal removal in the marsh. Thus, abundant pyrite occurred as framboidal grains, in addition to other minor sulfides of As, Zn and Cu as isolated particles. Moreover, high contents of elemental sulfur were found, which suggest partial sulfide oxidation, but marsh may have capacity to buffer potential release of contaminants. The importance of sulfur species was quantitatively confirmed by XANES, which also supports the accuracy of selective extraction schemes. Accordingly, managing pore-water quality through organic carbon-rich

* Corresponding author.
E-mail address: rafael.perez@dgeo.uhu.es (R. Pérez-López).

https://doi.org/10.1016/j.jhazmat.2018.02.001
Received 1 September 2017; Received in revised form 1 February 2018; Accepted 3 February 2018
Available online 08 February 2018

amendments over phosphogypsum stacks could lead to a decrease in contaminant loading of leakages resulting from weathering.

1. Introduction

Metal sulfide precipitation can exert a strong control on the species distribution and contaminant mobility under natural conditions in anoxic systems associated with decomposing organic matter. Activity of sulfate-reducing bacteria can be considered as the main mechanism for metal removal from pore-water through insoluble sulfide formation [1–4]. Microbially-mediated sulfate reducing processes can play a crucial role on the natural contamination attenuation in receiving media, as well as on artificial treatment systems [5,6].

Extensive anthropogenic activity and the lack of environmental regulation during the first half of the last century gave rise to many contaminated estuaries in industrialized and urbanized areas worldwide. Estuarine salt-marshes are often the sink of contaminants released from mining and industrial activity developed in the surrounding area. In these organic matter-rich environments, precipitation of sulfide minerals may sequester potentially toxic trace elements [7,8]. However, attenuation associated with these natural processes cannot be considered as a full replacement for restoration technologies, but it can sometimes help decision makers to optimize the best cost-effective and environmental friendly remediation practices [9].

Phosphogypsum is a waste from the production of phosphoric acid by phosphate fertilizer industry following wet chemical digestion of phosphate rock with sulfuric acid. This unwanted waste (mainly gypsum) is often disposed of in large stacks in coastal areas, close to the production plants, as a slurry along with leftover reactants and products from the industrial process [10]. This fact leads to the existence of highly-polluted acidic groundwaters in the waste pile containing high concentrations of metals and radionuclides [11]. Consequently, phosphogypsum stacks commonly constitute a potential source of contamination to the coastal environment [12].

The purpose of this study was to map redox zoning in the weathering profile of a phosphogypsum stack located on an estuarine marsh soil. We traced the formation and spatial distribution of reduced sulfur species in order to elucidate how sulfate-reducing processes in the marsh can control the fate of contaminants in the environment. To achieve this objective, quantitative S speciation data were obtained by combining chemical extractions with S K-edge X-ray absorption near-edge structure (XANES) spectroscopy and electron microscopic observations. Metal contents were analyzed both in pore-waters and in operationally defined selective extractants from solids for mobility discussion. As far as we know, no study has attempted to explore the sulfate-reduction processes associated with phosphogypsum waste and its impact on the environment, especially taking into account the combined use of selective extractions and synchrotron-based spectroscopic techniques. Moreover, this information will allow expanding the overall knowledge about the characteristics that regulate both the residence time and the potential release and transport of metals and metalloids from hazardous wastes to the environmental.

2. Materials and methods

2.1. Study site

The site investigated is a controversial phosphogypsum stack (100 Mt of stockpiled waste and 1200 ha of surface) located directly above salt-marshes of the Tinto River estuary (Huelva, SW Spain), less than 100 m from an urban area with similar extension (Fig. S1 of the Supporting information (SI)). The location of this phosphogypsum stack within the tidal prism makes it a potential source of pollution to the estuarine environment. The excess of highly-polluted acidic water stored in the pore-space of this anthropogenic aquifer emerges forming springs or edge outflows reaching the estuary. Moreover, there is a clear connection between the stack and the estuary, which leads to a potential weathering by seawater intrusion from the deepest part originating these edge outflows. This fact evidences the inefficiency of the preliminary restoration actions based on the addition of an artificial topsoil cover over the bare phosphogypsum [13]. In fact, all disposal modules of the stack, two non-restored zones and other two 'supposedly' restored zones (Fig. S1 of the SI), act as sources of edge outflow waters to the estuary [12].

However, sulfate-reduction and sulfide precipitation processes catalyzed by bacterial activity occur naturally in the salt-marshes supporting the stack and could attenuate some contamination [14]. This deposit area is currently in a legal limbo; the company must ensure environmental restoration of the marsh although only of those areas without previous restoration actions, while social turmoil advocates total restoration or even transportation of the waste to controlled landfills. In this scenario, studying natural processes, such as sulfate reduction in the marsh soils, could allow the optimization of possible effective remediation actions not only in the case of study but also in other estuarine systems affected by industrial waste releases around the world.

2.2. Phosphogypsum coring and sample processing

Phosphogypsum core samples were collected at approx. 0.5 m intervals from stack surface to the underlying marsh soils using a soil-sampling auger (Fig. S1 of the SI). The deepest sample corresponds to the first centimeters of underlying marsh soil (8.4 m at depth). Samples were transferred to polypropylene vacuum bags and rapidly taken to the laboratory within 15 min. At the laboratory, 0.1 μm-filtered pore-waters were collected through suction cup lysimeters under $N_{2(g)}$ atmosphere within a glove box. After pore-water extraction, solid samples were frozen and then lyophilized to complete dryness using a freeze-dryer.

2.3. Chemical and mineralogical analyses

For the pore-water, pH, redox potential (ORP, converted to Eh) and electrical conductivity (EC) were immediately measured after extraction. Determination of Fe(II)/(III) and H_2S concentrations was also immediately performed by spectrophotometric methods. Then, solutions were divided into two aliquots, one not acidified for anion analysis by high performance liquid chromatography (HPLC), and one acidified with HNO_3 to pH < 1 for analysis of major and trace elements by Inductively Coupled Plasma-Optical Emission Spectroscopy (ICP-OES) and Inductively Coupled Plasma-Mass Spectroscopy (ICP-MS), respectively. More details of the analytical procedures are described in the Section S1 of the SI.

For the solid samples, the bulk chemical composition was determined by acid digestion with *aqua regia* in Teflon vessels, and then followed by analysis with ICP-OES and ICP-MS. Sulfur speciation analyses were performed; acid-volatile sulfur (AVS, including amorphous Fe monosulfides (FeS), mackinawite, greigite as well as other HCl-soluble sulfides), pyrite-sulfur (Py-S) and elemental sulfur (ES) were differentiated by a three step sequential digestion, and their concentrations were determined using the method described by Duan et al. [15]. In order to study in detail the partitioning of metals, the following sequential extraction procedure from Rauret et al. [16] was also applied

to the solids: (F1) easily soluble fraction (interchangeable metals, associated with carbonates and those soluble in water or under slight acidic conditions), extracted with 0.11 M acetic acid; (F2) reducible fraction (metals bound to Fe and Mn oxyhydroxides), extracted with 0.1 M hydroxylamine hydrochloride at pH 2; (F3) oxidizable fraction (metals bound to organic matter and sulfides), extracted with hydrogen peroxide and 1 M ammonium acetate at pH 2; and (F4) residual fraction (non-mobile metals strongly bound to the crystalline structures), extracted with *aqua regia*. Solutions from sequential extraction were also analyzed by ICP-MS. Finally, the mineralogy was determined by conventional X-ray diffraction (XRD) with CuKα monochromatic radiation and scanning electron microscopy coupled with energy dispersive spectroscopy (SEM-EDS). Moisture content was determined gravimetrically.

Sulfur K-edge XANES data for the phosphogypsum profile and gypsum, pyrite and elemental sulfur standards were collected at the beamline XAFS of the Synchrotron Elettra Light Source (Trieste, Italy) [17]. XANES data analysis was performed according to standard procedures [18]. The spectra were taken in a range from 2300 to 2700 eV with 0.2 eV step size at the edge region. The spectra were normalized, after background subtraction, by means of Athena software within the IFFEFIT package [19]. The proportion of sulfur species in the samples was calculated by linear combination fitting software included in Athena. Data collection and analysis operations are described in the Section 2 of the SI.

3. Results and discussion

3.1. Sulfate reduction

Values of pH and Eh in the pore-waters along the profile are shown in Fig. 1a. The water table in the phosphogypsum stack was at a depth of approx. 3 m. Pore-waters were characterized by acidic conditions, with pH values that decreased from 3.0 to 2.2 in the unsaturated zone and then were stabilized to 2.1–2.2 in the saturated zone, though with a slight increase in the deepest part (Fig. 1a). This pH increase was more pronounced in the marsh soil surface in contact with phosphogypsum, with a pH of 4.1 (Fig. 1a). Eh values were maintained at around 480 mV in the first 7 m depth, but then decreased progressively toward the marsh to 320 mV (Fig. 1a).

Dissolved sulfate concentrations in pore-water increased gradually with depth from 1.3 to 6.2 g/L (Fig. 1b); while aqueous sulfide concentrations were below detection limit in the entire profile. Dissolved Fe concentrations also increased with depth from 2.4 mg/L in surface to 500 mg/L at 7.5 m depth, being the sharpest increase at this last depth (Fig. 1c). However, correlated to pH increase and Eh decrease, Fe concentrations decreased rapidly in the last meter of the profile up to 270 mg/L. Most of the total Fe corresponded to Fe(III) in the unsaturated zone, between 20 and 60% to Fe(II) in the first meters of the saturated zone, and finally percentages of 100% of Fe(II) are reached in the deepest samples (Fig. 1c).

The partitioning of the reduced sulfur species in the phosphogypsum solid with depth is shown in Fig. 1d. As expected, reduced sulfur species were inexistent in the shallowest 5.5 m depth. From 5.5 m depth, reduced sulfur species, mainly Py-S, were present in all samples down to the marsh base. Elemental sulfur and Py-S were the dominant species of reduced sulfur, especially in the deepest samples, i.e. basement of phosphogypsum stack and first centimeters of marsh, with values of up to 9.34 g/kg and 6.48 g/kg, respectively. AVS concentrations were much lower with values of up to 176 mg/kg in the deepest samples (Fig. 1d).

The geochemical evolution of the pore-water seems to be consistent with the presence of the reduced sulfur species in the solid. The decrease of Fe(II) in the last meter could be due to microbial sulfate reduction and pyrite sulfide precipitation. These processes might have contributed to the increase in pH of the pore-water, due to the alkalinity produced by bacterial activity, and to the decrease of Eh observed in the zone of interaction with salt marshes. Sulfate reduction conditions are commonly associated with Eh values ranging from −300 to 0 mV and circumneutral pH. However, the lower pH values and more positive redox potentials observed in this study have been also previously described in other sulfate-reducing environments [20]. This process naturally occur in acidic environments as long as there are anaerobic conditions, sufficient organic carbon, and the presence of acid-tolerant sulfate-reducing bacteria, as has been previously observed in the Tinto River sediments [21]. Other possibility is that bacterial activity is active in pore-water microenvironments that are more alkaline and reducing than the general solid chemistry.

AVS corresponds to Fe monosulfides which directly form by microbial sulfate reduction in presence of Fe(II) in solution. These monosulfides are the first phases that often precipitate in most natural aqueous systems and act as intermediate precursors necessary for the formation of most stable pyrite through reactions either with H_2S or with ES [22]. In anoxic sediments, Fe monosulfides together with ES can be also generated by abiotic reduction of Fe(III) oxides coupled to the oxidation of aqueous sulfide. The Fe monosulfides and ES so formed

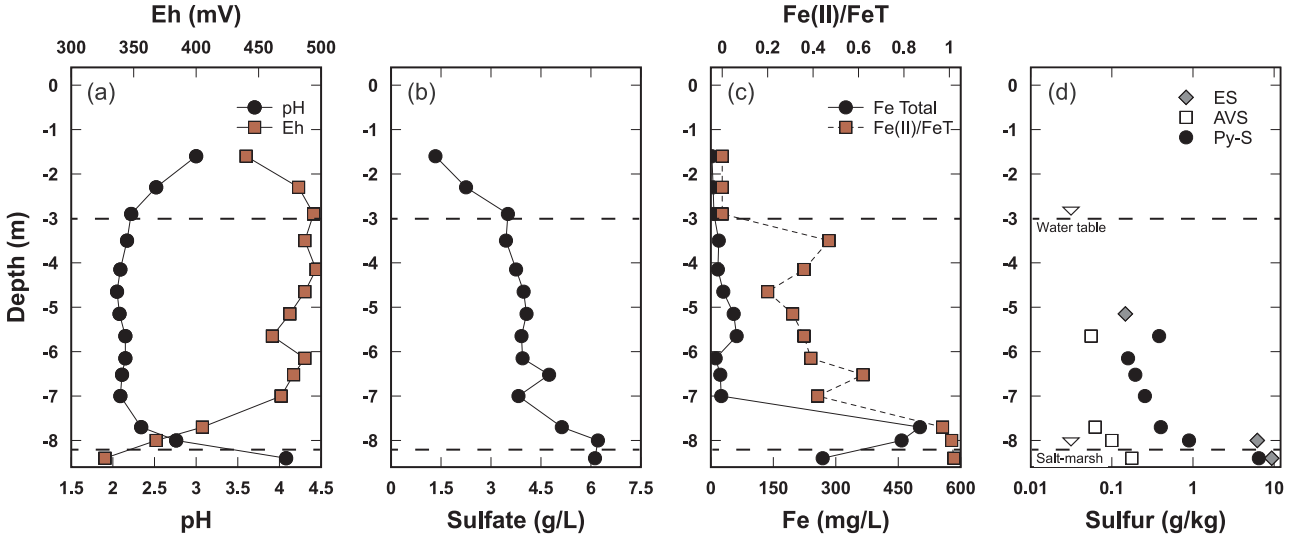

Fig. 1. Depth profiles of (a) pH and Eh, (b) sulfate and (c) Fe concentrations in pore-water solutions, and (d) reduced sulfur species in solid phosphogypsum. Fe(II)/Fe_{total} ratio for pore-waters is also shown in (c).

will react and produce pyrite. In the overall reaction, Fe monosulfides are produced in similar amounts as pyrite, which would explain values of AVS/Py-S ratio close to 1 [23,24]. Thus, the low values of AVS/Py-S ratios found in the deepest samples, 0.16, 0.11 and 0.03 at 7.5 m, 8 m and in the marsh contact, respectively, suggest that formation of Fe monosulfides and their transformation to pyrite is not controlled by the availability of Fe(III) minerals. The fact that the content of aqueous sulfide in pore-water is undetectable can be attributed to low iron-monosulfide solubility under Fe-rich conditions [25], which is reflected in a relatively high concentration of pore-water Fe(II) in the deepest samples. An abundance of pore-water Fe(II) in such depths can lead to iron-monosulfide accumulation due to rapid sequestration of bacterially produced H_2S.

Both AVS and Py-S contents in the deeper samples were within normal values compared to other anoxic sediments contaminated by metals [26–28]. However, ES concentrations were extremely high. This sulfur species is a product from oxidation of sulfides, mainly Fe monosulfides or AVS, as the known reductive processes do not yield free ES [29]. The high concentrations of ES found in this study could be indicative of that this oxidation process is not microbially mediated, since biotic oxidation is negligible due to competition from the very rapid abiotic oxidation rate [27]. The abiotic oxidation of AVS could be also associated to the fact that the Eh values are not as low as in other anoxic sulfide-forming environments. This oxidation process does not imply significant changes in the aqueous S concentration or changes in pH [25]. The oxidation in the contact with marsh sediments could be due to the possible hydrological connection between the stack and the estuary by saline intrusion, as already described in previous studies [12,13].

3.2. Influence on metal mobility

The depth profiles of the concentration of trace elements in pore-water and in phosphogypsum solid are shown in Fig. S2 of the SI. From these data, the percentages of trace elements dissolved in pore-water with respect to the total contents were calculated using sample moisture measurements following Clemente et al. [30] and then plotted in Fig. 2. Full details on these calculations can be found in the Section S3 of the SI. Percentages of dissolved elements in the pore-water space follow the same trend for all contaminants. Values increased with depth in the unsaturated zone until reaching a maximum at the middle of the saturated zone. However, in the last meter of the profile and, mainly, in the contact with the marsh, percentages of all dissolved elements drastically decreased until being depleted from solution (Fig. 2); despite their concentrations in the marsh solid were extremely high in comparison with the rest of the profile (Fig. S2 of the SI).

In the middle of the saturated zone, dissolved percentages reached maximum values of up to 100% for Zn, As and Cu (Fig. 2); i.e., the total amount of these elements was mobile in solution, with concentrations of up to 157, 34.2 and 6.23 mg/L, respectively (Fig. S2 of the SI). The most probable explanation of the high mobility of these contaminants, particularly As, could be related to the quality of the sulfuric acid used in the industrial process, as pointed out by Macías et al. [31]. The sulfuric acid was mainly obtained by roasting pyrite with up to 0.4 wt.% of As. The excess of As-loaded sulfuric acid from the industrial reaction is also deposited along with the phosphogypsum and explains the high mobility observed in the interstices of the stack, which evidences that this phosphogypsum is anomalous compared to others worldwide [31]. On the other hand, lower mobility was observed for the remaining pollutants in the middle of the saturated zone, with values of up to 25–35% for Ni and Sb, 10–20% for Cd, Cr and U, and approx. 5% for Co and Pb. Pore-solutions at these depths were characterized by concentrations of approx. 5 mg/L for U, 1–2 mg/L for Cd, Cr and Ni, and < 1 mg/L for Co, Pb and Sb. Furthermore, Th was absent in the pore-solutions of the entire profile due to its low solubility [32], despite reaching total concentrations of up 10 mg/kg in the solid (Fig. S2 of the SI).

The distribution of percentages of trace elements with respect to

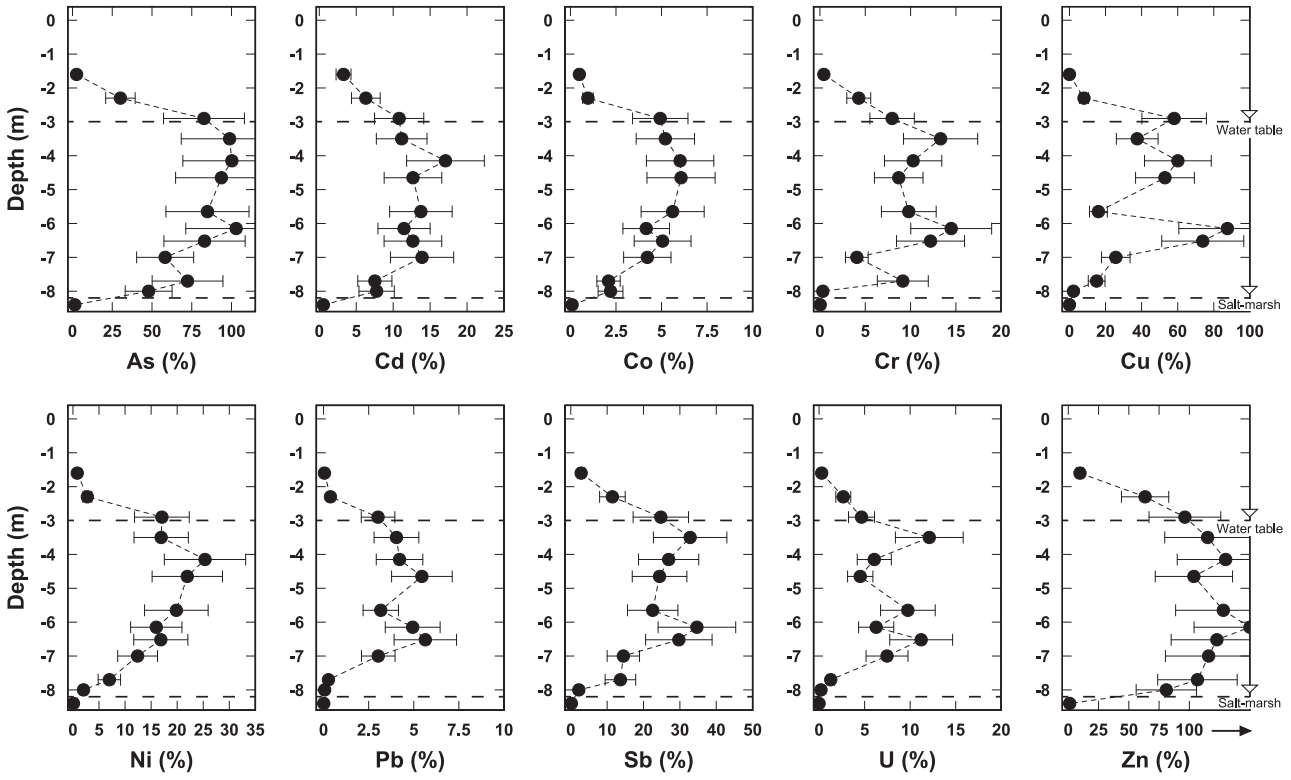

Fig. 2. Depth profiles of the percentages of all dissolved elements in the pore-space expressed as a fraction of the total content. Horizontal bars represent possible variations in the calculations associated with the range of densities found in the literature (see more details in the Section S3 of the SI).

total content with depth, obtained by sequential extraction, is shown in Fig. S3 of the SI. The results confirmed the information on contaminant mobility deduced from pore-water chemistry. Percentages leached in the easily-mobile fraction increased to a maximum value at middle of the saturated zone, particularly in the most abundant trace elements such as As (up to 93%), Zn (76%) and Cu (66%). However, these values sharply decreased towards the transition with the marsh basement. Moreover, a significant increase in the fraction bound to sulfides and organic matter, mainly Cu, Zn and to a lesser extent As, was recorded in the underlying marsh surface, with values of up to 74%, 64% and 11%, respectively (Fig. S3 of the SI). It seems therefore reasonable to suggest that the low availability of these potentially toxic trace elements could be controlled by precipitation of metal sulfides, as observed in numerous studies of estuary sediments affected by natural or anthropogenic sources [1,33–35].

As mentioned before, the AVS to Py-S ratio indicates spontaneous pyritization of AVS, which may be also expected to result in pyritization of trace elements associated with Fe monosulfides [36]. Accordingly, the molar ratio of elements, such as As, Cd, Cr, Cu, Fe, Ni, Pb and Zn, released by sequential extraction in the oxidizable fraction to sulfides could be used to differentiate immobilization by sulfate-reduction and sulfide precipitation from other processes that might occur in reducing conditions. In this sense, the sum of the molar concentration of these metals in the first centimeters of marsh (25.3 µmol/g) was much lower than the sum of AVS (5.50 µmol/g) plus Py-S (202 µmol/g). The molar ratio lower than one would suggest that precipitation of metal sulfides is the main mechanism that contributes to the low availability of metals in the pore-water. The molar deficit of metals could be attributed to that well-crystallized sulfides could become highly insoluble, survive the oxidizable step and be extracted in the non-mobile fraction of the sequential extraction [37]. Therefore, other mechanisms that may control the removal of contaminants in the marsh sediments, such as binding free metal ions in organic compounds [38–40], can be discarded.

On the other hand, uranium (most likely as U^{6+}) may be immobilized in the contact with the marsh by several reduction pathways that often occur in these organic-rich zones: abiotic reduction by iron sulfides that produce uraninite as well as biological mediation via enzymatic activity [41,42]. Due to its low mobility, Th seems to be bound to the insoluble residual phase, as shown by sequential extraction data (Fig. S3 of the SI) and also revealed by previous investigations on phosphogypsum [43].

3.3. Newly-formed solid-phase characterization

Conventional Cu-kα XRD analysis revealed that gypsum is the only crystalline phase in the entire phosphogypsum profile, together with quartz and clay minerals in the first centimeters of marshes (Fig. S4 of the SI). There are no well-defined peaks that allow the identification of the sulfide minerals leading to the contaminant immobilization.

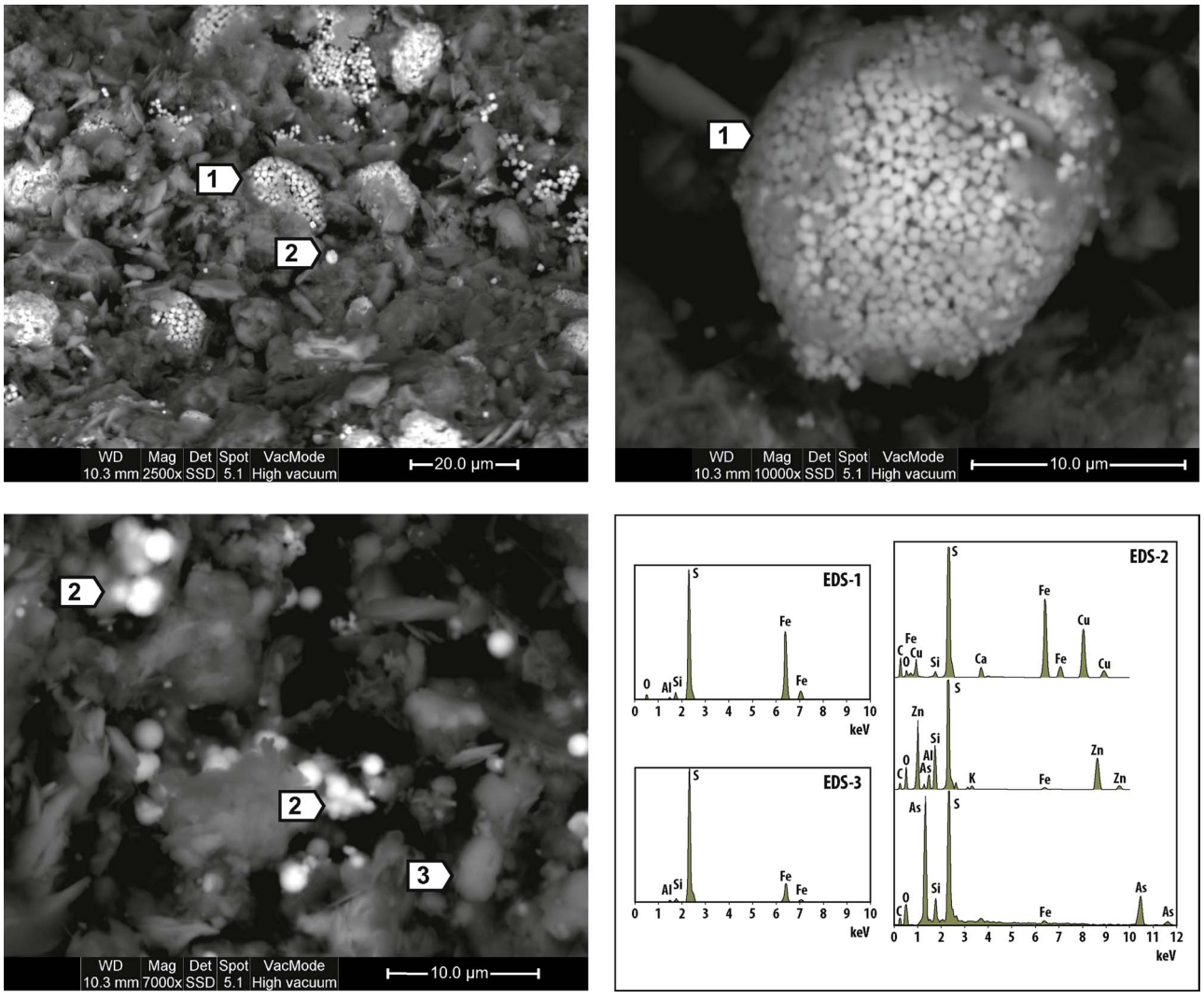

Fig. 3. SEM images and EDS spectra of newly-formed metal sulfides in the phosphogypsum samples located at 8 m depth and in the contact with the salt-marsh.

However, powder samples of the deepest zones examined with SEM contained abundance of authigenic sulfide mineral grains, as revealed by the typical morphology in framboids (Fig. 3). These newly-formed precipitates were not found with SEM in other depths other than near the contact with the marsh sediment. Framboids ranged from 5 to 30 μm in diameter with an average value of ~10 μm and corresponded to pyrite, as shown by EDS analysis (EDS-1; Fig. 3). Octahedral crystallites comprising individual framboids were of uniform size with less than 1 μm in diameter. Some individual spherical crystals of ~1 μm were also present and corresponded to other newly-formed sulfides containing Cu, Zn or As (EDS-2; Fig. 3). Moreover, some pellets or globule-like grains mainly composed by S were attributed to elemental sulfur (EDS-3; Fig. 3).

The lack of diffraction effects of sulfides using conventional X-rays must probably be due to that these newly-formed minerals of cryptocrystalline size precipitate within a set of more abundant and crystalline minerals such as gypsum. However, this limitation can be overtaken using techniques based on synchrotron radiation. Fig. 4 shows the sulfur K-edge XANES spectra of samples from 5 m depth to the first centimeters of marsh soil. The dominant presence of sulfate in all samples was clearly seen by the characteristic peak at ~2482 eV, as can be checked by comparing with the gypsum standard. In the deepest sample of phosphogypsum and in the marsh surface, spectra showed also peaks between 2472 and 2473 eV that could be characteristics of some inorganic sulfides such as pyrite and elemental sulfur, as can be deduced from the standard compounds (Fig. 4). Linear combination fitting of XANES data with contributions from reference standards suggested that gypsum comprised 100% of total S in the phosphogypsum samples to 7 m depth. However, XANES data of the deepest samples exhibited 30% of elemental sulfur in the phosphogypsum at 8 m depth and 29% of elemental sulfur and 6% of pyrite in the marsh contact (Fig. 4).

The relative abundance of the inorganic sulfides identified with XANES was comparable to data from reduced sulfur extraction. No iron monosulfides such as greigite and mackinawite, whose peaks in XANES spectra would be lower than 2472 eV [42], were detected. Therefore, Fe monosulfide concentrations found in the deepest zones, as well as some reduced sulfur species found between 5 and 8 m (Fig. 1d), should be below detection limit even by using synchrotron techniques. On the other hand, the absence of sulfur in organic forms in the deepest samples, whose peaks would be higher than 2473 eV [44], again suggests that the sulfide precipitation is the main mechanism that decreases mobility and, consequently, reduces bioavailability of contaminants, as above deduced by the ratio between sequential extraction oxidizable metals and sulfides. As mentioned previously, abundance of elemental sulfur suggests sulfide oxidation processes likely linked to a deep seawater recharge. Albeit, attenuating capacity of the sulfate-reduction processes seems to limit the potential re-release of metals during such oxidation.

4. Environmental implications

Given the uncertain future of the phosphogypsum stack, managing pore-water quality should be a priority action since excess of groundwater is currently the main vector of contamination through edge outflows to the Tinto River estuary. Chemical composition of edge outflows is very similar to that found in pore-water in the middle of the saturated zone, where maximum levels of contamination were observed, which would be indicative of stagnant and non-renewable waters near marshland basement associated to possible subsidence due to overpressure [13]. In these deepest zones, awareness of sulfate-reduction processes in the contact with marsh sediment could be critical before setting up any remediation attempt. In fact, this route of action could be occurring now in those previously restored zones.

Two of the four disposal modules forming the stack have similar characteristics; i.e., the same amount of phosphogypsum was approximately dumped, in the same period of time and using the same technical procedure. It would, therefore, be reasonable to assume that chemical characteristics of the edge outflow waters in both zones are also similar. The only difference is that one zone was already restored by a complex cover of artificial topsoil (zone 4; Fig. S1 of the SI) while the other zone remains unrestored (zone 3; Fig. S1 of the SI). Initially, the cover in the restored zone was installed to prevent weathering by rainwater infiltration and, thus, eliminate edge outflows. In contrast, despite such remediation actions, deep seawater intrusion continues with the leaching process and, hence, with the release of toxic elements to the estuary. However, edge outflows from the 'supposedly' restored zone are equally numerous although with 50% less contaminant loading, mainly As, Cr, Cu and U, than those of the unrestored zone [12].

One of the layers of the complex artificial-soil cover of the restored zone is an organic matter-rich vegetal level that, according to previous laboratory experiments [45], seems to be currently acting as a carbon source that enhances the activity of naturally-occurring sulfate-reducing bacteria in the phosphogypsum. This remediation mechanism was not initially expected, but it could contribute, together with that occurring in the marsh contact, to greater immobilization of pollutants by

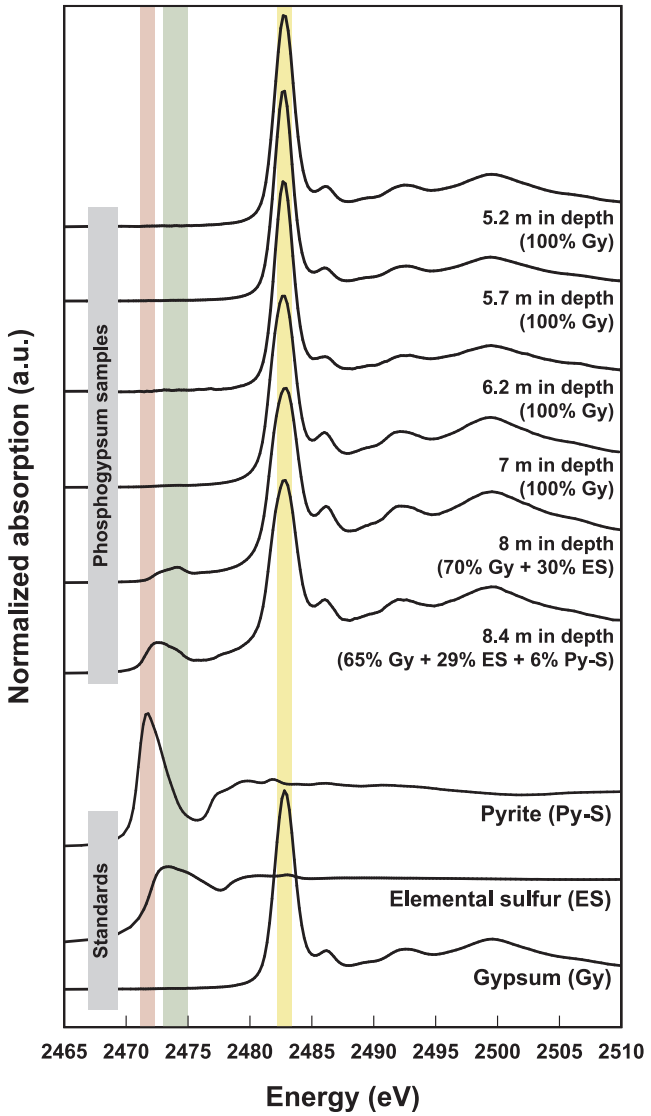

Fig. 4. Sulfur XANES spectra of phosphogypsum samples from 5 m depth to the first centimeters of salt-marsh, together with the reference compounds used for linear combination fitting and the obtained results.

sulfate-reduction processes than in the unrestored zone. In fact, it has been proven that in situ passive amendments of acidic pore-water bearing tailings with a small and dispersed mass of organic carbon have potential to support sulfate-reduction and minimize the associated contaminant loading to receiving waters [46,47]. Thus, these findings could help to optimize the guidelines for restoration actions that are currently being planned.

5. Conclusions

This research is focused on investigating the mobility of trace elements in phosphogypsum piles that have been dumped on estuarine salt-marshes at the bank of the Tinto River estuary (SW Spain) for years. The study describes some sulfate-reduction processes occurring at the contact between stack and marsh and naturally attenuating pollution reaching the estuary through edge outflows. According to the results here presented, expanding such sulfate-reduction processes to the entire phosphogypsum profile with the optimized use of organic carbon-rich amendments could reduce significantly the mobility of contaminants that are subsequently discharged to the Tinto River estuary, which should be taken into account in the already-started restoration. These findings also preclude the social demand of transportation to controlled landfills, because dredgeding and re-dumping polluted anoxic sediments can cause oxidation and release of trace elements bound to sulfides to the environment.

Acknowledgements

This work was supported by the Government of Andalusia through the research project FOREVER (P12-RNM-2260) and by the Spanish Ministry of Economic and Competitiveness through the research project CAPOTE (CGL2017-86050-R). The authors are very grateful to the funding support for the Committee of Experts on “The environmental diagnosis and the proposal of measures of restoration of the phosphogypsum stacks of Huelva”, appointed by the City Hall of Huelva. Very special thanks also go to the XAFS beamline staff at ELETTRA for their assistance during our XANES experiments (20140064 and 20145106). C.R. Cánovas was funded by the Talent consolidation program of the University of Huelva. The analytical assistance of María Jesús Vílchez from the CIDERTA of the University of Huelva is gratefully acknowledged. We would also like to thank Dr. Gerasimos Lyberatos for the editorial handling and two anonymous reviewers for the support and comments that significantly improved the quality of the original paper.

Appendix A. Supplementary data

Supplementary material related to this article can be found, in the online version, at doi:https://doi.org/10.1016/j.jhazmat.2018.02.001.

References

[1] J.W. Morse, G.W. Luther, Chemical influences on trace metal–sulfide interactions in anoxic sediments, Geochim. Cosmochim. Acta 63 (1999) 3373–3378.
[2] G. Billon, B. Ouddane, J. Laureyns, A. Boughriet, Chemistry of metal sulfides in anoxic sediments, Phys. Chem. 3 (2001) 3586–3592.
[3] D.B. Kosolapov, P. Kuschk, M.B. Vainshtein, A.V. Vatsourina, A. Wiebner, M. Kastner, R.A. Muller, Microbial processes of heavy metal removal from carbon-dericient effluents in constructed wetlands, Eng. Life Sci. 4 (2004) 403–411.
[4] L. Lesven, Y. Gao, G. Billon, M. Leermakers, B. Ouddane, J.C. Fischer, Early diagenesis processes aspects controlling the mobility of dissolved trace metals in three riverine sediment columns, Sci. Total Environ. 407 (2008) 447–459.
[5] S.G. Benner, W.D. Gould, D.W. Blowes, Microbial population associated with the generation and treatment of acid-mine drainage, Chem. Geol. 169 (2000) 435–448.
[6] A.H. Kaksonen, J.A. Puhakka, Sulfate reduction based bioprocesses for the treatment of acid mine drainage and the recovery of metals, Eng. Life Sci. 7 (2007) 541–564.
[7] W. Machado, M.F. Carvalho, R.E. Santelli, J.E.L. Maddock, Reactive sulfide relationship with metals in sediments from an eutrophicated estuary in Southeast Brazil, Mar. Pollut. Bull. 49 (2004) 89–92.
[8] E.D. Burton, I.R. Phillips, D.W. Hawker, Factors controlling the geochemical partitioning of trace metals in estuarine sediments, Soil Sediment. Contam. 15 (2006) 253–276.
[9] P. Werner, W. Bae, J.E. Odencrantz, Foreword (preface for the special issue on natural attenuation), Biodegradation 15 (2004) 347.
[10] H. Tayibi, M. Choura, F.A. López, F.J. Alguacil, A. López-Delgado, Environmental impact and management of phosphogypsum, J. Environ. Manage. 90 (2009) 2377–2386.
[11] P.M. Rutherford, M.J. Dudas, R.A. Samek, Environmental impacts of phosphogypsum, Sci. Total Environ. 149 (1994) 1–38.
[12] R. Pérez-López, F. Macías, C.R. Cánovas, A.M. Sarmiento, S.M. Pérez-Moreno, Pollutant flows from a phosphogypsum disposal area to an estuarine environment: an insight from geochemical signatures, Sci. Total Environ. 553 (2016) 42–51.
[13] R. Pérez-López, J.M. Nieto, J.D. de la Rosa, J.P. Bolívar, Environmental tracers for elucidating the weathering process in a phosphogypsum disposal site: implications for restoration, J. Hydrol. 529 (2015) 1313–1323.
[14] R. Pérez-López, J. Castillo, A.M. Sarmiento, J.M. Nieto, Assessment of phosphogypsum impact on the salt-marshes of the Tinto river (SW Spain): role of natural attenuation processes, Mar. Pollut. Bull. 62 (2011) 2787–2796.
[15] W.M. Duan, M.L. Coleman, K. Pye, Determination of reduced sulphur species in sediments – an evaluation and modified technique, Chem. Geol. 141 (1997) 185–194.
[16] G. Rauret, J.F. López-Sánchez, A. Sahuquillo, R. Rubio, C.I. Davidson, A. Ure, P. Quevauviller, Improvement of the BCR three step sequential extraction procedure prior to the certification of new sediment and soil reference materials, J. Environ. Monit. 1 (1999) 54–61.
[17] A. Di Cicco, G. Aquilanti, M. Minicucci, E. Principi, N. Novello, A. Cognigni, L. Olivi, Novel XAFS capabilities at ELETTRA synchrotron light source, J. Phys.: Conf. Ser. 190 (6) (2009) 012043.
[18] G. Bunker, Introduction to XAFS. A Practical Guide to X-Ray Absorption Fine Structure Spectroscopy, Cambridge University Press, New York, 2010.
[19] B. Ravel, M.J. Newville, ATHENA, ARTEMIS, HEPHAESTUS: data analysis for X-ray absorption spectroscopy using IFEFFIT, J. Synchrotron. Rad. 12 (2005) 537–541.
[20] C.D. Church, R.T. Wilkin, C.N. Alpers, R.O. Rye, R.B. McCleskey, Microbial sulfate reduction and metal attenuation in pH 4 acid mine water, Geochem. Trans. 8 (14) (2007) 10.
[21] A.P. Florentino, J. Weijma, A.J.M. Stams, I. Sánchez-Andrea, Sulfur reduction in acid rock drainage environments, Environ. Sci. Technol. 49 (2015) 11746–11755.
[22] R.A. Berner, Sedimentary pyrite formation, Am. J. Sci. 268 (1970) 1–23.
[23] D.T. Rickard, The kinetics and mechanisms of pyrite formation at low temperatures, Am. J. Sci. 275 (1975) 636–652.
[24] J.J. Middelburg, Organic carbon, sulphur, and iron in recent semi-euxinic sediments of Kau Bay, Indonesia, Geochim. Cosmochim. Acta 55 (1991) 815–828.
[25] E.D. Burton, R.T. Bush, L.A. Sullivan, R.K. Hocking, D.R.G. Mitchell, S.G. Johnston, R.W. Fitzpatrick, M. Raven, S. McClure, L.Y. Jang, Iron-monosulfide oxidation in natural sediments: resolving microbially mediated S transformations using XANES, electron microscopy, and selective extractions, Environ. Sci. Technol. 43 (2009) 3128–3134.
[26] J.W. Morse, J.C. Cornwell, Analysis and distribution of iron sulfide minerals in recent anoxic marine sediments, Mar. Chem. 22 (1987) 55–69.
[27] E.D. Burton, L.A. Sullivan, R.T. Bush, B. Powell, Iron-sulfide and trace element behaviour in sediments of Coombabah Lake, Moreton Bay (Australia), Mar. Pollut. Bull. 56 (2008) 1353–1358.
[28] A.M. Sarmiento, M. Olías, J.M. Nieto, C.R. Cánovas, J. Delgado, Natural attenuation processes in two water reservoirs receiving acid mine drainage, Sci. Total Environ. 407 (2009) 2051–2062.
[29] H. Troelsen, B.B. Jørgensen, Seasonal dynamics of elemental sulfur in two coastal sediments, Estuar. Coast. Shelf Sci. 15 (1982) 255–266.
[30] R. Clemente, N.M. Dickinson, N.W. Lepp, Mobility of metals and metalloids in a multi-element contaminated soil 20 years after cessation of the pollution source activity, Environ. Pollut. 155 (2008) 254–261.
[31] F. Macías, C.R. Cánovas, P. Cruz-Hernández, S. Carrero, M.P. Asta, J.M. Nieto, R. Pérez-López, An anomalous metal-rich phosphogypsum: characterization and classification according to international regulations, J. Hazard. Mater. 331 (2017) 99–108.
[32] M.B. Nisti, C.R. Saueia, L.H. Malheiro, G.H. Groppo, B.P. Mazzilli, Lixiviation of natural radionuclides and heavy metals in tropical soils amended with phosphogypsum, J. Environ. Radioact. 144 (2015) 120–126.
[33] P.M. Chapman, F. Wang, C. Janssen, G. Persoone, H.E. Allen, Ecotoxicity of metals in aquatic sediments: binding and release, bioavailability, risk assessment, and remediation, Can. J. Fish. Aquat. Sci. 55 (1998) 2221–2243.
[34] S.L. Simpson, L. Rochford, G.F. Birch, Geochemical influences on metal partitioning in contaminated estuarine sediments, Mar. Freshw. Res. 53 (2002) 9–17.
[35] P.R. Teasdale, S.C. Apte, P.W. Ford, G.E. Batley, L. Koehnken, Geochemical cycling and speciation of copper in waters and sediments of Macquarie Harbour, western Tasmania, Estuar. Coast. Shelf Sci. 57 (2003) 475–487.
[36] M.A. Huerta-Diaz, J.W. Morse, Pyritization of trace metals in anoxic marine sediments, Geochim. Cosmochim. Acta 56 (1992) 2681–2702.
[37] U. Förstner, Chemical forms and reactivities of metals in sediments, in: R. Leschber, R.D. Davis, P. L'Hermite (Eds.), Chemical Methods for Assessing Bio-Available Metals in Sludges and Soils, Elsevier, London, 1985, pp. 1–31.
[38] K.C. Yu, L.J. Tsai, S.H. Chen, S.T. Ho, Chemical binding of heavy metals in anoxic river sediments, Water Res. 35 (2001) 4086–4094.
[39] C.G. Ingersoll, D.D. MacDonald, W.G. Brumbaugh, B.T. Johnson, N.E. Kemble, J.L. Kunz, T.W. May, N. Wang, J.R. Smith, D.W. Sparks, D.S. Ireland, Toxicity assessment of sediments from the Grand Calumet River and Indiana Harbor Canal in northwestern Indiana, USA, Arch. Environ. Contam. Toxicol. 43 (2002) 156–167.

[40] K. Spencer, R. Dewhurst, P. Penna, Potential impacts of water injection dredging on water quality and ecotoxicity in Limehouse Basin, River Thames, SE England, UK, Chemosphere 63 (2006) 509–521.
[41] S.P. Hyun, J.A. Davis, K. Sun, K.F. Hayes, Uranium(VI) reduction by iron(II) monosulfide mackinawite, Environ. Sci. Technol. 46 (2012) 3369–3376.
[42] N. Janot, J.S. Lezama Pacheco, D.Q. Pham, T.M. O'Brien, D. Hausladen, V. Noël, F. Lallier, K. Maher, S. Fendorf, K.H. Williams, P.E. Long, J.R. Bargar, Physico-chemical heterogeneity of organic-rich sediments in the rifle aquifer, CO: impact on uranium biogeochemistry, Environ. Sci. Technol. 50 (2016) 46–53.
[43] A.J.G. Santos, B.P. Mazzilli, D.I.T. Fávaro, P.S.C. Silva, Partitioning of radionuclides and trace elements in phosphogypsum and its source materials based on sequential extraction methods, J. Environ. Radioact. 87 (2006) 52–61.
[44] J. Prietzel, J. Thieme, N. Tyufekchieva, D. Paterson, I. McNulty, I. Kögel-Knabner, Sulfur speciation in well-aerated and wetland soils in a forested catchment assessed by sulfur K-edge X-ray absorption near-edge spectroscopy (XANES), J. Plant Nutr. Soil Sci. 172 (2009) 393–403.
[45] J. Castillo, R. Pérez-López, A.M. Sarmiento, J.M. Nieto, Evaluation of organic substrates to enhance the sulfate-reducing activity in phosphogypsum, Sci. Total Environ. 439 (2012) 106–113.
[46] A.H.M. Hulshof, D.W. Blowes, W.D. Gould, Evaluation of in situ layers for treatment of acid mine drainage: a field comparison, Water Res. 40 (2006) 1816–1826.
[47] M.B.J. Lindsay, D.W. Blowes, P.D. Condon, C.J. Ptacek, Managing pore-water quality in mine tailings by inducing microbial sulfate reduction, Environ. Sci. Technol. 43 (2009) 7086–7091.

Water Research 140 (2018) 344–353

Contents lists available at ScienceDirect

Water Research

journal homepage: www.elsevier.com/locate/watres

Stable isotope insights into the weathering processes of a phosphogypsum disposal area

Evgenia-Maria Papaslioti [a, b, *], Rafael Pérez-López [b], Annika Parviainen [a], Francisco Macías [b], Antonio Delgado-Huertas [a], Carlos J. Garrido [a], Claudio Marchesi [c], José M. Nieto [b]

[a] Instituto Andaluz de Ciencias de la Tierra, CSIC & UGR, Avenida de las Palmeras 4, 18100 Armilla Granada, Spain
[b] Department of Earth Sciences & Research Center on Natural Resources, Health and the Environment, University of Huelva, Campus 'El Carmen', E-21071 Huelva, Spain
[c] Department of Mineralogy and Petrology, UGR, Avda. Fuentenueva s/n, E-18002 Granada, Spain

ARTICLE INFO

Article history:
Received 19 December 2017
Received in revised form
28 March 2018
Accepted 26 April 2018
Available online 28 April 2018

Keywords:
Isotopic tracers
Phosphogypsum
Huelva estuary
Weathering model
Water source
Ternary mixing

ABSTRACT

Highly acidic phosphogypsum wastes with elevated potential for contaminant leaching are stack-piled near coastal areas worldwide, threatening the adjacent environment. Huge phosphogypsum stacks were disposed directly on the marshes of the Estuary of Huelva (SW Spain) without any impermeable barrier to prevent leaching and thus, contributing to the total contamination of the estuarine environment. According to the previous weathering model, the process water ponded on the surface of the stack, initially used to carry the waste, was thought to be the main washing agent through its infiltration and subsequently the main component of the leachates emerging as the edge outflows. Preliminary restorations have been applied to the site and similar ones are planned for the future considering process water as the only pollution agent. Further investigation to validate the pollution pathway was necessary, thus an evaluation of the relationship between leachates and weathering agents of the stack was carried out using stable isotopes ($\delta^{18}O$, $\delta^{2}H$, and $\delta^{34}S$) as geochemical tracers. Quantification of the contribution of all possible end-members to the phosphogypsum leachates was also conducted using ternary mixing via the stable isotopic tracers. The results ruled out ponded process water as main vector of edge outflow pollution and unveiled a continuous infiltration of estuarine waters to the stack implying that is subjected to an open weathering system. The isotopic tracers revealed a progressive contribution downstream from fluvial to marine signatures in the composition of the edge outflows, depending on the location of each disposal zone within the different estuarine morphodynamic domains. Thus, the current study suggests that the access of intertidal water inside the phosphogypsum stack, for instance through secondary tidal channels, is the main responsible for the weathering of the waste in depth, underlying the necessity for new, more effective restorations plans.

1. Introduction

The phosphate fertilizer industry is responsible for the generation of a waste by-product, known as phosphogypsum (mainly gypsum, $CaSO_4 \cdot 2H_2O$), during the production of phosphoric acid (H_3PO_4) via the wet chemical digestion of phosphate ore (fluorapatite, $Ca_5(PO_4)_3F$) with sulphuric acid (H_2SO_4). The overall chemical reaction can be written ideally as (Eq. (1)):

$$Ca_5(PO_4)_3F + 5H_2SO_4 + 10H_2O \rightarrow 3H_3PO_4 + 5CaSO_4 \cdot 2H_2O + HF \quad (1)$$

The phosphate rock containing potentially toxic metal (loid)s and radionuclides as impurities is pre-concentrated by flotation, a process enhanced by reagents such as ammonium hydroxide or amine (Rutherford et al., 1994). Elevated concentrations of contaminants from the raw phosphate ore are then transferred into the

* Corresponding author. Instituto Andaluz de Ciencias de la Tierra, CSIC & UGR, Avenida de las Palmeras 4, 18100 Armilla Granada, Spain.
E-mail addresses: empapaslioti@correo.ugr.es (E.-M. Papaslioti), rafael.perez@dgeo.uhu.es (R. Pérez-López), aparviainen@iact.ugr-csic.es (A. Parviainen), francisco.macias@dgeo.uhu.es (F. Macías), antonio.delgado@csic.es (A. Delgado-Huertas), claudio@ugr.es (C.J. Garrido), carlos.garrido@csic.es (C. Marchesi), jmnieto@uhu.es (J.M. Nieto).

https://doi.org/10.1016/j.watres.2018.04.060
0043-1354/

resulting phosphogypsum (Rutherford et al., 1994; Bolívar et al., 2009; Pérez-López et al., 2010). Phosphogypsum, also, contains residual reagents and products from the industrial process trapped in its interstices, mainly phosphoric acid which is not fully separated in the factory, but also sulphuric and hydrofluorosilicic acids, increasing the acidity of the waste (Lottermoser, 2010). Thus, phosphogypsum is considered as a significant source of environmental contamination (Pérez-López et al., 2016).

The phosphate fertilizer industry is witnessing growth in order to maintain the farming production worldwide. Thus, huge amounts of phosphogypsum are also produced, while potential applications do not often meet the condition of high-consumption (Cánovas et al., 2018). The wet process that produces phosphoric acid requires a large volume of water, commonly known as process water, for a multitude of uses in the industrial complex. Process water is used, for instance, to slurry the phosphogypsum produced and transport it to storage in large stacks close to the fertilizer plants that are exposed to weathering conditions. Additionally, process water is often stored in ponds maintained on top of the stacks, forming a waste facility that can pose serious threat to the adjacent environment due to their potential leaching (Tayibi et al., 2009). Nevertheless, there are no formal regulations for the management of such hazardous material (Macías et al., 2017), despite its worldwide impact in many phosphogypsum disposal areas (see review in Tayibi et al., 2009).

Phosphoric acid plants and, hence, phosphogypsum stacks are often located in coastal areas, due to their relatively flat surface for the industrial activity, the nearby water availability and the proximity of the sea as a means of communication (Lysandrou and Pashalidis, 2008; Sanders et al., 2013; El Samad et al., 2014; El Zrelli et al., 2015). One of these paradigmatic phosphogypsum disposal areas is located at the Huelva Estuary (SW Spain), formed by the confluence of the Tinto and Odiel Rivers (Fig. 1a). Phosphogypsum was stack-piled on the salt-marshes of the right margin of the Tinto River estuary; however, similar, nearby salt marshes in the Odiel River, were declared as UNESCO Biosphere Reserve and RAMSAR-NATURA wetland with high-priority protection status. Acidic liquid effluents from the leaching of the stack, known as edge outflows, are highly concentrated in toxic elements and are a major source of contamination to the estuarine environment (Pérez-López et al., 2015). The Estuary of Huelva is, additionally, polluted by the Tinto and Odiel Rivers that are highly affected by acid mine drainage (AMD) resulting from sulphide oxidation in wastes from the abandoned mining activity in the Iberian Pyrite Belt (IPB) (Nieto et al., 2013).

Preliminary restorations have been already applied in some of the phosphogypsum modules and similar ones are planned for the future. These actions are based on the assumption that edge outflows originate mainly from the process water ponded on surface that infiltrates the piles and reaches the edge of the stack, hence, they focus on eliminating only that agent. However, Pérez-López et al. (2015) suggested that both types of phosphogypsum leachates are poorly connected using Cl/Br ratios and rare earth elements (REE) as geochemical tracers. Indeed, the absence of process water ponded on the surface of a 'supposedly' restored zone has not prevented the presence of numerous discharge points reaching the estuary until nowadays, which demonstrate the inefficiency of the restorations (Pérez-López et al., 2016). These authors proposed a possible pollutant dispersion pathway associated with the leaching of the phosphogypsum in depth through the input of estuarine waters.

Therefore, the current research aims to corroborate these previous studies by providing a full insight into the weathering processes occurring in the disposal area, to validate the main pollution pathway on which restorations should be based and more importantly, quantify the exact contribution of all the possible end-members as washing agents. Stable isotopes are widely used in many environmental studies as one of the most powerful tool for determining water sources and fluxes in a variety of systems (Peterson and Fry, 1987). One of their applications is the determination of the proportional contribution of more than one end-member to a final solution for the identification of pollution sources (Phillips, 2001; Zencich et al., 2002; Phillips and Gregg, 2003), hence in the present study they served as undeniable tracers for determining the main pollution source of the phosphogypsum waste. Stable hydrogen, oxygen and sulphur isotopes were used for the first time as geochemical tracers regarding the phosphogypsum, in order to identify and quantify -using ternary mixing-the contribution of the possible weathering agents (process water, seawater and river water) that lead to the formation of edge outflows. The validation of the pollution pathway would be of paramount importance for future effective restoration plans, as the appliance of the current measures does not prevent the contaminated leachates from reaching the estuarine and the coastal environments. The proposed methodology and the results obtained could be useful for further knowledge of the pollution pathway in phosphogypsum stacks located in coastal areas worldwide.

2. Study area

The industrial production of phosphoric acid in Huelva led to the disposal of around 100 Mt of phosphogypsum waste, between 1968 and 2010, directly on the salt marshes without any impermeable barrier to prevent leaching. Until 1997, phosphogypsum was transported as aqueous slurry to several decantation zones, in an open-circuit system, using seawater that was poured into the estuary after use. However, due to the enforcement of more strict environmental regulations, the factory was forced to avoid any direct discharge to the estuary according to the OSPAR convention (OSPAR, 2002; 2007). As such, from 1997 to 2010, the new waste management plan included the deposition of phosphogypsum in a large pyramidal pile over a single zone using a closed-circuit system with freshwater as process water. In this latter system, large superficial ponds were created on the stacks in order to contain the process water and lose it by evaporation, along with perimeter channels to collect all leachates from the piles.

At present, the disposal area is clearly divided into four zones (Fig. 1a and b); the zones 1 (35 Mt; 400 ha and 2–3 m in height) and 4 (30 Mt; 280 ha and 8–10 m in height) are currently considered as restored areas, i.e. without process water and with a top cover. In particular, zone 1 is covered by natural soil and vegetation, while zone 4 has a more complex cover including building wastes, industrial wastes and topsoil. On the other hand, the zones 2 (25 Mt; 240 ha and up to 30 m in height) and 3 (15 Mt; 200 ha and 8–12 m in height) are directly exposed to weathering without restoration actions, i.e. uncovered and with surface ponds of process water. The phosphogypsum of zones 1, 3 and 4 was deposited using the open-circuit system with seawater; on the other hand, the dumping sequence in the pyramidal zone 2 comprises a first filling stage with seawater before 1997 and a second stage with process water after 1997. As stated before, all disposal modules are source of numerous edge outflows discharging into the estuarine environment (Pérez-López et al., 2016).

The stacks are located within the tidal prism of the Huelva Estuary, which is between 37 and 82 hm^3 during a half cycle (6 h) (Grande et al., 2000). Its localization and the lack of composite liners at the bottom of the pile, could have a great influence on the possible weathering model of the phosphogypsum wastes by means of estuarine water, as can be elucidated simply by looking at the marshlands prior to the dumping. In 1956, numerous secondary

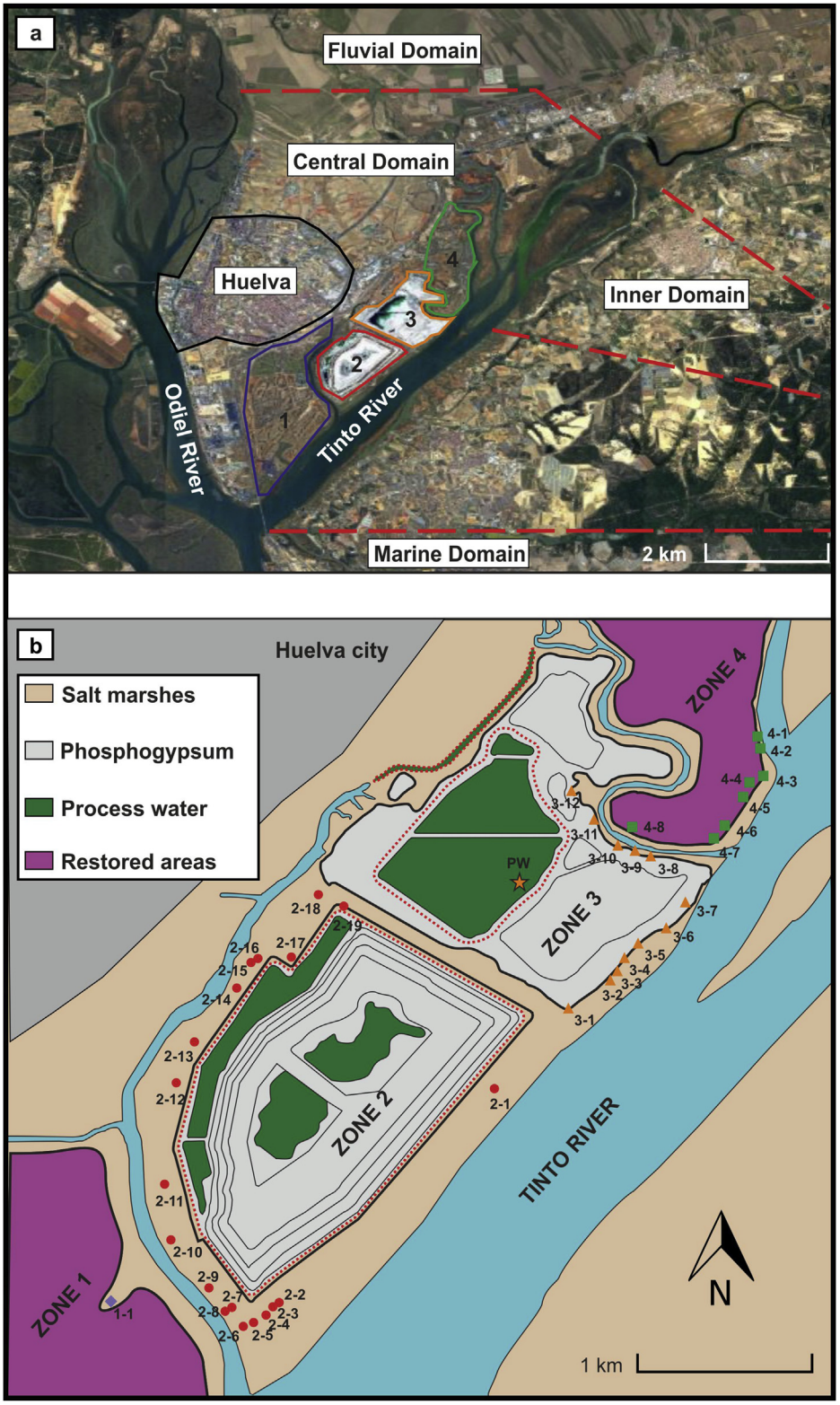

Fig. 1. Location map of the different zones of the phosphogypsum stack within the Estuary of Huelva: (a) Google Earth© image with the morphodynamc domains of the estuary according to Morales et al. (2008), and (b) Schematic image with the sampling points of edge outflows. Additional geographic details are available as Supplemental data.

tidal channels were present in the area, which were regularly flooded by the tides (Fig. S1a of the Supporting Information (SI)). Currently, those channels are covered by phosphogypsum, although they are probably preferential flow zones that allow the intertidal water to access the interior of the stack (Fig. S1b of the SI). In fact, some of the secondary tidal channels are sensed below the phosphogypsum stack and act as preferential via for the discharge of ponded process water in the zone 3 (Fig. S1c of the SI).

Accordingly, the weathering processes related to the leaching of the phosphogypsum stack could be influenced by the different morphodynamic domains in which the Estuary of Huelva is divided. The fluvial domain comprises the upper part of the estuary with a greater influence of the Tinto River and its pollution by AMD, the inner domain is characterised by mixing of fluvial and tidal waters, while the central and the marine domains are dominated by tidal-related processes (Morales et al., 2008). In this respect, zone 1 is close to the marine domain, zones 2 and 3 are in the central domain, and zone 4 is within the inner domain near the fluvial domain (Fig. 1a).

3. Materials and methods

3.1. Sampling and preparation

In June 2016, a total of 40 edge outflow samples were collected at different locations in the perimeter of the phosphogypsum stack (Fig. 1b); at zone 1 only one possible point was identified and sampled, whereas the most outflow points were sampled at zones 2 (n = 19), 3 (n = 12) and 4 (n = 8). One sample for each possible end-member associated with the weathering of the phosphogypsum stack was also collected for comparison purposes; close-circuit process water ponded on the surface of the zone 3 (PW) (Fig. 1b), AMD-affected fluvial water from the mouth of the Tinto River (TR) before the tidal influence, and seawater (SW) from the beach of Espigon closer to the oceanic coast in a contamination-free underway. Locations of all sampling points including the edge outflows and the end-members can be seen by Google Earth™ using the Keyhole Markup Language (KML) file available as electronic supplement.

Physicochemical parameters (pH, electrical conductivity (EC) and redox potential) of the solutions were measured *in-situ*, using a portable multi-parameter electrode (Hach, sensION™+ MM150) previously calibrated. Measured redox potential was referenced to standard hydrogen electrode (Eh), as proposed by Nordstrom and Wilde (1998). All samples were collected in polyethylene bottles and were transported directly to the laboratory for treatment. At the laboratory, the samples were immediately filtered (0.45 μm pore size), and subsequently two aliquots were stored in polyethylene vials, one for cation analysis after being acidified with 1% supra-pure nitric acid and another without acidification for anion analysis. Aliquots were also collected in polyethylene vials for analysis of the isotopic composition; one for ^{2}H and ^{18}O of H_2O and another for ^{34}S of sulphates.

3.2. Analytical methodology

3.2.1. Total elemental analysis

Concentrations of anions (F^-, Cl^-, Br^-, SO_4^{2-}, PO_4^{3-}) in all the unacidified samples were analysed by a high performance liquid chromatography system (HPLC) using a Metrohm 883 basic ion chromatograph equipped with Metrosep columns at the University of Huelva (Spain). Aluminium, Fe, Mn and trace elements (Cr, Co, Ni, Cu, Zn, As, Cd, Sb, Pb, and U) concentrations were determined in the acidified samples by Inductively Coupled Plasma-Mass Spectroscopy (ICP-MS) by an Agilent 8800 Triple quadrupole device at the Andalusian Institute of Earth Sciences (IACT, CSIC-UGR) in Granada (Spain). Detection limits were: 2 μg/L for Al; 0.5 μg/L for Fe; 0.04 μg/L for Mn and 0.02 μg/L for trace elements. Certified Reference Materials including SLRS-5 (river water) supplied by the National Research Council of Canada (CNRC) and 1640A (natural water) by the National Institute of Standards and Technology (NIST), were analysed by ICP-MS as external standards every four samples. Dilutions were performed to ensure that the concentration of the samples was within the concentration range of instrument calibration and blank solutions with the same acid matrix as the samples were also analysed. The average measurement error was below 5% for all analyses.

3.2.2. Isotopic measurements

All stable isotope analyses, including oxygen and hydrogen (from H_2O) and sulphur (from SO_4^{2-}), were carried out by Isotope-Ratio Mass Spectrometry (IRMS) at the Stable Isotope Laboratory of IACT. The stable isotope compositions are reported as δ values per mil (Eq. (2)):

$$\delta = (R_{sample}/R_{standard} - 1) * 1000 \quad (2)$$

Where $R = {}^{18}O/{}^{16}O$ for $\delta^{18}O$, $R = {}^{2}H/{}^{1}H$ for $\delta^{2}H$ (or δD) and $R = {}^{34}S/{}^{32}S$ for $\delta^{34}S$.

Oxygen isotope measurements were performed using a GasBench II peripheral system coupled with Delta Plus XP mass spectrometer (ThermoFinnigan, Bremen, Germany), using the CO_2–H_2O equilibration system (Epstein and Mayeda, 1953). H_2 and CO were produced by injecting the water sample onto a ceramic column containing a glassy carbon tube at 1400 °C, following the protocol described by Sharp et al. (2001). These gases were separated for H_2 isotopic measurement by chromatography using a helium carrier gas stream, connected online with a TC/EA interfaced with a Delta Plus XP mass spectrometer. The analytical error was ±1‰ for $\delta^{18}O$ and better than ±0.1‰ for $\delta^{2}H$. The standard for reporting oxygen and hydrogen is the V-SMOW (Vienna Standard Mean Ocean Water).

Samples were analysed for the isotopic composition of sulphur by means of combusting with V_2O_5 and O_2 at 1030 °C in a Carlo Elba NC1500 (Milan, Italy) elemental analyser online with a Delta Plus XL (ThermoQuest, Bremen, Germany) mass spectrometer (EA-IRMS), after the precipitation of SO_4^{2-} as $BaSO_4$ by adding a $BaCl_2$ solution. Commercial SO_2 was used for the preparation of three internal standards of +23.25‰, +6.03 and −6.38‰ compositions of $\delta^{34}S$. The precision calculated -after correction of the mass spectrometer daily drift-from standards systematically interspersed in analytical batches was better than ±0.2‰. The standard for reporting sulphur is the V-CDT (Vienna Canyon Diablo Troilite).

Mixing ratios of the three end-members influencing possibly the formation of the edge outflows were calculated based on the $\delta^{18}O$ and $\delta^{2}H$ compositions using the equations (Eq. (3) to (5)) provided at Clark (2015):

$$f_{TR} = (\delta^{2}H_S - \delta^{2}H_{SW} - f_{PW}(\delta^{2}H_{PW} - \delta^{2}H_{SW})) / (\delta^{2}H_{TR} - \delta^{2}H_{SW}) \quad (3)$$

$$f_{SW} = (\delta^{18}O_S - \delta^{18}O_{TR} - f_{PW}(\delta^{18}O_{PW} - \delta^{18}O_{TR})) / (\delta^{18}O_{SW} - \delta^{18}O_{TR}) \quad (4)$$

$$f_{PW} = 1 - f_{TR} - f_{SW} \quad (5)$$

Where f is the factor for each end-member (TR, SW and PW) and s (subscript) represents each measured edge outflow.

4. Results and discussion

4.1. Chemical characterisation

The high levels of acidity and EC characterize the edge outflow waters from both the restored (zones 1 and 4) and unrestored modules (zones 2 and 3) with mean pH values of 4.75, 2.27, 2.04 and 2.18 (Fig. 2), and mean EC values of 56.0, 54.4, 48.4 and 18.7 mS/cm, respectively. These characteristics are in accordance with the elevated concentrations of all the dissolved contaminants investigated here (SO_4^{2-}, PO_4^{3-}, Al, Cr, Fe, Co, Ni, Cu, Zn, As, Cd, Sb, Pb and U),

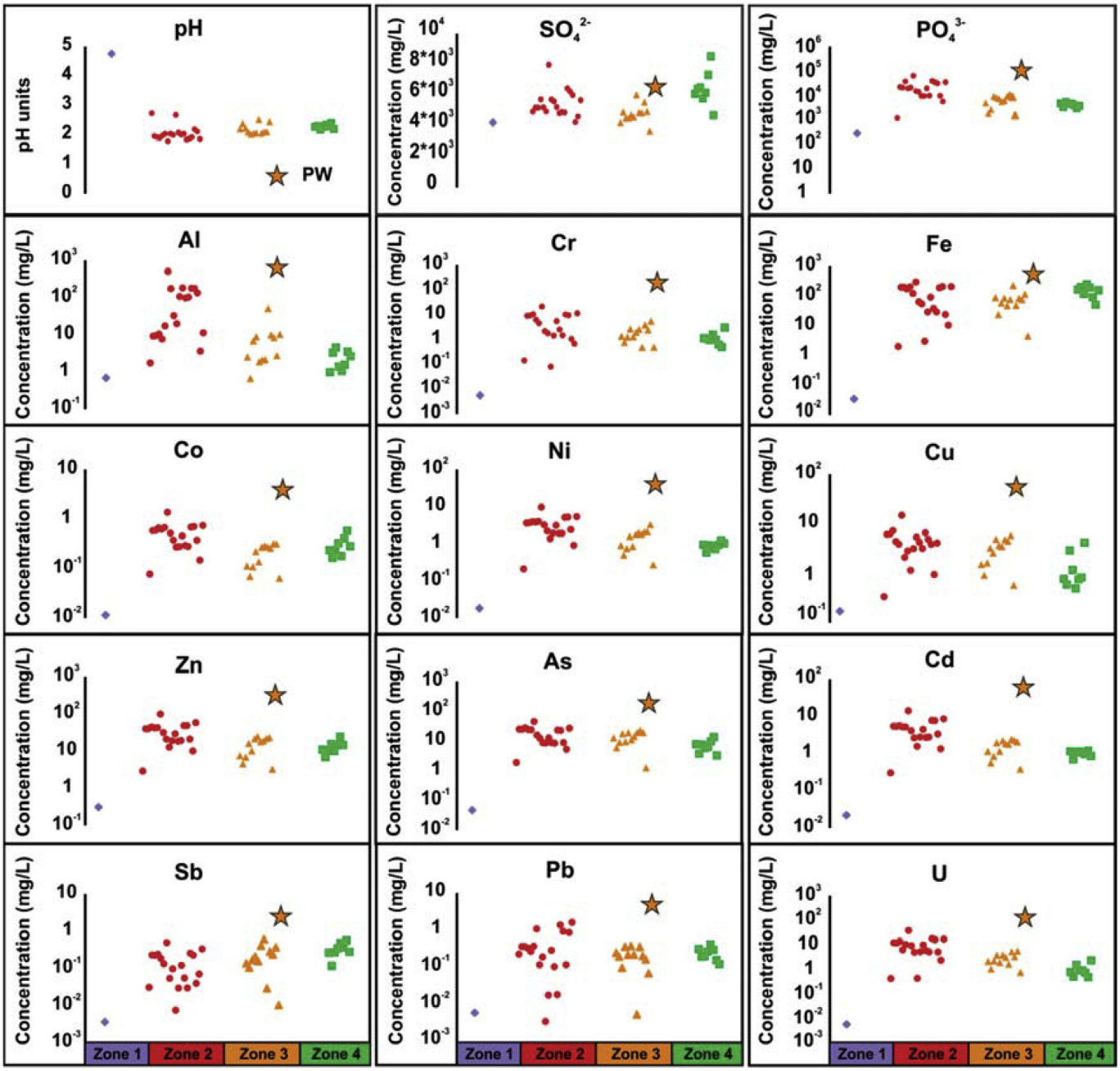

Fig. 2. Values of pH and total concentration of the phosphogypsum-related contaminants for the edge outflows and the process water (illustrated with a star) divided by zones of the stack (1–4).

with some variations depending on the zone of the stack. All the physicochemical parameters along with the total concentrations of the samples can be found in Table S1 of the SI.

The zones 1 and 4 are 'supposedly' restored, with no process water ponded on the surface of the stack and with a top cover. Regarding zone 1, only one edge outflow sample was obtained at a secondary tidal channel where interaction of estuarine water and outcropping phosphogypsum occurs during the rising tide (Pérez-López et al., 2016). This sample has lower acidity and metal concentrations than the leachates originated from the other zones (Fig. 2). All the obtained samples from zone 4 were acidic edge outflow waters with elevated elemental concentrations, though both acidity and concentrations were slightly lower than in the unrestored zones (Fig. 2). This can be owed to the complex soil cover that was applied to this zone as restoration measure, which includes a vegetation layer rich in organic matter that has the potential to act as carbon source for enhancing the activity of naturally-occurring sulphate reducing bacteria in the phosphogypsum (Castillo et al., 2012). Organic carbon-rich amendments over phosphogypsum stacks can lead to immobilization of part of the metal loading of leachates resulting from weathering by sulphide precipitation (Pérez-López et al., 2018). In phosphogypsum-related leachates, the sulphur is in excess in comparison to metals, which implies that sulphide precipitation can contribute to the low availability of metals in solution without significant changes in the aqueous sulphate concentration (Fig. 2).

Nevertheless, numerous edge outflow points still discharge to the estuary, with leachates significantly concentrated in many potentially toxic elements - e.g. Cu up to 4.16 mg/L, Zn up to 24.0 mg/L and As up to 13.4 mg/L. This is proof of the ineffectiveness of the current restoration measures and that the process water is not the only route of contamination, as there are no surface ponds in the zone 4.

The acidic edge outflows from the zones 2 and 3 presented even higher concentrations than those from the restored zones (Fig. 2). In turn, the zone 2 exhibited the highest contamination level; e.g. Cu, Zn and As reached values up to 14.8, 99.7 and 44.9 mg/L, respectively, whereas the corresponding values at zone 3 were up to 5.74, 24.4 and 22.1 mg/L. The process water from zone 3 (PW) exhibited conditions of extreme acidity (pH = 0.80) and contaminants concentration (EC = 108 mS/cm) far more elevated than in the edge outflows, as it is subjected to re-concentration by the closed-circuit and to a high level of evaporation; i.e. 50.2 mg/L for Cu, 285 mg/L for Zn and 146 mg/L for As, among others (Fig. 2).

4.2. Isotopic signatures

The measured values for the stable isotopes analysed, including $\delta^{18}O$, $\delta^{2}H$, and $\delta^{34}S$, for all the edge outflows are plotted in Fig. 3 and presented in Table S1 of the SI. The results for the three end-members representing the possible inputs of weathering agents, i.e. TR for the fluvial area, SW for the coastal area and PW for industrial water ponded on the stack surface, are also compiled in Fig. 3 and Table S1 of the SI.

4.2.1. $\delta^{18}O$ and $\delta^{2}H$ compositions

The $\delta^{18}O$ and $\delta^{2}H$ compositions for the three end-members were −3.98‰ and −25.0‰ for TR, 0.58‰ and 5.30‰ for SW, and 9.13 and 18.0‰ for PW, respectively. With respect to the edge outflows, the samples from the zones 3 and 4, as well as some samples from the zone 2, fall mainly along the mixing line between two end-members, TR and SW, while the point from zone 1 is significantly closer to the SW (red line in Fig. 3a). The different isotopic signatures observed reveal different ratios of influence from the two end-members depending on the location of each zone of the stack in the different morphodynamic domains within the estuary, from marine (closer to SW) to fluvial (closer to TR) influence. Thus, the leachate from zone 1 had the same isotopic signature as SW because zone 1 is under higher influence of tidal seawater in the marine domain. Zone 2 is located in the central domain, although also close to the marine and as such, those outflows falling between the TR and SW end-members had signatures closer to those of SW. On the other hand, zone 3 is located in the central domain, having all its leachates with negative values for both stable isotopes falling midway between the TR and the SW compositions and with nearly no influence of the PW end-member. Zone 4 is located in the inner domain, close to the fluvial influence and thus, some of the edge outflows had an isotopic signature closer to that of TR end-member. Nevertheless, other edge outflows from zone 4 presented heavier values, but these leakages were sampled in puddles of stagnant water, which can be subjected to evaporation, as indicated by their displacement along the evaporation tendency line (Fig. 3a).

However, many leachates originated from zone 2 exhibit a distinct pattern. As stated before, the dumping in zone 2 comprises two stages, with seawater before 1997 and with freshwater after 1997, following the change in phosphogypsum management policy. In this second stage, the continuous reuse of freshwater in a closed-loop system yielded highly acidic and pollutant-rich process water. Thus, edge outflows of zone 2 mainly show a seawater origin due to its location close to the marine domain, but with a notable contribution of the PW from the second filling stage in some edge outflows, as suggested by their distribution along the mixing line constructed in the $\delta^{18}O$ and $\delta^{2}H$ plot between the SW and PW end-members (black line in Fig. 3a). Moreover, the infiltration of process water stored on surface of the zone 2 could also contribute to these findings, mainly considering the proximity between some ponds and most of the samples found in this zone (Fig. 1b). The contribution of process water in the edge outflows from the zone 2 could be also the explanation for the highest contaminant concentrations observed in relation to edge outflows of the remaining zones.

4.2.2. $\delta^{34}S$ compositions

The $\delta^{34}S$ composition was 1.80‰ for the TR and 3.63‰ for the PW, both very close to most of the edge outflows at zones 2, 3 and 4 (Fig. 3b), and close to the composition range of the sulphides from the IPB (Velasco et al., 1998). The $\delta^{34}S$ signatures of TR and PW end-members, along with the majority of the outflows, indicated a typical continental origin with values that are consistent with sulphate from sulphide oxidation. In the case of TR, it is a reasonable outcome, as this water is severely affected by AMD that leads to high concentrations of sulphates and metal (loid)s due to the oxidation of the sulphide-rich mining wastes from the IPB. With respect to the PW, the sulphur composition was inherited from the sulphuric acid, which was produced by pyrite roasting and SO_2 recovery, used for the phosphoric acid manufacturing in Huelva during the wet chemical digestion. The pyrite used was obtained from the Tharsis Mine (IPB), which contained up to 0.4% of As – thus explaining the high level of As found in this waste (Macías et al., 2017).

On the contrary, the leachate from the zone 1 and a few samples belonging to zone 2 approached the SW signature, which gave a typical marine water signature at 20.3‰, corresponding to the amount of dissolved SO_4^{2-} contained in seawater (Fig. 3b). As such, they exhibited a signature between the typical marine and the continental one, implying a slightly higher influence from the seawater and the estuarine environments compared to the remaining outflows.

In general terms, the $\delta^{34}S$ signatures of the edge outflows also suggested a mixing behaviour between river water and seawater, where the plotting of the sample points would also seem to depend on the estuarine morphodynamic domain in which each zone is located. Thus, most of the edge outflows of zone 4 are closer to TR end-member, while the fluvial influence is progressively lost (increasing the marine influence) towards the zones 3, 2 and 1 (Fig. 3b). Numerous edge outflow points of zone 2 are distributed close to the PW end-member (Fig. 3b) confirming again the influence of the process water. However, the mixing behaviours are better defined from the $\delta^{18}O$ and $\delta^{2}H$ compositions, since the ^{34}S data for most of the edge outflows has less deviation probably due to that the origin of S in two of the three end-members (i.e. TR and PW) is the same (sulphides from IPB).

4.3. End-members contribution to edge outflows

The spatial distribution of the influence of the end-members to the edge outflows can be described based on their $\delta^{18}O$ and $\delta^{2}H$ compositions, as calculating the mixing fraction of three components requires two conservative parameters. The mixing ratio of the three end-members was calculated for each edge outflow (Fig. 4) following the ternary mixing described by Clark (2015). It is noteworthy that the isotopic signature of the only leachate collected in the zone 1 was identical to seawater (100% SW composition). Samples 4-2, 4-3, 4–6 and 4–7 were excluded from the graphs, as they cannot be considered as representative samples for zone 4, due to the evaporation of the stagnant puddles from where they were collected.

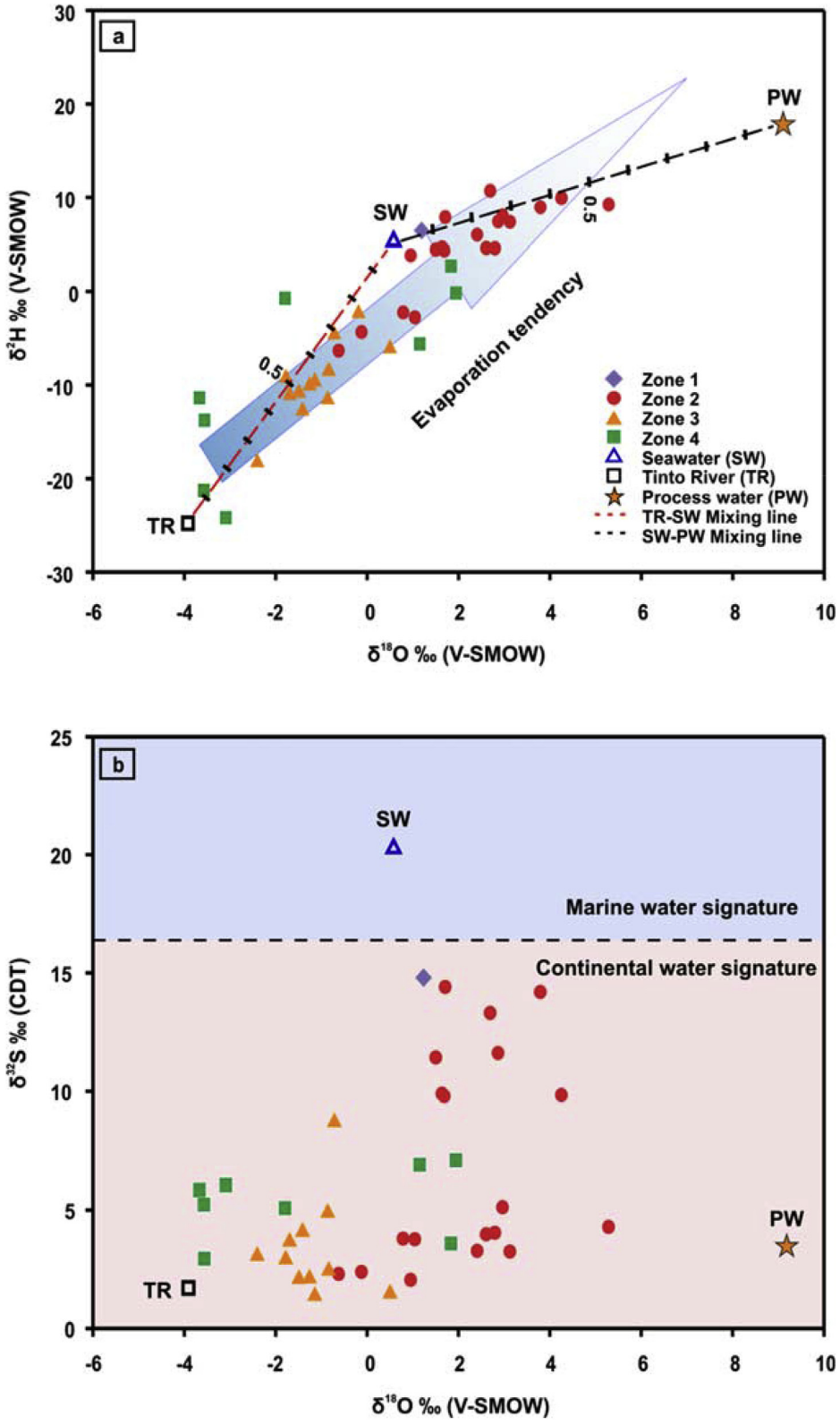

Fig. 3. Stable isotope signatures of edge outflows and end-members related with the phosphogypsum stack are plotted as (a) $\delta^{18}O$ vs. $\delta^{2}H$ and (b) $\delta^{18}O$ vs. $\delta^{34}S$. The two mixing lines connecting the Tinto River with the seawater (red line) on the one hand and the seawater with the process water (black line) on the other hand, are also provided. (For interpretation of the references to colour in this figure legend, the reader is referred to the Web version of this article.)

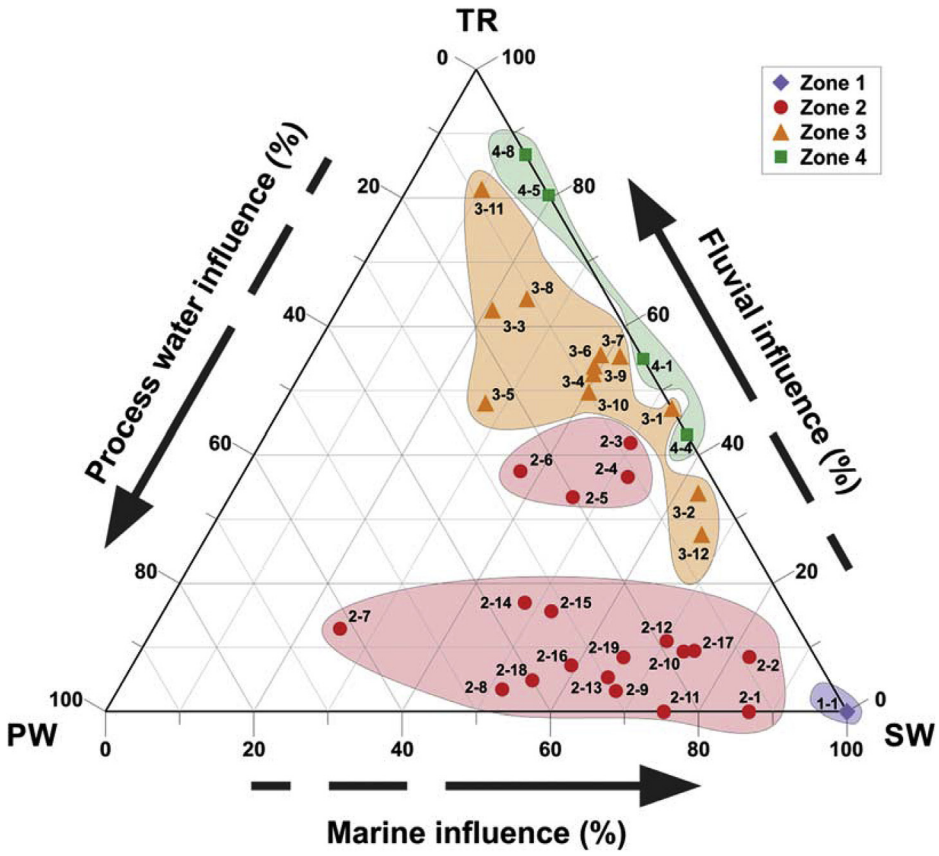

Fig. 4. Ternary diagram describing the contribution of end-members to the edge outflows based on their mixing ratios calculated by their $\delta^{18}O$ and $\delta^{2}H$ compositions.

At zone 2, edge outflows from 2–1 to 2–6 were collected towards the Tinto River estuary main channel compared to the remaining samples, and most of them at the southwest part of the zone (Fig. 1b). Thus, up to 87% of the composition of these samples was that of seawater (Fig. 4), as they are close to the marine domain. In addition, four samples out of these six (2–3, 2–4, 2–5 and 2–6) show a notable influence from the TR end-member (up to 42%), which is consistent taking into account their proximity to the main fluvial channel (Fig. 4). The contribution of process water increased moving to the western part (samples from 2–7 to 2–13) and the northern part of the zone (samples from 2–14 to 2–19) with a mixing ratio of up to 62%, but still the average proportion of seawater was higher in most of the samples, while the impact of river water was low (Fig. 4). On the other hand, the influence of Tinto River is evident in all edge outflows at zone 3, with seawater following, while a slight influence of process water, with an average of 9%, cannot be excluded. So the mixing ratio is mainly transitional between TR and SW end-members with an average of 52% and 38%, respectively, as shown in Fig. 4. Zone 4 belongs to the inner domain, close to the fluvial one and at the same time farther from the marine domain, so mainly TR (up to 87%) affects the composition of the respective edge outflows compared to SW (up to 20%), while there is no apparent influence from PW (Fig. 4).

4.4. Weathering model

The most significant outcome based on the $\delta^{18}O/\delta^{2}H/\delta^{34}S$ composition is that the edge outflows for all the zones are dominantly connected with the SW and/or the TR end-members, as they presented isotopic signatures denoting a clear estuarine influence. The contribution of the PW end-member to the isotopic signature of the edge outflows is nil for zones 1 and 4, low for zone 3, and more significant but not dominant for zone 2. In the restored zones, these findings are expected since there are no process water ponds. In zone 3, the process water stored on surface seems to be, geochemically, poorly connected to the edge outflows. Infiltration could occur but not reach the front or side edge of the stack where samples were taken due to the distance with respect to ponded process water. On the other hand, in zone 2 the influence of the process water seems to occur due to the second filling stage and/or from the infiltration from nearby surface ponds (Fig. 1b).

These findings on the source of the edge outflows and their geochemical difference with respect to the PW are consistent with the suggestions published by Pérez-López et al. (2015) which were based on REE and Cl/Br ratios as geochemical tracers. According to that study, process water had geochemical characteristics typical of phosphate fertilizers. On the contrary, the respective tracers of the edge outflows were identical to those of Tinto River estuary waters, indicating an estuarine origin. Therefore, the disconnection between the edge outflows and the PW, also suggested by the previous work, was a reasonable outcome. However, previous studies did not clarify whether the estuarine origin of edge outflows was related to the seawater used to transport phosphogypsum as a slurry.

In the current study, the $\delta^{18}O/\delta^{2}H/\delta^{32}S$ signatures validate that the phosphogypsum stack appertains to an open circulation system, where the continuously incoming estuarine water at the stack bottom appears to be the main mechanism of weathering of the waste in depth, ruling out the infiltration of the process water as the main source of contamination to the Estuary of Huelva (on which assumption the current restoration plan is based). The excess of (already acidic and contaminated) water discharges into the

estuary in the form of the edge outflows. In fact, zone 4 does not have ponds of process water and continues to leach edge outflow waters after restoration. Moreover, the type of estuarine water entering and washing the waste will depend on the location of each zone of the stack within the estuary, which clarifies the uncertainties of previous works. The isotopic signatures of the seawater used for phosphogypsum disposal seem to be 'erased' by the continuous deep washing through the edge outflows. However, process water used since 1997 for filling the upper part of zone 2 could contribute to their edge outflows. This is likely due to the fact that this higher pyramidal part is less washed by the deep input of estuarine water.

5. Conclusions

Phosphogypsum is a highly contaminated waste that threatens the environmental welfare through pollutant leaching in many coastal areas worldwide, where is usually disposed. This paper focuses on the weathering processes of a phosphogypsum stack in the Estuary of Huelva, which discharges highly acidic and contaminated edge outflows to the estuarine environment. The process water that was used to transfer the waste as slurry is ponded on the surface of the piles. It was believed until now that this extremely acidic and contaminated water was the main route of pollutant diffusion from phosphogypsum to the environment through its downward infiltration inside the stack and all restorations are based on that assumption. In the present study, we hypothesised that this is not the case and stable isotopes were used as geochemical tracers to describe the relation among the edge outflows and the phosphogypsum related end-members (process water, seawater and river water) with the aim to validate the pollution washing agent of the waste and quantify for the first time the contribution of each end-member to the leachates reaching the Estuary. Indeed, the isotopic signatures highlighted the poor geochemical connection between ponded process water and edge outflows ruling out the previous weathering model. Moreover, most of the outflows proved to be connected with the Tinto River and seawater end-members denoting an estuarine influence, depending on the morphodynamic domains to which the disposal zones belong. Before the deposition of the waste, secondary tidal channels flooded temporarily the salt marshes of the study area during the tidal cycles and are currently covered by the waste. As such, we suggest that the intertidal water access to the phosphogypsum stack through the secondary channels could act as one of the preferential paths that lead to the leaching mechanism.

Considering the high toxicity and acidity of the waste and that the current and the future restoration plans are based on the previous weathering mechanism (discarded by the present work), there is an urgent need for new effective measures to prevent phosphogypsum leachates from reaching the estuarine and subsequently, the coastal environment.

Acknowledgements

We would like to show our gratitude to I. Martinez Segura, M.J. Román Alpiste and A. Granados for their assistance in the laboratory work and the technical support. We are, also, immensely grateful to Dr. C.R. Cánovas for his great help during the sampling. This work was supported by the Regional Government of Andalusia through the "Junta de Andalucía" research projects P12-RNM-2260 and RNM-131 and by the Spanish Ministry of Economic and Competitiveness through the research project CAPOTE (CGL2017-86050-R). The authors are very grateful to the funding support for the Committee of Experts on "The environmental diagnosis and the proposal of measures of restoration of the phosphogypsum stacks of Huelva", appointed by the City Hall of Huelva. Dr. A. Parviainen acknowledges the 'Juan de la Cierva – Incorporación' (IJCI-2016-27412) Fellowship and Dr. C. Marchesi the "Ramón y Cajal" (RYC-2012-11314) Fellowship financed by the Spanish Ministry of Economy and Competitiveness (MINECO). Fellowships, research and infrastructure grants leading to this research have been (co)funded by the European Social Fund (ESF) and the European Regional Development Fund (ERFD) of the European Commission. Finally, we would also like to thank the three anonymous reviewers and the handling editor for the support and comments that significantly improved the quality of the original manuscript.

Appendix A. Supplementary data

Supplementary data related to this article can be found at https://doi.org/10.1016/j.watres.2018.04.060.

References

Bolívar, J.P., Martin, J.E., Garcia-Tenorio, R., Perez-Moreno, J.P., Mas, J.L., 2009. Behaviour and fluxes of natural radionuclides in the production process of a phosphoric acid plant. Appl. Radiat. Isot. 67 (2), 345–356.
Cánovas, C.R., Macías, F., Pérez-López, R., Basallote, M.D., Millán-Becerro, R., 2018. Valorization of wastes from the fertilizer industry: current status and future trends. J. Clean. Prod. 174, 679–690.
Castillo, J., Pérez-López, R., Caraballo, M.A., Nieto, J.M., Martins, M., Costa, M.C., Olías, M., Cerón, J.C., Tucoulou, R., 2012. Biologically-induced precipitation of sphalerite–wurtzite nanoparticles by sulfate-reducing bacteria: implications for acid mine drainage treatment. Sci. Total Environ. 423, 176–184.
Clark, I., 2015. Groundwater Geochemistry and Isotopes. CRC press.
El Samad, O., Aoun, M., Nsouli, B., Khalaf, G., Hamze, M., 2014. Investigation of the radiological impact on the coastal environment surrounding a fertilizer plant. J. Environ. Radioact. 133, 69–74.
El Zrelli, R., Courjault-Rad_e, P., Rabaoui, L., Castet, S., Michel, S., Bejaoui, N., 2015. Heavy metal contamination and ecological risk assessment in the surface sediments of the coastal area surrounding the industrial complex of Gabes city, Gulf of Gabes, SE Tunisia. Mar. Pollut. Bull. 101 (2), 922–929.
Epstein, S., Mayeda, T., 1953. Variations of the 018 content of waters from natural sources. Geochim. et Connochim. Acta 4, 213–224.
Grande, J.A., Borrego, J., Morales, J.A., 2000. A study of heavy metal pollution in the Tinto-Odiel estuary in southwestern Spain using factor analysis. Environ. Geol. 39, 1095–1101.
Lottermoser, B.G., 2010. Mine Wastes: Characterization, Treatment and Environmental Impacts, third ed. Springer-Verlag, Berlin, Heidelberg.
Lysandrou, M., Pashalidis, I., 2008. Uranium chemistry in stack solutions and leachates of phosphogypsum disposed at a coastal area in Cyprus. J. Environ. Radioact. 99 (2), 359–366.
Macías, F., Cánovas, C.R., Cruz-Hernández, P., Carrero, S., Asta, M.P., Nieto, J.M., Pérez-López, R., 2017. An anomalous metal-rich phosphogypsum: characterization and classification according to international regulations. J. Hazard Mater. 331, 99–108.
Morales, J.A., Borrego, J., San Miguel, E.G., López-González, N., Carro, B., 2008. Sedimentary record of recent tsunamis in the Huelva Estuary (southwestern Spain). Quat. Sci. Rev. 27 (7), 734–746.
Nieto, J.M., Sarmiento, A.M., Canovas, C.R., Olias, M., Ayora, C., 2013. Acid mine drainage in the Iberian Pyrite Belt: 1. Hydrochemical characteristics and pollutant load of the Tinto and Odiel rivers. Environ. Sci. Pollut. Res. Int. 20 (11), 7509–7519.
Nordstrom, D.K., Wilde, F.D., 1998. Reduction-oxidation potential (electrode method). In: National Field Manual for the Collection of Water Quality Data. U.S. Geological Survey Techniques of Water-Resources Investigations. Book 9, (chapter 6).5.
OSPAR, 2002. Discharges of Radioactive Substances into the Maritime Area by Nonnuclear Industry. Radioactive Substances Series. Publication No. 161. OSPAR Commission, London.
OSPAR, 2007. PARCOM Recommendation 91/4 on Radioactive Discharges: Spanish Implementation Report. Radioactive Substances Series. Publication No. 342. OSPAR Commission, London.
Pérez-López, R., Nieto, J.M., López-Coto, I., Aguado, J.L., Bolívar, J.P., 2010. Dynamics of contaminants in phosphogypsum of the fertilizer industry of Huelva (SW Spain): from phosphate rock ore to the environment. Appl. Geochem. 25 (5), 705–715.
Pérez-López, R., Nieto, J.M., Jesús, D., Bolívar, J.P., 2015. Environmental tracers for elucidating the weathering process in a phosphogypsum disposal site: implications for restoration. J. Hydrol. 529, 1313–1323.
Pérez-López, R., Macías, F., Cánovas, C.R., Sarmiento, A.M., Pérez-Moreno, S.M., 2016. Pollutant flows from a phosphogypsum disposal area to an estuarine environment: an insight from geochemical signatures. Sci. Total Environ. 553, 42–51.
Pérez-López, R., Carrero, S., Cruz-Hernández, P., Asta, M.P., Macías, F., Cánovas, C.R.,

Guglieri, C., Nieto, J.M., 2018. Sulfate reduction processes in salt marshes affected by phosphogypsum: geochemical influences on contaminant mobility. J. Hazard Mater. 350, 154–161.
Peterson, B.J., Fry, B., 1987. Stable isotopes in ecosystem studies. Annu. Rev. Ecol. Evol. Syst. 18 (1), 293–320.
Phillips, D.L., 2001. Mixing models in analyses of diet using multiple stable isotopes: a critique. Oecologia 127, 166–170.
Phillips, D.L., Gregg, J.W., 2003. Source partitioning using stable isotopes: coping with too many sources. Oecologia 136, 261–269.
Rutherford, P.M., Dudas, M.J., Samek, R.A., 1994. Environmental impacts of phosphogypsum. Sci. Total Environ. 149 (1–2), 1–38.
Sanders, L.M., Luiz-Silva, W., Machado, W., Sanders, C.J., Marotta, H., Enrich-Prast, A., Bosco-Santos, A., Boden, A., Silva, E.V., Santos, I.R., Patchineelam, S.R., 2013. Rare earth element and radionuclide distribution in surface sediments along an estuarine system affected by fertilizer industry contamination. Water Air Soil Pollut. 224, 1742–1749.
Sharp, Z.D., Atudorei, V., Durakiewicz, T., 2001. A rapid method for determination of hydrogen and oxygen isotope ratios from water and hydrous minerals. Chem. Geol. 178, 197–210.
Tayibi, H., Choura, M., López, F.A., Alguacil, F.J., López-Delgado, A., 2009. Environmental impact and management of phosphogypsum. J. Environ. Manag. 90 (8), 2377–2386.
Velasco, F., Sánchez-España, J., Boyce, A.J., Fallick, A.E., Sáez, R., Almodóvar, G.R., 1998. A new sulphur isotopic study of some Iberian Pyrite Belt deposits: evidence of a textural control on sulphur isotope composition. Miner. Deposita 34 (4). https://doi.org/10.1007/s001260050182.
Zencich, S.J., Froend, R.H., Turner, J.V., Gailitis, V., 2002. Influence of groundwater depth on the seasonal sources of water accessed by Banksia tree species on a shallow, sandy coastal aquifer. Oecologia 131, 8–19.

Marine Pollution Bulletin 127 (2018) 695–703

Contents lists available at ScienceDirect

Marine Pollution Bulletin

journal homepage: www.elsevier.com/locate/marpolbul

Effects of seawater mixing on the mobility of trace elements in acid phosphogypsum leachates

Evgenia-Maria Papaslioti[a,b,*], Rafael Pérez-López[b], Annika Parviainen[a], Aguasanta M. Sarmiento[c], José M. Nieto[b], Claudio Marchesi[a,d], Antonio Delgado-Huertas[a], Carlos J. Garrido[a]

[a] Instituto Andaluz de Ciencias de la Tierra, CSIC & UGR, Avenida de las Palmeras 4, 18100 Armilla, Granada, Spain
[b] Department of Earth Sciences & Research Center on Natural Resources, Health and the Environment, University of Huelva, Campus 'El Carmen', E-21071 Huelva, Spain
[c] Department of Mining Engineering, Mechanics, Energy and Construction, University of Huelva, 21819 Palos de la Frontera, Huelva, Spain
[d] Department of Mineralogy and Petrology, UGR, Avda. Fuentenueva s/n, E-18002 Granada, Spain

ARTICLE INFO

Keywords:
Phosphogypsum
Huelva Estuary
Seawater mixing
Geochemical processes
Contaminants mobility

ABSTRACT

This research reports the effects of pH increase on contaminant mobility in phosphogypsum leachates by seawater mixing, as occurs with dumpings on marine environments. Acid leachates from a phosphogypsum stack located in the Estuary of Huelva (Spain) were mixed with seawater to achieve gradually pH 7. Concentrations of Al, Fe, Cr, Pb and U in mixed solutions significantly decreased with increasing pH by sorption and/or precipitation processes. Nevertheless, this study provides insight into the high contribution of the phosphogypsum stack to the release of other toxic elements (Co, Ni, Cu, Zn, As, Cd and Sb) to the coastal areas, as 80–100% of their initial concentrations behaved conservatively in mixing solutions with no participation in sorption processes. Stable isotopes ruled out connexion between different phosphogypsum-related wastewaters and unveiled possible weathering inputs of estuarine waters to the stack. The urgency of adopting effective restoration measures in the study area is also stressed.

1. Introduction

The phosphate fertilizer industry produces huge amounts of a waste by-product, known as phosphogypsum (mainly gypsum, $CaSO_4{\cdot}2H_2O$) through the wet chemical digestion of phosphate ore (fluorapatite, $Ca_5(PO_4)_3F$) with sulphuric acid (H_2SO_4) to generate phosphoric acid (H_3PO_4). The theoretical overall chemical reaction is (Eq. (1)):

$$Ca_5(PO_4)_3F + 5H_2SO_4 + 10H_2O \rightarrow 3H_3PO_4 + 5CaSO_4{\cdot}2H_2O + HF \quad (1)$$

Most of the contaminants in the raw phosphate ore are transferred to the phosphoric acid during the wet chemical process (Bolivar et al., 2009; Pérez-López et al., 2010). Phosphogypsum has high acidity and concentration of contaminants due to the occurrence of residual phosphoric acid that has not been fully separated during the industrial process and that remains trapped in the interstices of gypsum grains. The waste also contains other chemical reagents and products from reaction (1), such as sulphuric and hydrofluoric acids, ammonium hydroxide or amine (Lottermoser, 2010). These impurities strongly limit the potential of phosphogypsum for recycling, e.g. as agricultural additives or for building materials (see review in Cánovas et al. (2018)).

Phosphogypsum wastes are often dumped directly in the marine environment and considered one of the major sources of seawater contamination, as occurs in the Gulf of Gabes (SE Tunisa) (El Zrelli et al., 2015). They are transported as an aqueous slurry and without any prior treatment are usually stockpiled in coastal areas close to phosphate fertilizer plants, where they are exposed to weathering conditions (Tayibi et al., 2009) and physical and geochemical processes associated with coastal systems (Sanders et al., 2013). These stacks are considered as a significant source of environmental contamination under leaching conditions (Lottermoser, 2010; Pérez-López et al., 2016).

Coastal systems are responsible for the mass flux of elements entering the deep ocean, because they serve as transition zones between freshwater and seawater environments. At coasts, significant modifications of seawater chemistry occur concerning salinity, ionic composition and redox conditions depending on the tidal cycles and the temporal variations in freshwater inputs (Hierro et al., 2014; Liang and

* Corresponding author at: Instituto Andaluz de Ciencias de la Tierra, CSIC & UGR, Avenida de las Palmeras 4, 18100 Armilla, Granada, Spain.
E-mail addresses: empapaslioti@correo.ugr.es (E.-M. Papaslioti), rafael.perez@dgeo.uhu.es (R. Pérez-López), aparviainen@iact.ugr-csic.es (A. Parviainen), aguasanta.miguel@dgeo.uhu.es (A.M. Sarmiento), jmnieto@dgeo.uhu.es (J.M. Nieto), claudio@ugr.es (C. Marchesi), antonio.delgado@csic.es (A. Delgado-Huertas), carlos.garrido@csic.es (C.J. Garrido).

https://doi.org/10.1016/j.marpolbul.2018.01.001
Received 2 November 2017; Received in revised form 29 December 2017; Accepted 1 January 2018

Wong, 2003). During mixing of wastewaters and seawaters, a variety of geochemical processes take place, such as precipitation and adsorption onto newly-formed solid phases or dissolution, desorption and migration, resulting in the change of elemental concentrations in solution (Asta et al., 2015; Hierro et al., 2014; Zhou et al., 2003). Given the frequent dumping of phosphogypsum on coastal systems worldwide, their leachates are often subjected to changes of pH induced by mixing with seawater, and subsequently to geochemical processes that regulate the behaviour of trace elements and control their partitioning into dissolved concentrations and solid phases. Thus, a clear insight into the geochemical processes occurring during the mixing of phosphogypsum leachates with seawater at coastal environments is vital for the assessment of the total metal loads transported to the oceans.

One of the principal parameters during the seawater mixing is the pH, which controls the resulting chemical composition of waters and the mineralogy and the precipitated solid phases. Therefore, this research focuses on the effect of pH increase on the mobility of contaminants in phosphogypsum leachates during seawater mixing. The aim of this contribution is to simulate and evaluate: i) the behaviour of contaminants including Al, As, Cd, Co, Cr, Cu, Fe, Ni, Pb, Sb, U and Zn when the leachates are released to the coast undergoing seawater mixing and pH rise, and ii) the driving geochemical processes that take place in these solutions. The main motivation of this study resides in the importance to understand the impact of seawater mixing on metal concentrations in phosphogypsum leachates before they attain the open oceans.

2. Materials and methods

2.1. Site description

A huge waste facility of phosphogypsum is located near the Atlantic coast of SW Spain, in an estuary formed by the confluence of the Odiel and Tinto Rivers (Huelva province), co-existing with one of the most important marsh ecosystems in Europe (Borrego et al., 2013). Although this first order ecological value, the Estuary of Huelva is one of the most polluted aquatic systems in the world due to the impacts of the abandoned mining industry in the Iberian Pyrite Belt (IPB) and the current activity in the Huelva Industrial Estate. The contamination related to abandoned mines is caused by the high concentrations of sulphates, metals and metalloids produced by the aqueous oxidation of sulphide-rich wastes -a process known as acid mine drainage (AMD)-, which are transported through the Tinto and Odiel Rivers (Nieto et al., 2013), while the industrial activity is responsible for, among others, the dumping of phosphogypsum wastes (Perez-Lopez et al., 2011).

Around 100 Mt of phosphogypsum were produced from 1968 to 2010 and stored in piles on 1200 ha of salt marshes at the right margin of the Tinto River without any type of isolation (Fig. 1). Phosphogypsum piles contain highly-contaminated groundwaters that are retained at depth by the marsh surface, forcing them to flow laterally and reach the edge of the stack. These acidic polluted leakages emerge, forming the so-called edge outflows, which are until nowadays a continuous source of pollution in the estuary (Pérez-López et al., 2015, 2016). Another source of contamination is the water stored on the surface of the piles, known as process water. The process water was used to slurry the phosphogypsum produced and transport it from the industry to the stack in a closed-circuit system implemented in 1997 for ensuring no wastage of water. Before 1997 phosphogypsum was transported using seawater in an opened-circuit system. Phosphogypsum stacks lie within the tidal prism of the estuary (Pérez-López et al., 2015), so that interaction of acid wastewaters and seawater occurs and the fate of contaminants after mixing must be elucidated.

Currently, four zones are recognised at the disposal area (Fig. 1). Zones 1 and 4 (3 m and 8 m of waste thickness, respectively) are considered already restored, as the piles are covered by natural soil and do not have surface process water ponds. On the contrary, zones 2 and 3 (30 m and 8–15 m of waste thickness, respectively) are still directly exposed to weathering conditions and are not totally watertight at present, with process water accumulated on their surface and numerous edge outflows reaching the estuary. However, the a priori restorations and the future restoration plans are not sufficient for preventing the phosphogypsum leachates reaching the estuary (Pérez-López et al., 2015, 2016), as zone 4, and to a lesser extent zone 1, discharge edge outflows ending up to the estuary.

2.2. Sampling and seawater mixing experiments

Seawater mixing experiments were performed to study the geochemical processes occurring when phosphogypsum leachates reach the estuary. Three leachate samples were collected to conduct such experiments. Two edge outflow waters were sampled at discharge points of the zones 3 and 4. This allows the comparison between restored and non-restored phosphogypsum areas in terms of mobilization of metals during seawater mixing. Process water from the surface pond of the zone 3 was also sampled for the mobility experiments, as this industrial water is released to the estuary in some point discharges (Pérez-López et al., 2016). To avoid additional contamination, seawater samples for the experimental mixtures were collected closer to the ocean coast in a contamination-free underway.

Fifteen experiments were carried out in total for the three different types of acidic phosphogypsum leachates (edge outflow waters from zones 3 and 4, and process water from zone 3) by mixing them with seawater to different ratios for obtaining pH values of approx. 3, 4, 5, 6, and 7. The adequate amounts of wastewaters, that would provide sufficient newly-formed precipitates for their characterisation, required huge volumes of seawater in order to obtain the target pH values. Therefore, mixtures were prepared directly on the coast site using plastic containers of 15 L. Titration curves were previously carried out in the laboratory for all the leachates in order to estimate the amount of seawater required for each target pH value.

The resulting solutions and precipitates from each mixing experiment were collected for further analyses. The pH, electrical conductivity and redox potential of the mixing solutions were in situ measured using a portable multi-parameter electrode (Hach, sensION™+ MM150). Measured redox potential was referenced to standard hydrogen electrode (Eh) as proposed by Nordstrom and Wilde (1998). In the laboratory, two aliquots were subsequently separated in polyethylene vials after filtering through 0.45 μm pore size filters; one for analysis of cation concentrations after being acidified with 1% suprapure nitric acid, and another unacidified for anion analysis. Two filtered aliquots were also collected in polyethylene vials for isotope analysis; one for δ^2H and $\delta^{18}O$ of H_2O and another for $\delta^{34}S$ and $\delta^{18}O$ of sulphates. Seawater and original phosphogypsum wastewaters were prepared in a similar manner as their mixtures. The solid precipitate samples for the different pH values were collected on filter paper (0.45 μm of pore size) by filtration of the total amount of the solutions using a vacuum pump. These solid samples were examined for mineralogical characterisation of newly-formed phases.

2.3. Analytical methodology

Major element (Ca, K, Mg and Na) concentrations were obtained via Inductively Coupled Plasma-Atomic Emission Spectroscopy (ICP-AES) by a Jobin Yvon Ultima 2 instrument at the University of Huelva (Spain). Concentrations of anions (F^-, Cl^-, Br^-, SO_4^{2-}, PO_4^{3-}) and ammonia were also analysed at the University of Huelva by a high performance liquid chromatography system (HPLC) using a Metrohm 883 basic ion chromatograph (IC) equipped with Metrosep columns. Aluminium, Fe, Mn and trace elements (Cr, Co, Ni, Cu, Zn, As, Cd, Sb, Pb, and U) were determined by Inductively Coupled Plasma-Mass Spectrometry (ICP-MS) by an Agilent 8800 Triple quadrupole device at the Andalusian Institute of Earth Sciences (IACT) in Granada (Spain).

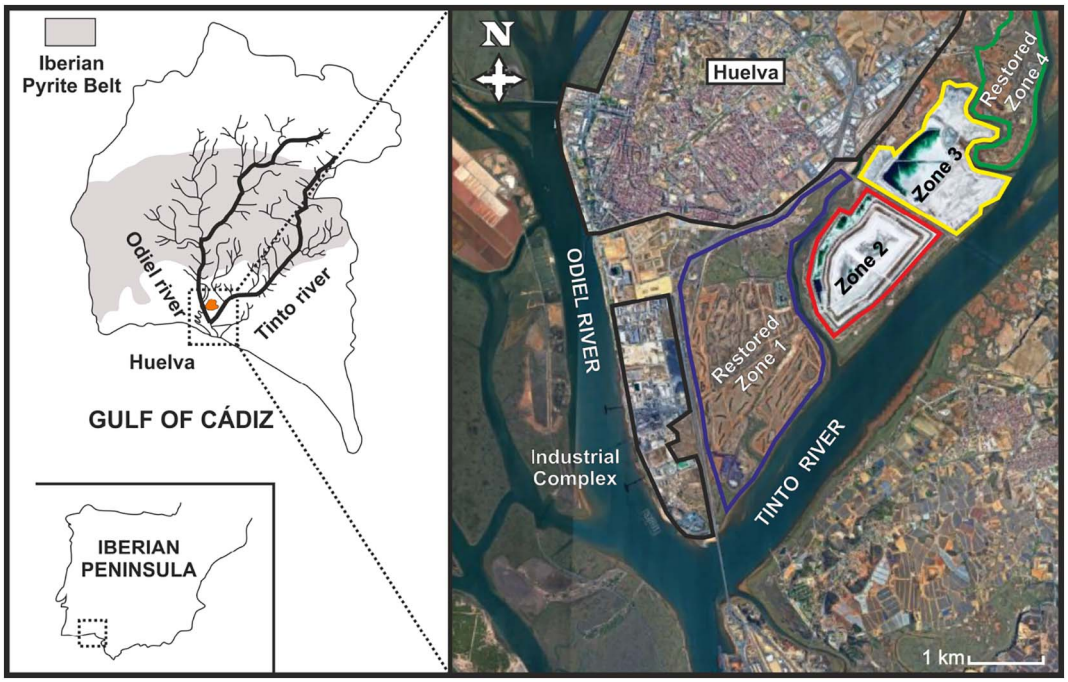

Fig. 1. Study area of the Huelva phosphogypsum stack, defining the different zones.

Detection limits were: 0.2 mg/L for S, 0.1 mg/L for Na, 0.05 mg/L for K and Mg, 0.02 mg/L for Ca and P, 0.002 mg/L for Al, 0.0005 mg/L for Fe, 0.04 µg/L for Mn and 0.02 µg/L for trace elements. Certified Reference Materials SLRS-5 (river water) and CASS5 (seawater) supplied by the National Research Council of Canada (CNRC), as well as 1640A (natural water) by the National Institute of Standards and Technology (NIST), were analysed by ICP-MS as external standards every four samples. Dilutions were performed to ensure that the concentrations of the samples were within the concentration range of instrument calibration and also to avoid clogging of the injection system. Blank solutions with the same acid matrix as the samples were also analysed. The average measurement error was below 5% for all the analyses. Determination of Fe(II) and total Fe (following reduction with hydroxylamine hydrochloride) in the phosphogypsum leachates was undertaken in the geochemical laboratory of the University of Huelva on the same day of the sampling by colorimetry at 510 nm using a SHIMADZU UVmini-1240 spectrophotometer. The detection limit was 0.3 mg/L and the measurement error was < 5%.

The solid phases precipitated from each mixture were analysed by a Field-Emission Scanning Electron Microscope with an AURIGA system (FESEM; ZEIS SMT) and an Environmental SEM (ESEM; FEI, QEMSCAN 650F), both coupled with Energy Dispersive x-ray Spectrometers (EDS), at the Instrumentation Centre of the University of Granada, Spain.

Geochemical calculations were performed for all mixing solutions by the PHREEQC-2 code (Parkhurst and Appelo, 2005) using the Minteq.v4 database (Allison et al., 1991), which allow determination of saturation indices (SI) with respect to relevant mineral phases that may play a key role in the mobility of the dissolved species. Negative SI indicates that the solutions are undersaturated with respect to the target minerals and, therefore, their dissolution is thermodynamically favored over precipitation. On the contrary, positive SI indicates that mineral precipitation is favored. Finally, SI close to zero indicates that solutions are close to equilibrium with respect to a given mineral phase.

2.4. Isotopic measurements

Stable isotopes including oxygen and hydrogen (from H_2O) and sulphur (from sulphates) isotopes were measured by Isotope-Ratio Mass Spectrometry (IRMS) at the Stable Isotope Laboratory of the IACT. The purpose of these analyses was to evaluate the source of the acidic leachates and their connection with the different end-members used for the experiments. The stable isotope compositions are reported as $\delta^{18}O$ and $\delta^{2}H$ (or δD) referred to the standard V-SMOW (Vienna Standard Mean Ocean Water) and $\delta^{34}S$ referred to the standard V-CDT (Vienna Canyon Diablo Troilite).

Oxygen isotope measurements were performed via a GasBench II peripheral system coupled with Delta Plus XP mass spectrometer (ThermoFinnigan, Bremen, Germany), using the CO_2–H_2O equilibration system (Epstein and Mayeda, 1953). H_2 and CO were produced following the protocol described by Sharp et al. (2001). These gases were separated for H_2 isotopic measurement by chromatography using a helium carrier gas stream, connected online with a TC/EA interfaced with a Delta Plus XP mass spectrometer. The analytical error was ± 1‰ for $\delta^{18}O$ and better than ± 0.1‰ for $\delta^{2}H$.

Sulphur isotopes were analysed by combustion with V_2O_5 and O_2 in a Carlo Elba NC1500 (Milan, Italy) elemental analyser online with a Delta Plus XL (ThermoQuest, Bremen, Germany) mass spectrometer (EA-IRMS). Different composition of internal standards with $\delta^{34}S$ = + 23.25‰, + 6.03 and − 6.38‰ (CDT) were prepared using commercial SO_2, after being compared with International Atomic Energy Agency (IAEA) standards. The precision was better than ± 0.2‰.

3. Results and discussion

3.1. Mixing ratios of seawater to phosphogypsum leachates

The respective amounts of seawater and acidic leachates used for each target pH, along with all the physicochemical parameters for all samples are compiled in Table 1. The phosphogypsum leachates displayed conditions of high acidity and extreme contamination, with pH values of 2.04 (edge outflow from zone 3), 2.19 (edge outflow from zone 4) and 1.37 (process water from zone 3), and electrical conductivities of 27.1, 40.5 and 55.6 mS/cm, respectively. On the other hand, seawater exhibited typical alkaline pH values of 7.94 and electrical conductivity of 55.2 mS/cm.

The extreme acidity of the leachates required large amounts of seawater to reach circumneutral pH values (Fig. 2); to produce pH around 7, 227 mL, 160 mL and 1.6 L of seawater were needed per each

Table 1
Physicochemical parameters, quantities of seawater and acidic leachates used for the experiments, major anion and cation concentrations (mg/L) in the starting and mixing solutions for each target pH.

Sample	pH	EC (mS/cm)	Eh (mV)	PG leachate (mL)	Seawater (mL)	Seawater-PG water ratio	Ammonium	Fluoride	Chloride	Bromide	Sulphate	Phosphate	Ca	K	Mg	Mn	Na
Seawater	7.94	55.2	n.a	–	–	–	2.40	111	21,666	69.0	3288	791	418	445	1301	0.01	10,985
Edge outflow-zone 3	2.04	27.1	482	–	–	–	58.0	874	13,827	36.7	4717	8911	1260	353	1039	6.49	8484
	3.14	55.4	500	700	9300	13.3	3.71	66.0	20,195	68.7	2829	1015	488	427	1340	0.45	11,065
	4.06	55.4	469	430	9570	22.3	1.38	37.0	20,442	66.2	2809	534	470	420	1224	0.33	11,346
	4.90	55.3	464	350	9650	27.6	28.4	30.3	20,331	65.9	2752	353	448	428	1346	0.34	11,230
	5.83	55.5	424	208	10,792	51.9	2.46	18.9	20,657	68.3	2735	346	445	421	1366	0.19	11,159
	6.38	55.6	396	90.0	10,010	111	2.23	7.34	20,844	73.2	2719	124	407	434	1351	0.10	11,128
	7.03	55.0	n.a	1.50	340	227	1.55	5.80	20,661	72.2	2681	127	428	431	1366	0.04	11,286
Edge outflow-zone 4	2.19	40.5	481	–	–	–	50.1	900	8143	16.7	4563	3751	931	282	871	12.9	6871
	3.07	54.1	496	990	9010	9.10	22.4	94.9	19,848	71.0	3011	416	451	415	1308	1.40	10,798
	4.02	54.4	445	445	9555	21.5	10.5	50.0	20,225	74.8	2810	221	434	426	1291	0.66	10,925
	4.85	54.4	462	390	9610	24.6	16.5	43.1	21,583	74.9	3159	252	454	434	1301	0.59	10,854
	6.65	54.4	443	295	10,705	36.3	3.65	28.4	20,758	79.2	2790	138	413	439	1317	0.41	11,099
	7.03	55.0	n.a	3.00	480	160	< 3	10.1	21,029	58.1	2711	58	416	440	1348	0.10	10,812
Process water-zone 3	1.37	55.6	638	–	–	–	997	1378	12,417	16.7	7556	95,671	2127	597	1757	24.6	8107
	3.10	55.9	522	82.0	10,018	122	9.88	32.6	20,892	63.0	2994	795	416	408	1264	0.35	11,155
	4.20	55.6	483	53.0	10,047	190	4.96	25.1	20,750	59.2	2950	529	409	410	1378	0.20	11,205
	4.98	55.4	462	44.0	10,066	229	2.65	20.5	20,575	62.3	2807	640	407	414	1259	0.19	10,922
	5.91	55.6	439	23.0	10,077	438	22.7	6.96	20,524	72.6	2654	277	403	425	1387	0.11	11,392
	7.05	55.0	n.a	0.15	240	1600	1.90	4.04	20,689	74.5	2677	100	399	419	1358	0.03	10,999

n.a not analysed.

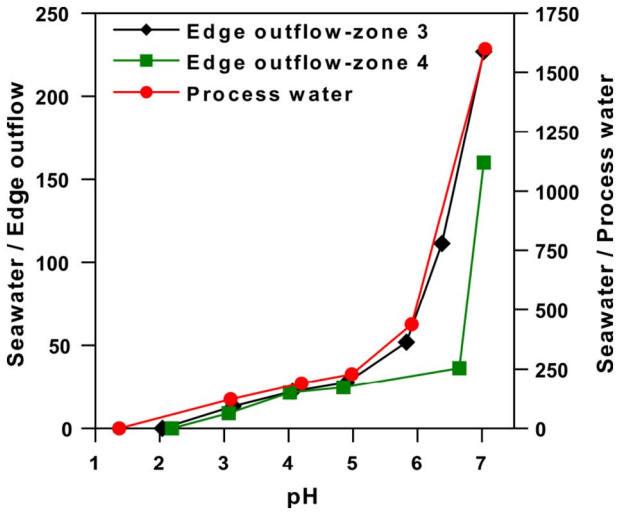

Fig. 2. Mixing ratios of seawater to phosphogypsum leachates used for the experiments for each target pH.

mL of edge outflows from zones 3 and 4 and process water, respectively (Table 1). Large seawater quantities explain the constant electrical conductivity of the mixing solutions at around 55 mS/cm, while the pH increased (Table 1). The ratio of seawater to phosphogypsum leachates corresponding to pH 7 was two to four times higher compared to that of pH 6 (Fig. 2), indicating a buffer zone for pH > 6 likely due to changes in the aqueous speciation or mineral solubility, that hinder further rise of the pH.

3.2. Chemical composition of starting solutions

The geochemical characteristics of starting and mixing solutions are summarized in Table 1 for major compounds and Table 2 for trace elements. As expected from extreme acidity and high conductivity, initial phosphogypsum-related wastewaters contain high concentrations of anions and cations, some of them being potentially toxic pollutants, e.g. concentrations in the edge outflow from the non-restored zone 3 were around 80 mg/L of Fe (mainly as Fe(II)), 20 mg/L of As and Zn, 10 mg/L of Al, 5 mg/L of U, Cu and Cr, 2 mg/L of Cd and Ni, and 0.5 mg/L of Sb, Pb and Co (Table 2).

Concentrations in the process water from the same non-restored zone were much higher than those found in the edge outflow, even between 3 and 10 times higher for PO_4 and metals (Tables 1 and 2). This owes to the fact that process water comes directly from the industrial process and is concentrated in a closed-circuit system (see Section 2.1). In addition, the geochemical characteristics of this type of water are related to the elevated evaporation rate taking place in the central ponds where it is stored, resulting in the accumulation of contaminants and increasing acidity (Pérez-López et al., 2015). On the other hand, concentrations of the edge outflow leachate from zone 4, in which some restoration actions have been undertaken, were within the same order of magnitude as those found in the edge outflow of zone 3, but with significantly lower values (Tables 1 and 2). Although contamination still persists in the restored zone 4 through edge outflows, relatively lower concentrations were observed likely due to that one of the layers of the complex artificial-soil cover is rich in organic matter, which seems to act as a carbon source that enhances the activity of naturally-occurring sulphate reducing bacteria in the phosphogypsum (Castillo et al., 2012), resulting in removal of part of the contamination.

In contrast, all the contaminants detected in the phosphogypsum leachates were in negligible abundances in seawater, and thus the latter does not contribute to the resulting concentrations after mixing experiments (Table 2).

Table 2
Trace elements concentrations (mg/L) in the starting and mixing solutions for each target pH. Isotopic signatures of δ^2H (δD), $\delta^{18}O$ and $\delta^{34}S$ are also shown.

Sample	pH	Al	Cr	Fe	Co	Ni	Cu	Zn	As	Cd	Sb	Pb	U	$\delta^{18}O$ (VSMOW)	δD (VSMOW)	$\delta^{34}S$ (CDT)
Seawater	7.94	0.13	1.02[a]	8.09[a]	0.11[a]	0.70[a]	4.26[a]	0.05	3.35[a]	0.23[a]	0.31[a]	2.99[a]	2.21[a]	0.58	5.33	20.3
Edge ouflow-zone 3	2.04	9.89	3.82	83.8	0.26	2.06	4.77	18.7	18.9	2.38	0.29	0.33	5.51	− 1.26	− 10.1	2.11
	3.14	1.00	0.16	3.43	0.02	0.12	0.29	1.20	1.34	0.16	0.02	0.02	0.34	− 2.07	− 6.81	17.7
	4.06	0.62	0.05	0.11	0.01	0.08	0.19	0.80	0.89	0.10	0.01	0.01	0.06	− 1.91	− 5.38	18.98
	4.90	0.64	0.02	0.04	0.01	0.08	0.16	0.77	0.81	0.09	0.01	2.02[a]	0.01	− 1.02	− 1.73	19.00
	5.83	0.13	0.68[a]	4.35[a]	0.01	0.04	0.07	0.33	0.41	0.04	0.01	0.68[a]	0.87[a]	− 1.27	2.10	19.4
	6.38	0.01	0.57[a]	0.01	2.54[a]	0.02	0.03	0.15	0.21	0.02	2.73[a]	0.18[a]	0.01	0.52	− 3.10	19.9
	7.03	0.01	0.89[a]	4.26[a]	0.96[a]	0.01	0.01	0.08	0.10	0.01	1.42[a]	0.03[a]	0.01	2.09	2.35	20.00
Edge ouflow-zone 4	2.19	2.66	3.01	155	0.28	1.02	4.16	14.6	3.22	0.85	0.28	0.11	2.47	− 3.57	− 21.3	5.24
	3.07	0.61	0.26	13.2	0.03	0.09	0.37	1.36	0.38	0.08	0.03	0.01	0.23	1.26	4.98	16.3
	4.02	0.28	0.08	1.33	0.01	0.04	0.18	0.65	0.17	0.04	0.01	2.96[a]	0.06	0.94	4.64	18.5
	4.85	0.25	0.03	0.01	0.01	0.04	0.14	0.55	0.14	0.03	0.01	0.61[a]	1.36[a]	1.03	4.65	18.7
	6.65	0.20	2.55[a]	0.01	0.01	0.03	0.10	0.41	0.11	0.02	0.01	0.17[a]	0.34[a]	0.86	6.39	19.1
	7.03	0.02	0.55[a]	4.11[a]	2.90[a]	0.01	0.02	0.10	0.03	0.01	2.06[a]	0.01[a]	0.01	2.06	4.58	19.7
Process water-zone 3	1.37	102	50.6	162	1.25	11.5	19.2	112	49.3	19.3	0.74	1.00	52.0	4.54	19.5	3.14
	3.10	1.75	0.21	0.45	0.01	0.11	0.19	1.13	0.61	0.19	0.01	0.02	0.47	− 0.96	− 15.9	19.5
	4.20	0.89	0.02	0.03	0.01	0.06	0.10	0.60	0.32	0.10	4.44[a]	0.01	0.09	− 0.73	− 12.7	19.8
	4.98	0.65	3.28[a]	0.01	0.01	0.05	0.08	0.53	0.29	0.09	4.01[a]	2.19[a]	0.03	2.20	− 7.45	19.7
	5.91	0.06	0.84[a]	0.01	3.09[a]	0.03	0.04	0.31	0.14	0.04	2.01[a]	0.47[a]	2.28[a]	0.66	− 16.4	19.7
	7.05	0.02	0.99[a]	4.22[a]	0.93[a]	0.01	0.01	0.08	0.04	0.01	0.75[a]	0.02[a]	0.01	1.51	8.11	20.2

[a] Values are in μg/L.

3.3. Trends in solution chemistry during mixing experiments

Given the high amounts of seawater used in the mixing experiments, the resulting solutions, reasonably, exhibited concentrations of major anions and cations almost duplicates of seawater, and as such, they exhibited a conservative trend during the experimental mixings (Tables 1 and 2). Exceptions to this case were phosphates, fluorides and, to a lesser extent, sulphates, as their concentrations decreased significantly, while the pH increased (Table 1). Thus, mainly fluoride and phosphate presented a non-conservative behaviour indicating precipitation processes at pH values higher than 3.

Concerning the contaminants, their concentrations decreased significantly from initial values in the pure phosphogypsum leachates as a result of dilution, although the concentrations observed in the mixing solutions at pH 7 were slightly higher than those found in seawater (Table 2). In order to evaluate the behaviour of the pollutants during the experimental runs, relative concentrations were calculated from the analysed concentrations by multiplying them by the dilution factor; i.e. the total amount of solution (leachate plus seawater) divided by the initial amount of leachate. Results are plotted in Fig. 3 and are described in the next two subsections according to the observed behaviour.

3.3.1. Non-conservative contaminants

Some metals such as Al, Fe, Cr, Pb and U exhibited a non-conservative behaviour throughout the seawater mixing experiments (Fig. 3a–c). Iron concentrations decreased with increasing mixing ratio and pH; only around 0.4–4.2% of Fe in relation to the initial concentration remained in solution at neutral pH, while most Fe was depleted from the solution at pH around 4. The solid phases that precipitated according to PHREEQC calculations are in accordance with the depletion of Fe from the solution (Table 3). Supersaturation in Fe(II) phosphates was noted in the form of strengite at pH > 3. Moreover, Fe (III) produced by Fe(II) oxidation, an increasingly rapid process as pH increases (Singer and Stumm, 1970), is predicted to precipitate as oxyhydroxide phases; i.e. goethite at pH > 4, lepidocrocite nearly at pH > 5 and ferrihydrite at pH > 6. According to the geochemical modelling, $Fe(OH)_{2.7}Cl_{0.3}$ is another supersaturated Fe phase at pH > 3, although minor compared to the other iron phases, as Cl behaved conservatively.

On the other hand, Al concentration also decreased but only at pH > 5, with 18–37% of the initial amount remaining in solution at neutral pH, except for the experiments regarding zone 4, where Al behaved conservatively. The aluminium phases that supersaturated in solution, according to the geochemical modelling, included phosphate, sulphate and oxyhydroxide minerals, i.e. plumbogummite, alunite, boehmite and gibbsite at pH > 6 (Table 3). Supersaturation in Al phases was reached at higher pH values and involved fewer phases in mixtures of zone 4 leachate compared to the other leachates, which could justify the conservative behaviour of Al in this case.

The non-conservative behaviour of phosphate concentration is consistent with geochemical modelling that indicated supersaturation in phosphate phases, not only strengite and plumbogummite, as indicated previously, but also $MnHPO_4$ at pH > 3, hydroxylapatite at pH > 5.5–7 and pyromorphite at pH 5.5–6.5. Major precipitation of hydroxylapatite at pH higher than 5.5–7 is expected due to the relative abundance of Ca in the starting solutions with respect to other cations (Table 1). The precipitation of most of newly-formed phases releases protons (Table 3), but probably hydroxyapatite precipitation reaction at pH 5.5–7 strongly contributes to the existence of the previously mentioned buffering zone for these pH values. The decrease in fluoride concentrations in solution as the pH increases is also consistent with the PHREEQC simulations that indicated supersaturation with respect to fluorite at all pH range (from 3 to 7) for the three acidic leachates (Table 3).

The amounts of minor Pb and Cr also decreased with increasing pH and the resulting neutral mixing solutions of the outflows and the process water contained only around 1–5% of the initial dissolved amounts of these metals (Fig. 3a–c). Both metals behaved similarly to iron and phosphates, implying that they were likely retained by sorption processes in Fe phosphate or oxyhydroxide precipitates, which can act as important sinks for trace elements. In addition, Pb probably precipitated as phosphate phases, a hypothesis consistent with the PHREEQC modelling, which showed supersaturation with respect to pyromorphite at pH around 5.5–6.5 and plumbogummite for the outflow of the zone 3 and the process water at pH 7, this last case in accordance with the behaviour of Al in solution (Table 3).

A different -although still non-conservative- pattern was observed for uranium in all three types of wastewaters, due to variations of U solubility during pH-induced seawater mixing. The amount of U in solution strongly decreased from pH 4 to pH 6 (0.5–1.2% of the initial value). No supersaturation in U phases was predicted by the geochemical modelling, probably indicating sorption processes onto other newly-formed phases. Indeed, some studies of this and other coastal

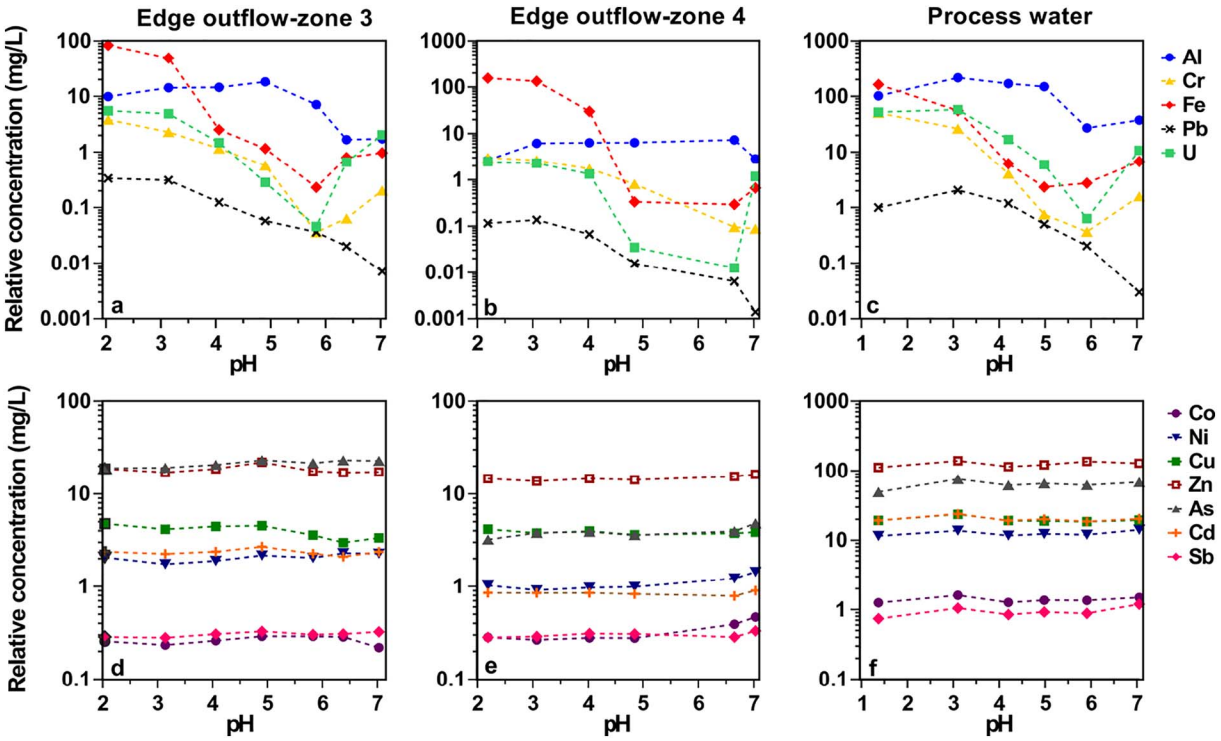

Fig. 3. Behaviour of non-conservative (a, b and c) and conservative (d, e and f) phosphogypsum-related contaminants with pH increase. The graphs are based on the relative concentrations in solution, calculated from the analysed concentrations multiplied by the dilution factor, which is the ratio of the total volume (leachate + seawater) to the volume of the leachate, for each experiment.

systems observed U adsorption onto Fe oxyhydroxide and aluminium particles (Hierro et al., 2013b; Hierro et al., 2014; McKee et al., 1987). However, increase of U in solution was again favored at pH > 6 (Fig. 3a–c), which could be due to a decrease of surface adsorption processes from the particulate phases and formation of soluble carbonate complexes (Hierro et al., 2013a), resulting in a positive U flux. The dissolved amount of U in the mixtures increased and 20–48% of the initial amount remained at neutral pH values. The same release behaviour was observed, although in a much lesser extent, for Fe and Cr at pH 7 (Table 2, Fig. 3a–c) probably due to a decrease in the supersaturation state of neutral solutions in relation to strengite according to the geochemical modelling performed (Table 3).

3.3.2. Conservative contaminants

On the contrary, increasing mixing ratio and pH rise had no significant impact on the concentrations of the majority of potentially toxic elements in the phosphogypsum leachates. Around 80–100% of Co, Ni, Cu, Zn, As, Cd and Sb were kept into solution until neutral pH with no fluctuations over the gradual pH increase (Fig. 3d–f). These trace elements thus exhibited a conservative behaviour during seawater mixing. This conservative trend is explained by the formation of ion complexes in the studied pH range, hindering the partitioning of these trace elements in precipitated solid phases. Indeed, this behaviour was supported by PHREEQC simulations, as no supersaturated phases containing these trace elements were predicted. In addition, these results show that sorption to other solid phases must not occur through the mixing experiments.

3.4. Solid phase characterisation

The chemical analyses of the mixing solutions showed that major elements, such as P, F, and Fe, were largely removed from solutions with increasing pH, implying that their concentrations decreased due to precipitation processes. Thus, the characterisation of these solid phases was required in order to provide a full insight into the geochemical processes controlling metal mobility during mixing of phosphogypsum leachates with seawater.

SEM-EDS images revealed that the newly-formed precipitates are submicrometer agglomerates of globular phases chemically composed mainly of iron (Fig. 4). Identification of individual phases was not possible due to the cryptocrystalline size of the solids. Semiquantitative microanalyses accomplished by SEM-EDS allowed to identify in the matrix the presence of aggregates constituted by P and Fe at pH > 4 (Fig. 4a), indicating phases similar to strengite, which is consistent with the geochemical modelling. More importantly, according to the EDS analysis, Fe oxyhydroxides precipitated at pH 3 from all types of wastewater mixtures, but the formation of Fe-rich phases was more abundant at pH values > 4 (Fig. 4b–e), being consistent with the decreasing amount of dissolved Fe in the solutions and the nature of solid phases calculated by PHREEQC (i.e. goethite, lepidocrocite and ferrihydrite). Other metals, such as Cr, were detected together with Fe in the aggregates of newly-formed phases at pH 5 and 6 (Fig. 4d), in agreement with the composition of solutions (Fig. 3a–c).

Despite chemical analyses showed the depletion of fluoride with increasing pH and PHREEQC calculations predicted the supersaturation of fluorite, fluoride phases were not detected by EDS analyses. This is probably due to the very small amount of fluoride precipitates, associated with phosphate or oxyhydroxide phases, which hinder their identification under the SEM.

EDS analyses detected significant concentrations of Ca and P in precipitates corresponding to pH 5.5–7, which can be attributed to the presence of hydroxyapatite (Fig. 4f). Other minor phases that were identified by SEM-EDS analyses included gypsum, Ca-Mg-aluminosilicates and quartz, in the form of particulate matter suspended in the acidic leachates and seawater used for the experiments.

3.5. Isotopic signature

The acidic leachates presented a different isotopic signature, at least in terms of $\delta^{18}O$ and $\delta^{2}H$, depending on the type of source water

Table 3
Ideal reactions, equilibrium constants and saturation indices (SI) for supersaturated minerals according to PHREEQC simulations from the database of model MINTEQ, at all the studied mixing solutions. Negative and positive SI indicate undersaturation and supersaturation, respectively.

Mineral	Reaction	LogKeq	Saturation index														
			Edge outflow-zone 3							Edge outflow-zone 4					Process water				
			3.14	4.06	4.90	5.83	6.38	7.03	3.07	4.02	4.85	6.65	7.03	3.10	4.20	4.98	5.91	7.05
Alunite	$KAl_3(SO_4)2(OH)_6 + 6H^+ \Leftrightarrow K^+ + 3Al^{+3} + 2SO_4^{-2} + 6H_2O$	−1.35	−24.8	−18.8	−12.8	−7.63	−3.81	−1.49	−26.4	−21.3	−16.0	−7.63	−1.32	−21.4	−15.6	−10.8	−4.56	0.04
Boehmite	$AlOOH + 3H^+ \Leftrightarrow Al^{+3} + 2H_2O$	8.58	−11.2	−8.31	−5.47	−2.84	−1.01	0.34	−11.9	−9.17	−6.63	−2.84	0.45	−10.1	−7.10	−4.74	−1.72	0.88
Diaspore	$AlOOH + 3H^+ \Leftrightarrow Al^{+3} + 2H_2O$	6.87	−9.54	−6.62	−3.78	−1.15	0.68	2.04	−10.2	−7.48	−4.94	−1.15	2.14	−8.42	−5.41	−3.05	−0.04	2.58
$Fe(OH)_{2.7}Cl_{0.3}$	$Fe(OH)_{2.7}Cl_{0.3} + 2.7H^+ \Leftrightarrow Fe^{+3} + 2.7H_2O + 0.3Cl^-$	−3.04	1.66	2.28	4.05	4.00	5.78	5.24	1.15	2.93	2.49	5.30	6.15	1.13	2.35	3.64	4.46	5.30
Ferrihydrite	$Fe(OH)_3 + 3H^+ \Leftrightarrow Fe^{+3} + 3H_2O$	4.89	−5.20	−4.30	−2.27	−1.16	−0.11	0.44	−4.83	−3.65	−2.97	−1.16	0.46	−5.74	−4.18	−2.67	−0.67	0.51
Fluorite	$CaF_2 \Leftrightarrow Ca^{+2} + 2F^-$	−11.0	1.79	1.55	1.33	1.01	0.10	−0.02	1.93	1.77	1.75	1.01	0.38	1.09	1.08	0.97	0.08	−0.36
Gibbsite	$Al(OH)_3 + 3H^+ \Leftrightarrow Al^{+3} + 3H_2O$	8.29	−11.5	−8.53	−5.69	−3.06	−1.23	0.13	−12.1	−9.39	−6.85	−3.06	0.23	10.3	−7.32	−4.96	−1.95	0.67
Goethite	$FeOOH + 3H^+ \Leftrightarrow Fe^{+3} + 2H_2O$	0.50	−0.74	0.16	2.19	3.30	4.33	4.89	−0.38	0.81	1.50	3.30	4.92	−1.27	0.27	1.79	3.79	4.95
Hematite	$Fe_2O_3 + 6H^+ \Leftrightarrow 2Fe^{+3} + 3H_2O$	−4.01	3.55	5.34	9.40	11.6	13.7	14.8	4.27	6.65	8.01	11.6	14.9	2.48	5.56	8.60	12.6	14.9
Hydroxylapatite	$Ca_5(PO_4)_3OH + H^+ \Leftrightarrow 5Ca^{+2} + 3PO_4^{-3} + H_2O$	−44.3	−12.8	−6.98	−1.55	3.98	5.80	8.56	−14.0	−8.60	−2.81	3.98	7.94	−13.5	−6.40	−1.22	4.22	8.89
Lepidocrocite	$FeOOH + 3H^+ \Leftrightarrow Fe^{+3} + 2H_2O$	1.37	−1.67	−0.77	1.26	2.36	3.42	3.97	−1.30	−0.13	0.56	2.36	3.99	−2.21	−0.66	0.86	2.85	4.03
$MnHPO_4$	$MnHPO_4 \Leftrightarrow Mn^{+2} + PO_4^{-3} + H^+$	−25.4	0.44	1.02	1.75	2.31	1.77	1.59	0.86	0.89	1.84	2.31	1.59	0.24	0.90	1.58	2.12	1.53
Plumbogummite	$PbAl_3(PO_4)_2(OH)_5{:}H_2O + 5H^+ \Leftrightarrow Pb^{+2} + 3Al^{+3} + 2PO_4^{-3} + 6H_2O$	−32.8	−28.4	−20.7	−12.8	−5.17	−2.20	0.11	−30.3	−24.3	−16.4	−5.17	−0.97	−25.2	−16.8	−10.6	−2.08	1.77
Pyromorphite	$Pb_5(PO_4)_3Cl \Leftrightarrow 5Pb^{+2} + 3PO_4^{-3} + Cl^-$	−84.4	−6.23	−4.55	−1.83	1.94	−0.90	−3.73	−7.50	−7.07	−3.05	1.77	−6.33	−6.87	−2.33	−1.41	1.57	−4.22
Strengite	$FePO_4{:}2H_2O \Leftrightarrow Fe^{+3} + PO_4^{-3} + 2H_2O$	−26.4	0.78	0.56	1.63	1.45	1.37	0.61	0.98	0.85	0.63	1.45	0.48	0.24	0.50	1.15	1.82	0.76

(Table 2). The process water revealed a higher level of evaporation compared to the outflow waters (Fig. 5a), in agreement with the elevated evaporation taking place in the surface ponds (see Section 3.2). Differences in the $\delta^{18}O$ and $\delta^{2}H$ compositions and, subsequently, in the degree of evaporation were also observed between the two studied edge outflows, with higher values in the outflow from zone 3. The minimal imprint of process water on the isotopic chemistry of leachates of zone 3 suggests poor connection between process water ponded on its surface and edge outflows. In addition, the edge outflows from zone 4, which still leak from the phosphogypsum stack despite the absence of ponded process water and the presence of a complex artificial soil cover, exhibited an isotopic signature very different from that of the process water.

The $\delta^{34}S$ compositions of pure edge outflows and process water were similar ($2‰ < \delta^{34}S < 5‰$) and indicated a continental signature implying that sulphates in the solutions derive from oxidation of sulphide ores (Fig. 5b). This outcome is unexpected considering that phosphogypsums in zones 3 and 4 were transported from the industry to the stack before 1997 using exclusively seawater, which exhibited a different $\delta^{34}S$ value (around 20‰). Thus, the $\delta^{34}S$ signature of the phosphogypsum leachates is more similar to the composition of sulphides from the IPB (median $\delta^{34}S = 0.8$ and SD = 7.1; Velasco et al., 1998). Accordingly, two possible origins could explain these similar values: (1) the existence of weathering inputs of the Tinto River estuarine water, which is affected by acid mine drainage from aqueous sulphide oxidation in IPB mining districts, to the interior of the stack, and/or (2) an inheritance of the sulphuric acid used during the wet chemical digestion for the phosphoric acid manufacturing in Huelva (reaction (1)), which is obtained by roasting of pyrite from the Tharsis Mine (IPB) and later recovering of the SO_2 from the gas with water.

With respect to the mixing solutions, their $\delta^{18}O$ and $\delta^{2}H$ compositions ranged from −2.07 to 2.2‰ and from −16.4 to 8.11‰, respectively (Fig. 5a). The isotopic signatures of the mixtures corresponding to the edge outflow from zone 3 are broadly between their two end-members (seawater and corresponding acidic leachate), whereas those of zone 4 plot close to the seawater composition. On the contrary, the mixtures with pH between 3 and 6 corresponding to the process water surprisingly presented lighter values of $\delta^{2}H$ and, in some mixing solutions of $\delta^{18}O$, than both end-members. The absence of other end-members could explain these discrepancies observed for $\delta^{18}O$ and $\delta^{2}H$ in the mixing solutions of the three types of leachates. On the other hand, the sulphur isotopic tracers presented, mainly, a marine influence for all the experimental mixtures, with $\delta^{34}S$ varying from 16.3 to 20.2‰ (Fig. 5b). The $\delta^{34}S$ values of mixtures with the three wastewater types are consistently closer to the seawater value ($\delta^{34}S$ ‰ around 20) with increasing amount of seawater used for each mixing solution.

Restoration actions in zones 1 and 4 and those planned for zones 2 and 3 are based on the assumption that infiltration of ponded process water through the porous media and its subsequent emergence as edge outflows is the main vector of contamination to the estuary. However, according to these isotopic findings, the apparent poor connection between the ponded process water and the edge outflows, the different isotopic fractionation observed in the interactions between phosphogypsum-related wastewaters and seawater, and the possible input of water from the Tinto River estuarine to the phosphogypsum stack, reveal a new focus on the weathering processes of the phosphogypsum related to its location in the tidal prism of the estuary, which confirms some suggestions previously reported by Pérez-López et al. (2015). Unfortunately, the lack of isotopic information on other disposal zones and end-members makes it impossible to further explore this possibility at present. Although these isotopic findings ought to prove the starting point, new studies should certainly be conducted in the future. As such, a full isotopic characterisation of the site including other possible end-members (e.g. Tinto and Odiel Rivers, estuarine waters along the main channel and pore-water solutions) and all the edge outflows from the four different zones should be performed.

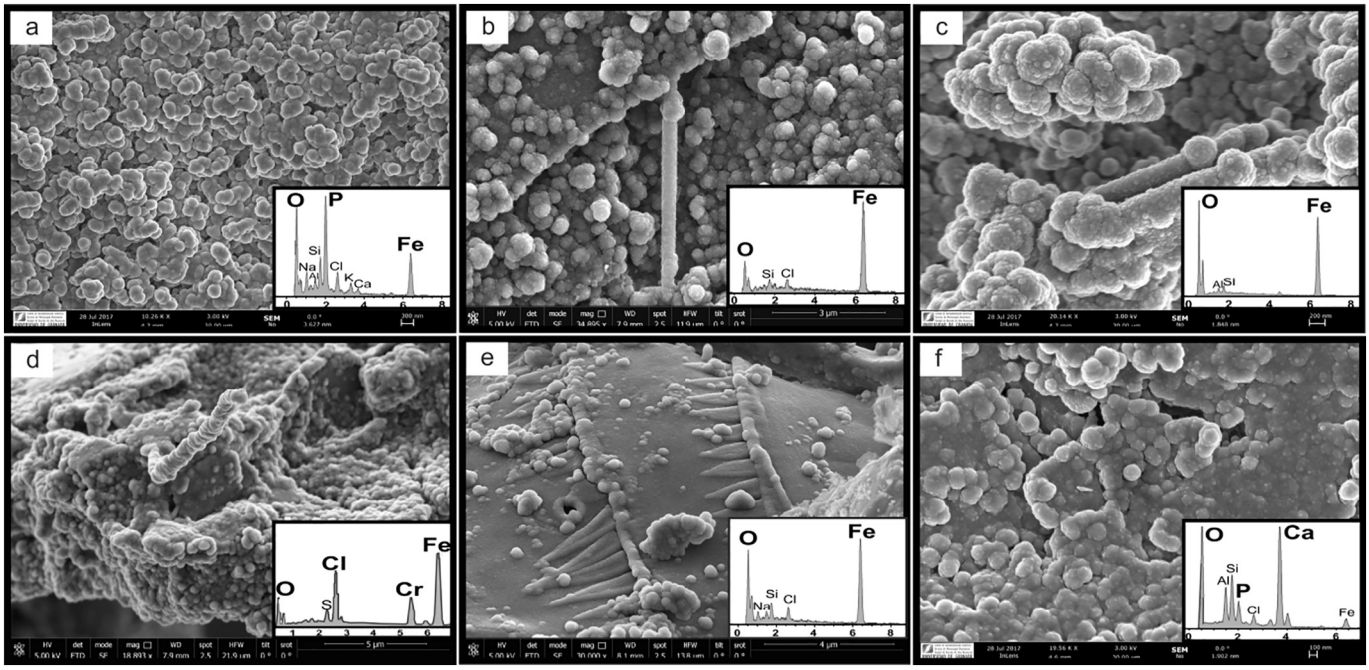

Fig. 4. SEM images and EDS spectra of the newly-formed precipitates collected from the mixing solutions at different target pH values: (a) aggregates of Fe-phosphates at pH 4, (b) and (c) Fe-oxyhydroxide phases in the shape of aggregated globules at pH 4 and 7 respectively, (d) plates and fibbers forming Fe-oxyhydroxide aggregates at pH 5, (e) horizontally aligned triangle-like structures of Fe-oxyhydroxide precipitates at pH 6 and (f) Ca-phosphate (i.e. hydroxylapatite) as phase identified among the major Fe phases at pH 6.

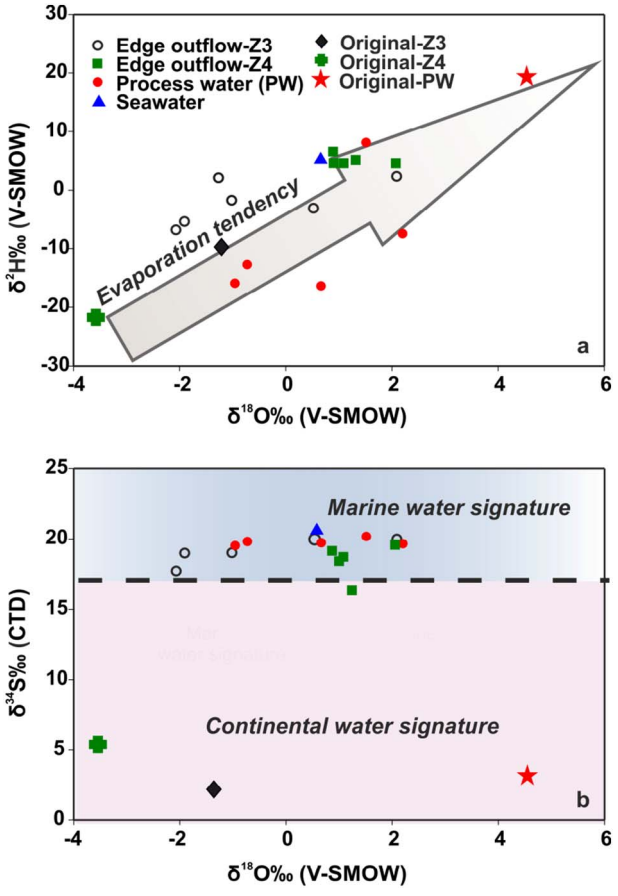

Fig. 5. Stable isotope signatures of the mixing solutions, the wastewater end-members (illustrated with diamond, cross and star for the edge outflow of zone 3, zone 4 and process water, respectively) and the seawater end-member; a) $\delta^{18}O$ vs. $\delta^{2}H$ (δD) composition, and b) $\delta^{18}O$ vs. $\delta^{34}S$ composition. (For interpretation of the references to color in this figure, the reader is referred to the web version of this article).

4. Environmental implications

The results of this study indicated that leaching of the phosphogypsum stack causes a continuous discharge of some of the most toxic contaminants, which threaten the environmental welfare, into the Estuary of Huelva. In addition to the other pollution sources of the study area, the highly acidic nature of these wastewaters, combined with their elevated dissolved concentrations of trace elements, contribute significantly to the total contamination of the Estuary of Huelva and subsequently of the Atlantic Ocean. The phosphogypsum stack is responsible for important amounts of contaminants reaching the Huelva Estuary, i.e. 42 ton/y of Fe, 12 ton/y of Zn, 6.9 ton/y of As, 1.6 ton/y of Cd, among others (Pérez-López et al., 2016), while the respective concentrations discharging to the estuary from IPB mining districts through Tinto and Odiel River basins were estimated to be 7922 ton/y of Fe, 3475 ton/y of Zn, 36 ton/y of As, and 11 ton/y of Cu (Olías et al., 2006). Accordingly, the phosphogypsum stack releases up to 16% of As and 13% of Cd of the total content reaching the estuary. The extent of phosphogypsum-related contamination is especially significant taking into account the small area covered by the stack (12 km^2) in comparison to both fluvial basins (3979 km^2). Moreover, the stack releases additional contaminants, e.g. phosphate, fluoride and uranium (Pérez-López et al., 2016), whose concentration ranges and geochemical behaviours have been highlighted in the current study. As such, this study reports that most of the released contaminants (i.e. Co, Ni, Cu, Zn, As, Cd and Sb) do not undergo a significant depletion in phosphogypsum leachates in spite of their mixing with more alkaline waters. These findings emphasise the necessity of adopting efficient restoration plans in order to manage successfully the phosphogypsum contamination at the Estuary of Huelva, and, more importantly, prevent these wastewaters from reaching the estuary.

5. Conclusions

The acidic and contaminant-rich leachates from a phosphogypsum stack discharge, up to day, directly into the Estuary of Huelva (SW Spain) and undergo seawater mixing. Seawater mixing experiments

were carried out in this study using three types of phosphogypsum leachates. Owing to mixing with the alkaline oceanic waters, different geochemical processes alter the concentrations and influence the mobility of the meta(loid)s contained in the leachates. The current research reports on two main conclusions through experimental and theoretical simulations of mixing of phosphogypsum wastewaters with seawater: a) the high acidity of the leachates hinders the rise of the pH requiring enormous amounts of seawater compared to the wastewaters in order to achieve circumneutral pH values, and b) most of the toxic contaminants including Co, Ni, Cu, Zn, As, Cd and Sb behave conservatively, whereas Fe, Al, Cr, Pb and U decrease significantly with increasing pH and participate in precipitation/sorption processes. According to the results of this study, the behaviour of the contaminants during the mixing experiments was similar among the different types of phosphogypsum leachates, suggesting that the origin of wastewater (edge outflows vs. process water) or the restoration actions (unrestored zone 3 vs. supposedly-restored zone 4) did not control their mobility.

Our findings have provided important insight into the problematic of the phosphogypsum waste worldwide and, more importantly, into the pollution of the Estuary of Huelva by phosphogypsum contaminants. The toxic elements that remain mobile after reaching the estuary, finally end up to the Atlantic Ocean contributing significantly to the total metal loads and threatening the environmental conditions of the littoral. It is, therefore, urgent to adopt effective restoration measures to minimize the impact of the studied phosphogypsum leachates on the estuarine environment and subsequently on the Atlantic Ocean, as well as of other phosphogypsum areas worldwide especially in coastal regions.

Acknowledgements

We would like to show our gratitude to I. Martinez Segura and M. J. Román Alpiste for their assistance in the laboratory work and the technical support in the ICP-MS analysis. We are, also, immensely grateful to Dr. C. Ruiz Cánovas and Dr. F. Macías for their great help during the sampling. This work was supported by the Regional Government of Andalusia through the research project FOREVER (P12-RNM-2260) and the Spanish Ministry of Economic and Competitiveness through the research project CAPOTE (CGL2017-86050-R). The authors are very grateful to the funding support for the Committee of Experts on "The environmental diagnosis and the proposal of measures of restoration of the phosphogypsum stacks of Huelva", appointed by the City Hall of Huelva. Dr. A Parviainen acknowledges the 'Juan de la Cierva – Formación' (FJCI-2014-19582) Fellowship and Dr. C. Marchesi the "Ramón y Cajal" (RYC-2012-11314) Fellowship financed by the Spanish Ministry of Economy and Competitiveness. We would also like to thank Dr. Parthasarathi Chakraborty (Associate Editor) and an anonymous reviewer for the support and comments that significantly improved the quality of the original paper.

References

Allison, J.D., Brown, D.S., Novo-Gradac, K.J., 1991. MINTEQA2/PRODEFA2, A Geochemical Assessment Model for Environmental Systems. Version 3. 0 User's Manual. Environmental Research Laboratory, Office of Research and Development, US Environmental Protection Agency, EPA/600/3-911021, Athens, GA.

Asta, M.P., Calleja, M.L., Perez-Lopez, R., Auque, L.F., 2015. Major hydrogeochemical processes in an acid mine drainage affected estuary. Mar. Pollut. Bull. 91 (1), 295–305.

Bolivar, J.P., Martin, J.E., Garcia-Tenorio, R., Perez-Moreno, J.P., Mas, J.L., 2009. Behaviour and fluxes of natural radionuclides in the production process of a phosphoric acid plant. Appl. Radiat. Isot. 67 (2), 345–356.

Borrego, J., Carro, B., Grande, J.A., De la Torre, M.L., Valente, T., Santisteban, M., 2013. Control factors on the composition of superficial sediments in estuaries of the coast of Huelva (SW Spain): a statistical approach/Factores de control sobre la composición de sedimentos superficiales de los estuarios de la costa de Huelva (SO de Espana): un acercamiento estadístico. J. Iber. Geol. 9 (2), 223.

Cánovas, C.R., Macías, F., Pérez-López, R., Basallote, M.D., Millán-Becerro, R., 2018. Valorization of wastes from the fertilizer industry: current status and future trends. J. Clean. Prod. 174, 678–690.

Castillo, J., Pérez-López, R., Caraballo, M.A., Nieto, J.M., Martins, M., Costa, M.C., ... Tucoulou, R., 2012. Biologically-induced precipitation of sphalerite–wurtzite nanoparticles by sulfate-reducing bacteria: implications for acid mine drainage treatment. Sci. Total Environ. 423, 176–184.

El Zrelli, R., Courjault-Radé, P., Rabaoui, L., Castet, S., Michel, S., Bejaoui, N., 2015. Heavy metal contamination and ecological risk assessment in the surface sediments of the coastal area surrounding the industrial complex of Gabes city, Gulf of Gabes, SE Tunisia. Mar. Pollut. Bull. 101 (2), 922–929.

Epstein, S., Mayeda, T., 1953. Variations of the 018 content of waters from natural sources. Geochim. et Connochim. Acta. 4, 213–224.

Hierro, A., Martín, J.E., Olías, M., García, C., Bolivar, J.P., 2013a. Uranium behavior during a tidal cycle in an estuarine system affected by acid mine drainage (AMD). Chem. Geol. 342, 110–118.

Hierro, A., Martín, J.E., Olías, M., Vaca, F., Bolivar, J.P., 2013b. Uranium behaviour in an estuary polluted by mining and industrial effluents: the Ría of Huelva (SW of Spain). Water Res. 47, 6269–6279.

Hierro, A., Olías, M., Ketterer, M.E., Vaca, F., Borrego, J., Cánovas, C.R., Bolivar, J.P., 2014. Geochemical behavior of metals and metalloids in an estuary affected by acid mine drainage (AMD). Environ. Sci. Pollut. Res. Int. 21 (4), 2611–2627.

Liang, Y., Wong, M.H., 2003. Spatial and temporal organic and heavy metal pollution at Mai Po Marshes Nature Reserve, Hong Kong. Chemosphere 52 (9), 1647–1658.

Lottermoser, B.G., 2010. Mine Wastes: Characterization, Treatment and Environmental Impacts, third ed. Springer-Verlag, Berlin, Heidelberg.

McKee, B.A., Demaster, D.J., Nittrouer, C.A., 1987. Uranium geochemistry on the Amazon shelf: evidence for uranium release from bottom sediments. Geochim. Cosmochim. Acta 51, 2779–2786.

Nieto, J.M., Sarmiento, A.M., Canovas, C.R., Olias, M., Ayora, C., 2013. Acid mine drainage in the Iberian Pyrite Belt: 1. Hydrochemical characteristics and pollutant load of the Tinto and Odiel rivers. Environ. Sci. Pollut. Res. Int. 20 (11), 7509–7519.

Nordstrom, D.K., Wilde, F.D., 1998. Reduction-oxidation potential (electrode method). In: National Field Manual for the Collection of Water Quality Data. U.S. Geological Survey Techniques of Water-Resources Investigations (Book 9, chapter 6.5).

Olías, M., Cánovas, C.R., Nieto, J.M., Sarmiento, A.M., 2006. Evaluation of the dissolved contaminant load transported by the Tinto and Odiel rivers (South West Spain). Appl. Geochem. 21 (10), 1733–1749.

Parkhurst, D.L., Appelo, C.A.J., 2005. PHREEQC-2 version 2.12: A hydrochemical transport model. US Geological Survey Central Region Research, USGS Water Resources Division. http://www.brr.cr.usgs.gov/projects/GWC_coupled/phreeqc.

Pérez-López, R., Macías, F., Cánovas, C.R., Sarmiento, A.M., Pérez-Moreno, S.M., 2016. Pollutant flows from a phosphogypsum disposal area to an estuarine environment: an insight from geochemical signatures. Sci. Total Environ. 553, 42–51.

Pérez-López, R., Nieto, J.M., Jesús, D., Bolívar, J.P., 2015. Environmental tracers for elucidating the weathering process in a phosphogypsum disposal site: implications for restoration. J. Hydrol. 529, 1313–1323.

Perez-Lopez, R., Nieto, J.M., López-Cascajosa, M.J., Díaz-Blanco, M.J., Sarmiento, A.M., Oliveira, V., Sánchez-Rodas, D., 2011. Evaluation of heavy metals and arsenic speciation discharged by the industrial activity on the Tinto-Odiel estuary, SW Spain. Mar. Pollut. Bull. 62 (2), 405–411.

Pérez-López, R., Nieto, J.M., López-Coto, I., Aguado, J.L., Bolívar, J.P., 2010. Dynamics of contaminants in phosphogypsum of the fertilizer industry of Huelva (SW Spain): from phosphate rock ore to the environment. Appl. Geochem. 25 (5), 705–715.

Sanders, L.M., Luiz-Silva, W., Machado, W., Sanders, C.J., Marotta, H., Enrich-Prast, A., Bosco-Santos, A., Boden, A., Silva, E.V., Santos, I.R., Patchineelam, S.R., 2013. Rare earth element and radionuclide distribution in surface sediments along an estuarine system affected by fertilizer industry contamination. Water Air Soil Pollut. 224 (10), 1742.

Sharp, Z.D., Atudorei, V., Durakiewicz, T., 2001. A rapid method for determination of hydrogen and oxygen isotope ratios from water and hydrous minerals. Chem. Geol. 178, 197–210.

Singer, P.C., Stumm, W., 1970. Acidic mine drainage: the rate determining step. Science 167, 1121–1123.

Tayibi, H., Choura, M., López, F.A., Alguacil, F.J., López-Delgado, A., 2009. Environmental impact and management of phosphogypsum. J. Environ. Manag. 90 (8), 2377–2386.

Velasco, F., Sánchez-España, J., Boyce, A.J., Fallick, A.E., Sáez, R., Almodóvar, G.R., 1998. A new sulphur isotopic study of some Iberian Pyrite Belt deposits: evidence of a textural control on sulphur isotope composition. Mineral. Deposita 34, 4. http://dx.doi.org/10.1007/s001260050182.

Zhou, J., Liu, Y., Abrahams, P., 2003. Trace metal behaviour in the Conwy estuary, North Wales. Chemosphere 51 (5), 429–440.

Chemosphere 242 (2020) 125174

Contents lists available at ScienceDirect

Chemosphere

journal homepage: www.elsevier.com/locate/chemosphere

Effects of redox oscillations on the phosphogypsum waste in an estuarine salt-marsh system

Evgenia-Maria Papaslioti [a, b, *], Rafael Pérez-López [b], Annika Parviainen [a], Van T.H. Phan [c], Claudio Marchesi [d], Alejandro Fernandez-Martinez [e], Carlos J. Garrido [a], José M. Nieto [b], Laurent Charlet [e]

[a] Instituto Andaluz de Ciencias de La Tierra, CSIC & UGR, Avenida de Las Palmeras 4, 18100, Armilla, Granada, Spain
[b] Department of Earth Sciences & Research Center on Natural Resources, Health and the Environment, University of Huelva, Campus 'El Carmen', E-21071, Huelva, Spain
[c] Institut de Planétologie et D'Astrophysique de Grenoble, CNRS, Université Grenoble Alpes, F-38000, Grenoble, France
[d] Department of Mineralogy and Petrology, UGR, Avda. Fuentenueva s/n, E-18002, Granada, Spain
[e] University Grenoble Alpes, CNRS, IRD, IFSTTAR, ISTerre, 38000, Grenoble, France

HIGHLIGHTS

- Estuarine salt-marsh systems are geochemically controlled by redox conditions.
- In the Huelva Estuary, phosphogypsum wastes are deposited directly on salt marshes.
- The waste and the marsh soil geochemistry was simulated under redox oscillations.
- Fe-phosphate abundance hinders sulphide formation and contaminants' immobilisation.
- Natural attenuation is impeded, leading to high pollution risk to the environment.

ARTICLE INFO

Article history:
Received 21 June 2019
Received in revised form
1 October 2019
Accepted 20 October 2019
Available online 23 October 2019

Handling Editor: Martine Leermakers

Keywords:
Phosphogypsum
Estuarine salt-marshes
Redox oscillations
Fe-phosphates
Trace elements mobility

ABSTRACT

Salt marshes are natural deposits of heavy metals in estuarine systems, where sulphide precipitation associated with redox changes often results in a natural attenuation of contamination. In the present study, we focus on the effects of variable redox conditions imposed to a highly-polluted phosphogypsum stack that is directly piled over the salt marsh soil in the Tinto River estuary (Huelva, Spain). The behaviour of contaminants is evaluated in the phosphogypsum waste and in the marsh basement, separately, in controlled, experimentally-induced oscillating redox conditions. The results revealed that Fe, and to a lesser extent S, control most precipitation/dissolution processes. Ferric iron precipitates in the form of phosphates and oxyhydroxides, while metal sulphide precipitation is insignificant and appears to be prevented by the abundant formation of Fe phosphates. An antagonistic evolution with changing redox conditions was observed for the remaining contaminants such as Zn, As, Cd and U, which remained mobile in solution during most of experimental run. Therefore, these findings revealed that high concentrations of phosphates inhibit the typical processes of immobilisation of pollutants in salt-marshes which highlights the elevated contaminant potential of phosphogypsum wastes on coastal environments.

1. Introduction

Significant pollution sources including metal mining, industrial activity and waste disposal have led to extensive contamination of environmental systems, such as marsh soils (*e.g.*, Vega et al., 2008, 2009). Such systems can act as important sinks for great loads of contaminants that are transferred through the estuarine water and the suspended sediments affected by tidal variations (Andrade et al., 2002, 2004; Vega et al., 2008).

The biogeochemical cycling and the behaviour of elements in

* Corresponding author. Instituto Andaluz de Ciencias de la Tierra, CSIC & UGR, Avenida de las Palmeras 4, 18100, Armilla, Granada, Spain.
E-mail address: empapaslioti@correo.ugr.es (E.-M. Papaslioti).

https://doi.org/10.1016/j.chemosphere.2019.125174
0045-6535/

such ecosystems depend on redox reactions, which play a key role, as they control the mobility, the chemical speciation and the toxicity of major and trace redox sensitive elements (*e.g.*, Fe, Mn, C, P, N, S, Cr, As and U), and the formation and/or dissolution of solid phases (Borch et al., 2009; Frohne et al., 2011); *i.e.*, the precipitation of sulphides is a driving process, conventionally met in estuarine marsh soil systems (Castillo et al., 2012; Pérez-López et al., 2018). Redox processes are usually kinetically controlled, and often mediated by microorganisms, so that oxic-anoxic oscillations of redox conditions have to be understood, as they are frequent in estuarine salt-marsh systems due to daily tides and subsequent changes of water table levels (Ann et al., 2000; Du Laing et al., 2009). According to Nernst equation, oxidation produces protons and thus, a drop in pH value, while the opposite happens during reduction (Yu et al., 2007), which means that pH and Eh may have, if not buffered, reversed behaviour during redox processes. Hence, the frequent Eh changes that occur in salt marsh soils due to oscillation of the water table, lead to subsequent pH alterations (Frohne et al., 2011), which are a key factor for elemental mobility.

Contaminants could be also released from the redox-dynamic marsh soil systems depending on the hydraulic regime (Ann et al., 2000). During dry periods, the near surface top soil is subjected to oxic conditions, while if flooded, *i.e.*, under water saturation, anaerobic conditions prevail, as the slow oxygen diffusion from the atmosphere does not balance O_2 consumption during organic material mineralisation by aerobic bacteria. Hence, microbial processes affect the mobility and speciation of redox-sensitive elements and the solubility/dissolution of mineral phases (Watts and Lloyd, 2013; Couture et al., 2015). Some non-redox sensitive elements (*e.g.*, Cu^{2+} and Co^{2+} in natural environments) could be also impacted indirectly by redox processes, *e.g.*, by natural organic matter mineralisation and Fe/Mn (hydr)oxide mineral phases reductive dissolution (Borch et al., 2009). The significance of studying redox processes, especially in anthropogenic contaminated environmental systems, lies to understanding whether natural attenuation occurs in these systems, or in the contrary, whether other remediation strategies, *e.g.*, based on microbial degradation or reductive sequestrations, must be implemented (Wu et al., 2006; Polizzotto et al., 2008).

Phosphogypsum wastes are generated by the phosphate fertiliser industry, during the production of phosphoric acid via the reaction of sulphuric acid with a phosphate ore (*i.e.*, apatite). It is estimated that the total amount of phosphogypsum produced worldwide until 2006 was about 6 billion tones (IAEA, 2013; Cánovas et al., 2018). In addition, around 1.1 and 1.2 billion tones of the waste had been generated worldwide only for 2015 and 2016, respectively (Cánovas et al., 2018) based on estimations made by USGS (2017) on the phosphate rock production.. This industry is usually located on coastal areas, whereas the waste is transported and deposited nearby, *e.g.*, on redox-dynamic estuarine salt-marsh systems. Redox fluctuations affect the stability or leaching of phosphogypsum-related contaminants by controlling the oxidation states of many compounds (*e.g.*, sulphur, iron and uranium) associated with these wastes and thus, their mobility (Papanicolaou et al., 2010). Large phosphogypsum disposal stacks could exhibit different redox gradients with depth as the upper unsaturated zones are likely to be subjected to oxidising conditions, particularly in stacks supported directly on organic matter-rich marsh soils (Lottermoser, 2007; Pérez-López et al., 2011).

2. Environmental setting and objectives

One singular case of redox-dynamic system is the phosphogypsum located in Huelva, SW Spain, that is directly stack-piled over the salt marshes of the Tinto River estuary without any impermeable barrier (Fig. 1). The marshes belong to one of the most important marsh ecosystems in Europe (Borrego et al., 2013), declared UNESCO Biosphere Reserve and RAMSAR-NATURA wetland with high-priority protection status. Between 1968 and 2010, this activity led to the disposal of approx. 100 Mt of phosphogypsum wastes in stacks covering an area of 12 km^2 on the salt marshes. The stacks are located within the tidal prism of the Huelva Estuary, which has a great influence on the weathering of phosphogypsum waste by means of estuarine tidal waters (Papaslioti et al., 2018). The highly-contaminated groundwater contained in the phosphogypsum piles migrates towards the edge of the stack forming acidic leakages, known as edge outflows, that have polluted the estuary until nowadays (Pérez-López et al., 2016; Papaslioti et al., 2018). Another source of contamination is the process water present on the surface of the piles, used to slurry the phosphogypsum and transport it from the industry.

The direct contact of the phosphogypsum stack with the organic matter-rich marsh soil basement leads to its weathering in deep zones under reducing conditions with stagnant and non-renewable waters. New insights have been provided into the interaction between the waste and its basement, showing that phosphogypsum leaching has an impact mainly near their contact, while the marsh soil act as a barrier, setting the basis for new treatment techniques (Guerrero et al., 2019). Detailed information on the permeability of the studied area and the aquifer development can be found at Rabi and Mohamad (2006). Anaerobic conditions are imposed by organic matter decomposition associated with microbial activity of sulphate-reducing bacteria (SRB), resulting in aqueous reduction of sulphate from phosphogypsum to sulphide. This process may lead to metal mobility restriction due to precipitation of metal sulphides (Pérez-López et al., 2011, 2018). However, partial oxidation of these sulphides in the marsh contact also occurs due to the hydrological connection between the stack and the estuary by saline intrusion (Pérez-López et al., 2018). Therefore, phosphogypsum can be subjected to weathering under reduction-oxidation cycles likely controlled by tidal variations.

Currently, the disposal area is divided into four zones (Fig. 1). Zones 2 and 3 are directly exposed to weathering, whereas zones 1 and 4 have been the subject of rehabilitation, *e.g.*, the implementation of a top soil cover (see Pérez-López et al., 2011, 2016 for further description of the zones). This cover includes a vegetation layer rich in organic matter that may act as carbon source, and thus enhance the activity of naturally-occurring SRB in the phosphogypsum (Castillo et al., 2012). Even small amounts of organic material could be enough to lead to dissolved oxygen depletion and consequently, to the establishment of anaerobic conditions (Pérez-López et al., 2011). Thus, the Huelva phosphogypsum is additionally affected by redox processes because of the applied complex soil cover. However, previous studies (Pérez-López et al., 2016; Papaslioti et al., 2018) have shown that the rehabilitation measures are ineffective and the edge outflows still leak to the estuary, highlighting the importance in improving the current remediation techniques.

The full awareness of the redox processes occurring in a redox-dynamic phosphogypsum stack under the prism of an estuarine system is the aim of the current study. It should provide important insights for an effective remediation to promote the contaminants attenuation to the environment. Therefore, this study evaluates the contaminant driving geochemical processes (i) in the phosphogypsum piles, and (ii) in its marsh soil basement, both present in an estuarine salt-marsh system, mimicked by experimentally induced redox oscillations, under controlled conditions.

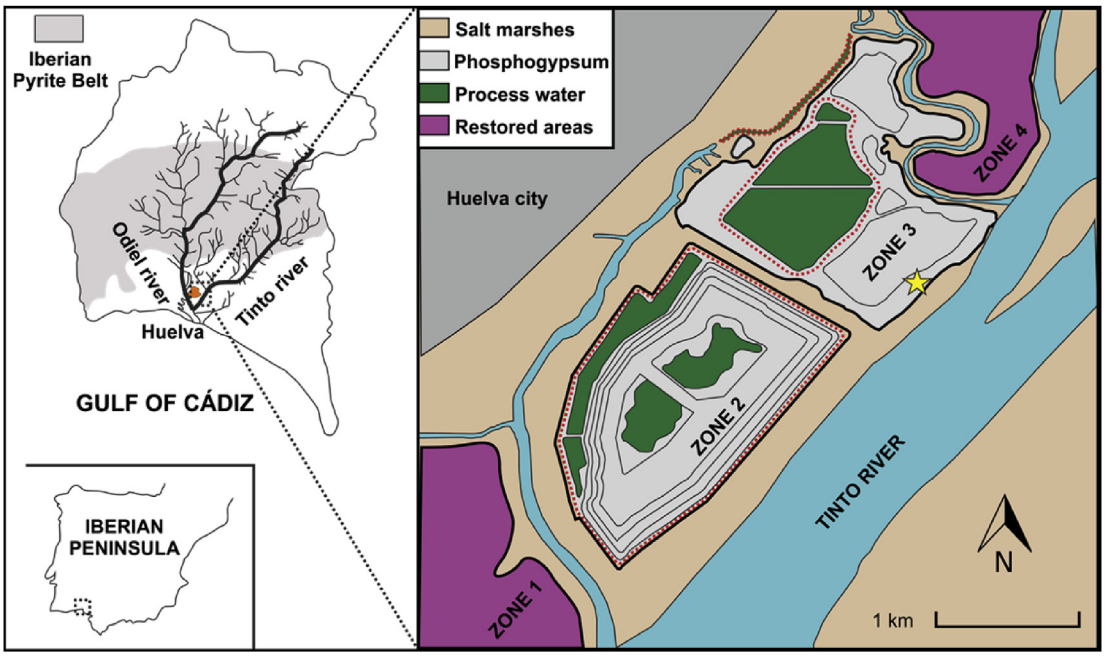

Fig. 1. Study area description showing the phosphogypsum stack disposed on the salt marsh soil. The star indicates the sampling point (geographical co-ordinates 37.254827−6.899216).

3. Materials and methods

3.1. Preparation of suspensions

For the redox oscillation experiments, two solid samples were collected from the stack surface in zone 3 (total thickness ranges from 8 to 12 m) using a soil-sampling auger (Fig. 1): (i) phosphogypsum at 5 m depth, where metals availability in the pore water is high (Pérez-López et al., 2018), and (ii) underlying salt marsh soil located at 8 m depth. The collected samples are considered representative regarding the studied phosphogypsum stack and more importantly, according to a recent geochemical study (Pérez-López et al., 2018), zone 3 is an oxidised and reduced area with redox cycles, and thus, the most suitable for the presented experimental work. Samples were preserved in heat sealed Mylar® bags under N_2 atmosphere until the experiments. This soil with high organic matter content could serve as a source of organic C and of bacteria.

Two soil suspensions of 1 L (<1 mm fraction, 100 g dry soil/L) were prepared for the experiments, one with phosphogypsum and another one with salt marsh soil. The suspensions were prepared by equilibrating in anoxic conditions each soil sample with synthetic degassed pore water for 1 week prior to the experiments. Each synthetic water was prepared by mimicking the solution composition of the phosphogypsum and the salt marsh soil in depth. For that purpose, Milli-Q water was enriched with an aliquot of salts (iron chloride, sodium arsenate, cadmium chloride, zinc sulphate, disodium hydrogen phosphate, calcium chloride, sodium chloride, sodium sulphate) and U_2O_5 Inductively Coupled Plasma-Mass Spectrometry standard solution, in order to simulate the natural waters (pore water) occurring within the soil samples (Table S1 of the Supplementary Information).

3.2. Experimental set-up and sample treatment

The experiment was performed using a custom two part Pyrex® glass redox stat bioreactor system designed by Thompson et al. (2006) and modified later by Parsons et al. (2013); a detailed description of the system can be found in similar, recent studies (Markelova et al., 2018; Phan et al., 2018, 2019) (Fig. S1). All parts of the equipment were washed with 5% HNO_3 and rinsed thoroughly in ultra-pure water prior to the experiment onset.

The suspensions were inserted in the reactors and were subjected to six cycles of 7 days each, by alternating oxic and anoxic conditions. To impose redox potential (Eh) change, the sparging gas was modulated between N_2:CO_2 (392 ppmv) during the anoxic cycle and compressed air O_2:N_2:CO_2 under constant pCO_2 ($10^{-3.5}$ atm) during oxic weeks. Samples were collected daily and then were centrifuged, filtered (0.45 μm) and stored in the fridge until analysis. Samples from anoxic weeks were taken daily, and treated and stored inside a N_2-filled anaerobic chamber ($O_{2(g)} < 1$ μL/L) to avoid oxidation. Reactors were covered with an aluminium foil during the experiments to prevent the formation of hydrogen peroxide and the photo-degradation of the contaminants. During the experiment, the bacteria present in the suspension are expected to consume the existing organic matter. Thus, 8.33 mmol/L of cellobiose ($C_{12}H_{22}O_{11}$ − Sigma-Aldrich) was added in the suspensions at the start of every reducing cycle in order to replace the labile organic matter that is needed to stimulate the bacteria in the bioreactors (Phan et al., 2018).

3.3. Eh-pH measurements

Continuous monitoring (every 30 min) of the Eh and pH was conducted during the 6-week experiments using electrodes inserted in the suspensions (Fig. S1). Solid polymer open junction pH and Eh electrodes (Mettler-Toledo Xerolyt, France) were placed inside the reactors through the corresponding connections. The electrode signals were connected to field-effect transistor (FET) instrumentation amplifiers with high input impedance. The signal was then passed to an Agilent acquisition/switching unit (34970a) connected to a PC running Agilent BenchLink Data Logger 3 software. The measured Eh values were corrected for the reference electrode's standard voltage (+207 mV at 25 °C) relative to the standard hydrogen electrode (SHE) and referred to Ag/AgCl (3 M

KCl) reference electrode.

A three-point calibration (pH 4, 7 and 10) was performed for the pH electrodes at the start and the end of the experiments showing that electrode response had not shifted importantly. Real values were calculated based on the calibration of the electrodes performed prior to the experiments.

3.4. Analytical methods

3.4.1. Aqueous elemental analysis

Major element (Ca, K, Mg and Na) concentrations and those of anions (F^-, Cl^-, Br^-, SO_4^{2-}, PO_4^{3-}) and ammonia were measured by Inductively Coupled Plasma-Atomic Emission Spectroscopy (ICP-AES) by a Jobin Yvon Ultima 2 instrument and by a high-performance liquid chromatography system (HPLC) using a Metrohm 883 basic ion chromatograph (IC) equipped with Metrosep columns, respectively. Aluminum, Fe, Mn and trace elements were determined by Inductively Coupled Plasma-Mass Spectrometry (ICP-MS) by an Agilent 8800 Triple quadrupole device. Detection limits were: 0.2 mg/L for S, 0.1 mg/L for Na, 0.05 mg/L for K and Mg, 0.02 mg/L for Ca and P, 2 μg/L for Al, 0.5 μg/L for Fe, 0.04 μg/L for Mn and 0.02 μg/L for trace elements. Certified Reference Materials SLRS-5 (river water) supplied by the National Research Council of Canada (CNRC) and 1640 A (natural water) by the National Institute of Standards and Technology (NIST), were analysed by ICP-MS as external standards every four samples. Blank solutions with the same acid matrix as the samples were also analysed. The average measurement error was below 5% for all the analyses.

Determination of inorganic arsenite (As^{3+}) and arsenate (As^{5+}) was conducted using coupling liquid chromatography LC (Thermo Scientific, SpectraSystem P4000) with ICP-MS with the internal standard Ge (Thermo Scientific, XSeries 2) according to the method described by Bohari et al. (2001). The detection limit was 0.09 μg/L for As^{3+} and 0.41 μg/L for As^{5+}, with a precision better than 5%.

The "methylene blue method" (Cline, 1969) was applied for the total S(-II) analysis in solution, in which standard stock Na_2S was used for the preparation of the standard solutions to build the calibration curve and to treat the results. For Fe^{2+} measurement, the ferrozine assay was used, modified according to Viollier et al. (2000). To obtain mobilised Fe^{2+} concentration in solution, an aliquot of sample was added to ferrozine solution. Standard stock solution was prepared using $FeCl_2{}^*4H_2O$ and standards of different concentrations were prepared via serial dilutions using HCl in order to mobilise Fe^{2+}. Samples and standards were measured immediately after preparation via UV−Vis spectroscopy (Lamda 35, Perkin Elmer) at 664 nm and 562 nm absorbance for sulphide and iron, respectively.

3.4.2. Dissolved Organic Carbon

Dissolved Organic Carbon (DOC) measurement of the filtered supernatants was conducted by Shimadzu VCSN analyser (TOC-5000 A, Shimadzu, France) via the direct NPOC (Non-purgeable Organic Carbon) method by pre-acidifying and pre-purging the sample to remove the Total Inorganic Carbon (TIC) and Purgeable Organic Carbon (POC), respectively. POC was partly removed from the sample by gas stripping, while the sample was acidified within pH 2 and 3 by adding a small portion of HCl and then TIC was removed from the acidified sample by purging with a purified gas. DOC was determined directly by means of Total Carbon (TC) measuring method as TC equal Total Organic Carbon. The detection limit was 0.3 mg/L and the precision was better than 2.5%.

3.4.3. Adenosine tri-phosphate

The adenosine tri-phosphate (ATP) test is a way to rapidly measure growing microorganisms through detection of ATP, a molecule found in and around active living cells. The ATP concentrations were determined by measuring luminescence levels in relative light units (RLU) using the BacTiter-Glo Microbial Cell Viability Assay Kit (G8233; Promega Corporation, Dübendorf, Switzerland), following an optimized procedure (Hammes et al., 2010). The detection limit of the luminescence-based ATP procedure is 0.0001 nM with a standard deviation of <5%. Measurements were performed by a Lumar LB 9507 luminometer (Berthold Technologies, Bad Wildbad, Germany). The ATP reagent -prepared by mixing the BacTiter-Glo™ Buffer with the BacTiter-Glo™ Substrate- was mixed with the slurry samples in a ratio of 1:1. The intensity measured (of each mixture) was correlated to ATP concentration using an ATP standard (BioThema Luminescent Assays, 45−051 ATP Standard 10 μM 5 mL, Sweden) for calibration.

3.5. Geochemical modelling

Geochemical calculations were performed for all the solutions, which were collected during the redox oscillations experiments, by the PHREEQC-3 code (Parkhurst and Appelo, 2013) using the Minteq.v4 database (Allison et al., 1991), allowing evaluation of the contaminants behaviour and the geochemical processes. The model was used to determine saturation indices (SI) with respect to relevant mineral phases that may play a key role in the mobility of the dissolved species under redox alterations. Negative SI indicates that the solutions are undersaturated with respect to the target minerals and, therefore, their dissolution is thermodynamically favoured over precipitation. On the contrary, positive SI indicates that mineral precipitation is favoured. Finally, SI close to zero indicates that solutions are close to equilibrium with respect to a given mineral phase and neither dissolution nor precipitation is thermodynamically predicted. All input data (physicochemical parameters, concentrations) are given in Tables 1 and 2, and the main reactions and their equilibrium constants are given in Table S2.

3.6. Solid phase analysis

Solid phase analysis was performed on the dried slurry collected during the redox experiments. The solid phases were analysed by a Field-Emission Scanning Electron Microscope with an AURIGA system (FESEM; ZEIS SMT) and a Scanning Electron Microscope of Variable Pressure (VPSEM; ZEIS SUPRA™ 40VP), both equipped with backscattered and secondary electron detectors coupled with Energy Dispersive X-ray Spectrometer (EDS).

4. Results

4.1. Eh and pH

The redox potential of the suspensions subjected to redox oscillations was relatively high, with Eh values systematically higher in the marsh soil (from 265 to 772 mV) than in the phosphogypsum experiment (from 170 to 560 mV) (Table 1; Fig. 2). Both suspensions followed similar trend, with an Eh decreasing in the 2nd and 3rd anoxic periods and increasing in the oxic ones (Fig. 2A and B). In principle, a negative correlation would be expected from Nerst equation between pH and Eh, but this was not observed in our experiments. Instead, both systems managed to have a well-buffered pH, with more acidic conditions observed in the marsh soil (from 3.16 to 3.51) than in the phosphogypsum system (from 4.59 to 4.69) (Table 1; Fig. 2A and B).

A weak positive correlation between Eh and pH was described in similar studies on other redox sensitive systems (Antić-Mladenović

Table 1
Physicochemical parameters, biological activity (as ATP) and organic matter amount (DOC) of the phosphogypsum and marsh soil suspensions during the redox experiments. Grey cells correspond to the anoxic and white to the oxic half-cycles. All concentrations are given in mmol/L, except for HS^-, Fe^{2+} and Fe^{3+} that are in μmol/L.

Sample	Day	Eh (mV)	pH	ATP (nM)	DOC	S	HS^-	Fe^{2+}	Fe^{3+}	F^-	Cl^-	P	Ca	K	Mg	Na
Phosphogypsum																
PG-01	1	170	4.60	0.04	11.1	90.5	2.76	110	278	2.10	472	23.2	32.0	n.a.	1.63	695
PG-02	2	175	4.62	0.04	12.3	74.8	1.65	260	1.60	1.87	472	14.9	21.6	0.82	0.98	435
PG-03	3	185	4.62	0.02	11.3	94.9	2.18	1.62	0.52	1.20	359	18.5	25.0	1.41	1.17	568
PG-04	4	189	4.62	0.03	5.36	72.5	2.08	1.62	2.41	1.08	318	19.1	26.0	1.56	1.26	566
PG-05	5	203	4.62	0.04	6.50	73.7	2.28	0.70	2.97	0.94	171	19.1	24.3	1.73	1.18	543
PG-06	8	227	4.61	4.91	7.23	71.7	2.42	<LD	0.13	2.03	480	20.1	26.3	2.22	1.27	561
PG-07	9	375	4.59	3.19	4.82	77.7	1.88	<LD	<LD	0.58	382	22.0	36.9	2.48	1.29	562
PG-08	10	399	4.59	6.85	3.52	72.4	1.83	<LD	0.36	0.57	463	20.4	26.1	2.59	1.28	559
PG-09	11	442	4.60	6.07	4.74	79.8	2.24	<LD	0.26	0.58	447	19.9	25.4	2.56	1.23	538
PG-10	12	450	4.60	5.36	1.75	80.6	1.97	<LD	0.17	0.70	315	21.0	26.6	2.84	1.29	570
PG-11	15	442	4.60	4.59	15.9	70.9	2.26	1.80	4.50	0.46	466	20.4	24.7	3.37	1.24	577
PG-12	16	387	4.60	2.52	17.1	72.0	0.34	<LD	<LD	0.53	470	21.4	27.3	0.13	1.31	543
PG-13	17	379	4.59	2.70	6.18	70.6	2.18	1.07	1.41	0.53	477	21.3	25.3	3.40	1.31	558
PG-14	18	369	4.60	1.80	12.7	77.7	2.08	<LD	1.93	0.55	478	23.8	29.1	4.24	1.42	606
PG-15	19	366	4.60	1.55	2.69	75.9	2.21	<LD	0.85	0.58	480	21.8	27.3	3.77	1.33	578
PG-16	22	502	4.68	2.38	2.34	76.1	2.08	<LD	0.48	0.86	486	22.1	27.3	4.31	1.26	577
PG-17	23	507	4.68	4.02	3.35	64.2	2.36	<LD	0.20	0.81	481	19.4	24.4	3.63	1.15	503
PG-18	24	517	4.68	2.05	1.92	76.2	1.93	<LD	0.42	0.84	486	23.2	27.4	4.68	1.33	619
PG-19	25	529	4.68	1.47	2.49	75.2	2.13	<LD	1.01	0.83	481	24.1	27.4	4.86	1.39	599
PG-20	26	542	4.68	2.90	2.19	74.8	2.53	<LD	0.32	0.61	481	22.6	27.6	4.90	1.30	578
PG-21	29	554	4.67	1.14	15.8	78.6	2.18	0.74	<LD	0.91	474	23.6	29.0	5.01	1.38	606
PG-22	30	532	4.66	2.18	5.54	63.6	2.24	1.25	1.40	0.60	498	19.8	23.7	4.55	1.15	505
PG-23	31	509	4.66	2.81	2.09	55.6	0.62	0.88	5.62	0.45	477	20.9	24.4	6.79	2.49	515
PG-24	32	512	4.66	3.50	4.32	62.9	1.94	0.52	0.45	0.60	482	18.7	22.8	5.37	1.29	518
PG-25	33	518	4.66	4.66	6.25	67.0	2.16	1.44	1.59	0.78	482	20.0	24.0	5.87	1.37	557
PG-26	36	562	4.66	2.10	7.19	n.a.	1.57	<LD	<LD	0.67	495	n.a.	n.a.	n.a.	n.a.	n.a.
PG-27	37	562	4.69	2.48	1.31	n.a.	2.08	<LD	<LD	0.74	488	n.a.	n.a.	n.a.	n.a.	n.a.
PG-28	38	562	4.67	2.19	1.20	62.0	1.99	1.07	<LD	0.73	486	18.5	22.6	5.78	1.33	500
PG-29	39	561	4.66	1.99	1.21	63.8	2.44	<LD	0.36	0.70	489	19.9	23.1	5.17	1.14	490
PG-30	40	561	4.66	3.39	1.24	68.2	1.94	<LD	0.16	0.73	491	21.3	24.6	5.70	1.28	509

et al., 2011; Frohne et al., 2014). The dynamics of pH often reflect the presence of microorganisms and organic matter (Husson, 2013; Wang et al., 2013), the oxidation of pyrite (Phan et al., 2018) or the hydrolysis of Fe (Karimian et al., 2018), all generating acidity to the system, they may lead to the continuously low pH conditions during the present experiments.

4.2. DOC consumption and ATP levels as tracers of the microbial activity

Both suspensions subjected to redox oscillations followed similar DOC trend. Phosphogypsum samples presented slightly lower values (from 1.20 to 17.1 mmol/L) than those corresponding to the marsh soil (from 0.47 to 29.9 mmol/L) (Table 1). After the addition of the cellobiose at the onset of every anoxic cycle, the DOC amount decreased constantly until reaching the lowest levels at the subsequent oxidising half cycles (Fig. 2D), as it was consumed by bacteria faster than it is replenished by hydrolysis (Parsons et al., 2013), and/or due to respiration and oxidation of Fe^{2+}, S and As (Phan et al., 2018). The correlations between DOC with Eh and pH were not significant, also described by Frohne et al. (2011).

At the first half of the phosphogypsum experiment, ATP concentration was minimal during the anoxic conditions and higher during the oxic cycles indicating the presence of aerobic bacteria (Fig. 2C). On the contrary, the microbial inactiveness in the marsh soil suspension was highlighted during the same period at both conditions (Fig. 2C). This behaviour was expected due to the strong anoxic environment that exists naturally in the marsh soil because of the high content in decomposing organic matter, which probably does not favour the aerobic bacteria growth. Nevertheless, microbial activity slightly increased at the second half of the marsh soil experiment consistent with the higher Eh conditions. Higher ATP values were observed during anoxic conditions in both systems at that period, indicating that the rates of the microbially mediated solubilisation of POM (Particulate Organic Matter) exceeded the rates of DOC consumption by heterotrophic metabolism, as also observed in Parson et al. (2013) and Phan et al. (2018). This microbial activity increase cannot be supported by the development of SRB due to the low pH conditions and the limited sulphate reduction and thus, to the low sulphide concentrations in both our systems, corroborating the fact that anaerobic conditions could not be effectively reached, as shown by the constantly elevated Eh values (Fig. 2A and B).

Marsh soil																
MS-01	1	265	3.51	0.04	9.23	53.4	1.89	129	279	2.23	470	26.9	30.9	4.59	3.25	545
MS-02	2	273	3.48	0.02	5.01	n.a.	1.78	552	57.2	2.06	270	n.a.	n.a.	n.a.	n.a.	n.a.
MS-03	3	281	3.43	0.04	15.2	53.2	1.99	652	38.1	2.69	490	29.0	33.0	5.69	3.52	545
MS-04	4	287	3.40	0.04	13.9	58.1	1.88	619	90.3	2.85	495	33.5	36.0	6.12	3.94	579
MS-05	5	291	3.36	0.33	11.2	57.7	1.81	507	222	2.87	512	32.8	36.0	6.29	3.64	563
MS-06	8	312	3.28	0.71	8.80	49.1	2.05	117	733	2.89	444	22.4	30.1	6.17	3.31	504
MS-07	9	394	3.16	0.34	3.55	52.6	2.08	4.38	86.4	2.91	436	23.9	27.2	5.66	2.86	481
MS-08	10	471	3.18	0.22	3.73	54.4	2.04	1.22	2.54	3.32	503	29.2	32.2	7.37	3.68	519
MS-09	11	480	3.21	0.19	5.07	56.7	1.81	0.86	1.66	3.32	505	30.7	34.1	7.37	3.61	585
MS-10	12	484	3.22	0.28	3.91	53.5	1.78	1.23	2.00	2.62	500	27.3	31.0	6.75	3.19	506
MS-11	15	480	3.22	0.45	29.9	55.4	1.94	3.43	3.53	2.84	496	30.1	34.0	7.70	3.55	554
MS-12	16	449	3.22	0.65	15.0	54.6	1.67	17.8	4.30	2.78	503	29.4	34.1	7.39	3.38	527
MS-13	17	436	3.22	0.57	7.27	53.7	1.72	3.27	3.90	2.91	507	30.1	33.1	7.60	3.52	535
MS-14	18	430	3.21	0.70	0.47	55.1	1.77	13.6	29.2	2.91	505	29.8	34.7	7.80	3.45	542
MS-15	19	428	3.21	0.61	5.61	n.a.	1.73	9.89	<LD	2.70	514	n.a.	n.a.	n.a.	n.a.	n.a.
MS-16	22	712	3.43	0.92	4.31	54.0	1.93	7.50	2.56	3.21	508	29.6	33.1	8.10	3.48	550
MS-17	23	717	3.43	1.29	3.68	46.8	1.99	1.25	1.48	3.12	509	25.7	28.5	7.25	3.14	477
MS-18	24	727	3.44	1.84	3.08	54.8	1.49	6.77	0.18	3.15	509	30.1	34.2	8.12	3.49	545
MS-19	25	739	3.43	2.68	2.97	56.1	1.59	3.46	3.37	3.21	510	30.9	33.3	8.99	3.59	548
MS-20	26	752	3.42	1.86	3.13	53.6	1.65	0.97	1.65	3.02	519	28.5	32.1	8.48	3.46	539
MS-21	29	764	3.41	1.59	14.9	53.1	1.80	1.97	1.28	3.04	510	29.7	32.3	8.18	3.49	543
MS-22	30	735	3.38	1.79	2.43	49.9	1.77	1.82	0.31	3.20	508	27.5	30.8	7.58	3.15	498
MS-23	31	723	3.39	2.41	7.50	62.8	1.73	5.11	0.88	3.17	561	25.5	28.9	6.71	2.31	551
MS-24	32	729	3.39	1.57	4.70	54.8	1.72	1.44	0.98	2.96	513	28.3	32.8	8.18	3.47	530
MS-25	33	745	3.39	2.73	2.18	53.3	1.72	2.33	<LD	3.11	519	29.3	33.3	8.95	3.62	544
MS-26	36	772	3.37	1.17	2.05	n.a.	1.72	<LD	<LD	3.16	519	n.a.	n.a.	n.a.	n.a.	n.a.
MS-27	37	772	3.31	0.88	2.11	61.7	2.01	<LD	<LD	3.22	521	29.1	39.9	9.10	3.61	524
MS-28	38	772	3.34	1.20	2.02	43.2	1.75	<LD	2.61	3.15	521	22.5	26.4	8.28	3.45	461
MS-29	39	771	3.36	0.80	2.10	47.3	1.64	<LD	2.15	2.08	535	24.6	28.1	9.16	3.62	475
MS-30	40	771	3.37	1.18	2.22	42.4	1.41	<LD	2.08	3.21	522	22.8	26.6	8.52	3.36	492

n.a. = not analysed; LD = limit of detection

4.3. Sulphur release and iron cycling

The total amount of S in solution presented no correlation with the Eh in both systems and no significant differences between oxic and anoxic conditions were found. Despite following similar pattern, S concentrations presented higher values in the phosphogypsum compared to the marsh soil (Table 1; Fig. 3A and B). Aqueous HS^- concentration did not present important or consistent variations, and was constantly present at low concentrations in both systems, with only occasional decrease under anoxic conditions (e.g. 31st day in the phosphogypsum), (Fig. 3A and B), indicating limited sulphate reduction during the anoxic half-cycles. Nevertheless, supersaturation with respect to some sulphide phases was predicted by PHREEQC calculations, e.g. chalcopyrite and pyrite (Table S2), that can be related with occasional sulphide precipitation.

In phosphogypsum both total Fe and Fe^{2+} decreased dramatically soon after the first days of the experiment, already on the 3rd day (from 338 to 2.14 μmol/L) (Table 1). The low Fe^{2+} values were preserved in each oxic phase, the higher pH (4.5) favouring slightly Fe^{2+} oxidation by O_2. Ferrous iron increased during the anoxic half cycles, while it was almost depleted from solution at the oxic ones, as it was likely oxidised to Fe^{3+} and precipitated as newly-formed phase explicating the decrease in total Fe (Fig. 3C). On the contrary, in marsh soil, Fe^{2+} was very close to the total Fe, even in oxic periods, and the first drop was observed at the onset of the first oxic phase (9th day from 408 to 90.8 μmol/L), probably due to the limited oxidation by O_2 (Fig. 3D).

The depletion of Fe from the solution was consistent with the solid phases that tended to precipitate according to PHREEQC calculations; Fe^{3+} produced by Fe^{2+} oxidation was predicted to precipitate as oxyhydroxide phases; *i.e.*, goethite and lepidocrocite (Table S2). This was mainly evident in the phosphogypsum and less in the marsh soil, where the calculated SI corresponded either to undersaturation or close to saturation with respect to the Fe phases, a case consistent with the poor oxidation of Fe during the oxic cycles. Moreover, supersaturation in Fe^{3+} phosphates was noted in the form of strengite at both experiments (Table S2), while Fe phosphate precipitation would explain the decrease of the iron amount in solution in the marsh soil experiment during the oxic cycles, despite there is no strong oxidation of Fe.

4.4. Mobility of trace elements

The range of trace elements' concentrations (Zn, As, Cd, U) was small indicating mostly a conservative behaviour during the experiments with no consistent alternations between oxic and anoxic conditions (Fig. 4); *e.g.*, As fluctuated only between approx. 0.03 to 0.07 and 0.08 to 0.11 mmol/L, in the phosphogypsum and the marsh soil, respectively (Table 2). The higher contaminant mobility in the marsh soil system is consistent with the lower pH values. Concerning As speciation, the results indicated that most of the total amount was present as As^{5+}, while As^{3+} was present at minimal concentrations (Fig. 4A and B).

Table 2
Total elemental concentrations in the phosphogypsum and the marsh soil suspensions during the redox experiments. Aluminium, Cu, Zn, As and Cd are given in mmol/L, while the remaining in μmol/L. Grey cells correspond to the anoxic and white to the oxic half-cycles.

Sample	Day	Al	Cr	Mn	Co	Ni	Cu	Zn	As	Cd	Sb	Pb	U
Phosphogypsum													
PG-01	1	0.05	0.85	4.73	0.45	0.16	0.03	0.09	0.04	0.01	0.35	0.009	0.028
PG-02	2	0.01	<LD	3.64	0.36	0.16	0.01	0.04	0.03	0.01	0.34	<LD	0.031
PG-03	3	0.01	0.16	2.96	0.31	0.12	0.004	0.05	0.03	0.01	0.17	0.005	0.026
PG-04	4	0.01	0.21	4.60	0.50	0.18	0.01	0.06	0.03	0.01	0.25	0.014	0.061
PG-05	5	0.001	<LD	<LD	<LD	<LD	<LD	0.06	0.04	0.01	<LD	<LD	0.059
PG-06	8	0.002	0.02	2.81	0.29	0.11	0.004	0.04	0.03	0.01	0.21	0.001	0.013
PG-07	9	0.01	<LQ	3.54	0.36	0.16	0.01	0.06	0.04	0.01	0.35	0.045	0.027
PG-08	10	0.003	0.02	3.60	0.38	0.14	0.01	0.05	0.03	0.01	0.27	0.005	0.019
PG-09	11	0.004	<LD	3.59	0.38	0.15	0.01	0.05	0.04	0.01	0.29	0.005	0.020
PG-10	12	0.002	<LD	3.31	0.35	0.13	0.004	0.04	0.03	0.01	0.24	0.002	0.017
PG-11	15	0.004	<LD	3.45	0.38	0.14	0.004	0.04	0.03	0.01	0.24	0.006	0.033
PG-12	16	<LD	<LD	4.42	0.46	0.20	0.01	0.04	0.03	0.01	0.38	<LD	0.033
PG-13	17	0.003	<LD	2.76	0.32	0.11	0.004	0.04	0.03	0.01	0.20	0.003	0.024
PG-14	18	0.003	<LD	3.47	0.37	0.15	0.005	0.04	0.03	0.01	0.24	0.007	0.023
PG-15	19	0.004	<LD	3.30	0.37	0.14	0.005	0.05	0.03	0.01	0.26	0.006	0.031
PG-16	22	0.005	<LD	3.35	0.38	0.15	0.004	0.05	0.03	0.01	0.24	0.003	0.027
PG-17	23	<LD	<LD	3.34	0.36	0.16	0.004	0.04	0.04	0.01	0.28	<LD	0.032
PG-18	24	0.005	<LD	3.40	0.41	0.15	0.004	0.04	0.03	0.01	0.24	0.005	0.031
PG-19	25	0.01	<LD	3.35	0.37	0.14	0.004	0.04	0.03	0.01	0.25	0.005	0.039
PG-20	26	0.003	<LD	3.20	0.35	0.14	0.004	0.04	0.03	0.01	0.23	0.004	0.035
PG-21	29	0.004	<LD	3.26	0.38	0.14	0.003	0.05	0.03	0.01	0.23	0.005	0.034
PG-22	30	<LD	<LD	3.21	0.40	0.15	0.004	0.04	0.04	0.01	0.26	<LD	0.033
PG-23	31	0.18	0.19	11.0	0.48	0.16	0.11	0.12	0.07	0.01	0.11	0.020	0.499
PG-24	32	0.01	<LD	3.11	0.38	0.13	0.004	0.04	0.03	0.01	0.22	0.003	0.041
PG-25	33	0.01	<LD	3.15	0.38	0.14	0.004	0.04	0.03	0.01	0.24	0.005	0.048
PG-26	36	<LD	<LD	3.37	0.35	0.17	0.004	0.04	0.04	0.01	0.26	<LD	0.035
PG-27	37	0.01	<LD	3.41	0.36	0.17	0.003	0.04	0.04	0.01	0.25	<LD	0.030
PG-28	38	0.01	<LD	3.06	0.35	0.14	0.003	0.04	0.03	0.01	0.22	0.004	0.034
PG-29	39	0.01	<LD	2.90	0.35	0.13	0.003	0.03	0.03	0.01	0.20	0.002	0.031
PG-30	40	0.01	<LD	3.52	0.38	0.17	0.003	0.04	0.04	0.01	0.26	<LD	0.037

4.5. Solid phase characterisation

The chemical analyses of the aqueous phases of both phosphogypsum and marsh soil systems after 3 redox oscillation cycles showed that Fe is largely removed from the solution and SEM-EDS analyses revealed the dominant presence of Fe solid phases at precipitates. In both systems, Fe phosphate is the most commonly identified Fe solid phase, and is detected independently of the redox conditions (Fig. 5A and B). Chromium was found to be adsorbed to them to some extent. Iron oxyhydroxides were not detected until completion of the second full cycle, while certain identification of the exact phases was not feasible. They carried Cr, Cu and Zn as species in oxic, and to a lesser extent, in anoxic conditions (Fig. 5C and D). Iron was also detected in the spectra corresponding to major phases already present in the original phosphogypsum and soil materials, including gypsum, barite or fluoride.

The identification of metal sulphides was challenging in both matrices, probably, due to their low quantities that were difficult to be identified by SEM-EDS analysis. Nevertheless, some metal sulphide phases (*e.g.*, FeS_2 and (Cu,-Fe) S_2) were detected in the solid samples of both experiments (Fig. 5E and F), in agreement with the phases predicted to precipitate according to PHREEQC calculations (Table S2).

5. Discussion

5.1. Fe and S redox processes' effect on metal behaviour

In our experiments, soon after organic matter addition in each anoxic half-cycle, aqueous Fe concentration first increased, as observed in other studies (*e.g.*, Parsons et al., 2013). However, the limited amount of Fe released in solution might be attributed to the little total Fe present in the solid phases and to the slow dissolution kinetics of iron oxyhydroxides. The fast drop of Fe^{+2} that follows indicates the precipitation of Fe phosphates (Kocar and Fendorf, 2009; Weigand et al., 2010), with phosphate ion being predominant in such phosphogypsum, and the fast sorption on remaining Fe oxides or occasional fast FeS precipitation (Wolthers et al., 2005). After this dramatic drop in the phosphogypsum first anoxic half-cycle and the marsh soil first oxic half-cycle, the initial amount of total Fe was never recovered and remained continuously low. The onset of Fe oxyhydroxides reduction, in the initial and subsequent reducing periods on the phosphogypsum, is sharp (no Fe^{2+} present

Marsh soil													
MS-01	1	0.18	1.01	10.6	0.44	0.15	0.05	0.25	0.09	0.01	0.13	0.006	0.318
MS-02	2	0.36	0.70	11.7	0.44	0.18	0.02	0.25	0.11	0.01	0.11	<LD	0.600
MS-03	3	0.27	0.82	12.1	0.53	0.18	0.02	0.25	0.11	0.02	0.10	0.009	0.481
MS-04	4	0.28	0.61	11.4	0.45	0.16	0.02	0.23	0.10	0.01	0.10	0.009	0.511
MS-05	5	0.23	0.53	10.2	0.42	0.15	0.02	0.21	0.09	0.01	0.11	0.009	0.474
MS-06	8	0.28	0.46	10.5	0.47	0.16	0.01	0.21	0.10	0.01	0.11	0.007	0.803
MS-07	9	0.41	0.45	11.6	0.46	0.18	0.04	0.24	0.11	0.01	0.12	<LD	0.349
MS-08	10	0.30	0.42	11.3	0.47	0.16	0.14	0.22	0.10	0.01	0.11	0.016	0.454
MS-09	11	0.25	0.29	9.24	0.40	0.14	0.13	0.18	0.08	0.01	0.09	0.013	0.381
MS-10	12	0.30	0.32	10.9	0.47	0.17	0.16	0.21	0.10	0.01	0.10	0.016	0.471
MS-11	15	0.28	0.32	10.6	0.46	0.15	0.18	0.20	0.09	0.01	0.11	0.019	0.462
MS-12	16	0.41	0.38	11.2	0.44	0.18	0.18	0.23	0.10	0.01	0.12	<LD	0.404
MS-13	17	0.28	0.30	10.4	0.46	0.15	0.17	0.21	0.09	0.01	0.11	0.017	0.468
MS-14	18	0.31	0.36	11.1	0.47	0.16	0.18	0.22	0.10	0.01	0.11	0.026	0.553
MS-15	19	n.a.	n.a.	n.a.	n.a.	n.a.	n.a.	n.a.	n.a.	n.a.	n.a.	n.a.	n.a.
MS-16	22	0.31	0.29	11.1	0.47	0.17	0.16	0.21	0.10	0.01	0.12	0.023	0.499
MS-17	23	0.30	0.26	12.1	0.47	0.19	0.22	0.19	0.09	0.01	0.11	0.017	0.413
MS-18	24	0.31	0.23	11.09	0.50	0.16	0.23	0.21	0.10	0.01	0.11	0.019	0.515
MS-19	25	0.32	0.24	11.32	0.51	0.17	0.23	0.22	0.10	0.01	0.12	0.054	0.538
MS-20	26	0.34	0.23	11.78	0.50	0.18	0.27	0.22	0.10	0.02	0.13	0.020	0.546
MS-21	29	0.31	0.18	10.78	0.49	0.17	0.25	0.23	0.10	0.01	0.12	0.026	0.505
MS-22	30	0.29	0.19	10.91	0.59	0.16	0.24	0.19	0.08	0.01	0.17	0.017	0.510
MS-23	31	0.28	0.01	2.87	0.35	0.13	0.10	0.13	0.06	0.01	0.23	0.006	0.053
MS-24	32	0.30	0.15	10.92	0.44	0.16	0.24	0.20	0.09	0.01	0.11	0.020	0.518
MS-25	33	0.34	0.19	10.76	0.50	0.17	0.25	0.21	0.10	0.01	0.11	0.021	0.541
MS-26	36	0.40	0.17	12.24	0.47	0.20	0.27	0.24	0.11	0.01	0.13	<LD	0.413
MS-27	37	0.38	0.19	11.43	0.45	0.19	0.26	0.23	0.11	0.01	0.12	<LD	0.380
MS-28	38	0.35	0.19	12.01	0.54	0.17	0.27	0.22	0.10	0.02	0.13	0.022	0.556
MS-29	39	0.31	0.18	10.64	0.46	0.15	0.24	0.20	0.09	0.01	0.12	0.020	0.495
MS-30	40	0.31	0.18	12.03	0.47	0.19	0.26	0.23	0.11	0.01	0.13	0.019	0.382

n.a.= not analysed; LD= limit of detection

during the oxic periods) and corresponds to the cellobiose (organic matter) addition. Although organic matter could a priori reduce directly Fe oxyhydroxides present in the phosphogypsum, this reduction is generally found in the literature to be catalysed by iron reductive bacteria (e.g. Phan et al., 2019). Nevertheless, this could be attributed to the time needed for the development of anaerobic microbial activity (Rinklebe and Langer, 2008; Langer and Rinklebe, 2009), which could be longer compared to our short one week anoxic periods (Frohne et al., 2014), or to the acidic conditions that hindered the establishment of the anoxic environment (Phan et al., 2018). These conditions may arise from the zero formation of Fe oxyhydroxides during oxic periods due to the main precipitation of phosphate.

In the phosphogypsum experiment, Fe^{2+} in solution first decreases in the oxic half cycles as Eh increases, and free Fe^{2+} oxidatively precipitates as FeOOH, a phenomenon catalysed by adsorption of Fe^{2+} on mineral surfaces (Silvester et al., 2005), or as amorphous Fe^{3+} phosphates. The oxidation of Fe^{2+} originating from pyrite oxidation and Fe-(oxyhydr)oxides to Fe^{3+} phases was, also, described in similar studies (*e.g.*, Phan et al., 2019). The rapid precipitation of poorly crystalline Fe^{3+} minerals under oxic conditions has been described by Megonigal et al. (2003). In turn, these precipitated Fe phases re-dissolved in the subsequent anoxic cycle releasing Fe, which was again reduced to Fe^{2+}, as previously reported (Antić-Mladenović et al., 2011; Frohne et al., 2011, 2014), which implies the formation of high surface/volume ratio particles, i.e. Fe^{2+} nanoparticles. The precipitation of Fe^{+3} bearing solid phases following Fe^{2+} oxidation in the studied systems is one of the driving processes of "The Iron Wheel" geochemical cycling, which is used to describe the alternating reductive dissolution and oxidation-precipitation processes of iron. This cycling can interact with P leading to the abundant formation of Fe phosphates (*i.e.*, vivianite and strengite), as already described by Busigny et al. (2016). This process is consistent with the low sulphide concentrations in our systems that allows the dissolved Fe to accumulate (Davison, 1993; Busigny et al., 2016).

Oxidation of Fe^{2+} and consequently, Fe precipitation were less important during the marsh soil experiment, indicating its resistance to oxidation (i) by low pH, and (ii) by competence with Dissolved Organic Matter (DOM); the Fe^{2+} oxygenation kinetics are highly pH dependent, and thus, faster at pH 4.5 than at pH 3.5. Nevertheless, the differences between Fe^{2+} and Fe-total were slightly higher in oxic cycles implying the presence of *e.g.*, Fe^{3+} organic complexes in the solution.

The conservative behaviour of the metals in the present experiments indicated their poor adsorption to Fe minerals and their poor co-precipitation, *i.e.*, in the case of As due to SO_4^{2-} competition, while Fe^{2+} is oxidised, a case in agreement with other studies (Frohne et al., 2011, 2014). Low pH conditions could have prevented those processes, as the adsorption capacity of trace elements to Fe minerals is low in acidic environments (Schulz-Zunkel and Krüger, 2009), as both the surface of those minerals and the metals of

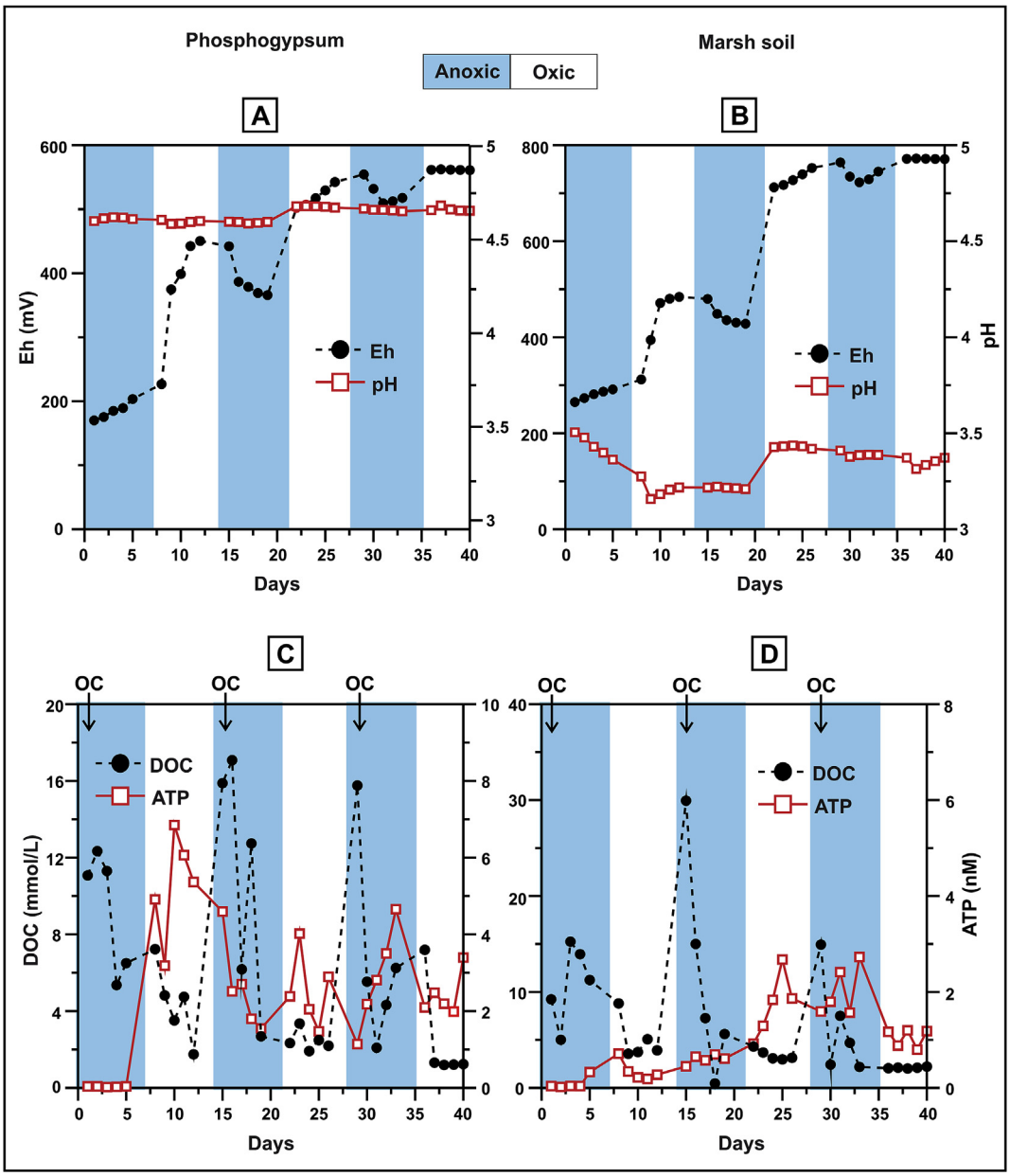

Fig. 2. Eh-pH parameters (**A** and **B**), microbial activity and organic matter (**C** and **D**) in the phosphogypsum and marsh soil systems, respectively. The OC arrow indicates the addition of cellobiose at the beginning of the anoxic cycles.

interest (Zn, Cd and U) are positively charged. Thus, the results revealed higher soluble concentrations than expected and a general conservative behaviour, especially for Zn, As and Cd concentrations in solution. High mobilization of metals during acidic conditions was also detected in other studies on redox dynamics (*e.g.*, Chuan et al., 1996; Wiegand et al., 2009; Miller et al., 2010), showing that natural attenuation is not favoured. Organic matter is another important parameter that controls the fate of metals in redox dynamics, as reported by Grybos et al. (2007), due to its high affinity to complex and adsorb metal cations (Cd, Cu, Ni and Zn) on negatively surface charged carboxyl groups (Laveuf and Cornu, 2009; Frohne et al., 2011). The synergic effect of various contaminants included in the same suspension at the beginning of the experiment could, also, affect each other's behaviour and compete for ion complexation (Couture et al., 2015). The exceptional decrease of the available trace elements during the marsh soil experiment (i.e. at the 31st day at the last anoxic cycle; Fig. 4B and D) could indicate their occasional co-precipitation to the available Fe minerals.

In anoxic and acidic environments (around pH 4), the sulphur produced during the oxidation of organic matter is expected to react with the dissolved Fe^{2+} to form monosulphides of insoluble Fe (Berner, 1970). The overall reaction would be (Eq. (1)):

$$4FeOOH_{(s)} + 4SO_4^{2-} + 9CH_2O + 8H^+ \rightarrow 4FeS_{(s)} + 9CO_2 + 15H_2O \quad (1)$$

Therefore, the available Fe and the remaining metal ions released during the anoxic half cycles could precipitate as metal sulphides. However, this process did not seem to be important in the current experiments, as indicated by the minimal decrease of sulphide concentration (Fig. 3A) and the poor metal sulphide identification during mineralogical analysis. The limited activity of

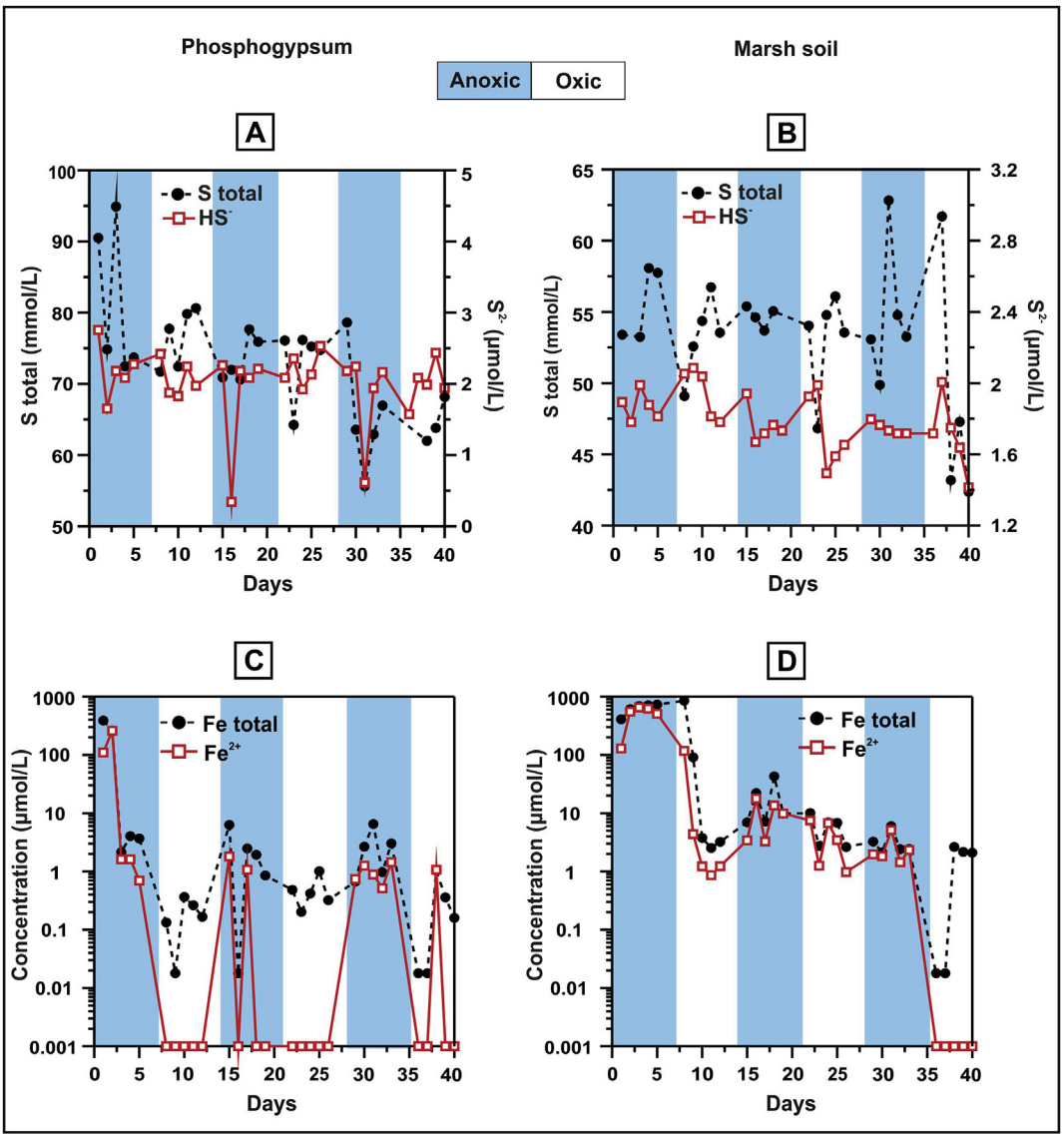

Fig. 3. Concentrations of total S and HS^- (**A** and **B**), and concentrations in log scale of total Fe, and Fe^{2+} (**C** and **D**), in the phosphogypsum and the marsh soil systems, respectively.

SRB could be responsible for this effect, and the established acidic conditions might have inhibited their development (Blodau, 2006; Karimian et al., 2018) and subsequently, prevented the microbial sulphate reduction (Phan et al., 2018). The low pH conditions might have prevented the preservation of the potential sulphide precipitates, leading also, to their poor identification, as they are reported to be rather soluble under acidic conditions (Liu et al., 2009; Frohne et al., 2011). Given the more acidic conditions prevailing in the marsh soil system, sulphate reduction and sulphide precipitation was zero. Hence, in both systems, sulphide concentrations were too low to favour metal sulphide precipitation. More importantly the dominant Fe phosphate precipitation should have prevented the formation of sulphides, being the main precipitation process that controlled the mobility of Fe^{2+}. Therefore, the conventional driving process of sulphide precipitation expected in estuarine salt marsh systems is not favoured when the source of the contaminants is a waste rich in phosphates, as occurs in the studied area.

In addition, the available metal ions appeared in higher concentrations than the aqueous sulphide ions. This could be explained by the dissolution of some solid phases on which the metals were adsorbed (*e.g.*, Fe oxyhydroxides) and their subsequent release. This would imply the coupled reaction **(1)** of reductive dissolution of Fe oxyhydroxides and sulphate reduction with precipitation of metal sulphides. However, since there is no evident decrease of trace metals during oxic cycles despite Fe oscillation, the Fe oxyhydroxides that dissolved could be also contained in the initial phosphogypsum, concomitant with the identified phases by SEM-EDS analysis. With respect to the marsh soil experiment, the abnormal behaviour of sulphide with respect to the marsh soil -low peaks (although not significant) during the last two oxic half cycles (Fig. 3B)- could be explained by the decomposition of the present organic matter that favoured the development of anoxic microenvironments.

5.2. As and U behaviour

Arsenic was detected mostly as As^{5+} under both oxic and anoxic conditions, so no correlation was identified between As species and redox conditions. Arsenate, on the contrary to As^{3+}, is chemically

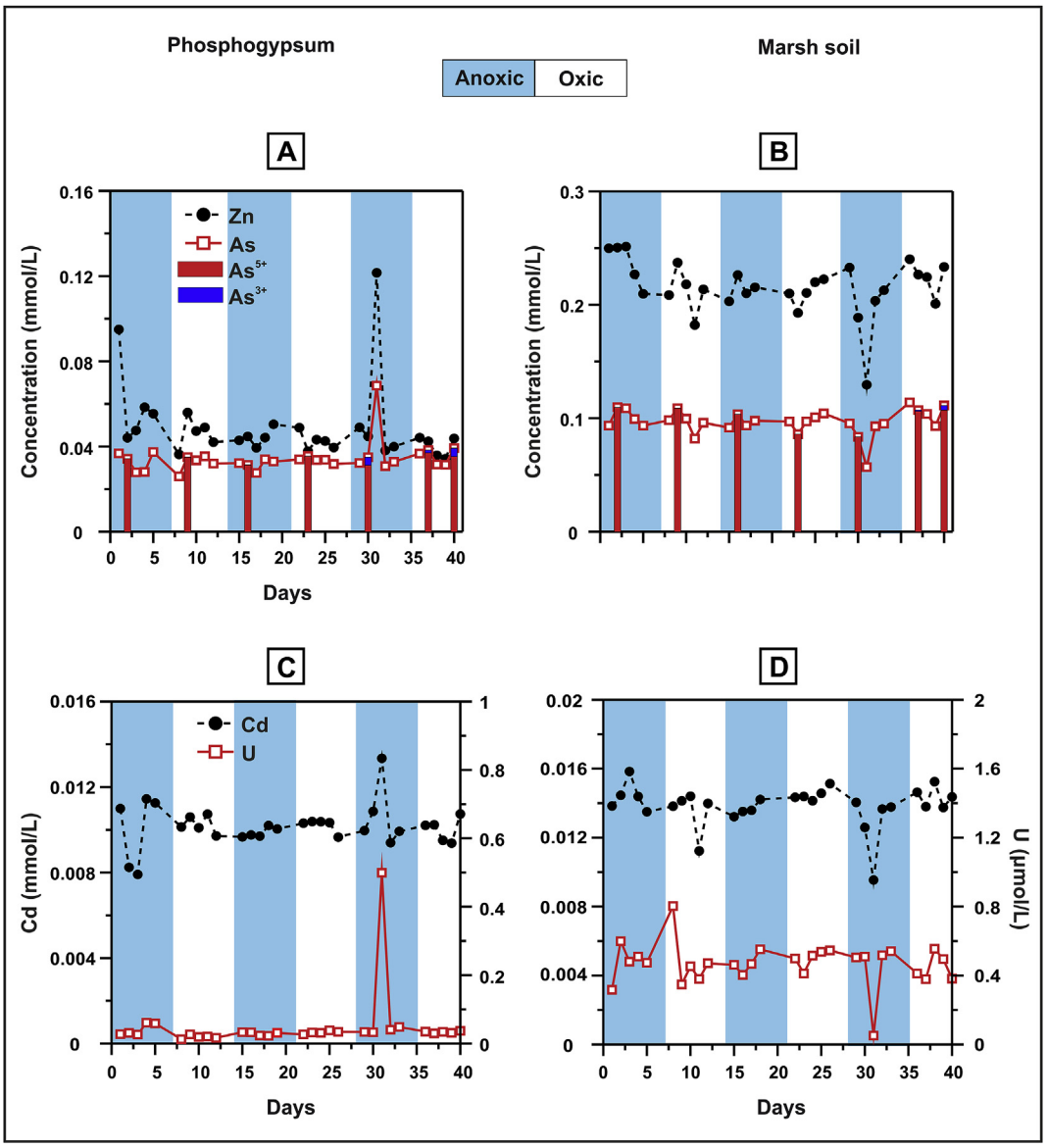

Fig. 4. Concentrations of trace elements during the redox experiments in the phosphogypsum (**A** and **C**), and in the marsh soil (**B** and **D**). Arsenic speciation is also presented for representative samples in each half-cycle (**A** and **B**).

similar to phosphate, so they compete for the same cations or binding sites in soils (Manning and Goldberg, 1996; Signes-Pastor et al., 2007). Huge aqueous phosphate concentrations present in both phosphogypsum and marsh soil suspensions could be responsible for As high mobility, as As^{5+} was the predominant species during the experiment. Phosphate is competing effectively with As in terms of sorption processes on iron minerals and has a strong affinity to sorb onto iron oxide minerals (Manning and Goldberg, 1996; Gao and Mucci, 2001; Dixit and Hering, 2003), hence preventing the As immobilisation during the presented experiments. In addition, As^{5+} was not reduced to As^{3+} during the anoxic conditions and thus, not favouring the formation of arsenic sulphide minerals, as only As^{3+} among arsenic ions has a strong affinity for S (Signes-Pastor et al., 2007). Some exceptions to the mobility of As, *e.g.*, day 31 at the marsh soil, could be attributed to As^{5+} sorption onto Fe^{3+} phosphate minerals, as has been reported by Lenoble et al. (2005).

Uranium presented a less conservative behaviour during redox cycling than the rest of the contaminants, as it displayed often fluctuations even during the same half cycle. Uranium is most likely present as U^{6+} in oxic conditions, while it could be reduced to the less soluble form of U^{4+} in anoxic conditions and thus, be immobilised by precipitation of $UO_{2(s)}$ or monomeric U^{+5} (Couture et al., 2015). This process could occur through several reduction pathways in organic-rich zones, including the materials of the presented experiments that are organic matter rich, such as abiotic reduction by iron sulphides that produces uraninite or as biological mediation via enzymatic activity (Hyun et al., 2012). This was more evident in the marsh soil experiment and especially, at the last two anoxic half cycles, being in agreement with the elevated values of organic matter (Figs. 2D and 3D).

6. Conclusions

Phosphogypsum disposal areas in estuarine salt marsh systems, such as the Huelva phosphogypsum pile, are sensitive to redox

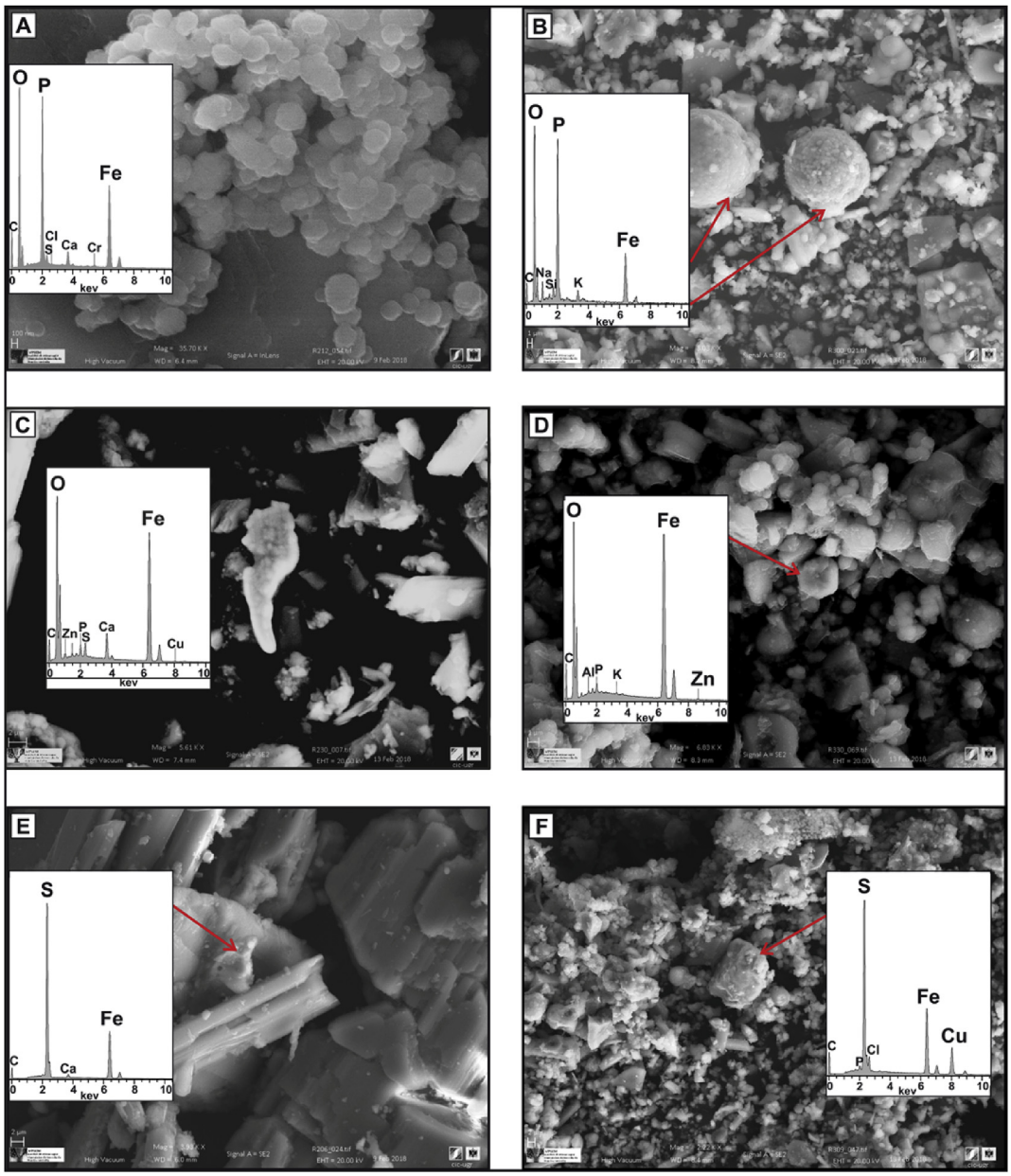

Fig. 5. Solid phases identified by SEM-EDS analysis in the precipitates collected during the experiments. **A** and **B**: Fe phosphate in the second anoxic cycle of the phosphogypsum and the marsh soil systems, respectively; **C** and **D**: Iron oxyhydroxide as a sink for Cu and Zn in the last oxic cycle of the phosphogypsum and the marsh soil systems, respectively; **E** and **F**: Fe sulphide (i.e. pyrite) in the second anoxic cycle of the phosphogypsum and the marsh soil systems, respectively; Cu substitution in Fe sulphide (in **F**).

conditions, which control the behaviour of the dominant redox sensitive species, *i.e.*, Fe and S, and subsequently, the geochemical processes and the mobility of the potentially toxic trace elements that discharge from the waste. Our results reveal a rapid and significant decrease of aqueous Fe upon the start of anoxic conditions in the phosphogypsum experiment and upon the start of the oxic period in the marsh soil experiment, coherent with a fast precipitation of Fe phosphate. Iron decrease from solution was also consistent, to a lower extent, with precipitation of Fe(III) oxyhydroxides. In contrast, sulphate reduction and FeS precipitation, usually very active in estuarine salt marsh systems, were not favoured in the current study, consistent with the absence of SRB. In addition, the insufficient amount of sulphide available compared to trace elements concentrations hinders Fe, Cd or Zn sulphide precipitation processes. Therefore, the formation of metal sulphides appeared to be secondary compared to the precipitation of Fe phosphates, which in turn controls the mobility of the metal ions independently of the redox conditions. Immobilisation of the contaminants of interest (Zn, As, Cd, U) was not favoured during the current experiments, possibly due to prevailing acidic conditions, elevated concentrations of organic matter, and the synergetic effect of various contaminants competing for the same precipitated phases. In general, the studied trace elements are more mobile in the salt marsh soil than in the phosphogypsum stack, due to repetitively lower pH and higher Eh values.

Although SRB activity can be favoured by a cover rich in organic matter and abundant of sulphate -as already implemented in parts of the waste- this study shows that this process cannot provide a substantial improvement in the quality of the leachates, given that contaminants mobility is not affected importantly by redox

oscillations. Based on the experiments, natural attenuation does not seem to work in this industrial ecosystem, and different remediation actions are necessary. Accordingly, further studies on the optimisation of treatment systems for the acid leachates based on alkaline addition would be needed since they might be postulated as the only feasible way to prevent contaminants from reaching the Estuary of Huelva. Nevertheless, an alternative possible pathway for Fe depletion is described in the current study, uncoupled from the microbial activity, that could be at use under conditions with poor microbial activity development.

Acknowledgements

This work was supported by the Regional Government of Andalusia through the "Junta de Andalucía" research projects and RNM-131 and by the Spanish Ministry of Economy and Competitiveness through the research project CAPOTE (CGL2017-86050-R). The authors are very grateful to the funding support for the Committee of Experts on "The environmental diagnosis and the proposal of measures of restoration of the phosphogypsum stacks of Huelva", appointed by the City Hall of Huelva. Dr. E. M. is grateful to the funding support of International Mobility launched by the University of Granada and CEI-BIOTIC Granada 2015/2016. Dr. A. Parviainen acknowledges the 'Juan de la Cierva – Incorporación' (IJCI-2016-27412) Fellowship and Dr. C. Marchesi the "Ramón y Cajal" (RYC-2012-11314) Fellowship financed by the Spanish Ministry of Economy and Competitiveness (MINECO).

We are immensely grateful to Dr. C.R. Cánovas and Dr. F. Macías for their help during the sampling. We also thank Dr. Delphine Tisserand and Dr. Sarah Bureau for their assistance during laboratory and analytical work. Redox oscillation experiments were performed within the analytical chemistry platform of ISTerre (OSUG France). We acknowledge the University of Huelva (Spain) and the Andalusian Institute of Earth Sciences (IACT) in Granada (Spain) for the solution elemental analyses, the University of Montpellier (France) (AETE-ISO platform, OSU-OREME/Université de Montpellier) for the aqueous As speciation, the Institute of Geosciences of the Environment (IGE) and the Institute of Earth Sciences (ISTerre) in Grenoble (France) for the ATP measurements, and for DOC, S and Fe analyses, respectively. Solid phase characterisation took place at the Instrumentation Centre (CIC) of the University of Granada, Spain.

Appendix A. Supplementary data

Supplementary data to this article can be found online at https://doi.org/10.1016/j.chemosphere.2019.125174.

References

Allison, J.D., Brown, D.S., Novo-Gradac, K.J., 1991. MINTEQA2/PRODEFA2, A Geochemical Assessment Model for Environmental Systems. Version 3. 0 User's Manual. EPA/600/3-911021. Environmental Research Laboratory, Office of Research and Development, US Environmental Protection Agency, Athens, GA.

Andrade, M.L., Reyzabal, M.L., Marcet, P., Montero, M.J., 2002. Industrial impact on marsh soils at the bahia blanca ria, Argentina. J. Environ. Qual. 31 (2), 532–538.

Andrade, M.L., Covelo, E.F., Vega, F.A., Marcet, P., 2004. Effect of the Prestige oil spill on salt marsh soils on the coast of Galicia (northwestern Spain). J. Environ. Qual. 33 (6), 2103–2110.

Ann, Y., Reddy, K.R., Delfino, J.J., 2000. Influence of redox potential on phosphorus solubility in chemically amended wetland organic soils. Ecol. Eng. 14 (1–2), 169–180.

Antić-Mladenović, S., Rinklebe, J., Frohne, T., Stärk, H.J., Wennrich, R., Tomić, Z., Ličina, V., 2011. Impact of controlled redox conditions on nickel in a serpentine soil. J. Soils Sediments 11 (3), 406–415.

Berner, R.A., 1970. Sedimentary pyrite formation. Am. J. Sci. 268 (1), 1–23.

Blodau, C., 2006. A review of acidity generation and consumption in acidic coal mine lakes and their watersheds. Sci. Total Environ. 369 (1e3), 307e332.

Bohari, Y., Astruc, A., Astruc, M., Cloud, J., Angot, A.P., 2001. Improvements of hydride generation for the speciation of arsenic in natural freshwater samples by HPLC-HG-AFS. Anal Atomic Spectrometry 16, 774–778.

Borch, T., Kretzschmar, R., Kappler, A., Cappellen, P.V., Ginder-Vogel, M., Voegelin, A., Campbell, K., 2009. Biogeochemical redox processes and their impact on contaminant dynamics. Environ Sci & Technol 44 (1), 15–23.

Borrego, J.F., Carro, B.M., Gil, J.A.G., De la Torre, M.L., Valente, T., Santisteban, M., 2013. Control factors on the composition of superficial sediments in estuaries of the coast of Huelva (SW Spain): a statistical approach. Cuadernos de Geología Ibérica= Journal of Iberian Geology: an international publication of earth sciences 39, 223–232.

Busigny, V., Jézéquel, D., Cosmidis, J., Viollier, E., Benzerara, K., Planavsky, N.J., Michard, G., 2016. The iron Wheel in lac pavin: interaction with phosphorus cycle. In: Lake Pavin. Springer, Cham, pp. 205–220.

Cánovas, C.R., Macías, F., Pérez-López, R., Basallote, M.D., Millán-Becerro, R., 2018. Valorization of wastes from the fertilizer industry: current status and future trends. J. Clean. Prod. 174, 678–690.

Castillo, J., Pérez-López, R., Sarmiento, A.M., Nieto, J.M., 2012. Evaluation of organic substrates to enhance the sulfate-reducing activity in phosphogypsum. Sci. Total Environ. 439, 106–113.

Chuan, M.C., Shu, G.Y., Liu, J.C., 1996. Solubility of heavy metals in a contaminated soil: effects of redox potential and pH. Water Air Soil Pollut. 90 (3–4), 543–556.

Cline, J.D., 1969. Spectrophotometric determination of hydrogen sulfide in natural waters. Limnol. Oceanogr. 14 (3), 454–458.

Couture, R.M., Charlet, L., Markelova, E., Made, B., Parsons, C.T., 2015. On–off mobilization of contaminants in soils during redox oscillations. Environ sci & techno 49 (5), 3015–3023.

Davison, W., 1993. Iron and manganese in lakes. Earth Sci. Rev. 34 (2), 119–163.

Dixit, S., Hering, J.G., 2003. Comparison of arsenic (V) and arsenic (III) sorption onto iron oxide minerals: implications for arsenic mobility. Environ sci & techno 37 (18), 4182–4189.

Du Laing, G., Rinklebe, J., Vandecasteele, B., Tack, F.M.G., 2009. Trace metal behaviour in estuarine and riverine floodplain soils and sediments: a review. Sci. Total Environ. 407, 3972–3985.

Frohne, T., Rinklebe, J., Diaz-Bone, R.A., Du Laing, G., 2011. Controlled variation of redox conditions in a floodplain soil: impact on metal mobilization and biomethylation of arsenic and antimony. Geoderma 160 (3), 414–424.

Frohne, T., Rinklebe, J., Diaz-Bone, R.A., 2014. Contamination of floodplain soils along the Wupper River, Germany, with As, Co, Cu, Ni, Sb, and Zn and the impact of pre-definite redox variations on the mobility of these elements. Soil Sediment Contam.: Int. J. 23 (7), 779–799.

Gao, Y., Mucci, A., 2001. Acid base reactions, phosphate and arsenate complexation, and their competitive adsorption at the surface of goethite in 0.7 M NaCl solution. Geochem. Cosmochim. Acta 65 (14), 2361–2378.

Grybos, M., Davranche, M., Gruau, G., Petitjean, P., 2007. Is trace metal release in wetland soils controlled by organic matter mobility or Fe-oxyhydroxides reduction? J. Colloid Interface Sci. 314 (2), 490–501.

Guerrero, J.L., Gutiérrez-Álvarez, I., Mosqueda, F., Olías, M., García-Tenorio, R., Bolívar, J.P., 2019. Pollution evaluation on the salt-marshes under the phosphogypsum stacks of Huelva due to deep leachates. Chemosphere 230, 219–229.

Hammes, F., Goldschmidt, F., Vital, M., Wang, Y., Egli, T., 2010. Measurement and interpretation of microbial adenosine tri-phosphate (ATP) in aquatic environments. Water Res. 44 (13), 3915–3923.

Husson, O., 2013. Redox potential (Eh) and pH as drivers of soil/plant/microorganism systems: a transdisciplinary overview pointing to integrative opportunities for agronomy. Plant Soil 362 (1–2), 389–417.

Hyun, S.P., Davis, J.A., Sun, K., Hayes, K.F., 2012. Uranium (VI) reduction by iron (II) monosulfide mackinawite. Environ sci & techno 46 (6), 3369–3376.

IAEA, 2013. Radiation Protection and Management of Norm Residues in the Phosphate Industry. Safety Reports Series No. 78 d Vienna. International Atomic Energy Agency, p. 308.

Karimian, N., Johnston, S.G., Burton, E.D., 2018. Iron and sulfur cycling in acid sulfate soil wetlands under dynamic redox conditions: a review. Chemosphere 197, 803–816.

Kocar, B.D., Fendorf, S., 2009. Thermodynamic constraints on reductive reactions influencing the biogeochemistry of arsenic in soils and sediments. Environ Sci & Technol 43 (13), 4871–4877.

Langer, U., Rinklebe, J., 2009. Lipid biomarkers for assessment of microbial communities in floodplain soils of the Elbe River (Germany). Wetlands 29 (1), 353–362.

Laveuf, C., Cornu, S., 2009. A review on the potentiality of rare earth elements to trace pedogenetic processes. Geoderma 154 (1–2), 1–12.

Lenoble, V., Laclautre, C., Deluchat, V., Serpaud, B., Bollinger, J.C., 2005. Arsenic removal by adsorption on iron (III) phosphate. J. Hazard Mater. 123 (1–3), 262–268.

Liu, J., Valsaraj, K.T., DeLaune, R.D., 2009. Inhibition of mercury methylation by iron sulfides in an anoxic sediment. Environ. Eng. Sci. 26, 833–840.

Lottermoser, B.G., 2007. Mine Wastes: Characterization, Treatment, Environmental Impacts, second ed. Springer-Verlag, Berlin Heidelberg.

Manning, B.A., Goldberg, S., 1996. Modeling competitive adsorption of arsenate with phosphate and molybdate on oxide minerals. Soil Sci. Soc. Am. J. 60 (1), 121–131.

Markelova, E., Couture, R.M., Parsons, C.T., Markelov, I., Madé, B., Van Cappellen, P., Charlet, L., 2018. Speciation dynamics of oxyanion contaminants (As, Sb, Cr) in argillaceous suspensions during oxic-anoxic cycles. Appl. Geochem. 91, 75–88.

Megonigal, J.P., Hines, M.E., Visscher, P.T., 2003. Anaerobic metabolism: linkages to trace gases and aerobic processes. In: Holland, H.D., Turekian, K.K. (Eds.), Treatise on Geochemistry. Pergamon, Oxford, p. 317e424.
Miller, F.S., Kilminster, K.L., Degens, B., Firns, G.W., 2010. Relationship between metals leached and soil type from potential acid sulphate soils under acidic and neutral conditions in Western Australia. Water Air Soil Pollut. 205 (1–4), 133.
Papanicolaou, F., Antoniou, S., Pashalidis, I., 2010. Redox chemistry of sulphate and uranium in a phosphogypsum tailings dump. J. Environ. Radioact. 101 (8), 601–605.
Papaslioti, E.M., Pérez-López, R., Parviainen, A., Macías, F., Delgado-Huertas, A., Garrido, C.J., Marhesi, C., Nieto, J.M., 2018. Stable isotope insights into the weathering processes of a phosphogypsum disposal area. Water Res. 140, 344–353.
Parkhurst, D.L., Appelo, C.A.J., 2013. PHREEQC Version 3: a Computer Program for Speciation, Batch-Reaction, One-Dimensional Transport, and Inverse Geochemical Calculations (No. 6-A43). US Geological Survey.
Parsons, C.T., Couture, R.M., Omoregie, E.O., Bardelli, F., Greneche, J.M., Roman-Ross, G., Charlet, L., 2013. The impact of oscillating redox conditions: arsenic immobilisation in contaminated calcareous floodplain soils. Environ. Pollut. 178, 254–263.
Pérez-López, R., Castillo, J., Sarmiento, A.M., Nieto, J.M., 2011. Assessment of phosphogypsum impact on the salt-marshes of the Tinto river (SW Spain): role of natural attenuation processes. Mar. Pollut. Bull. 62 (12), 2787–2796.
Pérez-López, R., Macías, F., Cánovas, C.R., Sarmiento, A.M., Pérez-Moreno, S.M., 2016. Pollutant flows from a phosphogypsum disposal area to an estuarine environment: an insight from geochemical signatures. Sci. Total Environ. 553, 42–51.
Pérez-López, R., Carrero, S., Cruz-Hernández, P., Asta, M.P., Macías, F., Cánovas, C.R., Guglieri, C., Nieto, J.M., 2018. Sulfate reduction processes in salt marshes affected by phosphogypsum: geochemical influences on contaminant mobility. J. Hazard Mater. 350, 154–161.
Phan, V.T., Bardelli, F., Le Pape, P., Couture, R.M., Fernandez-Martinez, A., Tisserand, D., Bernier-Latmani, R., Charlet, L., 2018. Interplay of S and as in Mekong Delta sediments during redox oscillations. Geosci. Front.
Phan, V.T., Bernier-Latmani, R., Tisserand, D., Bardelli, F., Le Pape, P., Frutschi, M., Gehin, A., Couture, R.M., Charlet, L., 2019. As release under the microbial sulfate reduction during redox oscillations in the upper Mekong delta aquifers, Vietnam: a mechanistic study. Sci. Total Environ.
Polizzotto, M.L., Kocar, B.D., Benner, S.G., Sampson, M., Fendorf, S., 2008. Near-surface wetland sediments as a source of arsenic release to ground water in Asia. Nature 454 (7203), 505–508.
Rabi, J.A., Mohamad, A.A., 2006. Parametric modelling and numerical simulation of natural-convective transport of radon-222 from a phosphogypsum stack into open air. Appl. Math. Model. 30 (12), 1546–1560.
Rinklebe, J., Langer, U., 2008. Floodplain soils at the Elbe River, Germany, and their diverse microbial biomass. Arch. Agron Soil Sci. 54 (3), 259–273.
Schulz-Zunkel, C., Krüger, F., 2009. Trace metal dynamics in floodplain soils of the River Elbe: a review. J. Environ. Qual. 38 (4), 1349–1362.
Signes-Pastor, A., Burló, F., Mitra, K., Carbonell-Barrachina, A.A., 2007. Arsenic biogeochemistry as affected by phosphorus fertilizer addition, redox potential and pH in a West Bengal (India) soil. Geoderma 137 (3–4), 504–510.
Silvester, E., Charlet, L., Tournassat, C., Gehin, A., Grenèche, J.M., Liger, E., 2005. Redox potential measurements and Mössbauer spectrometry of FeII adsorbed onto FeIII (oxyhydr) oxides. Geochem. Cosmochim. Acta 69 (20), 4801–4815.
Thompson, A., Chadwick, O.A., Rancourt, D.G., Chorover, J., 2006. Iron-oxide crystallinity increases during soil redox oscillations. Geochem. Cosmochim. Acta 70, 1710–1727. https://doi.org/10.1016/j.gca.2005.12.005.
USGS, 2017. Geological Survey, 2017, Mineral Commodity Summaries 2017. U.S. Geological Survey, p. 202.
Vega, F.A., Covelo, E.F., Andrade, M.L., 2008. Impact of industrial and urban waste on the heavy metal content of salt marsh soils in the southwest of the province of Pontevedra (Galicia, Spain). J. Geochem. Explor. 96 (2–3), 148–160.
Vega, F.A., Covelo, E.F., Cerqueira, B., Andrade, M.L., 2009. Enrichment of marsh soils with heavy metals by effect of anthropic pollution. J. Hazard Mater. 170 (2–3), 1056–1063.
Viollier, E., Inglett, P.W., Hunter, K., Roychoudhury, A.N., Van Cappellen, P., 2000. The ferrozine method revisited: Fe (II)/Fe (III) determination in natural waters. Appl. Geochem. 15 (6), 785–790.
Wang, Y., Tang, C., Wu, J., Liu, X., Xu, J., 2013. Impact of organic matter addition on pH change of paddy soils. J. Soils Sediments 13 (1), 12–23.
Watts, M.P., Lloyd, J.R., 2013. Bioremediation via microbial metal reduction. In: Microbial Metal Respiration. Springer Berlin Heidelberg, pp. 161–201.
Weigand, H., Mansfeldt, T., Bäumler, R., Schneckenburger, D., Wessel-Bothe, S., Marb, C., 2010. Arsenic release and speciation in a degraded fen as affected by soil redox potential at varied moisture regime. Geoderma 159 (3–4), 371–378.
Wiegand, J., Aschan, G., Kraus, U., Piontek, J., Mederer, J., 2009. Chemical fractionation and soil-to-plant transfer characteristics of heavy metals in a sludge deposit field of the river Ruhr, Germany. Soil Sediment Contam. 18 (1), 14–29.
Wolthers, M., Charlet, L., van Der Linde, P.R., Rickard, D., van Der Weijden, C.H., 2005. Surface chemistry of disordered mackinawite (FeS). Geochem. Cosmochim. Acta 69 (14), 3469–3481.
Wu, W.M., Carley, J., Gentry, T., Ginder-Vogel, M.A., Fienen, M., Mehlhorn, T., Yan, H., Caroll, S., Pace, M.N., Nyman, J., Luo, J., Gentile, M.E., Fields, M.W., Hickey, R.F., Gu, B., Watson, D., Cirpka, O.A., Zhou, J., Fendorf, S., Kitanidis, P.K., Jardine, P.M., Criddle, C.S., 2006. Pilot-scale in situ bioremedation of uranium in a highly contaminated aquifer. 2. Reduction of U(VI)andgeochemical control of U(VI) bioavailability. Environ Sci & Technol 40, 3986–3995.
Yu, K., Böhme, F., Rinklebe, J., Neue, H.-U., DeLaune, R.D., 2007. Major biogeochemical processes in soils — a microcosm incubation from reducing to oxidizing conditions. Soil Sci. Soc. Am. J. 71, 1406–1417.